UNIVERSIDADE ESTADUAL PAULISTA "JÚLIO DE MESQUITA FILHO"
INSTITUTO DE BIOCIÊNCIAS – CAMPUS DE BOTUCATU

PÓS-GRADUAÇÃO EM CIÊNCIAS BIOLÓGICAS
ZOOLOGIA

TESE DE DOUTORADO

Qual o impacto da pesca de arrasto sobre a assembleia de camarões em áreas costeiras marinhas? Uma análise temporal de populações a ecossistema no litoral norte de São Paulo

Júlia Fernandes Perroca
Orientador: Prof. Dr. Rogerio Caetano da Costa

BOTUCATU
2023

UNIVERSIDADE ESTADUAL PAULISTA "JÚLIO DE MESQUITA FILHO"
INSTITUTO DE BIOCIÊNCIAS – CAMPUS DE BOTUCATU

PÓS-GRADUAÇÃO EM CIÊNCIAS BIOLÓGICAS
ZOOLOGIA

Qual o impacto da pesca de arrasto sobre a assembleia de camarões em áreas costeiras marinhas? Uma análise temporal de populações a ecossistema no litoral norte de São Paulo

Júlia Fernandes Perroca
Orientador: Prof. Dr. Rogerio Caetano da Costa

Tese apresentada ao programa de Pós-Graduação em Ciências Biológicas do Instituto de Biociências da Universidade Estadual Paulista – UNESP, Campus de Botucatu, como parte dos requisitos para a obtenção do título de Doutora em Ciências Biológicas –Zoologia.

BOTUCATU
2023

FICHA CATALOGRÁFICA ELABORADA PELA SEÇÃO TÉC. AQUIS. TRATAMENTO DA INFORM.
DIVISÃO TÉCNICA DE BIBLIOTECA E DOCUMENTAÇÃO - CÂMPUS DE BOTUCATU - UNESP
BIBLIOTECÁRIA RESPONSÁVEL: ROSEMEIRE APARECIDA VICENTE-CRB 8/5651

Perroca, Júlia Fernandes.
Qual o impacto da pesca de arrasto sobre a assembleia de camarões em áreas costeiras marinhas? : uma análise temporal de populações a ecossistema no litoral norte de São Paulo / Júlia Fernandes Perroca. - Botucatu, 2023

Tese (doutorado) - Universidade Estadual Paulista "Júlio de Mesquita Filho", Instituto de Biociências de Botucatu
Orientador: Rogerio Caetano da Costa
Capes: 20402007

1. Camarão - População. 2. Pesca de arrastão. 3. Pesca artesanal. 4. Mudanças climáticas. 5. Decápodes.

Palavras-chave: Bycatch; Decapoda; El Niño Southern Oscillation; Pesca artesanal; Pesca de arrastão.

“Mas, quando estou fazendo meu trabalho, me sinto viva e eu mesma. É isso que eu faço. Tenho certeza de que existem outras versões de felicidade, mas essa é a minha”

- Lynsey Addario

Agradecimentos

À Deus, pela dádiva da vida e por poder experenciar as maravilhas da natureza. Ao professor *Dr. Rogerio Caetano da Costa* pela oportunidade de iniciar minha vida científica logo no primeiro ano da faculdade. Obrigada professor, por todos os ensinamentos, confiança e amizade. Nestes dez anos de parceria o *LABCAM* se tornou um lar para mim!

À *Fundação de Amparo à Pesquisa do Estado de São Paulo (FAPESP)* pelo auxílio financeiro concedido por meio da bolsa de doutorado – *FAPESP* (Proc. 2019/01308-5). À *FAPESP* pelos recursos financeiros concedidos por meio do projeto Temático (Proc. 2018/13685-5), o qual foram imprescindíveis para a realização deste trabalho, e aos coordenadores do projeto: *Prof. Dr. Fernando L. M. Mantelatto*, *Prof. Dr. Fernando José Zara*, *Prof. Dr. Sérgio Bueno* e *Prof. Dr. Rogerio Caetano Costa*. Ao auxílio regular *FAPESP* (Proc. 95/02833-0) sob a responsabilidade do *Dr. Fernando Luis Mantelatto*; ao auxílio Biota *FAPESP*, subprojeto Biodiversidade ambiente não consolidado (Proc. 98/07090-3) sob a responsabilidade do *Dr. Adilson Fransozo*; auxílio *Programa Jovem Pesquisador FAPESP* (Proc. 04/07309-8) sob a responsabilidade do *Dr. Rogerio Caetano da Costa*; às bolsas de doutorado *FAPESP* processos 97/12108-6, 97/12106-3 e 97/12107-0 supervisionadas pelo *Dr. Adilson Fransozo*. Ao *Conselho Nacional para o Desenvolvimento Científico e Tecnológico (CNPq)* no edital Pesca processo 406006/2012-1.

Ao professor *Dr. Jorge Luiz Rodrigues Filho*, muito obrigada por todos os ensinamentos, pela paciência, sugestões e amizade. Aprendi muito com você nestes anos de parceria!!!

Ao *Ministério do Meio Ambiente (MMA)* e ao *Instituto Brasileiro do Meio Ambiente e dos Recursos Naturais Renováveis (IBAMA)* por conceder a licença para coleta de material na área de estudo.

À *Pós-Graduação em Ciências Biológicas (Zoologia)* da UNESP de Botucatu e ao Departamento de Zoologia (IB Unesp-Botucatu) no qual realizei meu doutoramento.

Ao *Departamento de Ciências Biológicas*, Faculdade de Ciências da UNESP de Bauru, no qual o *Laboratório de Biologia de Camarões Marinhos e de Água Doce* está vinculado.

Ao *Instituto Oceanográfico da USP*, base de Ubatuba, e equipe pela gentil recepção, pela disponibilização do espaço para hospedagem e manipulação do material durante as coletas, e pelas deliciosas refeições.

Ao ilustre pescador *Djalma Rosa*, vulgo passarinho, por fazer parte da equipe durante todos os anos de amostragem, por todo o auxílio, ensino e carinho. Ao pescador *Oseas Lopes de Oliveira* pelo auxílio durante o último ano de coletas e encarar as pescarias "mortais" com nossa equipe.

Ao time do arrasto *Gabriel de Lucca*, *Gabriel Gois* e *Milena* pelo companheirismo e resiliência frente as adversidades do campo, sem vocês este trabalho não seria o mesmo. A todos que participaram das amostragens de campo na Enseada de Ubatuba desde 1995, sem o árduo esforço de todos, este trabalho não teria sido realizado.

Ao *José Fernando Gomes* vulgo *Sr. Fernando*, motorista da Unesp, que nos levou a Ubatuba na maioria das coletas referentes ao último período de amostragem e nos "cuidou" com muito carinho e atenção.

Aos membros atuais do LABCAM, *Daphine*, *Regis*, *Caio*, *Ana*, *Milena*, *Nádia*, *Sara*, *Helena*, *Leo*, *Sene*, e aos ex-membros *Rafa*, *Andrea*, *Natalia*, *Lizandra*, *João*, *Abner*, *Chuck*, *Sara*, *Woody*, *de Lucca*, pelo companheirismo e troca de conhecimentos e vivências. Um agradecimento especial para *Caio*, *Rafinha*, *Milena* e *Gois* pelas tardes divertidas e produtivas no cultivo e por toda a amizade.

Agradeço aos amigos de Botucatu, *Isabela Moraes* por sempre me receber em sua

casa com muito carinho e ao *Alexandre Silva* (Dino) pelos conselhos científicos.

Às minhas companheiras de "*Women in Crustacean Science*", *Isabela Moraes*, *Milena Jaconis* e *Amanda Horsch* pela amizade e suporte emocional. Fazer parte deste projeto com vocês é algo do qual muito me orgulho.

Às minhas amigas irmãs *Angélica e Nathália* por crescerem comigo e me acompanharem em todas as etapas.

E por fim, o meu maior agradecimento ao meu bem mais precioso minha Família. Gostaria de agradecer aos meus amados pais *José Roberto* e *Angela* por sempre me incentivarem nos estudos e em meus sonhos desde pequena. Sempre escutei que poderia fazer o que eu quisesse contanto que eu desejasse e me esforçasse. A confiança de vocês foi imprescindível para que eu nunca desistisse. Agradeço a minha amada avó *Lourdes*, por sempre cuidar de mim e me acompanhar desde bebê, sua força e amor me inspiram. À Miu, pelo suporte emocional!

Sumário

Considerações iniciais

Camarões marinhos são commodities amplamente comercializadas, representando mundialmente o segundo recurso pesqueiro em termos de valor (FAO, 2018). As pescarias de camarões ocorrem em uma amplitude de sistemas marinhos e estuarinos ao redor do mundo (Gillet, 2008), sendo que em ambientes tropicais e subtropicais, a atividade se concentra em áreas rasas sobre estoques de organismos da superfamília Penaeoidea (Garcia & Le Reste, 1986).

No Brasil, os camarões-rosa *Farfantepenaeus paulensis* (Pérez Farfante, 1967) e *F. brasiliensis* (Latreille, 1817), o camarão-branco *Litopenaeus schmitti* (Burkenroad, 1936) e o camarão-sete-barbas *Xiphopenaeus kroyeri* (Heller, 1862) constituíam as principais pescarias de camarão nas regiões Sul e Sudeste. No entanto, a tendência decrescente da produção das espécies de camarão-rosa a partir da década de 1990, forçou a adoção de pescarias multiespecíficas. Isto, estimulou a captura do camarão-barba-ruça *Artemesia longinaris* Spence Bate, 1888 e do camarão-santana *Pleoticus muelleri* (Spence Bate, 1888), sendo ambas, as espécies consideradas como fauna acompanhante das pescarias tradicionais citadas anteriormente (Dias Neto, 2011).

Independentemente da espécie alvo, as pescarias de camarões marinhos são comumente realizadas por arrasto de fundo (Vendeville, 1990), o qual se configura, atualmente, como um dos principais métodos de pesca comercial em nível mundial (Burridge et al., 2006). Se por um lado este método é eficaz na captura de espécies alvo, por outro apresenta uma ampla e discutida problemática ambiental (Diamond et al., 2004; Hall & Mainprize, 2005), associada à diversos impactos negativos sobre as populações e ecossistemas explotados (Almeida et al., 2017). Dentre seus impactos negativos, destacam-se a captura incidental de organismos não alvo da pesca (bycatch) e a

modificação física do fundo oceânico, ocasionadas, respectivamente, pela baixa seletividade das redes (Davies et al., 2009) e pela ação mecânica do petrecho contra o sedimento (Pusceddu et al., 2014).

Cerca de 70% do fundo do mar é composto por substratos não consolidados (Snelgroove, 1999), que podem ser altamente heterogêneos devido a variações físicas naturais e à alteração biológica (e.g. conchas, tubos de animais, buracos e tocas), sendo estas variações imprescindíveis aos processos de assentamento de muitos organismos (Thrush et al., 2002; Gray et al., 2006). No entanto, a pesca de arrasto tende a homogeneizar o sedimento, reduzindo a estrutura tridimensional acima e abaixo da interface sedimento água (Gray et al., 2006), e além disso ocasiona a ressuspensão de grandes quantidades de material e alterações nas características físicas e químicas do substrato (Oberle et al., 2016).

Os arrastos também acarretam em mortalidade de organismos marinhos por outras formas: muitas espécies bentônicas são esmagadas diretamente pela rede, enquanto outras são capturadas e morrem quando levadas para o convés ou devolvidas ao mar (Jennings et al., 2001). Sobre este grupo de espécies capturados involuntariamente, denominado como bycatch, sabe-se que as pescarias de camarão são as principais geradoras de biomassa (Hall, 2005) em nível mundial (Kelleher, 2005).

Dentre os organismos que compõem o bycatch ou a fauna acompanhante de pescarias de camarão-sete-barbas *X. kroyeri*, um importante recurso pesqueiro no Brasil explorado em toda costa brasileira (Costa et al., 2007; IBAMA, 2011), os crustáceos após os peixes, constituem o segundo maior recurso capturado em termos de biomassa e diversidade de espécies (Severino-Rodrigues et al., 2002). Ainda no caso das pescarias de *X. kroyeri*, há uma grande captura e por conseguinte mortalidade de juvenis de crustáceos (Rodrigues-Filho et al., 2016), decorrente da atividade ocorrer próximo à costa

e em baixas profundidades, áreas que geralmente são habitats de recrutamento de várias espécies (Caley et al., 1996).

As espécies de camarões que constituem a fauna acompanhante possuem, em geral, baixo ou nenhum valor comercial (Branco et al., 2015). No entanto, por serem continuamente removidas em elevadas biomassas pela pesca, acabam sendo impactadas de forma similar àquelas que são alvo da atividade. Exemplos destes táxons são os peneideos *Rimapenaeus constrictus* (Stimpson, 1871) e *Sicyonia dorsalis* Kingsley, 1878, o camarão *Nematopalaemon schmitti* (Holthuis, 1950) pertencente à superfamília Palaemonoidea Rafinesque, 1815 e *Exhippolysmata oplophoroides* (Holthuis, 1948) pertencente à superfamília Alpheoidea Rafinesque, 1815 (Costa et al., 2016; Mantelatto et al., 2016).

Além dos mencionados impactos diretos sobre as populações capturadas, a pesca de arrasto acarreta em impactos indiretos, como por exemplo alterações na estrutura das comunidades bentônicas, bem como em interações tróficas entre espécies (NRC, 2002). Os efeitos deletérios sobre as interações entre os indivíduos em áreas de pesca resultam em efeitos que se prolongam por toda teia trófica, diminuindo tanto a diversidade estrutural como a funcional dos ecossistemas, e, presumivelmente, também sua resiliência (Coleman & Williams, 2002).

Possivelmente associado aos impactos diretos e indiretos da pesca de arrasto, a Lista Nacional das Espécies de Invertebrados Aquáticos e Peixes de 2004 apontou como espécies ameaçadas de sobre-explotação cinco camarões peneídeos: *F. brasiliensis*, *F. paulensis*, *F. subtilis* (Pérez-Farfante, 1967), *L. schmitti* e *X. kroyeri* (Dias Neto, 2011). Entretanto, na avaliação do estado de conservação dos crustáceos brasileiros de 2010 a 2014, chegou-se à conclusão que dados biológicos ainda são insuficientes para um prognóstico fidedigno dos Penaeoidea (Boos et al., 2016) e de *E. oplophoroides*

(Christoffersen, 2016).

Em uma tentativa de compensar a mortalidade dos indivíduos pela sobrepesca, e para prevenir a explotação de camarões pequenos com pouco valor comercial, uma medida de ordenação amplamente adotada na pesca nas regiões tropicais e subtropicais é o período do Defeso (Gulland, 1989; Ye, 1998). Nas pescarias brasileiras de camarão, a normativa de instrução IBAMA nº 189/2008 proibia a pesca no período de recrutamento de juvenis de camarão-rosa de 1º de março a 31 de maio na área marinha entre as paralelas 21º18'04,00 "S (fronteira dos estados do Espírito Santo e Rio de Janeiro) e 33º40'33,00 "S (Foz do Arroio Chuí, RS). No entanto, havia uma extensa discussão sobre a assertividade deste defeso, visto que que o período não contemplava todas as espécies de camarões (Simões et al., 2017), sobretudo àquelas que não são alvo das pescarias. A partir de 2023, a portaria SAP/MAPA nº 656 alterou a vigência do defeso para 28 de janeiro a 30 de abril, contemplando a mesma extensão geográfica da normativa anterior, buscando adequar o fechamento da pesca com o período de recrutamento dos camarões-rosa.

Ações que levam em consideração apenas a biologia de um grupo especifico são possivelmente equivocadas e não asseguram a manutenção do sistema, visto que há evidências robustas que considerar um maior grupo de espécies (e.g Ecosystem-Based Fisheries Management) é uma opção mais efetiva de manejo (FAO, 1995). No entanto, manejos multiespecíficos demandam uma elevada quantidade de informações, sendo uma situação rara quando se trata de espécies descartadas como bycatch (Dell et al., 2009), sobretudo em países sem legislação pesqueira restritiva para a pesca de arrasto como o Brasil (Guanais et al., 2015).

Neste sentido, há uma elevada demanda por estudos que busquem avaliar ao máximo as espécies capturadas na pesca de arrasto, compreendendo suas relações com variáveis ambientais, ecológicas e pesqueiras (Soykan et al., 2008; Lewison et al., 2011).

Tais estudos servem como base para compreender e eventualmente manejar o impacto da atividade camaroeira sobre o sistema (Sboutzuski et al., 2001). Alguns estudos de curto prazo foram realizados na área para as espécies citadas previamente, a saber: *X. kroyeri* (Costa et al., 2007; Carvalho et al., 2015; Castilho et al., 2015), *A. longinaris* (Costa et al., 2005a; Castilho et al., 2007), *L. schmitti* (Capparelli et al., 2011; Bochini et al., 2014; Carvalho et al., 2015), *P. muelleri* (Costa et al., 2004; Lopes et al., 2014), *F. paulensis* e *F. brasiliensis* (Costa & Fransozo, 1999; Costa et al., 2016), *R. constrictus* (Costa & Fransozo, 2004a,b), *S. dorsalis* (Costa et al., 2005b; Castilho et al., 2008b), *N. schmitti* (Almeida et al., 2011, 2012), e *E. oplophoroides* (Fransozo et al., 2005).

Heckler (2014) avaliou a variação temporal da abundância e distribuição de *X. kroyeri* na Enseada de Ubatuba e a sua relação com a temperatura e salinidade num período de 13 anos. Entretanto, recentemente descobriu-se que *X. kroyeri* tratava-se de um complexo de espécies, e uma outra espécie foi registrada ocorrendo na área de estudo, *Xiphopenaeus dincao* (Carvalho-Batista, Terossi, Zara, Mantelatto, Costa, 2020).

Ademais, ainda não se estudou as variações a longo prazo da abundância das demais espécies de camarões a fim de explicar temporalmente o que causa estas variações e qual o papel dos fatores ambientais e climáticos nos ecossistemas marinhos brasileiros a longo prazo, bem como a influência da pesca no ecossistema como um todo.

Considerando que a dinâmica dos fatores ambientais varia no tempo e no espaço, e que a variação de fatores ambientais importantes como a temperatura, salinidade, tipo e estrutura do sedimento podem afetar a abundância e ocorrência de camarões (Dall, 1990; Castilho et al., 2008), o estudo a longo prazo de populações é imprescindível para a obtenção de informações e para o manejo dos estoques. Estas mudanças na ocorrência e abundância de espécies, bem como a alteração nos fatores abióticos do ambiente podem acarretar em variações temporais na composição específica de comunidades (Magurran

& Henderson, 2010).

Outros fatores ambientais, como os eventos atmosféricos-oceânicos de larga escala (e.g Oscilação Sul El Niño) são conhecidos por afetar a pluviosidade no Sul e Sudeste do país, controlando a entrada de *F. paulensis* na lagoa dos Patos (RS) (Pereira & D'Incao, 2012), e estimulando o recrutamento na Enseada de Ubatuba durante períodos de El Niño (Perroca et al., 2022). Ainda, a dinâmica de massas d'água marinhas, como a Água Central do Atlântico Sul (ACAS), é notadamente conhecida por alterar a dinâmica populacional de *X. kroyeri* quando ressurge, ou em áreas próximas a ressurgência (Davanso et al., 2017).

Desta maneira, presume-se que as variáveis e os fatores ambientais, bem como eventos climáticos atuem sobre as populações de camarões, gerando padrões específicos de variação. Por exemplo, no caso de *Artemesia longinaris* e *Pleoticus muelleri*, que são espécies que apresentam distribuição subtropical e temperada em relação às outras aqui mencionadas, reputa-se a respeito de que maneira os eventos de ENOS influenciariam a variação da abundância e biomassa de tais espécies. Espera-se que a entrada da ACAS (massa d'água caracterizada por baixas temperaturas) influencie temporalmente estas espécies, aumentando a captura das mesmas na primavera e verão. Quanto a *X. kroyeri* e *R. constrictus*, espera-se que a escassez de chuvas gere uma maior salinidade na área e, consequentemente, uma maior produção destas espécies.

Relativizando pela assembleia de camarões, indaga-se o efeito deletério da pesca ao longo dos anos de monitoramento. A pesca contínua de arrasto nas localidades de estudo pode ter acarretado em homogeneização do sistema, o que consequentemente torna o sistema menos diverso entre seus habitats constituintes. De forma a complementar as hipóteses acima, foram formuladas as seguintes questões: (i) Há um padrão na influência das variáveis ambientais sobre a abundância das populações acompanhantes ao longo do

tempo? (ii) Existem tendências temporais que indiquem depleções das populações não alvo da pesca? (iii) A pesca tradicional alterou a diversidade no ecossistema explotado ao longo dos anos?

O resultado desta investigação foi organizado em dois capítulos. O primeiro capítulo "The influence of environmental and ocean-climatic drivers in the abundance of shrimps in a shallow subtropical marine area" buscou avaliar a influência temporal dos fatores ambientais e oceano-climáticos na distribuição espaço-temporal dos camarões na Enseada de Ubatuba. O segundo capítulo foi intitulado "Long-term trends in shrimp abundance and diversity in a tropical bay" avaliou a associação entre as espécies que compõem a Assembleia de camarões na Enseada de Ubatuba, e se a abundância das espécies capturadas diminuiu ou aumentou ao longo dos anos. No segundo capítulo também foi avaliada a variação temporal da diversidade de camarões para a área de estudo.

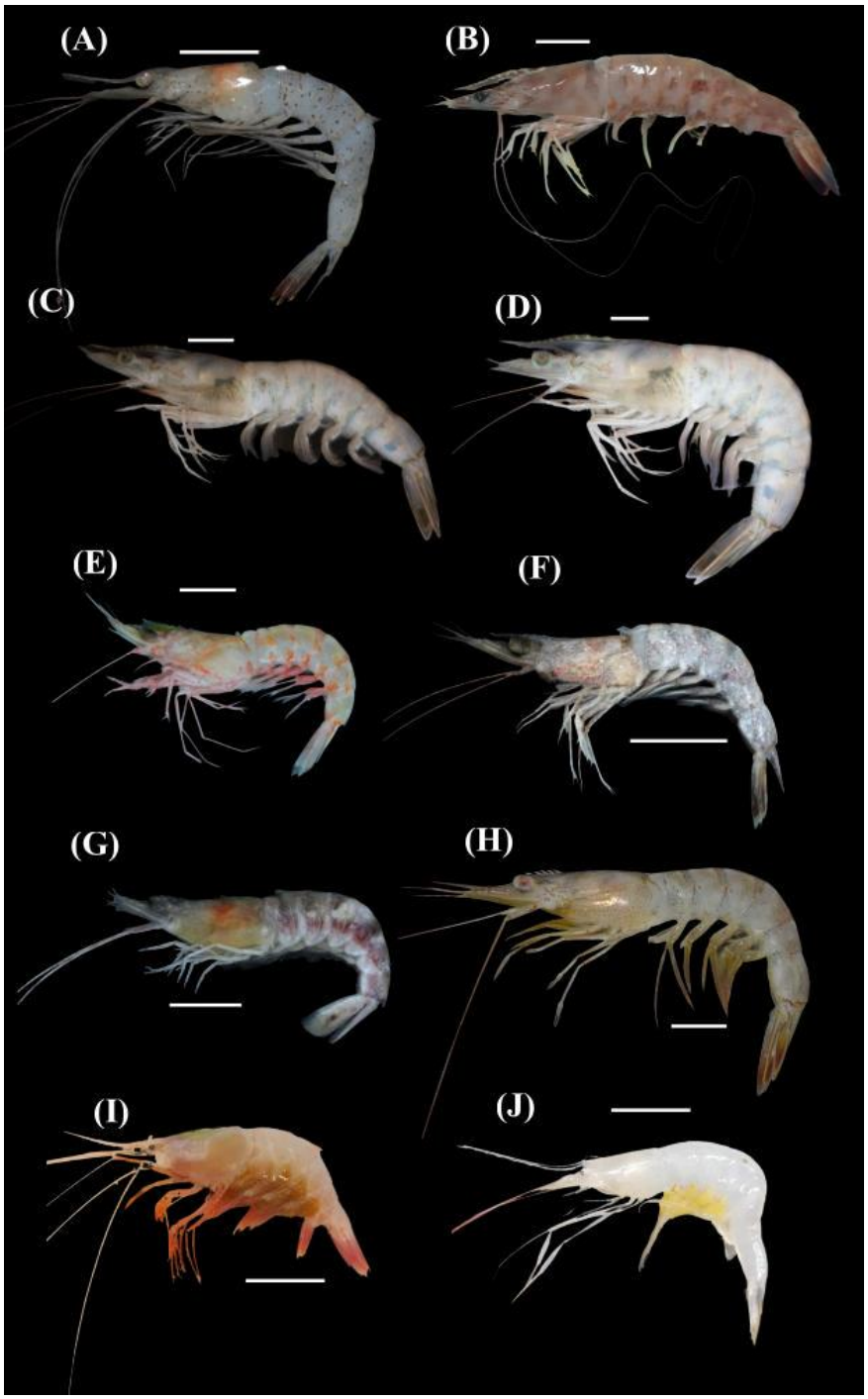

Figura 1 – (A) *Artemesia longinaris* Spence Bate, 1888; (B) *Farfantepenaeus brasiliensis* (Latreille, 1817); (C) *Farfantepenaeus paulensis* (Pérez Farfante, 1967); (D) *Litopenaeus schmitti* (Burkenroad, 1936); (E) *Pleoticus muelleri* (Spence Bate, 1888); (F) *Rimapenaeus constrictus* (Stimpson, 1871); (G) *Sicyonia dorsalis* Kingsley, 1878; (H) *Xiphopenaeus* spp. – Penaeoidea; (I) *Exhippolysmata oplophoroides* (Holthuis, 1948); (J) *Nematopalaemon schmitti* (Holthuis, 1950) – Caridea. Photographs by J. Perroca (A-D, I-J) and M.S. Jaconis (H). Photographs by R.C. Buranelli (E-G) – in Mantelatto et al. 2022 (doi.org/10.11646/zootaxa.5121.1.1).

Referências

Almeida, A.C.; Fransozo, V.; Teixeira, G.M.; Furlan, M.; Hiroki, K.A.N & Fransozo, A. 2011. Population structure and reproductive period of whitebelly prawn *Nematopalaemon schmitti* (Holthuis 1950) (Decapoda: Caridea: Palaemonidae) on the southeastern coast of Brazil. Invertebrate Reproduction & Development, 55(1): 30-39.

Almeida, A.C.; Fransozo, A.; Teixeira, G.M.; Furlan, M.; Hiroki, K.A.N & Bertini, G. 2012. Ecological distribtution of the shrimp *Nematopalaemon schmitti* (Crustacea: Decapoda: Caridea) in the three bays on the south-eastern coast of Brazil. African Journal of Marine Science, 34(1): 93-102.

Almeida, M.; Frutos, I.; Company, J.B.; Martin, D.; Romano, C & Cunha, M.R. 2017. Biodiversity of suprabenthic peracarid assemblages from the Blanes Canyon region (NW Mediterranean Sea) in relation to natural disturbance and trawling pressure. Deep-Sea Research II, 137: 390-403.

Bauer, R.T. 1992. Testing generalizations about latitudinal variation in reproduction and recruitment patterns with sicyoniid and caridean shrimp species. Environmental Control and Climate Change, 22(1-3): 193-202. doi.org/10.1080/07924259.1992.9672272

Bochini, G.L.; Fransozo, A.; Castilho, A.L.; Hirose, G.L & Costa, R.C. 2014. Temporal and spatial distribution of the commercial shrimp *Litopenaeus schmitti* (Dendrobranchiata: Penaeidae) in the south-eastern Brazilian coast. Journal of the Marine Biological Association of the United Kingdom, 1-8.

Boos, H.; Costa, R.C.; Santos, R.A.F.; Dias-Neto, J.; Severino-Rodrigues, E.; Rodrigues, L.F.; D'Incao, F.; Ivo,

Branco, J. O.; Freitas Júnior, F.; Christoffersen, M.L. 2015. Bycatch fauna of seabob shrimp trawl fisheries from Santa Catarina State, southern Brazil. Biota Neotropica. 15(2): 1-14.

Burridge, C.Y.; Pitcher, C.R.; Hill, B.J.; Wassenberg, T.J & Poiner, I.R. 2006. A comparison of demersal communities in an area closed to trawling with those in adjacent areas open to trawling: A study in the Great Barrier Reef Marina Park, Australia. Fisheries Research, 79: 64-74.

Caley, J., Carr, M.H., Hixon, M.A., Hughes, T.P., Jones, G.P & Menge, B.A. 1996. Recruitment and the local dynamics of open marine populations. Annual Review of Ecology, Evolution, and Systematics, 27:477-500.

Capparelli, M.V.; Kasten, P.; Castilho, A.L & Costa, R.C. 2011. Ecological distribution of the shrimp *Litopenaeus schmitti* (Burkenroad, 1936) (Decapoda, Penaeoidea) in Ubatuba Bay, São Paulo, Brazil. Invertebrate Reproduction & Development, 1-7.

Castilho, A.L.; Costa, R.C.; Fransozo, A & Boschi, E.E. 2007. Reproductive pattern of the South American endemic shrimp *Artemesia longinaris* (Decapoda: Penaeoidea), off São Paulo State, Brazil. Tropical Biology, 55(1): 39-48.

Castilho, A.L.; Furlan, M.; Costa, R.C & Fransozo, V. 2008a. Abundance and temporal-spatial distribution of the rock shrimp *Sicyonia dorsalis* Kinsgley, 1878 (Decapoda, Penaeoidea) from the northern coast of São Paulo state, Brazil. Seckenbergiana Maritima, 38(1): 75-83.

Castilho, A.L.; Pie, M.R.; Fransozo, A.; Pinheiro, A.P & Costa, R.C. 2008b. The relationship between environmental variation and species abundance in shrimp community (Crustacea: Decapoda: Penaeoidea) in south-eastern Brazil. Journal of the Marine Biological Association of the United Kingdom, 88(1): 119-123.

Castilho, A.L.; Bauer, R.T.; Freire, F.A.M.; Fransozo, V.; Costa, R.C.; Grabowski, R.C & Fransozo, A. 2015. Lifespan and reproductive dynamics of the commercially important sea bob shrimp *Xiphopenaeus kroyeri* (Penaeoidea): synthesis of a 5-year study. Journal of Crustacean Biology, 35(1): 30-40.

Christoffersen, M. 2016. Avaliação de *Exhippolysmata oplophoroides* (Holthuis, 1948) (Decapoda: Lysmatidae). Cap. 16: p. 203-211. In: Pinheiro, M. & Boos, H. (Org.). Livro Vermelho dos Crustáceos do Brasil: Avaliação 2010-2014. Porto Alegre, RS, Sociedade Brasileira de Carcinologia - SBC, 466 p.

Coleman, F.C & Williams, S.L. 2002. Overexploiting marine ecosystem engineers: potential consequences for biodiversity. Trends in Ecology & Evolution, 17(1): 40-44.

Costa, R.C & Fransozo, A. 1999. A nursey ground for two tropical pink-shrimp Penaeus species: Ubatuba bay, northern coast of São Paulo, Brazil. Nauplius, (7): 73-81.

Costa, R.C & Fransozo, A., 2004a. Abundance and ecologic distribution of the shrimp *Rimapenaeus constrictus* (Crustacea: Penaeidae) in the northern coast of São Paulo State, Brazil. Journal of Natural History, 38:901-912.

Costa, R.C & Fransozo, A. 2004b. Reproductive biology of the shrimp *Rimapenaeus constrictus* (Decapoda, Penaeidae) in the Ubatuba region of Brazil. Journal of Crustacean Biology, 24(2): 274-281.

Costa, R.C., Fransozo, A & Pinheiro, A.P. 2004. Ecological distribution of the shrimp *Pleoticus muelleri* (Bate, 1888) (Decapoda: Penaeoidea) of Southeastern Brazil. Hydrobiologia, 529: 195-203.

Costa, R.C.; Fransozo, A.; Castilho, A.L & Freire, F.A.M. 2005a. Annual, seasonal and spatial variation of abundance of the shrimp *Artemesia longinaris* (Decapoda: Penaeoidea) in south-eastern Brazil. Journal of the Marine Biological Association of the United Kingdom, 85: 107-112.

Costa, R.C.; Fransozo, A & Negreiros-Fransozo, M.L. 2005b. Ecology of the rock shrimp *Sicyonia dorsalis* Kinglsey 1878 (Crustacea: Sicyioniidae) in a subtropical region of Brazil. Gulf and Carribbean Research, 17: 1-8.

Costa, R.C.; Fransozo, A.; Freire, F.A.M & Castilho, A.L. 2007. Abundance and ecological distribution of the "Sete- barbas" shrimp *Xiphopenaeus kroyeri* (Heller, 1862) (Decapoda: Penaeoidea) in three bays of the Ubatuba region, southeastern Brazil. Gulf and Carribean Research, 19: 33-41.

Costa, R.C.; Lopes, M.; Castilho, A.L.; Fransozo, A. & Simões, S.M. 2008. Abundance and distribution of juvenile pink shrimps *Farfantepenaeus* spp. In a mangrove estuary and adjacent bay on the northern shore of São Paulo State, southern Brazil. Invertebrate Reproduction and Development, (52): 51-58.

Costa, R.C.; Bochini, G.L.; Simões, S.M.; Lopes, M.; Sancinetti, G.; Castilho, A.L. & Fransozo, A. 2016. Distribution pattern of juveniles of the pink shrimps *Farfantepenaeus brasiliensis* (Latreille, 1817) and *F. paulensis* (Pérez-Farfante, 1967) on the southern Brazilian coast. Nauplius, 24: 1-10.

Boos, H.; Costa, R.C.; Santos, R.A.; Neto, J.D.; Rodrigues, E.S.; Rodrigues, L.F.; D'Incao, F.; Ivo, C.T.C & Coelho, P.A. 2016. Avaliação dos Camarões Peneídeos (Decapoda: Penaeidae). Cap. 23: p. 300-317. In: Pinheiro, M. & Boos, H. (Org.). Livro Vermelho dos Crustáceos do Brasil: Avaliação 2010-2014. Porto Alegre, RS, Sociedade Brasileira de Carcinologia - SBC, 466 p.

Dall, W.; Hill, B.J.; Rothlisberg, N.W & Staples, D.J. 1990. The biology of Penaeidae. Advances in Marine Biology, 27: 1–484.

Dell, Q.; Brewer, D.T.; Griffiths, S.P.; Heales, D.S & Tonks M.L. 2009. Bycatch in a tropical schooling—Penaeid fisheries and comparisons with a related, specialized trawl regime. Fisheries Management and Ecology, 16 (3): 191–201.

Davanso, T.M.; Hirose, G.L.; Herrera, D.R.; Fransozo, A & Costa, R.C. 2017. Does the upwelling phenomenon influence the population dynamics and management of

the seabob shrimp *Xiphopenaeus kroyeri* (Heller, 1862) (Crustacea, Penaeidae)? Hydrobiologia, 795: 295-311.

Davies, R.W.D.; Cripps, S.J.; Nickson, A & Porter, G. 2009. Defining and estimating global marine fisheries bycatch. Marine Policy, 33: 661-672.

Diamond, S.L. 2004. "Bycatch Quotas in the Gulf of Mexico Shrimp Trawl Fishery: Can they Work?". Reviews in Fish Biology and Fisheries, 14: 207–237.

Dias Neto, J .2011. Proposta de Plano nacional de Gestão para uso sustentável de Camarões marinhos do Brasil. Brasília: IBAMA.

FAO. 1995. FAO Code of Conduct for Responsible Fisheries. FAO, Rome, Italy.

FAO. 2018. The State of World Fisheries and Aquaculture 2018 - Meeting the sustainable development goals. Rome. Licence: CC BY-NC-SA 3.0 IGO.

Fransozo, V.; Costa, R.C.; Bertini, G & Cobo, V.J. 2005. Population biology of spiny shrimp *Exhippolysmata oplophoroides* (Holthuis) (Caridea, Hyppolitidae) in a subtropical region, São Paulo, Brazil. Revista Brasileira de Zoologia, 22(4): 1078-1084.

Garcia, S. & Le Reste, L. 1986. Ciclo vitales, dinámica explotación y ordenación de las poblaciones de camarones peneidos costeros. FAO, (203):180 p.

Gillett, R. 2008. Global study of shrimp fisheries. FAO Fisheries Technical Papers, 475

Graça-Lopes, R.; Santos, E.P.; Severino-Rodrigues, E.; Braga, F.S.M & Puzzi, A. 2007. Contributions to the knowledge of the sea-bob shrimp (*Xiphopenaeus kroyeri* Heller, 1862) biology and fishery in the Sao Paulo State littoral, Brazil. Boletim do Instituto de Pesca, 33(1): 63-84.

Guanais, J.H.G.; Medeiros, R.P & McConney, P.A. 2015. Designing a framework for addressing bycatch problems in Brazilian small-scale trawl fisheries. Marine Policy, 51: 111-118.

Gulland, J.A. 1989. The optimum opening date in shrimp fishing: a sensitivity analysis. Kuwait Bulletin of Marine Science, 10: 71–79.

Gray, J.S.; Dayton, P.; Thrush, S & Kaiser, M.J. 2006. On effects of trawling, benthos and sampling design. Marine Pollution Bulletin, 52: 840-843.

Hall, S.J & Mainprize B.M. 2005. "Managing By-catch and Discards: How much Progress are we Making and How can we do Better?". Fish and Fisheries, 6: 134–155.

Heckler, G.S.; Costa, R.C.; Fransozo, A.; Rosso, S & Shimizu, R.M. 2014. Long-term patterns of spatial and temporal distribution in the seabob shrimp *Xiphopenaeus kroyeri* (Decapoda: Penaeidae) population in southeastern Brazil. Journal of Crustacean

Biology, 34(3): 326-333.

IBAMA. 2011. Boletim estatístico da aquicultura e pesca no Brasil. Ministério do Meio Ambiente, Brasília. IBAMA (Brazilian Institute of Environment and Renewable Natural Resources) – http://www.ibama.gov.br/biodiversidade-aquatica/periodos-dedefeso/defesos (last accessed 12 September 2018).

Jennings, S.; Dinmore, T.A.; Duplisea, D.E.; Warr, K.J & Lancaster, J.E. 2001. Trawling disturbance can modify benthic production processes. Journal of Animal Ecology, 70: 459-47

Kelleher, K. 2005. Discards in the world's marine fisheries. An update. FAO Fisheries Technical Paper Nº 470, Food and Agriculture Organization of the United Nations, Rome, Italy, 22p. http://www.fao.org/3/a-y5936e.pdf

Lewison, R.L.; Soykan, C.U.; Cox, T.; Peckham, H.; Pilcher, N.; LeBoeuf, N.; McDonald, S.; Moore, J.; Safina, C & Crowder, L.B. 2011. Ingredients for addressing the challenges of fisheries bycatch. Bulletin of Marine Science, 87(2):235–250.

Lopes, M.; Fransozo, A.; Castilho, A.L & Costa, R.C. 2014. Diel variation in abundance and size of the south American red shrimp *Pleoticus muelleri* (Spence Bate, 1888) (Decapoda, Solenoceridae) in the Ubatuba region, Southeastern Brazil. Brazilian Journal of Oceanography, 62(3): 225-234.

Magurran, A & Henderson, P. 2010. Temporal turnover and the maintenance of diversity in ecological assemblages. Philosophical Transactions of the Royal Society B-Biological Sciences, 365: 3611-3620.

Mantelatto, F.L.; Bernardo, C.H.; Silva, T.E.; Bernardes, V.P.; Cobo, V.J & Fransozo, A. 2016. Composição e distribuição de crustáceos decápodes associados à pesca do camarão-sete-barbas *Xiphopenaeus kroyeri* (Heller, 1862) no litoral norte do Estado de São Paulo. Boletim do Instituto de Pesca, São Paulo, 42(2): 307-326.

Martin J.W & Davis G.E. 2001. An Updated Classification of the Recent Crustacea Natural History Museum of Los Angeles County, Los Angeles, California.

NRC – National Research Council. 2002. Effects of Trawling and Dredging on Sea-floor Habitat. The National Academies Press, Washington DC, 136 pages.

Oberle, F.K.J.; Swarzenski, P.W.; Reddy, C.M.; Nelson, R.K.; Baasch, B & Hanebuth, T.J.J. 2016. Deciphering the lithological consequences of bottom trawling to sedimentary habitats on the shelf. Journal of Marine Systems, 159: 120-131.

Pereira, N & D'Incao, F. 2012. Relationship between rainfall, pink shrimp harvest (*Farfantepenaeus paulensis*) and adult stock, associated with El Niño and La Niña

phenomena in Patos Lagoon, southern Brazil. Journal of the Marine Biological Association of the United Kingdom, 92(7): 1451–1456.

Perroca, J.F.; Rodrigues-Filho, J.L.; Fransozo, A & Costa, R.C. 2022. Variations in pink-shrimps *Farfantepenaeus brasiliensis* and *F. paulensis* juvenile abundance: clarifying ecological patterns and providing subsidies to management in shallow marine ecosystems. Fisheries Research 256: 106482. doi.org/10.1016/j.fishres.2022.106482

Programa de Monitoramento da Atividade Pesqueira Marinha e Estuarina do Instituto de Pesca (PMAP). www.propesq.pesca.sp.gov.br (acessado por último em 12 janeiro de 2019).

Pusceddu, A.; Bianchelli, S.; Martin, J.; Puig, P.; Palanques, A.; Masqué, R & Danovaro, R. 2014. Chronic and intensive bottom trawling impairs deep-sea biodiversity and ecosystem function. Proceedings of the National Academy of Sciences U.S.A, 111: 8861-8866.

Rodrigues-Filho, J.L.; Couto, E.C.G.; Barbieri, E. & Branco, J.O. 2016. Ciclos sazonais da carcinofauna capturada na pesca do camarão-sete-barbas, *Xiphopenaeus kroyeri* no litoral de Santa Catarina. Boletim dos Instituto de Pesca, São Paulo, 42(3): 648-661.

Severino-Rodrigues, E.; Guerra, D.S.F. & Graça-Lopes, R. 2002. Carcinofauna acompanhante da pesca dirigida ao camarão-sete-barbas (*Xiphopenaeus kroyeri*) desembarcada na praia do Perequê, Estado de São Paulo, Brasil. Boletim do Instituto de Pesca, São Paulo, 28(1): 33-48.

Simões, S.M.; Heckler, G.S & Costa, R.C. 2017. Reproductive period and recruitment of Penaeoidea shrimp on the southeastern Brazilian coast: implications for the closed season. Crustaceana, 90:1177-1192.

Soykan, C.U.; Moore, J.E.; Zydelis, R.; Crowder, L.B.; Safina, C & Lewison, R.L. 2008. Why study bycatch? An introduction to the Theme Section on fisheries bycatch. Endangered Species Research, 5:91–102

Snelgroove, P.V.R. 1999. Getting to the bottom of marine biodiversity: sedimentary habitats – ocean bottoms are the most widespread habitat on Earth and support high biodiversity and key ecosystem services. Bioscience, 49: 129- 138.

Stobutzki, I. C., M. J. Miller, J. P. Jones, and J. P. Salini. 2001. Bycatch diversity and variation in penaeid fisheries; the implications for monitoring. Fisheries Research, 53:283–301

Thrush, S.F & Dayton, P.K. 2002. Disturbance to Marine Benthic Habitats by

Trawling and Dredging: Implications for Marine Diversity. Annual Review of Ecology, Evolution, and Systematics, 33: 449-473.

Vendeville, P. 1990. Tropical shrimp fisheries: types of fishing gear used and their selectivity. FAO Fisheries Technical Paper 261 (Revision), Food and Agriculture. Organization of the United Nations, Rome, Italy, 75 p.

Ye, Y. 1998. Assessing effects of closed seasons in tropical and subtropical penaeid shrimp fisheries using a length-based yield-per-recruit model. ICES Journal of Marine Science, 55: 1112–1124.

Capítulo 1

The influence of environmental and ocean-climatic drivers in the abundance of shrimps in a shallow subtropical marine area

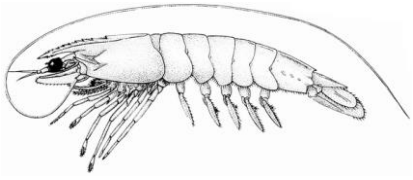

The influence of environmental and ocean-climatic drivers in the abundance of shrimps in a shallow subtropical marine area

Abstract

Different life cycles lead to differences in species niche and in their ecological requirements. In this study we registered the spatial and temporal variance in abundance in eight shrimp species by analyzing a dataset that spanned a 27-year period. We also assessed the influence of ocean-climatic and environmental factors in their abundance. Periods of neutrality favored the increase in abundance of *Artemesia longinaris, Pleoticus muelleri*, *Rimapenaeus constrictus*, *Sicyonia dorsalis* and *Nematopalaemon schmitti*. The shrimps *P. muelleri* and *S. dorsalis* also showed higher abundances in periods of La Niña. In La Niña and neutral periods, there is a shift in the atmospheric pressure gradient favoring Northeast winds, that enhances the SACW intrusion and weakens the Coastal Water. Thus, species that responds negatively to elevated temperatures, as *P. muelleri* and *S. dorsalis*, in El Niño will migrate to deeper areas, which were not sampled in this study. As for El Niño events, it favored the abundance of *Litopenaeus schmitti* and *R. constrictus*. El Niño is known to increase water surface temperature in southeast Brazil, so the increase in temperature is benefic to these species whose abundances increase in elevated temperatures. All species were associated with sediments of silt and clay. Long-term monitoring of the communities of species of commercial interest or accidentally captured, are essential for establishing standards and measures to protect ecosystems.

Keywords: Bycatch, Caridea, Decapoda, ENSO, Penaeoidea, SACW

Introduction

Shallow coastal environments, especially in the tropics, are used as nursing and foraging grounds by several marine species (Caley et al., 1996). Among these species, shrimps constitute one of the most diverse and abundant taxa (Martin & Davis, 2001). Shrimps can roughly be classified into two groups: the superfamily Penaeoidea (suborder Dendrobranchiata) and infraorder Caridea (suborder Pleocyemata).

Unlike carideans who incubate embryos to advanced zoeal larvae in their pleon, penaeoid shrimps spawn eggs that are fertilized and released into the plankton, where they hatch as nauplius and the embryonic development takes place (Bauer, 1992). Regardless, both groups are important fishery resources and are extensively explored by fleets in different grounds (Ingólfsson et al., 2022; Turschwell et al., 2022). Carideans of commercial interest are usually fished by industrial fleets in deeper waters (e.g 200 to 600 m deep), where larger species and therefore more profitable are found, such as *Pandalus borealis* Krøyer, 1838 (Larsen et al., 2018) and *Crangon crangon* (Linnaeus, 1758) (Temming et al., 2022).

Penaeoids are fished offshore by industrial fleets (e.g., *Aristeus antennatus* (Risso 1816)), and in coastal waters by artisanal ones (e.g., *Xiphopenaeus kroyeri* (Heller, 1862)) (Graça Lopes et al., 2007; Gorelli et al., 2016). Species belonging to *Litopenaeus* spp. and *Farfantepenaeus* spp. for example might be targeted by both fleets due to their life cycle. These organisms present life cycle type II, as proposed by Dall (1990), in which reproduction and spawning occurs offshore, and the nauplius develops into the stage of mysis and is carried through tidal waves and currents to estuaries and coastal lagoons, where they'll grow into juveniles, and then recruit into the adult population (Garcia & Le Reste, 1981). Other coastal penaeoids such as *Artemesia longinaris* Spence Bate, 1888

present life cycle type III (Dall, 1990), in which the whole life cycle takes place independently from brackish waters.

Different life cycles lead to differences in species niche and in their ecological requirements. Ocean-climatic (e.g., El Niño Southern Oscilation) and environmental factors (e.g., temperature, salinity, grain size and composition, organic matter content) influence the abundance of such organisms and their ability of occupying the environment (Villareal & Hernandez-Llamas, 2005; Pereira & D'Incao, 2012). These environmental variables might oscillate overtime, and consequently influence organisms' abundance and population dynamics. Therefore, long term studies are important to monitor species abundance, especially in fishing grounds.

To assess the influence of environmental factors on the shrimp assemblage of a tropical bay, we evaluated a dataset from fishery-independent trawls conducted in the Ubatuba Bay for nine years spanning a 27-year period. Located in the Northern coast of São Paulo State, Ubatuba Bay, is a traditional seabob shrimp *Xiphopenaeus kroyeri* (Heller, 1862) fishing area, with over a hundred trawling boats targeting this resource (IP/APTA/SAA/SP, 2021). With a total area of 8 Km^2, the bay is 4.5 km wide at its entrance, with its width decreasing towards the beach (Mantelatto & Fransozo, 1999). Three water masses influence this region: Coastal Water (Temperature > 20°C and Salinity < 36); Tropical Water (Temperature > 20°C and Salinity > 36); and South Atlantic Central Water (Temperature < 18°C and Salinity > 36) (Castro-Filho et al., 1987). The influence of these water masses coupled with the presence of several embayments formed by the Serra do Mar Mountain range (Suguio & Martin, 1978), and also the transition from the tropical zone to the temperate zone, make of Ubatuba a biodiversity hotspot for several marine organisms.

Nine shrimp species are frequently captured as seabob shrimp bycatch at the bay.

The Penaeoidea *A. longinaris*, *Farfantepenaeus brasiliensis* (Latreille, 1817), *F. paulensis* (Pérez Farfante, 1967), *Litopenaeus schmitti* (Burkenroad, 1936), *Pleoticus muelleri* (Spence Bate, 1888), *Rimapenaeus constrictus* (Stimpson, 1871), and *Sicyonia dorsalis* Kingsley, 1878. Also, the carideans *Exhippolysmata oplophoroides* (Holthuis, 1948) and *Nematopalaemon schmitti* (Holthuis, 1950). The influence of environmental factors (e.g., bottom water temperature and salinity, sediment size, organic matter content, rainfall, ENSO events) in the abundance of *F. brasiliensis* and *F. paulensis* in the area was already investigated by Perroca et al. (2022), thus the study did not include data concerning these species.

The study investigated the long-term trends between shrimp species abundance and ecological patterns in Ubatuba Bay by answering the following questions: (i) how species abundance varies through months and sampling sites at the bay? (ii) how environmental variables influences shrimp abundance?

Material and Methods

Data collection

Sampling was conducted monthly during nine years between September 1995 to June 2022 (Table 1) in four sites at the bay (Figure 1). Shrimps were captured through the years with the same shrimp fishing vessel, equipped with double rig nets, with 20 mm mesh in the wings and 18 mm mesh at the cord end, and towed at an average speed of 1.7 knots. Four hauls (half an hour per site – 18,000 m^2 per trawl) were carried out during daylight in the study area (Figure 1). The sites were chosen considering their position at the bay, depth and wave exposition. Site 1 is deeper and more exposed while Site 3 is the shallowest. As for Site 2, it is most influenced by wave action, whereas Site 4 is the most sheltered, with less wave action (Perroca et al., 2022). An echo sounder coupled to a GPS (Global Positioning System) was used to measure the depth of each sampling site and guarantee the location of the trawling (Table 2).

The material was sorted on the boat and stored in plastic bags with crushed ice, labeled and taken to the Laboratory of Biology of Marine and Freshwater Shrimps (LABCAM), where the individuals were identified according to Pérez-Farfante and Kensley (1997) and Costa et al. (2003), and counted (n). With the description of a new seabob shrimp (i.e.; *Xiphopenaeus dincao* Carvalho-Batista, Terossi, Zara, Mantelatto, Costa, 2020) for the area, and the impossibility of identification of past sampled years all data regarding *X. kroyeri* will be considered in this work as *Xiphopenaeus* spp.

Table 1 – Sampling years between 1995 and 2022 in Ubatuba Bay, southeastern coast of Brazil

1st year	September 1995 to August 1996
2nd year	January to December 1998
3rd year	January to December 1999
4th year	July 2001 to June 2002
5th year	July 2002 to June 2003
6th year	July 2006 to June 2007
7th year	July 2013 to June 2014
8th year	October 2016 to September 2017
9th year	July 2021 to June 2022

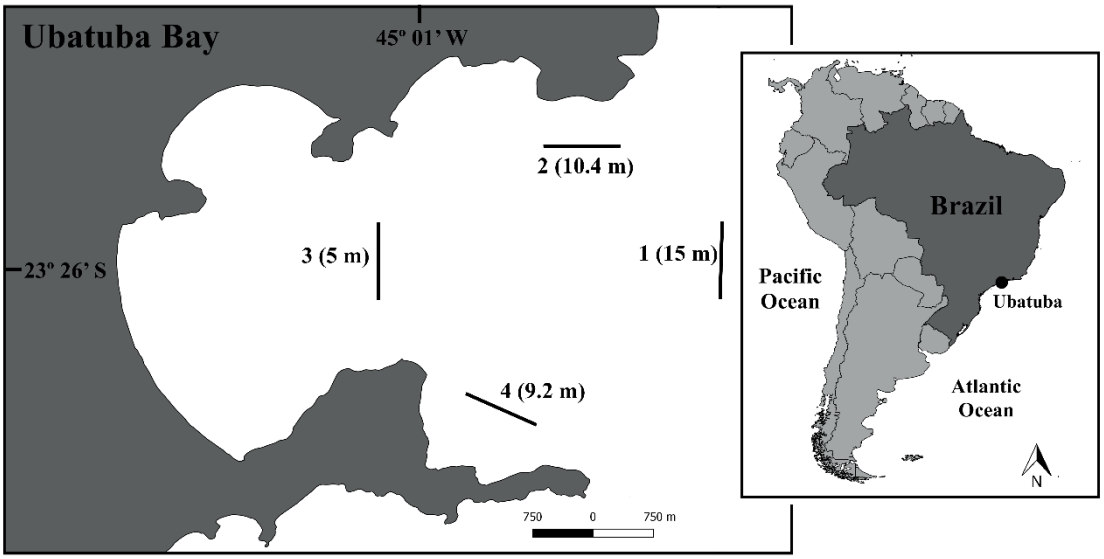

Figure 1 – The sampling sites (1, 2, 3 and 4) in Ubatuba Bay, São Paulo State, Brazil

Table 2 – Depth (m) and location (GPS) of each collection site.

Site	Depth (m)	Location (GPS)
1	15 m	23° 26' S / 44° 59' W
2	10.4 m	23° 25' S / 45° 00' W
3	5 m	23° 26' S / 45° 02' W
4	9.2 m	23° 26' S / 45° 03' W

Additionally, in each haul, a Van Dorn bottle was used to sample bottom water used to measure temperature (mercury thermometer, ºC) and salinity (specific optical refractometer). A Van Veen grab was used to collect sediment samples used to measure granulometry and organic matter content.

In the laboratory, the sediment was dried at 70°C for 72 h. For particle size composition analysis, two 50-g subsamples were treated with 250 mL of a 0.2 N NaOH solution, agitated for 5 min to release silt and clay particles, and then rinsed on a 0.063-mm sieve. Sediments were sieved through 2 mm (gravel), 2.0–1.01 mm (very coarse sand), 1.0–0.51 mm (coarse sand), 0.50–0.26 mm (medium sand), 0.25–0.126 mm (fine sand), and 0.125–0.063 mm (very fine sand). Smaller particles were classified as silt-clay. The particle size categories followed the American standard (Wentworth, 1999), and fractions were expressed on the Phi (ϕ) scale, i.e., according to the formula: $\phi = - \log_2 d$, where d = grain diameter (mm) (Tucker, 1988). For example, $-1 = \phi < 0$ (very coarse sand), $0 = \phi < 1$ (coarse sand), $1 = \phi < 2$ (intermediate sand), $2 = \phi < 3$ (fine sand), $3 = \phi < 4$ (very fine sand), and $\phi \geq 4$ (silt + clay) (Hakanson & Jansson, 1983). Phi was calculated by cumulative particle size curves plotted on a computer using the f scale, with values corresponding to the 16th, 50th, and 84th percentiles used to determine the mean diameter of the sediment using the formula $Md = (\phi 16 + \phi 50 + \phi 84)/3$ (Tucker, 1988). Organic matter content (%) was determined by weighing ash 3 aliquots of 10 g per transect were placed in porcelain crucibles, heated at 500°C for 3 h, and then reweighed (Mantelatto & Fransozo, 1999).

The samples were carried out by the NEBECC (Study Group on Crustacean Biology, Ecology and Culture) and LABCAM (Laboratory of Biology of Marine and Freshwater Shrimps) study groups of the São Paulo State University, as part of several master's and doctoral research projects.

To assess which explanatory covariate drive abundance of shrimp assemblage in the bay (response variables), we chose eight environmental and climatic variables based on prior knowledge from the scientific literature (Table 3). Rainfall data for Ubatuba was obtained from the Department of Waters and Electric Energy (DAEE, 2018), and from the National Center for Monitoring and Early Warning of Natural Disasters (CEMADEN, 2022). From the rainfall variable we obtained two new variables (i.e.; Rain – 1 and Rain – 2), by realigning the original data with abundance, with time lag of "k" units, in which k represents the number of lagged months (i.e.; one month, two months) (Moraes et al., 2012). El Niño Southern Oscillation (ENSO) data was obtained from the Climate Prediction Center (Climate Prediction Center, 2022). The Oceanic Niño Index (ONI) was chosen as the index to represent ENSO events (Table 3) (Awange et al., 2016). When surface temperature in the Niño 3.4 region (5°N–5°S, 120–170°W) exceeded + / - 0.5 ◦C for at least five consecutive months, events were classified as El Niño and La Niña respectively (Trenberth & Stepaniak, 2001).

Table 3 – Covariates evaluated in statistical models of temporal variance in abundance of the shrimp assemblage in Ubatuba Bay, Brazil.

Covariate	**Justification**	**References**
Rainfall (Rain), Rainfall -1 (Rain1) and Rainfall -2 (Rain2)	Affects salinity and nutrient discharge in aquatic environments	Pereira & D'Incao 2012, Bochini et al., 2014
Bottom water salinity (Sal)	Influence shrimp physiology, reproduction and habitat availability	Brito et al., 2000; Bochini et al., 2014
Bottom water temperature (Temp)	Influence shrimp physiology, reproduction and habitat availability	Vilarreal & Hernandez-Llamas, 2005
Organic matter content (OM)	Food availability	Davanso et al., 2017
Granulometry (Phi)	Many shrimps display burrowing behavior	Somers, 1987
ENSO	Affects rainfall, sea surface temperature and levels, abundance and recruitment	Pereira & D'Incao, 2012; Perroca et al. 2022

Data analysis

Abundance of each species was used to estimate indices of catch-per-unit-of-effort ($CPUE_n$: shimp.h^{-1}) to standardize response variables. Our dataset comprised eight response variables ($CPUE_n$ *A. longinaris*, $CPUE_n$ *L. schmitti*, $CPUE_n$ *P. muelleri*, $CPUE_n$ *R. constrictus*, $CPUE_n$ *S. dorsalis*, $CPUE_n$ *Xiphopenaeus* spp., $CPUE_n$ *E. oplophoroides*, $CPUE_n$ *N. schmitti*) and nine explanatory variables (Rain, Rain -1, Rain -2, Bottom water salinity, Bottom water temperature, Organic matter content, Phi, Months, ENSO).

To assess each species abundance variation in the area, we analyzed the monthly variation in $CPUE_n$ and its relationship with ENSO events at sampling sites (i.e., spatio-temporal models) with Generalized Additive Models (GAM). We selected GAMs because the relationships between the variables were nonlinear (Supplementary material) and models like GAMs show adequacy to analyze such data (Wood, 2017). From data exploration (Zuur et al., 2009), it was noticeable that the residuals from the species models were non-normal and nonhomogeneous, having nonlinear and curvilinear patterns, high number of zeros, over-dispersed species data, temporal dependency, and a possible interaction between ENSO and Month. Based on data exploration results, we fitted to each species, GAMs with factor-smooth interaction between months and ENSO variables, and a linear term to sites (see table 6). We then tested the effect of removing the variables ENSO and Site, to access their importance to model fitting. To determine the best model, we used the Second-Order Information Criterion (AICc), and the models with the lower AICc were selected as best model (Sugiura, 1978). All fitted models presented negative binomial distribution, due to the excess of zeros in the dataset, and used link function identity and ARMA (Autoregressive Moving Average) correlation structure because of the temporal correlation detected in $CPUE_n$ variables.

All analyses were performed in the software R version 4.0.3. The negative

binomial models were fitted using the package mgcv (Wood, 2017). The AICCc values were estimated with function AICc() from MuMin package (Barton, 2009) and the graphical outputs with packages ggplot (Wickham, 2016) and visreg (Breheny & Burchett, 2017).

To investigate relationships between shrimp abundance and environmental variables (i.e., ecological models), we followed the same data exploration routine. Due to an initially high number of covariates (eight), we checked for collinearity to avoid type II errors in modeling using scatter plots and Pearson correlation coefficients (Zuur et al., 2009). Also, we selected the more representative rain variable to each species, to avoid collinearity, considering that rain variables originated from the same variable by lagging rain months. The relationship between rain variables and species may be observed in table 4. In the ecological models, we fitted a global negative binomial GAM with monthly mean values of all explanatory variables and explored the effect of dropping terms on model selection. All models considered additive, interactive, and isolated relationships between the explanatory variables and, to select the best GAM, we calculated the AICc for each one. We used the criterion that models with $\Delta AICc < 2$ have substantial support for being the best model (Burnham & Anderson, 2002). From best model, we extracted the predicted values to plot against explanatory covariates to highlight effects on $CPUE_n$ patterns.

Table 4 – Spearman correlation coefficients of response variables and rain variables.

Response variable	Rainfall proxy	ρ
A. longinaris abundance	Rain	0.017
	Rain -1	-0.010
	Rain -2	-0.141*
L. schmitti abundance	Rain	-0.526*
	Rain -1	-0.404
	Rain -2	-0.178
P. muelleri abundance	Rain	-0.244*
	Rain -1	-0.227
	Rain -2	-0.116
R. constrictus abundance	Rain	-0.193*
	Rain -1	-0.143
	Rain -2	0.011
S. dorsalis abundance	Rain	0.022
	Rain -1	0.159
	Rain -2	0.259*
Xiphopenaeus spp. abundance	Rain	-0.200
	Rain -1	-0.299
	Rain -2	-0.304*
E. oplophoroides abundance	Rain	0.054
	Rain -1	0.041
	Rain -2	0.061*
N. schmitti abundance	Rain	-0.162*
	Rain -1	-0.043
	Rain -2	-0.019

Results

Environmental factors

Higher values of rainfall were registered in austral summer followed by spring. Autumn was the season in which the lower rainfall values were registered (Fig. 2A). Mean values of bottom water salinity varied similar through seasons; however, spring showed the lower amplitudes followed by summer (Fig. 2B). As for bottom water temperature, higher mean values were recorded in summer, followed by spring. Winter showed the lower mean values of temperature (Fig. 2C). Higher mean values of organic matter content occurred in autumn and winter, while the lower mean values occurred in spring (Fig. 2D). Phi varied similarly through seasons, reaching higher amplitudes in May and July (Fig. 2E).

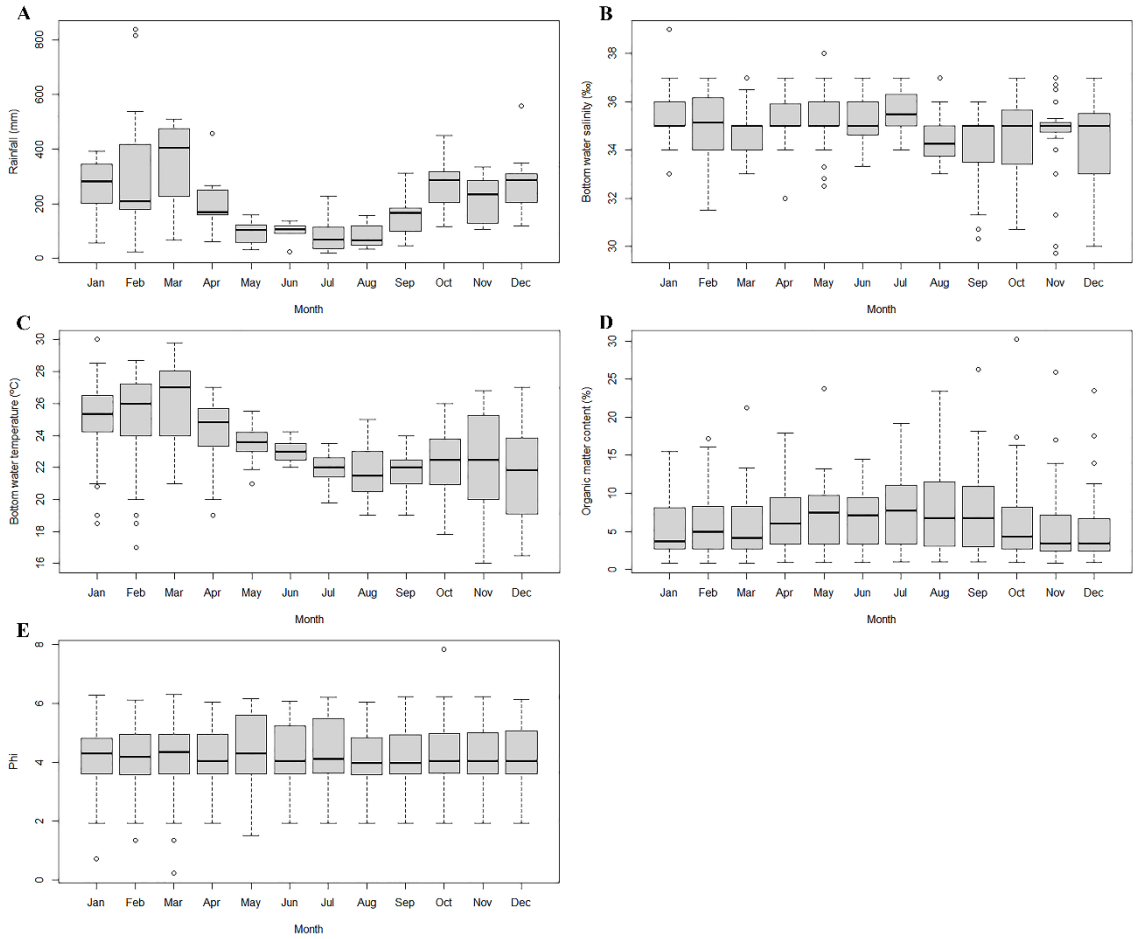

Figure 2 – Mean values, and minimum and maximum amplitudes of [A] Rainfall (mm), [B] Bottom water salinity (‰), [C] Bottom water temperature (◦C), [D] Organic matter content, [E] Phi during the sampling period. (Mean; SD = standard deviation; Min = minimum; Max = maximum; Circles = outliers).

Abundance of sampled species

A total of 566,141 shrimps were caught in the Ubatuba Bay during the sampling period. The abundance of species per year may be observed in table 4. Among penaeoideans, *Xiphopenaeus* spp. was the most abundant (82.19%) with 460,268 individuals captured, followed by *A. longinaris* with 51,163 individuals (9.14%) and *P. muelleri* with 12,048 individuals (2.15 %). The least abundant species were *L. schmitti* (0.56%).

Table 5 – Shrimp abundance per sampling year in Ubatuba Bay, São Paulo, Brazil.

	Number of individuals									
Species	**95/96**	**98**	**99**	**01/02**	**02/03**	**06/07**	**13/14**	**16/17**	**21/22**	**Total**
A. longinaris	414	4,717	340	31,844	8,321	287	2,803	2,379	58	51,163
L. schmitti	59	726	224	184	335	288	341	750	256	3,163
P. muelleri	614	36	928	3,757	578	474	791	4,636	234	12,048
R. constrictus	346	892	757	1,930	751	284	2,044	2,556	412	9,972
S. dorsalis	213	397	306	1,547	196	51	1,116	2,478	218.5	6,523
Xiphopenaeus spp.	52,415	89,770	58,761	80,850	34,949	56,046	20,061	126,839	21,370	460,268
E. oplophoroides	2,279	2,211	4,182	1,835	84	na	549	2,834	728.5	14,703
N. schmitti	na	913	711	na	na	na	171	50	280	2,125

*na – abundance was not registered

Spatio-temporal models: months, ENSO and site

The best model for the spatio-temporal variation in *A. longinaris* contained an interactive term between ENSO and months, and a linear term on sites, and explained 70.9% of abundance variation (Deviance explained) (Table 6). *Artemesia longinaris* was more abundant in the summer and in periods of neutrality (ENSO) (Fig. 3A). Abundance was higher in site 1, the deepest, followed by site 2 (Fig. 3B).

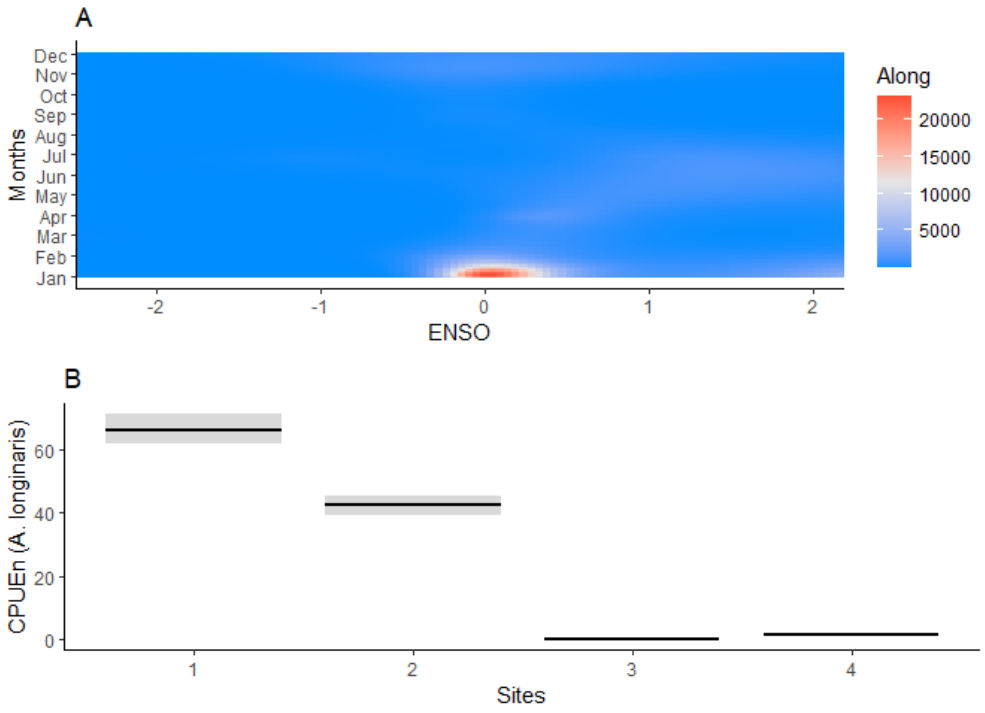

Figure 3 – Predicted effect of months and ENSO interaction (A) and sites (B) on *A. longinaris* $CPUE_n.hour^{-1}$ in the Ubatuba Bay.

The best model for the variation in *L. schmitti* contained an interactive term between ENSO and months, and an additive term on sites, and explained 32.9% of abundance variation (Deviance explained) (Table 6). Captures were higher from April to July, and increased in periods of El Niño (Fig. 4A). Abundance was higher in site 3 (i.e., 5 m deep – shallowest site) followed by site 4 (i.e., 9.2 m deep – most sheltered site) (Fig. 4B).

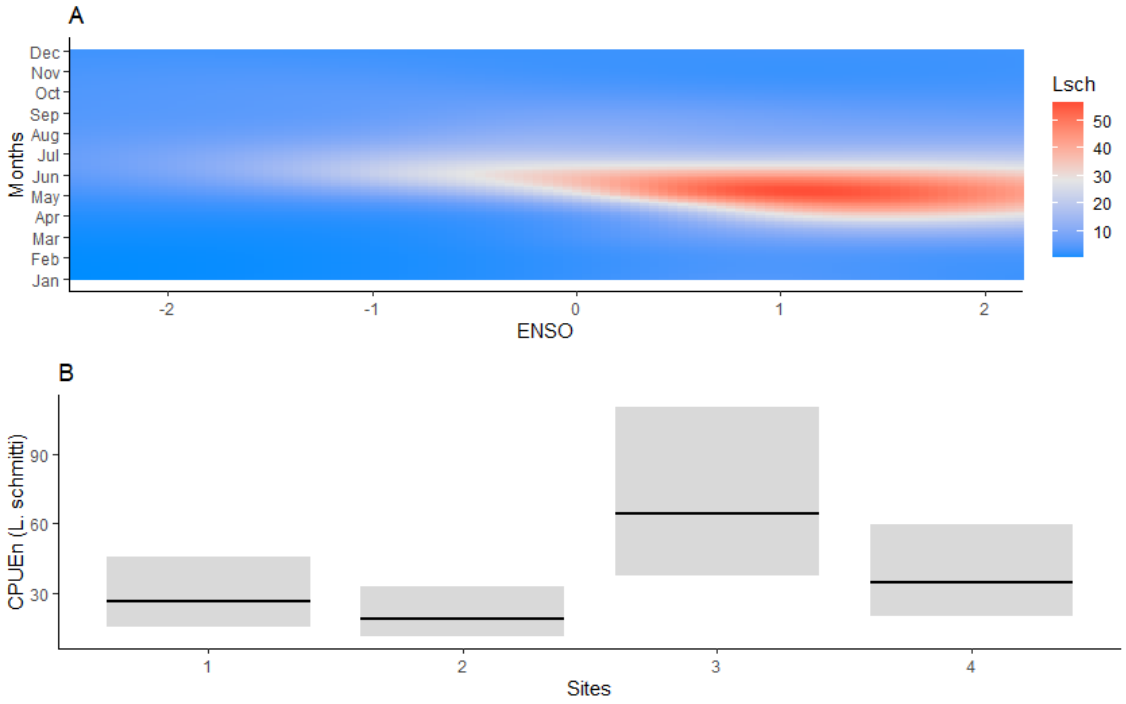

Figure 4 – Predicted effect of months and ENSO interaction (A) and sites (B) on *L. schmitti* $CPUE_n.hour^{-1}$ in the Ubatuba Bay.

The best model for the variation in *P. muelleri* contained an interactive term between ENSO and months, and an additive term on sites, and explained 38% of abundance variation (Deviance explained) (Table 6). Abundance peaks were registered from May to July, and in November (Fig. 5A). In periods of neutrality and weak La Niña abundance was higher (Fig. 5A). Site 1 presented the higher abundance, followed by site 2 (Fig. 6B).

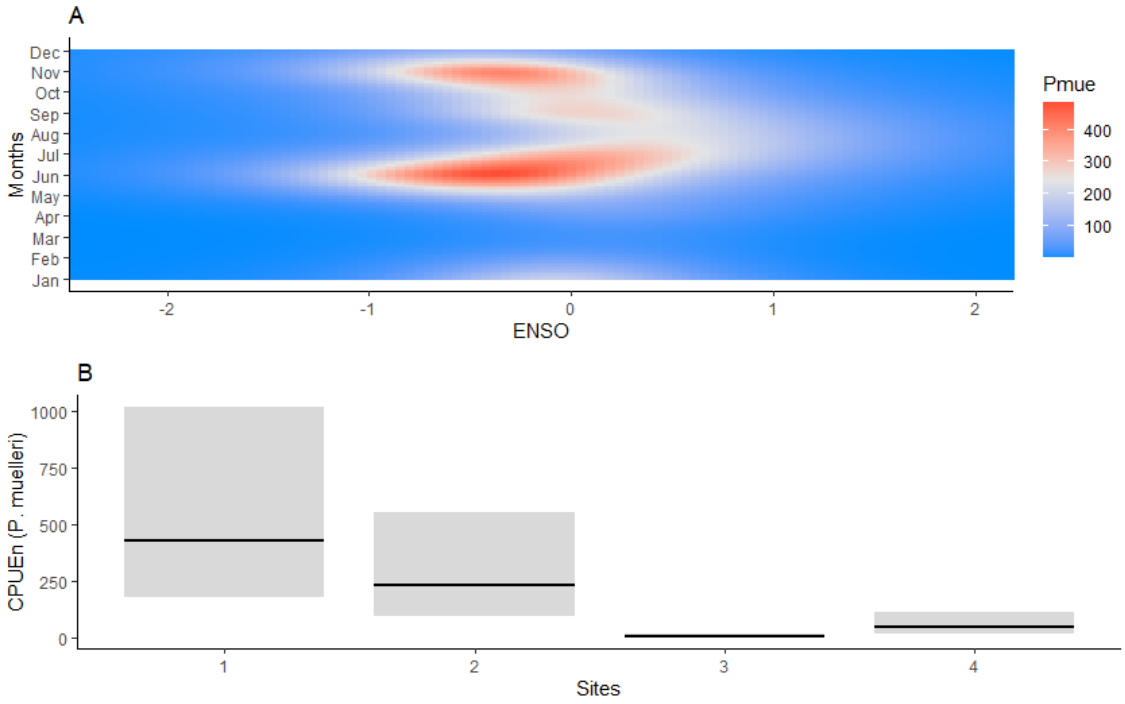

Figure 5 – Predicted effect of months and ENSO interaction (A) and sites (B) on *P. muelleri* $CPUE_n.hour^{-1}$ in the Ubatuba Bay.

The best model fitted for the *R. constrictus* contained the variables months, ENSO and sites, and explained 15.9% of variation in abundance (Deviance explained) (Table 6). Higher abundance was registered from June to August and in periods of neutrality and weak El Niño (Fig. 6A). Site 3 showed the higher abundance, followed by site 4, with a slightly lower abundance (Fig. 6B).

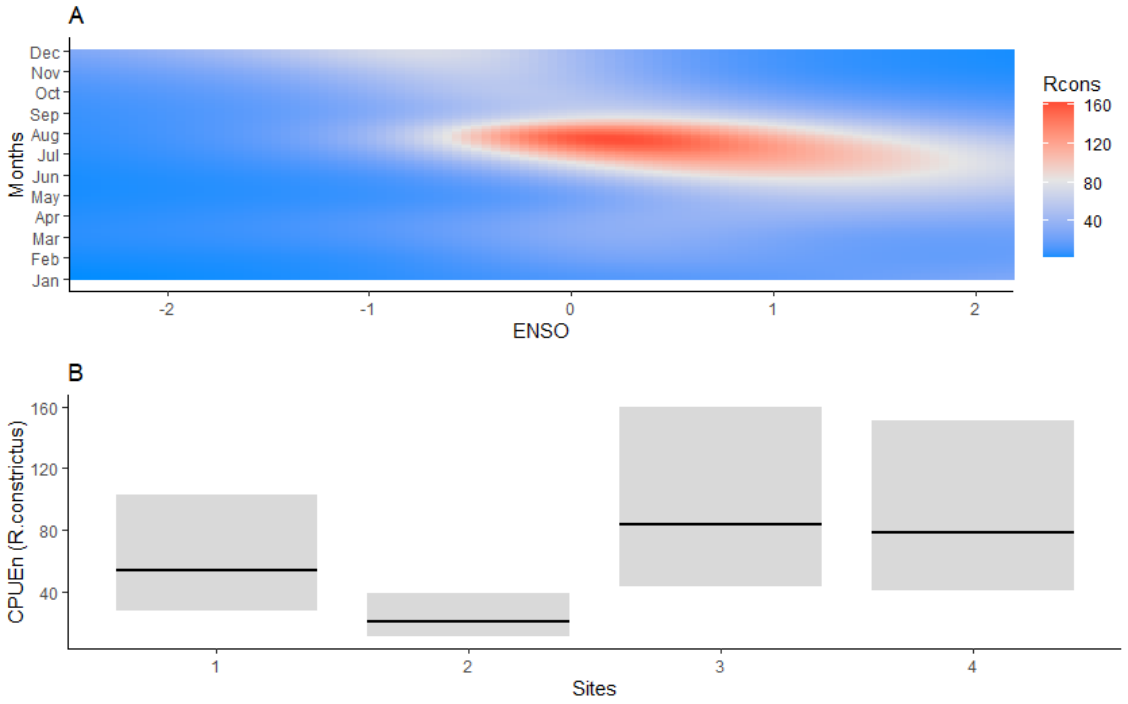

Figure 6 – Predicted effect of months and ENSO interaction (A) and sites (B) on *R. constrictus* $CPUE_n.hour^{-1}$ in the Ubatuba Bay.

The best model fitted for *S. dorsalis* explained 30.8% of variation in abundance (Deviance explained) and contained the interaction between variables months and ENSO, and a linear term to sites (Table 6). The higher abundances were recorded from October to January, with and additional peak in June and July (Fig. 7A). Periods of neutrality and weak La Niña also registered increase in abundance (Fig. 7A). In relation to the spatial distribution, site 3 showed the higher abundance, followed by site 4 (Fig. 7B).

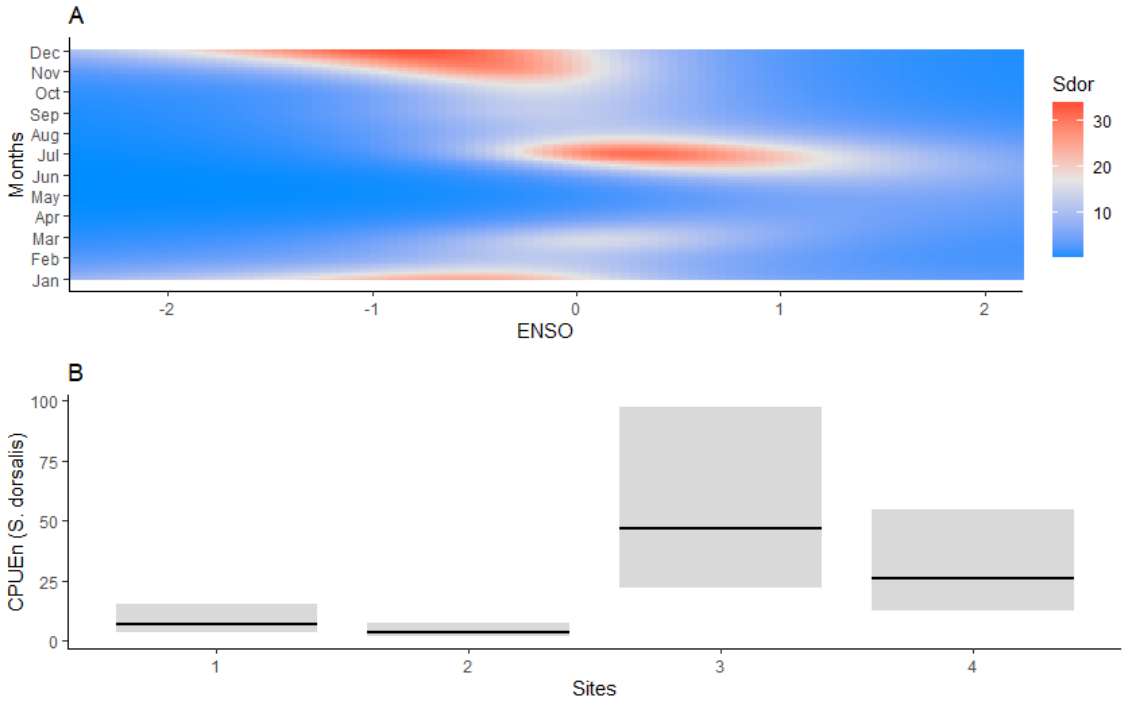

Figure 7 – Predicted effect of months and ENSO interaction (A) and sites (B) on *S. dorsalis* $CPUE_n.hour^{-1}$ in the Ubatuba Bay.

The best model for the spatio-temporal variation in *Xiphopenaeus* spp. contained the variable month, and a linear term on sites, and explained 25.8% of abundance variation (Deviance explained) (Table 6). Abundance was higher from April to July, and decreased in the following months (Fig. 8A). Site 3 showed the higher abundance of *Xiphopenaeus* spp. (Fig. 8B).

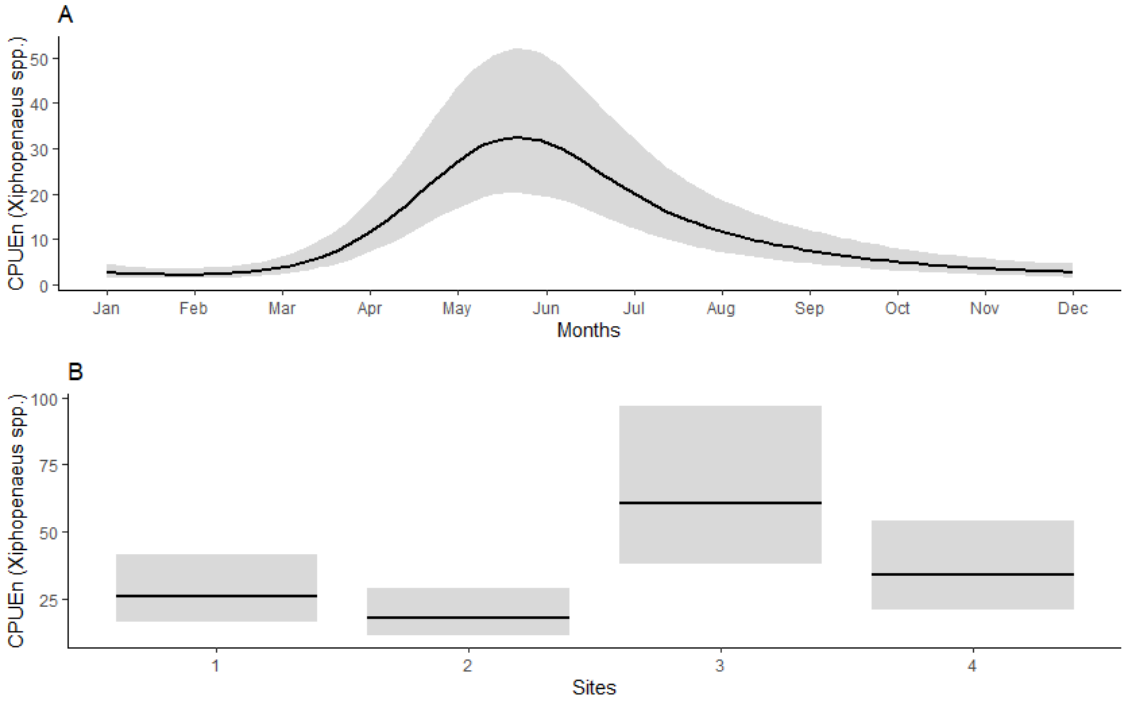

Figure 8 – Predicted effect of months (A) and sites (B) on *Xiphopenaeus* spp. $CPUE_n.hour^{-1}$ in the Ubatuba Bay.

The best model fitted for *E. oplophoroides* contained the variable month, and an linear term on sites, and explained 19.1% of abundance variation (Deviance explained) (Table 6). Higher abundance was registered from August to December (Fig. 9A). The abundance was also significantly higher in site 2 (Fig. 9B).

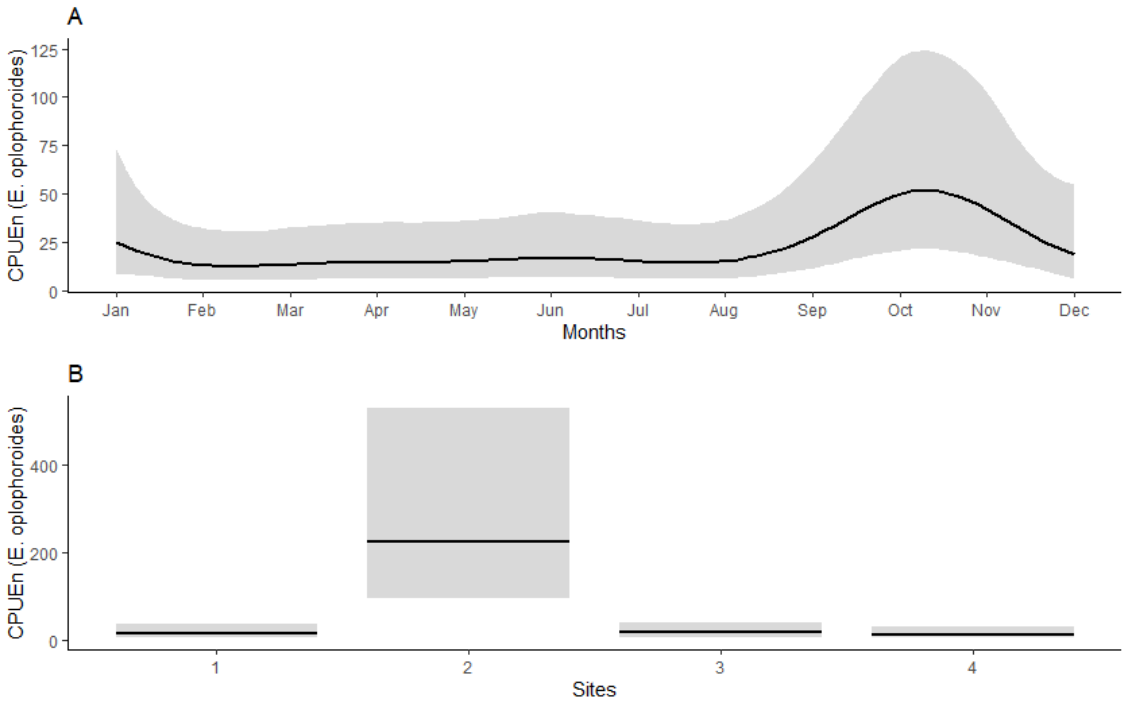

Figure 9 – Predicted effect of months (A) and sites (B) on *E. oplophoroides*. $CPUE_n.hour^{-1}$ in the Ubatuba Bay.

The best model for the spatio-temporal variation in *N. schmitti* contained an interactive term between ENSO and months, and a linear term on sites, and explained 54.4% of abundance variation (Deviance explained) (Table 6). In periods of neutrality and weak La Niña, abundance was higher from June to July. In periods of El Nino however, abundance was higher from May to August, and increased with event intensity (Fig. 10A). Site 2 showed the highest abundance of *N. schmitti* (Fig. 10B).

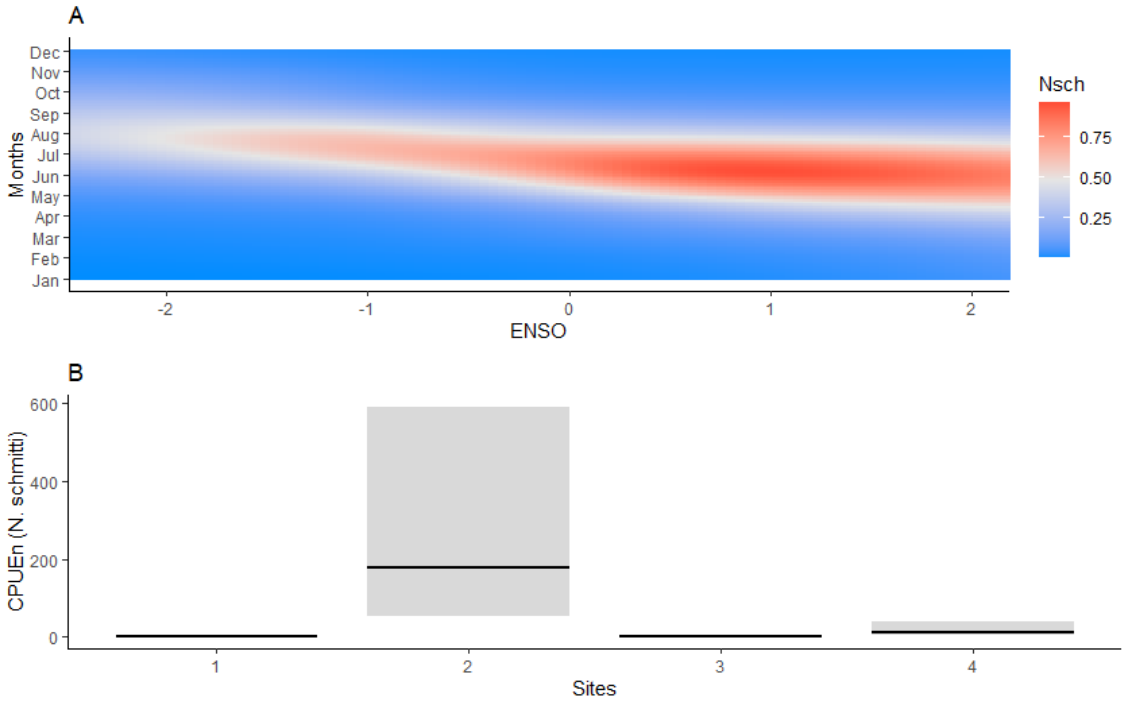

Figure 10 – Predicted effect of months (A) and sites (B) on *N. schmitti* $CPUE_n.hour^{-1}$ in the Ubatuba Bay.

Table 6 – Negative binomial GAMs fitted for response variables. corARMA = Autoregressive Moving Average correlation. s = smooth factor. * Best model.

Response variable	Parameters	Temporal correlation	AICc
$CPUE_n$ *A. longinaris*	s(Month,ENSO)+ Site	corARMA(form = ~ Month, p = 1, q = 1)	175817.3*
	s(Month,ENSO)		307101.6
	s(Month) + Site		317613.0
$CPUE_n$ *L. schmitti*	s(Month,ENSO)+ Site	corARMA(form = ~ Month, p = 1, q = 1)	2591.714*
	s(Month,ENSO)		2615.546
	s(Month) + Site		2613.849
$CPUE_n$ *P. muelleri*	s(Month,ENSO)+ Site	corARMA(form = ~ Month, p = 1, q = 1)	2551.461*
	s(Month,ENSO)		2642.906
	s(Month) + Site		2580.572
$CPUE_n$ *R. constrictus*	s(Month,ENSO)+ Site	corARMA(form = ~ Month, p = 1, q = 1)	3410.407*
	s(Month,ENSO)		3428.435
	s(Month) + Site		3429.790
$CPUE_n$ *S. dorsalis*	s(Month,ENSO)+ Site	corARMA(form = ~ Month, p = 1, q = 1)	2690.408*
	s(Month,ENSO)		2753.061
	s(Month) + Site		2734.982
$CPUE_n$ *Xiphopenaeus* spp.	s(Month,ENSO)+ Site	corARMA(form = ~ Month, p = 1, q = 1)	7147.960
	s(Month,ENSO)		2615.588
	s(Month) + Site		2613.919*
$CPUE_n$ *E. oplophoroides*	s(Month,ENSO)+ Site	corARMA(form = ~ Month, p = 1, q = 1)	2517.800
	s(Month,ENSO)		2571.266
	s(Month) + Site		2517.593*
$CPUE_n$ *N. schmitti*	s(Month,ENSO)+ Site	corARMA(form = ~ Month, p = 1, q = 1)	732.7579*
	s(Month,ENSO)		789.7508
	s(Month) + Site		734.7650

Ecological models: environmental variables

Model selection for variance in *A. longinaris* yielded two models with ΔAICc < 2 that may be considered as best model (Table 7). The first model contained the variables "OM", "Phi", "Sal" and explained 31.6% of the variation in *A. longinaris* (Deviance explained). The second model contained the variables "OM" and "Phi" and explained 30.8% of the variation (Deviance explained). Abundance decreased with the increase in organic matter content (Fig. 11A). There was an increase in abundance in Phi of 4.5 (Fig. 11B), and $CPUE_n.h^{-1}$ increases with higher salinity values (Fig. 11C).

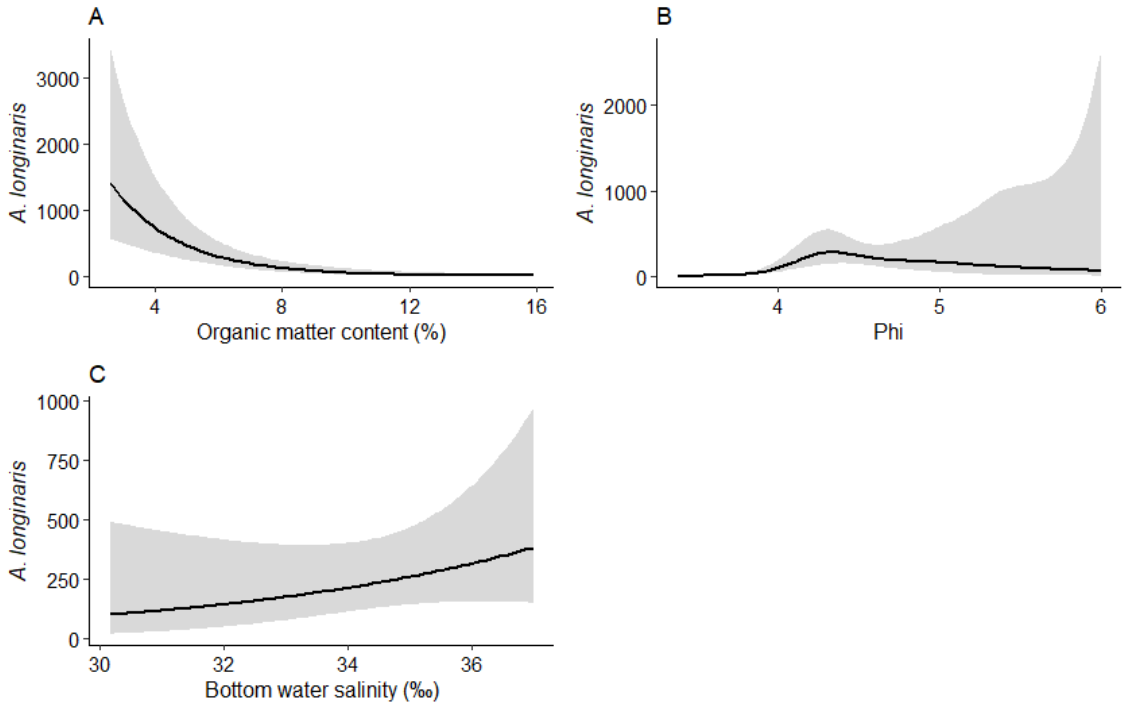

Figure 11 – Variation of abundance ($CPUE_n.hour^{-1}$) of *Artemesia longinaris* and its relationship with the covariates selected in the best model: [A] Bottom water temperature (ºC), [B] Bottom water salinity, [C] Rainfall -2 (mm), [D] Organic matter (%), and [E] Granulometry.

Table 7 – Generalized additive models (GAM) adjusted for *A. longinaris* $CPUE_n.hour^{-1}$. Models with ΔAICc < 2 = best model. df = Degrees of freedom; logLik = Log likelihood of a model.

Rank	Parameters	DF	logLik	AICc	ΔAICc
Gam28	Along ~ s(Rain2) + s(Sal) + s(Temp)	5.96	-532.29	1077.32	42.74
Gam12	Along ~ s(Rain2) + s(Sal)	5.14	-532.77	1076.45	41.87
Gam20	Along ~ s(Rain2) + s(Temp)	4.54	-532.93	1075.44	40.86
Gam24	Along ~ s(Sal) + s(Temp)	5.14	-532.13	1075.16	40.58
Gam4	Along ~ s(Rain2)	3.20	-533.82	1074.31	39.73
Gam8	Along ~ s(Sal)	4.27	-532.65	1074.28	39.71
Gam16	Along ~ s(Temp)	3.00	-533.23	1072.70	38.12
Gam29	Along ~ s(OM) + s(Rain2) + s(Sal) + s(Temp)	6.00	-522.55	1057.94	23.36
Gam30	Along ~ s(Phi) + s(Rain2) + s(Sal) + s(Temp)	11.64	-515.62	1057.61	23.03
Gam22	Along ~ s(Phi) + s(Rain2) + s(Temp)	9.30	-517.70	1055.96	21.38
Gam21	Along~ s(OM) + s(Rain2) + s(Temp)	5.00	-522.64	1055.87	21.29
Gam25	Along ~ s(OM) + s(Sal) + s(Temp)	5.00	-522.62	1055.83	21.25
Gam13	Along ~ s(OM) + s(Rain2) + s(Sal)	5.00	-522.57	1055.72	21.14
Gam26	Along ~ s(Phi) + s(Sal) + s(Temp)	10.97	-515.35	1055.38	20.80
Gam14	Along ~ s(Rain2) + s(Phi) + s(Sal)	9.89	-516.49	1054.98	20.40
Gam18	Along ~ s(Phi) + s(Temp)	8.42	-517.83	1054.10	19.52
Gam17	Along ~ s(OM) + s(Temp)	4.00	-522.72	1053.84	19.26
Gam5	Along ~ s(OM) + s(Rain2)	4.00	-522.68	1053.75	19.17
Gam9	Along ~ s(OM) + s(Sal)	4.00	-522.64	1053.66	19.08
Gam10	Along ~ s(Phi) + s(Sal)	9.16	-516.26	1052.75	18.17
Gam6	Along ~ s(Phi) + s(Rain2)	7.24	-518.32	1052.32	17.74
Gam1	Along ~ s(OM)	3.00	-522.77	1051.76	17.18
Gam2	Along ~ s(Phi)	6.24	-518.53	1050.42	15.84
Gam_global	Along ~ s(Temp) + s(Sal) + s(Rain2) + s(OM) + s(Phi)	11.31	-508.15	1041.82	7.24
Gam23	Along ~ s(OM) + s(Phi) + s(Rain2) + s(Temp)	10.27	-508.69	1040.33	5.75
Gam27	Along ~ s(OM)+ s(Phi) + s(Sal)+ s(Temp)	10.16	-508.30	1039.27	4.69
Gam19	Along ~ s(OM) + s(Phi) + s(Temp)	9.12	-508.91	1037.94	3.36
Gam15	Along ~ s(OM) + s(Phi) + s(Rain2) + s(Sal)	9.47	-508.44	1037.87	3.29
Gam7	Along ~ s(OM) + s(Phi) + s(Rain2)	8.49	-509.06	1036.73	2.15
Gam11	*Along ~ s(OM) + s(Phi) + s(Sal)*	*8.47*	*-508.52*	*1035.60*	*1.02*
Gam3	*Along ~ s(OM) + s(Phi)*	*7.46*	*-509.19*	*1034.58*	*0*

Model selection for variance in *L. schmitti* yielded one model with ΔAICc < 2 that may be considered as best model (Table 8). This model contained the variables "OM", "Phi", "Rain" and "Temp", and explained 61.3% of variance in abundance (Deviance explained). Abundance was non-linearly related to all selected variables, and it slightly increased in values of Phi > 5.5 (Fig. 12A). However, abundance decreased in values of rainfall higher than 200 mm (Fig. 12B). Higher captures were registered between 22.5°C e 25°C (Fig. 12C) and 8 and 12% of organic matter content (Fig. 12D).

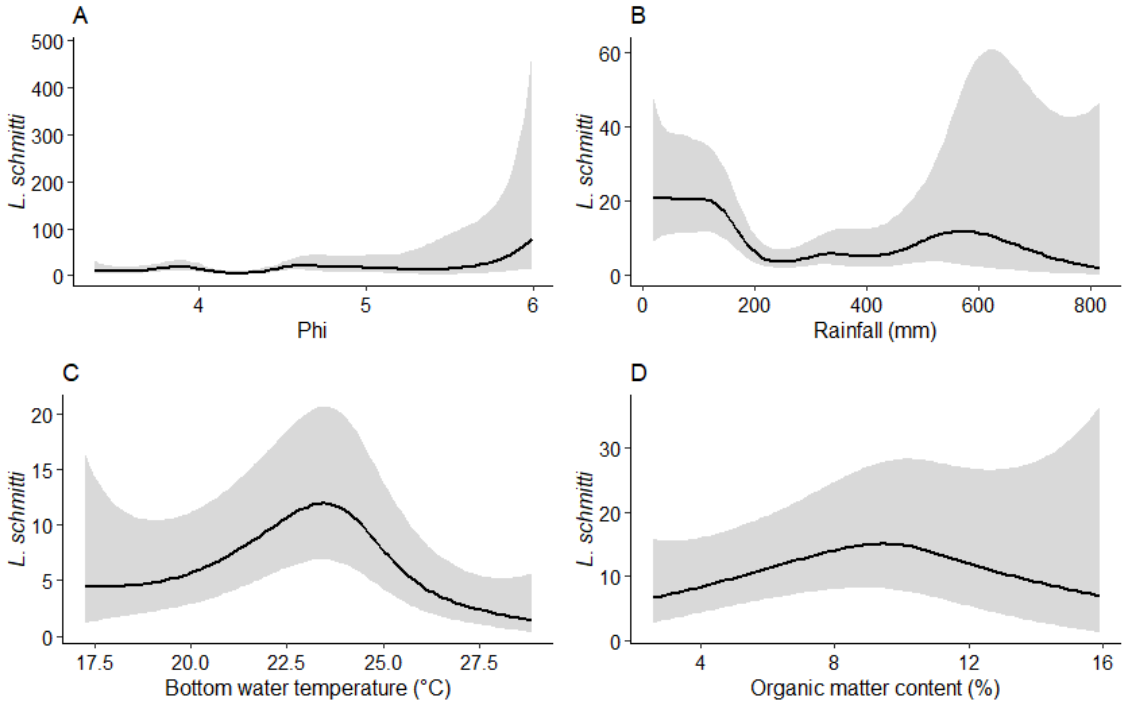

Figure 12 – Variation of abundance ($CPUE_n.hour^{-1}$) of *Litopenaeus schmitti* and its relationship with the covariates selected in the best model: [A] Phi, [B] Rainfall (mm), [C] Bottom water temperature (ºC), and [D] Organic matter content (%).

Table 8 – Generalized additive models (GAM) adjusted for *L. schmitti* $CPUE_n.hour^{-1}$. Models with ΔAICc < 2 = best model. df = Degrees of freedom; logLik = Log likelihood of a model.

Rank	Parameters	DF	logLik	AICc	ΔAICc
Gam8	s(Sal)	3.00	-388.20	782.63	47.19
Gam2	s(Phi)	5.41	-384.88	781.27	45.82
Gam10	s(Phi) + s(Sal)	5.27	-383.40	777.98	42.54
Gam1	s(OM)	6.37	-381.28	776.22	40.78
Gam9	s(OM) + s(Sal)	6.61	-380.07	774.37	38.92
Gam16	s(Temp)	6.53	-379.50	773.06	37.61
Gam3	s(OM) + s(Phi)	9.22	-375.28	770.94	35.49
Gam18	s(Phi) + s(Temp)	9.79	-373.55	768.84	33.39
Gam11	s(OM) + s(Phi) + s(Sal)	7.70	-375.68	768.12	32.67
Gam17	s(OM) + s(Temp)	10.73	-370.89	765.84	30.39
Gam24	s(Sal) + s(Temp)	8.97	-372.30	764.37	28.92
Gam25	s(OM) + s(Sal) + s(Temp)	11.24	-368.82	762.99	27.55
Gam26	s(Phi) + s(Sal) + s(Temp)	10.83	-368.88	762.08	26.64
Gam13	s(OM) + s(Rain) + s(Sal)	13.15	-362.63	755.53	20.09
Gam12	s(Rain) + s(Sal)	10.25	-365.41	753.70	18.25
Gam19	s(OM) + s(Phi) + s(Temp)	17.94	-355.02	753.54	18.09
Gam5	s(OM) + s(Rain)	12.53	-361.97	752.58	17.14
Gam15	s(OM) + s(Phi) + s(Rain) + s(Sal)	14.02	-359.69	751.96	16.52
Gam4	s(Rain)	9.34	-365.29	751.23	15.78
Gam27	s(OM) + s(Phi) + s(Sal)+ s(Temp)	18.91	-352.30	750.96	15.51
Gam14	s(Rain) + s(Phi) + s(Sal)	11.30	-361.94	749.38	13.94
Gam7	s(OM) + s(Phi) + s(Rain)	13.52	-358.86	748.98	13.54
Gam6	s(Phi) + s(Rain)	11.13	-361.10	747.28	11.83
Gam29	s(OM) + s(Rain) + s(Sal) + s(Temp)	17.41	-352.51	746.99	11.55
Gam28	s(Rain) + s(Sal) + s(Temp)	14.20	-355.63	744.31	8.87
Gam21	s(OM) + s(Rain) + s(Temp)	16.96	-351.71	744.10	8.65
Gam20	s(Rain) + s(Temp)	13.37	-355.60	742.04	6.59
Gam30	s(Phi) + s(Rain) + s(Sal) + s(Temp)	15.57	-351.41	739.61	4.16
Gam22	s(Phi) + s(Rain) + s(Temp)	15.44	-350.87	738.17	2.73
Gam_global	s(Temp) + s(Sal) + s(Rain) + s(OM) + s(Phi)	24.80	-336.48	738.15	2.71
Gam23	*s(OM) + s(Phi) + s(Rain) + s(Temp)*	*24.29*	*-336.00*	*735.44*	*0.00*

Model selection for *P. muelleri* resulted in two best models (Table 9). The first model explained 32.1% of variance in abundance (Deviance explained) and contained the variables “Phi”, “Sal”, “Temp” (Table 9). The second model explained 32.9% of variance in abundance (Deviance explained) and contained the variables “OM”, “Phi”, “Sal” and “Temp” (Table 9). While *P. muelleri* abundance decreased with temperature increase (Fig. 13A), it increased non-linearly in higher salinity values (Fig. 13B). Abundance decreased with the increase in OM (Fig. 13C), and increased in Phi >5 (Fig. 13D).

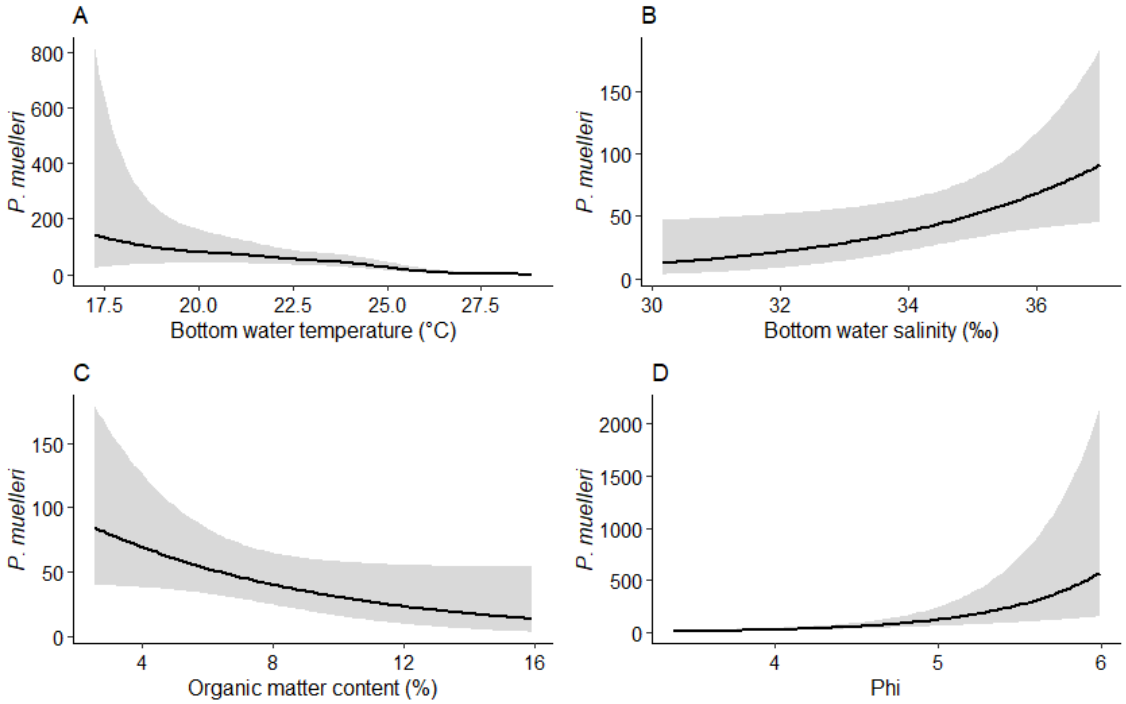

Figure 13 – Variation of abundance ($CPUE_n.hour^{-1}$) of *Pleoticus muelleri* and its relationship with the covariates selected in the best model: [A] Bottom water temperature (ºC), [B] Bottom water salinity, [C] Organic matter content (%), and [D] Phi.

Table 9 – Generalized additive models (GAM) adjusted for *P. muelleri* $CPUE_n.hour^{-1}$. Models with ΔAICc < 2 = best model. df = Degrees of freedom; logLik = Log likelihood of a model.

Rank	Parameters	DF	logLik	AICc	ΔAICc
Gam1	s(OM)	3.00	-462.01	930.26	33.82
Gam8	s(Sal)	3.00	-459.68	925.59	29.15
Gam9	s(OM) + s(Sal)	4.00	-458.29	924.97	28.52
Gam4	s(Rain)	3.00	-457.89	922.00	25.56
Gam12	s(Rain) + s(Sal)	4.00	-455.96	920.30	23.86
Gam5	s(OM) + s(Rain)	4.00	-455.01	918.41	21.97
Gam13	s(OM) + s(Rain) + s(Sal)	5.00	-453.77	918.12	21.68
Gam2	s(Phi)	3.00	-455.70	917.63	21.19
Gam3	s(OM) + s(Phi)	4.00	-453.92	916.24	19.79
Gam6	s(Phi) + s(Rain)	4.00	-452.48	913.35	16.91
Gam11	s(OM) + s(Phi) + s(Sal)	5.00	-450.69	911.97	15.53
Gam10	s(Phi) + s(Sal)	4.01	-451.72	911.84	15.40
Gam14	s(Rain) + s(Phi) + s(Sal)	5.71	-449.71	911.60	15.16
Gam16	s(Temp)	5.52	-449.40	910.56	14.11
Gam7	s(OM) + s(Phi) + s(Rain)	5.00	-449.96	910.52	14.08
Gam20	s(Rain2) + s(Temp)	7.29	-447.32	910.44	14.00
Gam15	s(OM) + s(Phi) + s(Rain) + s(Sal)	6.00	-448.48	909.79	13.35
Gam21	s(OM) + s(Rain) + s(Temp)	8.16	-445.40	908.63	12.19
Gam17	s(OM) + s(Temp)	6.48	-447.23	908.40	11.96
Gam28	s(Rain2) + s(Sal) + s(Temp)	8.99	-444.17	908.15	11.71
Gam24	s(Sal) + s(Temp)	7.44	-445.90	907.93	11.49
Gam29	s(OM) + s(Rain) + s(Sal) + s(Temp)	9.40	-443.49	907.78	11.34
Gam25	s(OM) + s(Sal) + s(Temp)	7.84	-444.93	906.95	10.51
Gam22	s(Phi) + s(Rain) + s(Temp)	7.93	-442.28	901.86	5.42
Gam23	s(OM) + s(Phi) + s(Rain) + s(Temp)	8.96	-440.32	900.38	3.94
Gam30	s(Phi) + s(Rain) + s(Sal)+ s(Temp)	10.11	-438.82	900.18	3.73
Gam18	s(Phi) + s(Temp)	6.78	-442.63	899.87	3.43
Gam_global	s(Temp) + s(Sal) + s(Rain) + s(OM) + s(Phi)	10.02	-438.25	898.82	2.38
Gam19	s(OM) + s(Phi) + s(Temp)	8.09	-440.52	898.71	2.27
Gam26	*s(Phi) + s(Sal) + s(Temp)*	*8.95*	*-439.07*	*897.86*	*1.41*
Gam27	*s(OM)+ s(Phi) + s(Sal) + s(Temp)*	*8.95*	*-438.36*	*896.44*	*0.00*

Model selection for *R. constrictus* yielded in 5 models that may be considered as best model (Table 10). The model that contained the variables "OM", "Phi", "Sal" and "Temp" showed the higher deviance explained, and explained 24.2% of the variance in abundance (Table 10). Abundance decreased with the increase in bottom water temperature (Fig. 14A), and increased in OM around 7% (Fig. 14B). It also increased in values of Phi > 4.5 (Fig. 14C).

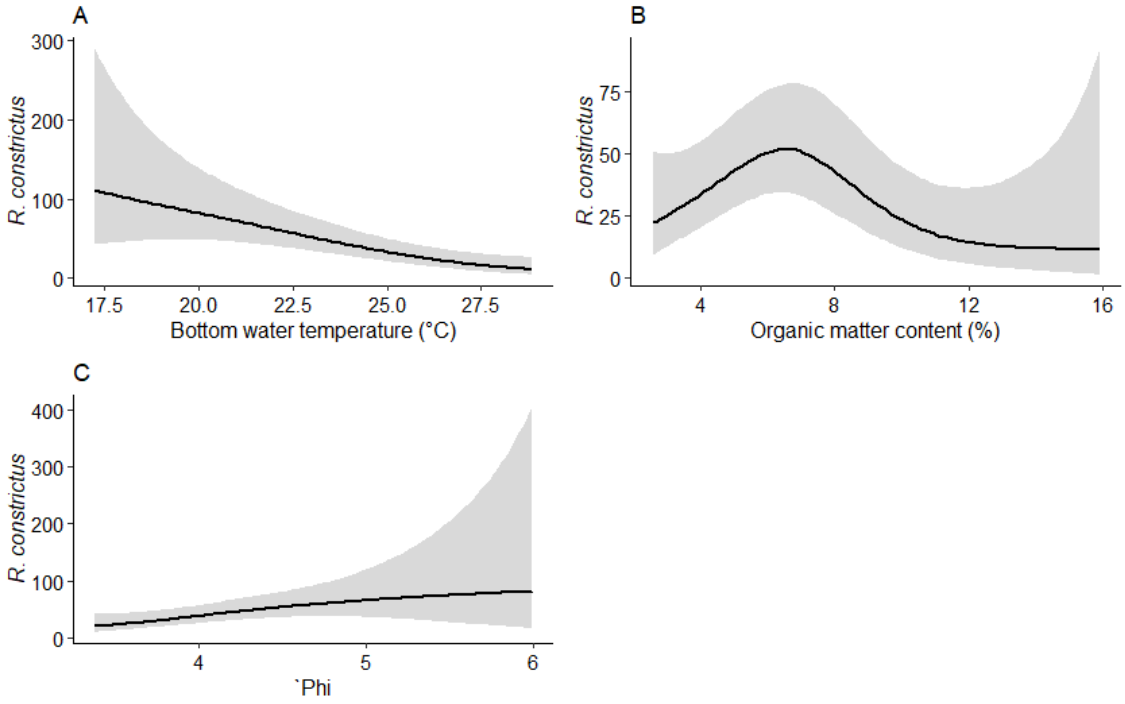

Figure 14 – Variation of abundance ($CPUE_n$.hour^{-1}) of *Rimapenaeus constrictus* and its relationship with the covariates selected in the best model: [A] Bottom water temperature (ºC), [B] Organic matter content (%), and [C] Phi.

Table 10 – Generalized additive models (GAM) adjusted for *R. constrictus* $CPUE_n.hour^{-1}$. Models with ΔAICc < 2 = best model. df = Degrees of freedom; logLik = Log likelihood of a model.

Rank	Parameters	DF	logLik	AICc	ΔAICc
Gam13	s(OM) + s(Rain) + s(Sal)	9.45	-505.88	1032.69	13.05
Gam9	s(OM) + s(Sal)	8.48	-506.78	1032.13	12.49
Gam5	s(OM) + s(Rain)	5.18	-510.53	1032.05	12.41
Gam7	s(OM) + s(Phi) + s(Rain)	7.23	-507.97	1031.59	11.95
Gam12	s(Rain) + s(Sal)	6.94	-508.24	1031.47	11.83
Gam6	s(Phi) + s(Rain)	4.54	-510.89	1031.37	11.73
Gam8	s(Sal)	5.64	-509.49	1031.00	11.36
Gam1	s(OM)	4.71	-510.47	1030.88	11.24
Gam14	s(Rain) + s(Phi) + s(Sal)	9.10	-505.32	1030.70	11.06
Gam4	s(Rain)	3.00	-512.16	1030.55	10.91
Gam15	s(OM) + s(Phi) + s(Rain) + s(Sal)	11.73	-501.80	1030.19	10.55
Gam3	s(OM) + s(Phi)	6.33	-508.02	1029.64	10.00
Gam2	s(Phi)	3.01	-511.59	1029.43	9.79
Gam10	s(Phi) + s(Sal)	7.37	-506.44	1028.85	9.21
Gam11	s(OM) + s(Phi) + s(Sal)	10.70	-502.33	1028.65	9.01
Gam30	s(Phi) + s(Rain) + s(Sal) + s(Temp)	11.53	-499.73	1025.55	5.91
Gam29	s(OM) + s(Rain) + s(Sal) + s(Temp)	11.32	-499.70	1024.96	5.32
Gam22	s(Phi) + s(Rain) + s(Temp)	8.93	-502.56	1024.78	5.14
Gam28	s(Rain) + s(Sal) + s(Temp)	6.31	-505.43	1024.39	4.75
Gam_global	s(Temp) + s(Sal) + s(Rain) + s(OM) + s(Phi)	14.31	-495.13	1023.61	3.96
Gam26	s(Phi) + s(Sal) + s(Temp)	10.54	-499.68	1022.97	3.33
Gam25	s(OM) + s(Sal) + s(Temp)	10.49	-499.62	1022.72	3.08
Gam20	s(Rain) + s(Temp)	5.28	-505.73	1022.67	3.03
Gam24	s(Sal) + s(Temp)	5.33	-505.41	1022.14	2.50
Gam21	s(OM) + s(Rain) + s(Temp)	8.80	-501.16	1021.66	2.02
Gam27	*s(OM)+ s(Phi) + s(Sal)+ s(Temp)*	*13.55*	*-495.06*	*1021.45*	*1.81*
Gam23	*s(OM) + s(Phi) + s(Rain) + s(Temp)*	*10.85*	*-498.42*	*1021.21*	*1.57*
Gam18	*s(Phi) + s(Temp)*	*6.83*	*-503.19*	*1021.10*	*1.46*
Gam16	*s(Temp)*	*4.29*	*-505.72*	*1020.45*	*0.81*
Gam17	*s(OM) + s(Temp)*	*7.74*	*-501.42*	*1019.68*	*0.04*
Gam19	*s(OM) + s(Phi) + s(Temp)*	*10.01*	*-498.67*	*1019.64*	*0.00*

As for *S. dorsalis*, two models were selected as best models (Table 11). The first model contained the variables "OM", "Phi", "Rain2", "Temp", and explained 23% of abundance variation (Deviance explained). The second model also explained 23% of abundance variation (Deviance explained) and contained the variables "OM", "Phi", "Temp" (Table 11). Abundance decreased with the increase in OM (Fig. 15A), and slightly increased in values of Phi close to 6 (Fig. 15B). As for rainfall (Fig. 15C) and temperature (Fig. 15D) the increase in these variables' values lead to a decrease in abundance.

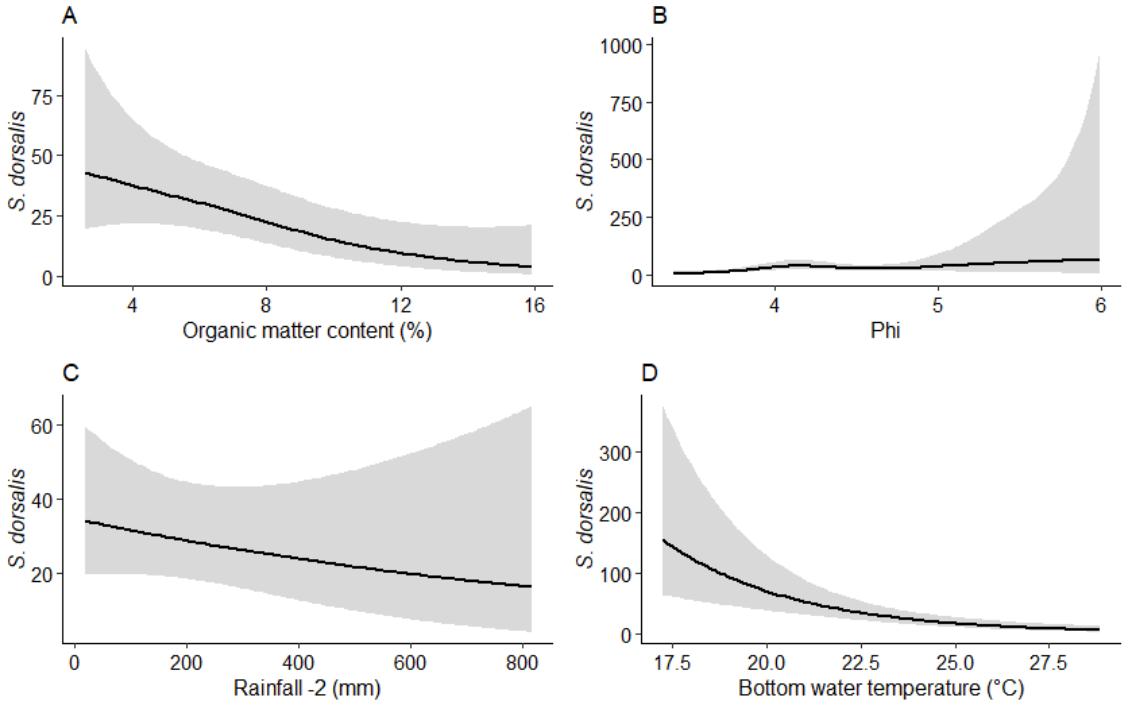

Figure 15 – Variation of abundance ($CPUE_n.hour^{-1}$) of *Sicyonia dorsalis* and its relationship with the covariates selected in the best model: [A] Organic matter content (%), [B] Phi, [C] Rainfall -2, and [D] Bottom water temperature (ºC).

Table 11 – Generalized additive models (GAM) adjusted for *S. dorsalis* $CPUE_n.hour^{-1}$. Models with ΔAICc < 2 = best model. df = Degrees of freedom; logLik = Log likelihood of a model.

Rank	Parameters	DF	logLik	AICc	ΔAICc
Gam12	s(Rain2) + s(Sal)	4.00	-440.42	889.24	20.45
Gam13	s(OM) + s(Rain2) + s(Sal)	5.78	-437.90	888.15	19.36
Gam15	s(OM) + s(Phi) + s(Rain2) + s(Sal)	11.62	-430.67	887.66	18.88
Gam4	s(Rain2)	3.00	-440.60	887.43	18.65
Gam8	s(Sal)	3.00	-440.48	887.19	18.40
Gam14	s(Rain2) + s(Phi) + s(Sal)	6.24	-436.74	886.87	18.08
Gam9	s(OM) + s(Sal)	4.55	-438.14	885.89	17.10
Gam5	s(OM) + s(Rain2)	4.00	-438.36	885.10	16.32
Gam6	s(Phi) + s(Rain2)	4.97	-437.16	884.85	16.06
Gam10	s(Phi) + s(Sal)	5.21	-436.84	884.73	15.94
Gam11	s(OM) + s(Phi) + s(Sal)	8.17	-433.18	884.22	15.43
Gam7	s(OM) + s(Phi) + s(Rain2)	6.57	-434.71	883.56	14.77
Gam1	s(OM)	3.00	-438.46	883.15	14.36
Gam2	s(Phi)	3.85	-437.34	882.74	13.95
Gam3	s(OM) + s(Phi)	5.30	-434.98	881.20	12.41
Gam29	s(OM) + s(Rain2) + s(Sal) + s(Temp)	8.88	-428.23	875.99	7.21
Gam28	s(Rain2) + s(Sal)+ s(Temp)	5.00	-432.50	875.59	6.81
Gam24	s(Sal) + s(Temp)	4.00	-433.07	874.53	5.74
Gam_global	s(Temp) + s(Sal) + s(Rain2) + s(OM) + s(Phi)	13.12	-422.15	874.48	5.70
Gam30	s(Phi) + s(Rain2) + s(Sal) + s(Temp)	8.82	-427.48	874.36	5.57
Gam25	s(OM) + s(Sal) + s(Temp)	8.40	-427.74	873.89	5.10
Gam20	s(Rain2) + s(Temp)	4.00	-432.49	873.38	4.59
Gam26	s(Phi) + s(Sal) + s(Temp)	7.85	-428.04	873.18	4.39
Gam21	s(OM) + s(Rain2) + s(Temp)	5.96	-430.19	873.13	4.34
Gam16	s(Temp)	3.00	-433.06	872.36	3.57
Gam27	s(OM) + s(Phi) + s(Sal) + s(Temp)	12.58	-421.76	872.29	3.50
Gam22	s(Phi) + s(Rain2) + s(Temp)	7.77	-427.57	872.05	3.26
Gam17	s(OM) + s(Temp)	5.59	-429.96	871.81	3.03
Gam18	s(Phi) + s(Temp)	6.79	-428.15	870.94	2.15
Gam23	*s(OM) + s(Phi) + s(Rain2) + s(Temp)*	*10.37*	*-423.59*	*870.37*	*1.58*
Gam19	*s(OM) + s(Phi) + s(Temp)*	*9.73*	*-423.59*	*868.79*	*0.00*

Model selection for *Xiphopenaeus* spp. yielded three best models (Table 12). The first model contained the variables "Phi" and "Rain2", and explained 11.8% of abundance variation (Deviance explained). The second model contained the variables "OM" and "Rain2", and explained 14.8% of variation (Deviance explained". The third model contained the variable "Rain2", and explained 11.6% of abundance variation (Deviance explained). Abundance was higher in values of OM around 8% (Fig. 16A), and in values of Phi > 4.5 (Fig. 16C). Abundance values decreased with rainfall increase (Fig. 16B).

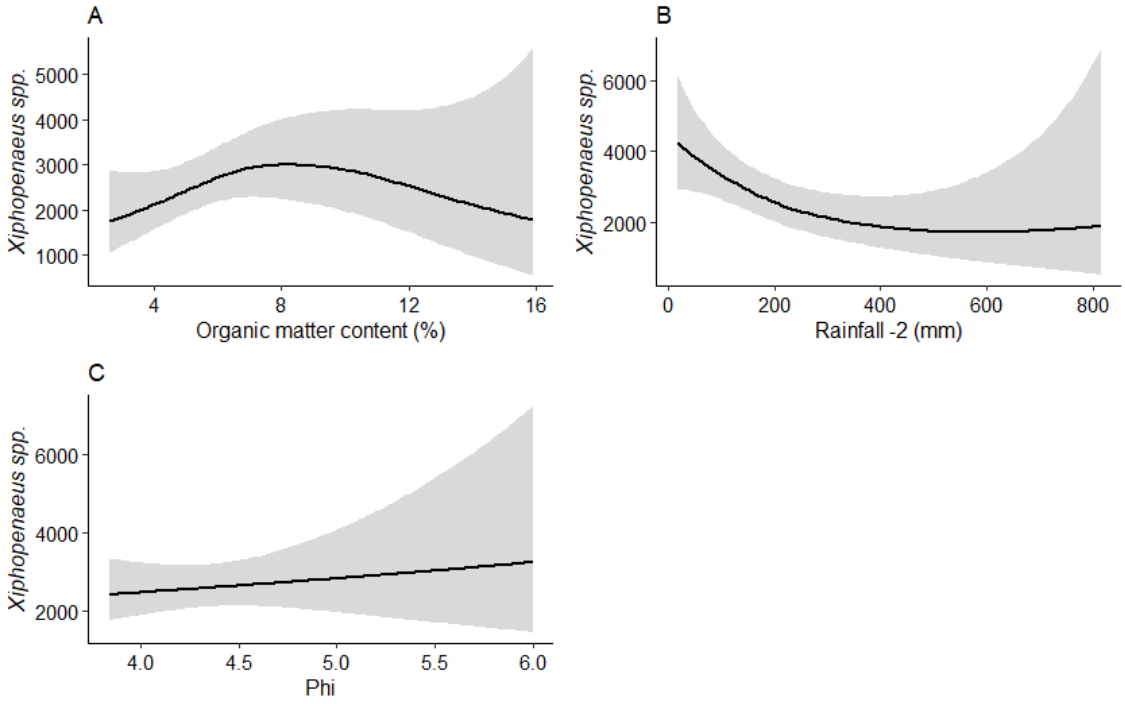

Figure 16 – Variation of abundance ($CPUE_n.hour^{-1}$) of *Xiphopenaeus* spp. and its relationship with the covariates selected in the best model: [A] Organic matter content (%), [B] Rainfall -2, and [C] Phi.

Table 12 – Generalized additive models (GAM) adjusted for *Xiphopenaeus* spp. $CPUE_n.hour^{-1}$. Models with ΔAICc < 2 = best model. df = Degrees of freedom; logLik = Log likelihood of a model.

Rank	Parameters	DF	logLik	AICc	ΔAICc
Gam24	s(Sal) + s(Temp)	4.00	-930.33	1869.06	163.71
Gam16	s(Temp)	3.04	-930.52	1867.36	162.01
Gam8	s(Sal)	3.00	-930.34	1866.91	161.56
Gam26	s(Phi) + s(Sal) + s(Temp)	5.46	-852.81	1717.33	11.98
Gam18	s(Phi) + s(Temp)	4.62	-852.83	1715.48	10.13
Gam10	s(Phi) + s(Sal)	4.36	-852.94	1715.11	9.76
Gam27	s(OM) + s(Phi) + s(Sal) + s(Temp)	8.21	-848.22	1714.61	9.26
Gam25	s(OM) + s(Sal) + s(Temp)	7.01	-849.51	1714.32	8.97
Gam2	s(Phi)	3.54	-852.95	1713.35	7.99
Gam_global	s(Temp) + s(Sal) + s(Rain2) + s(OM) + s(Phi)	10.05	-845.18	1713.09	7.74
Gam17	s(OM) + s(Temp)	6.11	-849.64	1712.49	7.14
Gam19	s(OM) + s(Phi) + s(Temp)	7.28	-848.17	1712.27	6.92
Gam11	s(OM) + s(Phi) + s(Sal)	7.25	-848.19	1712.26	6.91
Gam9	s(OM) + s(Sal)	6.04	-849.48	1712.01	6.66
Gam30	s(Phi) + s(Rain2) + s(Sal) + s(Temp)	7.65	-847.55	1711.91	6.56
Gam29	s(OM) + s(Rain2) + s(Sal) + s(Temp)	8.99	-845.67	1711.41	6.06
Gam15	s(OM) + s(Phi) + s(Rain2) + s(Sal)	9.07	-845.20	1710.67	5.31
Gam23	s(OM) + s(Phi) + s(Rain2) + s(Temp)	9.07	-845.18	1710.63	5.27
Gam1	s(OM)	5.14	-849.61	1710.21	4.86
Gam3	s(OM) + s(Phi)	6.30	-848.14	1709.92	4.57
Gam28	s(Rain2) + s(Sal) + s(Temp)	6.71	-847.62	1709.83	4.48
Gam14	s(Rain2) + s(Phi) + s(Sal)	6.67	-847.55	1709.59	4.24
Gam22	s(Phi) + s(Rain2) + s(Temp)	6.67	-847.52	1709.53	4.17
Gam13	s(OM) + s(Rain2) + s(Sal)	7.99	-845.75	1709.12	3.77
Gam21	s(OM) + s(Rain2) + s(Temp)	8.03	-845.64	1708.99	3.64
Gam7	s(OM) + s(Phi) + s(Rain2)	8.09	-845.19	1708.26	2.91
Gam12	s(Rain2) + s(Sal)	5.73	-847.65	1707.62	2.27
Gam20	s(Rain2) + s(Temp)	5.72	-847.60	1707.51	2.16
Gam6	*s(Phi) + s(Rain2)*	*5.68*	*-847.52*	*1707.27*	*1.91*
Gam5	*s(OM) + s(Rain2)*	*7.02*	*-845.72*	*1706.76*	*1.41*
Gam4	*s(Rain2)*	*4.74*	*-847.64*	*1705.35*	*0.00*

Model selection for *E. oplophoroides* resulted in five models that could be considered as best model (Table 13). The model that explained better the abundance variation contained the variables "OM", "Phi" and "Rain2", and explained 11.2% of the variation (Deviance explained). Abundance of *E. oplophoroides* was higher in values of organic matter content of 10% (Fig. 17A). Also, abundance was higher in Phi > 4.5 (Fig. 17B) and when rainfall exceeded 400 mm (Fig. 17C).

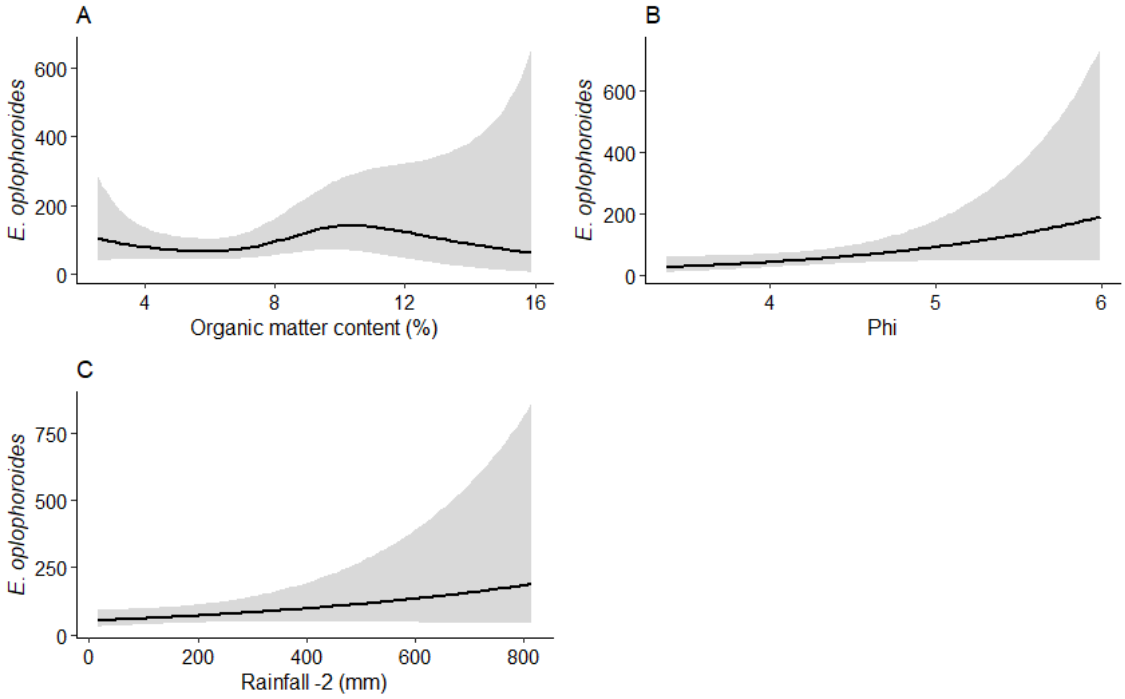

Figure 17 – Variation of abundance ($CPUE_n.hour^{-1}$) of *Exhyppolysmata oplophoroides* and its relationship with the covariates selected in the best model: [A] Organic matter content (%), [B] Phi, and [C] Rainfall -2 (mm).

Table 13 – Generalized additive models (GAM) adjusted for *E. oplophoroides* $CPUE_n.hour^{-1}$. Models with ΔAICc < 2 = best model. df = Degrees of freedom; logLik = Log likelihood of a model.

Rank	Parameters	DF	logLik	AICc	ΔAICc
Gam26	s(Phi) + s(Sal) + s(Temp)	6.07	-491.55	996.21	7.50
Gam_global	s(Temp) + s(Sal) + s(Rain2) + s(OM) + s(Phi)	12.00	-484.14	996.04	7.33
Gam29	s(OM) + s(Rain2) + s(Sal) + s(Temp)	9.36	-487.22	995.43	6.72
Gam24	s(Sal) + s(Temp)	4.92	-492.17	994.83	6.12
Gam25	s(OM) + s(Sal) + s(Temp)	9.15	-486.93	994.32	5.61
Gam27	s(OM) + s(Phi) + s(Sal) + s(Temp)	12.30	-482.83	994.21	5.50
Gam10	s(Phi) + s(Sal)	5.09	-491.53	993.93	5.22
Gam30	s(Phi) + s(Rain2) + s(Sal) + s(Temp)	6.79	-489.57	993.91	5.20
Gam28	s(Rain2) + s(Sal) + s(Temp)	6.14	-490.21	993.68	4.97
Gam15	s(OM) + s(Phi) + s(Rain2) + s(Sal)	10.79	-484.46	993.52	4.81
Gam23	s(OM) + s(Phi) + s(Rain2) + s(Temp)	9.19	-486.43	993.43	4.72
Gam21	s(OM) + s(Rain2) + s(Temp)	7.25	-488.64	993.15	4.44
Gam13	s(OM) + s(Rain2) + s(Sal)	8.43	-487.15	992.98	4.27
Gam8	s(Sal)	4.04	-492.17	992.87	4.16
Gam18	s(Phi) + s(Temp)	8.04	-487.49	992.72	4.01
Gam11	s(OM) + s(Phi) + s(Sal)	11.09	-483.41	992.20	3.49
Gam9	s(OM) + s(Sal)	8.27	-486.86	992.03	3.32
Gam16	s(Temp)	3.01	-492.84	991.96	3.25
Gam19	s(OM) + s(Phi) + s(Temp)	9.70	-485.02	991.88	3.17
Gam17	s(OM) + s(Temp)	6.80	-488.52	991.84	3.13
Gam14	s(Rain2) + s(Phi) + s(Sal)	5.93	-489.50	991.78	3.07
Gam12	s(Rain2) + s(Sal)	5.03	-490.29	991.31	2.60
Gam20	s(Rain2) + s(Temp)	4.41	-490.93	991.21	2.50
Gam2	s(Phi)	3.00	-492.45	991.16	2.45
Gam22	s(Phi) + s(Rain2) + s(Temp)	5.00	-490.24	991.16	2.45
Gam5	s(OM) + s(Rain2)	6.26	-488.72	990.98	2.27
Gam7	*s(OM) + s(Phi) + s(Rain2)*	*7.54*	*-487.03*	*990.61*	*1.39*
Gam3	*s(OM) + s(Phi)*	*8.17*	*-486.02*	*990.10*	*1.39*
Gam1	*s(OM)*	*5.83*	*-488.66*	*989.86*	*1.15*
Gam6	*s(Phi) + s(Rain2)*	*4.00*	*-490.23*	*988.90*	*0.20*
Gam4	*s(Rain2)*	*3.01*	*-491.22*	*988.71*	*0.00*

As for *N. schmitti*, model selection resulted in one best model, that contained the variables "Phi" and "Temp", and explained 58.1% of abundance variation (Deviance explained) (Table 14). Abundance was higher in values of Phi between 4.5 and 5 (Fig. 18A). There was also a higher abundance in temperature of 23ºC (Fig. 15B).

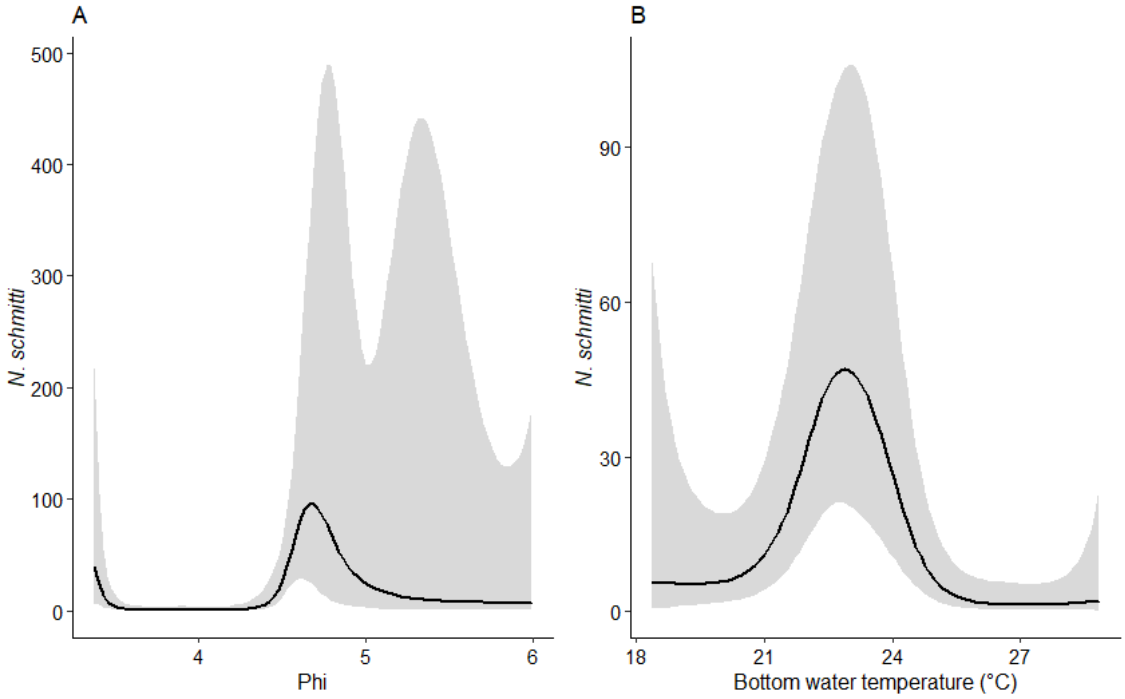

Figure 18 – Variation of abundance ($CPUE_n.hour^{-1}$) of *Nematopalaemon schmitti* and its relationship with the covariates selected in the best model: [A] Phi, and [B] Bottom water temperature (ºC).

Table 14 – Generalized additive models (GAM) adjusted for *N. schmitti* $CPUE_n.hour^{-1}$. Models with ΔAICc < 2 = best model. df = Degrees of freedom; logLik = Log likelihood of a model.

Rank	Parameters	DF	logLik	AICc	ΔAICc
Gam9	s(OM) + s(Sal)	4.42	-183.70	377.13	20.70
Gam25	s(OM) + s(Sal) + s(Temp)	9.73	-176.53	376.75	20.31
Gam8	s(Sal)	3.00	-185.04	376.51	20.07
Gam5	s(OM) + s(Rain)	6.71	-180.24	375.88	19.44
Gam1	s(OM)	3.51	-183.98	375.55	19.11
Gam_global	s(Temp) + s(Sal) + s(Rain) + s(OM) + s(Phi)	20.11	-156.39	374.83	18.40
Gam17	s(OM) + s(Temp)	8.35	-176.77	373.32	16.89
Gam4	s(Rain)	3.00	-183.44	373.31	16.88
Gam29	s(OM) + s(Rain) + s(Sal) + s(Temp)	10.47	-173.61	373.12	16.69
Gam21	s(OM) + s(Rain) + s(Temp)	9.67	-174.47	372.45	16.02
Gam13	s(OM) + s(Rain) + s(Sal)	7.05	-177.90	372.08	15.65
Gam24	s(Sal) + s(Temp)	7.40	-177.42	372.06	15.62
Gam12	s(Rain) + s(Sal)	4.00	-181.47	371.67	15.24
Gam28	s(Rain) + s(Sal) + s(Temp)	7.39	-177.17	371.51	15.07
Gam20	s(Rain) + s(Temp)	7.05	-177.03	370.34	13.91
Gam16	s(Temp)	6.39	-177.45	369.49	13.06
Gam15	s(OM) + s(Phi) + s(Rain) + s(Sal)	14.38	-165.28	369.25	12.81
Gam23	s(OM) + s(Phi) + s(Rain) + s(Temp)	17.96	-157.88	368.28	11.85
Gam7	s(OM) + s(Phi) + s(Rain)	13.97	-165.35	367.93	11.49
Gam27	s(OM) + s(Phi) + s(Sal) + s(Temp)	16.34	-160.77	367.52	11.08
Gam11	s(OM) + s(Phi) + s(Sal)	10.26	-170.32	365.90	9.47
Gam10	s(Phi) + s(Sal)	8.87	-171.28	363.81	7.38
Gam3	s(OM) + s(Phi)	9.31	-170.45	363.36	6.93
Gam14	s(Rain) + s(Phi) + s(Sal)	9.89	-169.56	363.28	6.85
Gam6	s(Phi) + s(Rain)	9.63	-169.86	363.11	6.67
Gam30	s(Phi) + s(Rain) + s(Sal) + s(Temp)	14.51	-161.74	362.63	6.19
Gam19	s(OM) + s(Phi) + s(Temp)	14.81	-160.95	362.13	5.69
Gam2	s(Phi)	7.94	-171.18	361.04	4.60
Gam26	s(Phi) + s(Sal) + s(Temp)	14.88	-160.15	360.78	4.35
Gam22	s(Phi) + s(Rain) + s(Temp)	14.28	-160.32	358.97	2.54
Gam18	*s(Phi) + s(Temp)*	*13.64*	*-160.18*	*356.43*	*0*

Discussion

The spatial distribution of shrimp species in the Bay is directly associated with the life cycle of the studied species and their stage of development. *Litopenaeus schmitti*, was more abundant in site 3, the shallowest, and closest to the estuaries. This species presents life cycle type II, as proposed by Dall (1990). Reproduction and spawning occur offshore, and then post-larvae migrate to estuaries where they will complete their juvenile development, and when pre-adults, recruit to the adult population in deeper waters (Garcia & Le Reste 1986; Cházaro-Olvera et al., 2009). Due to the small sized estuaries in Ubatuba Bay (Costa et al., 2008), which are subjected to quick shifts in salinity gradient, the permanence of *L. schmitti* in these environments will depend on its specific tolerance limits.

Litopenaeus schmitti post-larvae are able to tolerate values of salinity lower than 15, although their optimum is around, which allows them to inhabit these estuaries (Rosas et al., 1997). Similar was observed for *F. paulensis*, but not to *F. brasiliensis* by Perroca et al. (2022) in the same Bay. Thus, juveniles of *L. schmitti* and *F. paulensis* remains in the estuaries for longer periods, while *F. brasiliensis* concentrates at the estuaries entrance or at adjacent shallow areas at the bay. After a few months, juveniles of the three species migrate to the "5 m deep region" (site 3), the shallowest sampled area, where they were captured more abundantly in this study and in Perroca et al. (2022), and also to site 4, a sheltered area with low wave action. In the present study, *R. constrictus* and *S. dorsalis* also were more abundant in site 3, regardless of their life cycle being independent from estuaries. The presence of these species in the sampling site is related to their ecological requirements (i.e., organic matter concentration, phi, bottom water temperature).

Xiphopenaeus spp. was also more abundant in site 3. Despite of Dall et al. (1990) including *X. kroyeri* in the type II life cycle, Castro et al. (2005) and Costa et al. (2007)

observed that, for the northern coast of São Paulo, seabob shrimp juveniles do not enter estuaries to complete their development. This probably occur due to the small sized estuaries in the area, and *Xiphopenaeus* spp. tolerance in relation to salinity gradients, as it is observed for *F. brasiliensis* (Costa et al., 2016). This species differs mainly in their habits as adults. While pink shrimp adult migrates to deeper offshore areas (between 40 and 100 m deep), the seabob shrimps remain in shallower areas (up to 20 m deep) (Costa et al., 2007). *Artemesia longinaris* and *P. muelleri* were more abundant in site 1, and the carideans *E. oplophoroides* e *N. schmitti* were more abundant in site 2. These species present life cycle type III, in which post-larvae prefer coastal waters with elevated salinity (Dall, 1990).

Temporally, it was also possible to notice different patterns in species distribution. The higher abundance of *A. longinaris* was recorded during summer, being accentuated in period of neutrality. Its presence in site 1 and 2 through summer is associated with the intrusion of the South Atlantic Central Water (SACW), which its reflexes in the deeper portions of the bay lead to decrease in bottom water temperature and increase in salinity. The pattern observed here corroborates with the literature (Costa et al., 2005, 2010; Carvalho-Batista et al., 2011, 2018).

The white shrimp *L. schmitti* was more abundant in autumn and winter, and when bottom water temperature varied between 22.5ºC and 25ºC. Despite of its abundance increasing in El Niño events, the rainfall increase affected negatively its abundance. In Brazil, El Niño leads to a significant increase in seasonal precipitation in the southern and southeast regions, especially in spring (Grimm et al., 1998, 2000), and an increase in sea surface water temperature (Cavalcanti et al., 2009). However, Perroca et al. (2022) did not found correlation between El Niño events and increase in pluviosity for the area, possibly because the northern coast of São Paulo State has the highest total precipitation

for the country, especially in the summer (Seluchi et al., 2011; Pezzoli et al., 2013). Therefore, increase in precipitation in winter and autumn possibly leads to an early recruitment to the adult population in the offshore area, once most individuals captured at the bay are juveniles. Otherwise, authors observed a positive effect of rainfall in this species abundance a few months after it increased in areas with larger estuaries (Santos & Freitas, 2004; Santos et al., 2008). *L. schmitti* was more abundant in the shallower portions of the Bay (site 3, followed by site 4). Bochini et al. (2014) registered the same for this species in three different bays in Ubatuba. Sites 3 and 4, are less hydrodynamic, and present sediment composed mostly of silt and clay, which contains a higher concentration of organic matter content available as a food resource and allows these shrimps to burrow.

Pleoticus muelleri was more abundant from May to July (autumn-winter), and its abundance decreased with increase in temperature, and on the contrary, increased with salinity increase. This species showed preference for deeper areas of the bay (site 1, followed by site 2). These results corroborate the findings of Costa et al. (2004), and also according to Castilho et al. (2008), reproduction peaks from late spring to early summer. So, it is possible that this peak in abundance registered in this study reflects the juvenile recruitment at the bay.

As for *R. constrictus*, it was more abundant from June to August. Also, periods of neutrality and weak El Niño influenced positively in this species abundance. They were more abundant in site 3, followed by site 4, the shallowest and more sheltered areas of the bay. The models suggested decrease in abundance in elevated temperatures, however, this resulted from the analysis methodology and does not reflect the species true occurrence. To the ecological models, in order to decrease data dispersion, the monthly mean of abundance and environmental factors was used. The result from this indicated

that in periods in which the mean temperature at the bay was around 17.5ºC, these individuals were more abundant in sites 3 and 4, once they probably migrate from deeper areas of the bay with lower temperature, to the warmer shallower sites. It is important to notice that *R. constrictus* is a tropical species with preference for elevated temperatures (Costa & Fransozo, 2004).

The rock shrimp *S. dorsalis* was also more abundant in sites 3 and 4, respectively, however from October to January, and with an additional peak in June and July. Its abundance increased in periods of neutrality and La Niña, and also in temperature values of 17.5ºC. This is probably due to reflexes of the SACW intrusion, as was observed by Castilho et al. (2008). Also, *S. dorsalis* is often found associated with macroalgae, that are abundant in the less hydrodynamic sites of the bay, as we observed in the field. *Xiphopenaeus* spp. was more abundant from April to July through the years. This is an important result since the peak in abundance occurred within the closed season (March 1 to May 31), and these stocks are already overexploited (Miazaki, 2021).

For the carideans, *E. oplophoroides* was more abundant from August to December (spring), and site 2, as was observed by Fransozo et al. (2005). As for *N. schmitti*, it was more abundant from June to July in periods of neutrality and weak La Niña. However, in periods of El Niño, abundance was higher from May to August. *N. schmitti* was also more abundant in site 2. According with Almeida et al. (2012), individuals of *N. schmitti* migrates during summer and spring to other areas, since the SACW intrusion leads to decrease in water temperature, and this species shows preference for elevated temperatures. The SACW intrusion also transport detritus and vegetal fragments to other areas, decreasing the habitat and food availability for these organisms (Herrera et al., 2017; Marques et al., 2021).

All species that had Phi as explanatory variable in the models, showed preference

for sediments with finer texture (i.e., Silt and clay). These preference for finer sediments is common to several Penaeoidea species, once these sediments make burrowing easier, as was observed for *A. longinaris* (Fransozo et al., 2004; Costa et al., 2005), *Farfantepenaeus* spp. (Williams, 1984; Costa et al., 2016), *L. schmitti* (Bochini et al., 2014; Santos et al., 2020), *P. muelleri* (Costa et al., 2004), *S. dorsalis* (Castilho et al., 2008; Piantkoski et al., 2021) and *Xiphopenaeus* spp. (Costa et al., 2007; Almeida et al. 2012).

The carideans *N. schmitti* and *E. oplophoroides* also showed preference for silt and clay. Fransozo et al. (2005) registered for *E. oplophoroides* preference for very fine sand. This is similar to what was found by Bernardes et al. (2020) for *R. constrictus*. Costa and Fransozo (2004), showed the preference of *R. constrictus* for greater sediment, however, Bernardes et al. (2020) comparing samples from 1995 and 2017, observed that a sedimentation process occurred overtime at the bay, diminishing the environmental heterogeneity and increasing the proportion of silt and clay in the sediment. The authors believe that this process occurred due to the great rainfall events linked to intense El Niño episodes (1997-1998 and 2015-2016), coupled with the urbanization at the area and increase in trawling. The *R. constrictus* population probably adapted to this change in sediment availability, and the same may have occurred for *E. oplophoroides*.

With regard to ENSO events, periods of neutrality favored the increase in abundance of *A. longinaris*, *P. muelleri*, *R. constrictus*, *S. dorsalis* e *N. schmitti*. The shrimps *P. muelleri* and *S. dorsalis* also showed higher abundances in periods of La Niña. In La Niña and neutral periods, there is a shift in the atmospheric pressure gradient favoring Northeast winds, that enhances the SACW intrusion and weakens the Coastal Water (Castro-Filho et al., 1987; Enfield & Mayer, 1997). Thus, species that responds negatively to elevated temperatures, as *P. muelleri* and *S. dorsalis,* in El Niño will migrate

to deeper areas, which were not sampled in this study. As for El Niño events, it favored the abundance of *L. schmitti* and *R. constrictus*. El Niño is also known to increase water surface temperature in southeast Brazil (Cavalcanti et al., 2009), thus the increase in temperature is benefic to these species whose abundances increase in elevated temperatures.

The combination of all these factors makes the Ubatuba Bay a hotspot for several species of shrimp and other organisms. Therefore, long-term studies of the communities living there, caught as species of commercial interest or accidentally, are essential for establishing standards and measures to protect this ecosystem.

References

Almeida, A.C.; Fransozo, A.; Teixeira, G.M.; Hiroki, K.A.N.; Furlan, M & Bertini, G. 2012. Ecological distribution of the shrimp *Nematopalaemon schmitti* (Crustacea: Decapoda: Caridea) in three bays on the south-eastern coast of Brazil. African Journal of Marine Science, 34: 93-102.

Awange, J.L.; Mpelasoka, F & Gonçalves, R.M. 2016. When every drop counts: Analysis of droughts in Brazil for the 1901-2013 period. Science of the Total Environment, 566-567, 1472-1488. doi.org/10.1016/j.scitotenv.2016.06.031.

Barton, K. 2009. Mu-MIn: Multi-model inference. R Package Version 0.12.2/r18

Bernardes, V.P.; Souza, A.N.; Bernardo, C.H.; Teixeira, G.M.; Costa, R.C.; Mantelatto, F.L & Fransozo, A. 2020. Comparison of the spatio-temporal distribution of the roughneck shrimp *Rimapenaeus constrictus* (Stimpson, 1874) (Crustacea, Penaeoidea) from monthly samples collected 20 years apart: Effects of a marine protected area in southeastern Brazil. Marine Ecology, 41: e12605. doi: 10.1111/maec.12605

Bochini, G.L; Fransozo, A.; Castilho, A.L.; Hirose, G.L & Costa, R.C. 2014. Temporal and spatial distribution of the commercial shrimp *Litopenaeus schmitti* (Burkenroad, 1936) (Dendrobranchiata: Penaeidae) in the southeastern Brazilian coast. Journal of the Marine Biological Association of the United Kingdom, 94: 1001-1008. doi:10.1017/S0025315414000265

Breheny, P & Burchett, W. 2017. "Visualization of Regression Models Using visreg." The R Journal 9: 56–71.

Brito, R.; Chimal, M.E & Rosas, C. 2000. Effect of salinity in survival, growth, and osmotic capacity of early juveniles of *Farfantepenaeus brasiliensis* (decapoda: penaeidae). Journal of Experimental Marine Biology and Ecology, 244: 253-263.

Burnham, K. P. & Anderson, D.R. 2002. Model Selection and Multimodel Inference: A Practical Information-Theoretic Approach. Springer, New York, NY.

Caley, J., Carr, M.H., Hixon, M.A., Hughes, T.P., Jones, G.P & Menge, B.A. 1996. Recruitment and the local dynamics of open marine populations. Annual Review of Ecology, Evolution, and Systematics, 27:477-500.

Carvalho-Batista, A.; Simões, S.M.; Lopes, M & Costa, R.C. 2011. Ecological distribution of the shrimp *Pleoticus muelleri* (Bate, 1888) and *Artemesia longinaris* Bate, 1888 (Decapoda: Penaeoidea) in the Southeastern Brazilian littoral. Nauplius, 19: 135-143. doi:10.1590/S0104-64972011000200005.

Carvalho-Batista, A.; Terossi, M.; Zara, F.J.; Mantelatto, F.L & Costa, R.C. 2019. A multigene and morphological analysis expands the diversity of the seabob shrimp *Xiphopenaeus* Smith, 1869 (Decapoda: Penaeidae), with descriptions of two new species. Scientific Reports, 9: 15281.

Castilho, A.L., Furlan, M., Costa, R.C & Fransozo, V. 2008. Abundance and temporal-spatial distribution of the rock shrimp *Sycionia dorsalis* Kingsley, 1878 (Decapoda, Penaeoidea) from the northern coast of São Paulo state, Brazil. Senckenbergiana marítima, 38:75-83.

Castro, R.H., Costa, R.C., Fransozo, A., Mantelatto, F.L.M. 2005. Population structure of the seabob shrimp *Xiphopenaeus kroyeri* (Heller, 1862) (Crustacea, Penaeoidea) in the littoral of São Paulo, Brazil. Scientia Marina, 69:105-112.

Castro-Filho, B.M.; Miranda, L.B & Myao, S.Y. 1987. Condições hidrográficas na plataforma continental ao largo de Ubatuba: Variações sazonais e em média escala. Boletim do Instituto Oceanográfico, 35:13-51.

Cavalcanti, I.F.A.; Ferreira, N.J.; Silva, M.G.A.J & Dias, M.A.F.S. 2009. Tempo e Clima no Brasil. Oficina de Textos, São Paulo: 463p.

Cházaro-Olvera, S.; Winfield, I & Coria-Olvera, V. 2009. Transport of *Farfantepenaeus aztecus* postlarvae in three lagoon-system inlets in the southwestern Gulf of Mexico. Crustaceana 82: 425-437. doi:10.1163/156854008X400612

CEMADEN. 2022. National Center for Monitoring and Early Warning of Natural Disasters. Available at www2.cemaden.gov.br/mapainterativo/#. Last accessed September 9, 2022.

Costa, R.C.; Fransozo, A.; Melo, G.A.S & Freire, F.A.M. 2003. An illustrated key for Dendrobranchiata shrimps from the northern coast of São Paulo state, Brazil. Biota Neotropica, 3 (1): 1-12.

Costa, R.C. & A. Fransozo. 2004. Abundance and ecologic distribution of the shrimp *Rimapenaeus constrictus* (Crustacea: Penaeidae) in the northern coast of São Paulo State, Brazil. Journal of Natural History, 38:901-912.

Costa, R.C.; Fransozo, A & Pinheiro, A. 2004. Ecological distribution of the shrimp *Pleoticus muelleri* (Bate, 1888) (Decapoda: Penaeoidea) in southeastern Brazil. Hydrobiologia, 529: 195-203.

Costa, R.C.; Fransozo, A.; Castilho, A.L & Freire, F.A.M. 2005. Annual, seasonal and spatial variation of abundance of the shrimp *Artemesia longinaris* (Decapoda: Penaeoidea) in south-eastern Brazil. Journal of Marine Biological Association of United

Kingdom, 85: 107–112. doi:10.1017/S0025315405010908h

Costa, R.C.; Fransozo, A.; Freire, F.A.M & Castilho, A.L. 2007. Abundance and ecological distribution of the "sete-barbas" shrimp *Xiphopenaeus kroyeri* (Heller, 1862) (Decapoda: Penaeoidea) in three bays of the Ubatuba region, Southeastern, Brazil. Gulf and Caribbean Research, 19: 33-41. doi:10.18785/gcr.1901.04

Costa, R.C.; Lopes, M.; Castilho, A.L.; Fransozo, A & Simões, S.M. 2008. Abundance and distribution of juvenile pink shrimps *Farfantepenaeus* spp. In a mangrove estuary and adjacente bay on the northern shore of São Paulo State, southern Brazil. International Journal of Invertebrate Reproduction and Development, 52: 51-58. doi:10.1080/07924259.2008.9652272

Costa, R.C.; Branco, J.O.; Machado, I.F.; Campos, B.R & Avila, M.G. 2010. Population biology of shrimp *Artemesia longinaris* Bate, 1888 (Crustacea, Decapoda, Penaeidae) from the South coast of Brazil. Journal of Marine Biological Association of United Kingdom, 90: 663-669. doi:10.1017/S002531540999124X

Costa, R.C.; Carvalho-Batista, A.; Herrera, D.R.; Pantaleão, J.A.F.; Teodoro, S.S.A & Davanso, T. 2016. Carcinofauna acompanhante da pesca do camarão-sete-barbas *Xiphopenaeus kroyeri* em Macaé, Rio de Janeiro, sudeste brasileiro. Boletim do Instituto de Pesca, 43: 611-624. doi: 10.20950/1678-2305.2016v42n3p611

CPC (Climate Prediction Center). 2021. National Oceanic and Atmospheric Administration (NOAA). El Niño-Southern Oscillation (ENSO) data. http://cpc.ncep.noaa.gov/products/analysis_monitoring/ensostuff/ensoyears.shtml (last accessed 05 June 2021).

DAEE (Department of Waters and Electric Energy) – (2018). Rainfall data. http://www.hidrologia.daee.sp.gov.br (last accessed 05 June 2018).

Dall, W., Hill, B.J., Rothlisberg, P.C. & Staples, D.J. 1990. The biology of the Penaeidae. In: Blaxter, J.H.S. & Southward, A.J. (Eds). Advanced Marine Biology, San Diego, Academic press.

Enfield, D.B & Mayer, D.A. 1997. Tropical Atlantic sea surface temperature variability and its relation to El Nino-Southern Oscillation. Journal of Geophysical Research, American Geophysical Union, 102(C1): 929-945.

Fransozo, A.; Costa, R.C.; Castilho, A.L & Mantelatto, F.L.M. 2004. Ecological distribution of the shrimp "barba-ruça" *Artemesia longinaris* (Decapoda: Penaeidae) in Fortaleza Bay, Ubatuba, Brazil. Revista de Investigación y Desarrollo Pesquero, 16:45-53.

Fransozo, V.; Costa, R.C.; Bertini, G & Cobo, V.J 2005. Population biology of spine shrimp *Exhippolysmata oplophoroides* (Holthuis) (Caridea, Hippolytidae) in a subtropical region, São Paulo, Brazil. Revista Brasileira de Zoologia, 22:1078-1084.

Garcia, S. & L. Le Reste. 1981. Life cycles, dynamics, exploitation and management of coastal penaeid shrimp stocks. FAO Fish. Tech. Pap. 203, 215 p

Gorelli, G.; Sardà, F & Company, J.B. 2016. Fishing Effort Increase and Resource Status of the Deep-Sea Red Shrimp *Aristeus antennatus* (Risso 1816) in the Northwest Mediterranean Sea Since the 1950s. Reviews in Fisheries Science & Aquaculture, 24(2): 192-202. doi.org/10.1080/23308249.2015.1119799

Grimm, A. M.; Ferraz, S.E.T & Gomes, J. 1998. Precipitation anomalies in Southern Brazil associated with El Niño and La Niña events. Journal of Climate, 11:2863-2880. doi:10.1175/1520-0442(1998)011<2863:PAISBA>2.0.CO;2

Grimm, A.M.; Barros, V.R & Doyle, M.E. 2000. Climate variability in Southern South America associated with El Niño and La Niña events. Journal of Climate, 13: 35-58. doi:10.1175/1520-0442(2000)013<0035:CVISSA>2.0.CO;2

Hakanson, L & Jansson, M. 1983. Principles of Lake Sedimentology. Springer-Verlag, Berlin, Heidelberg, New York, Tokyo.

Herrera, D.R.; Pescinelli, R.A & Costa, R.C. 2017. Ecological distribution of *Nematopalaemon schmitti* and *Exhippolysmata oplophoroides* (Crustacea: Caridea) near an upwelling area off southeastern Brazil. Latin American Journal of Aquatic Research, 45(1), 149-158. doi: 10.3856/vol45-issue1-fulltext-14

IP/APTA/SAA/SP. 2022. Estatística Pesqueira Marinha e Estuarina do Estado de São Paulo. Consulta On-line. Programa de Monitoramento da Atividade Pesqueira Marinha e Estuarina do Estado de São Paulo. Instituto de Pesca (IP), Agência Paulista de Tecnologia dos Agronegócios (APTA), Secretaria de Agricultura e Abastecimento do Estado de São Paulo (SAA/SP). [accessed: 2022 January 20]. http://www.propesq.pesca.sp.gov.br/.

Ingólfsson, O.A.; Jørgensen, T.; Sistiaga, M..; Herrmann, B & Kvalvik, L. 2022. Increasing catch efficiency for *Nephrops* in deep-water shrimp (*Pandalus borealis*) trawl fisheries. Fisheries Research, 254: 106394. doi.org/10.1016/j.fishres.2022.106394

Larsen, R.B.; Herrmann, B.; Sistiaga, M.; Brinkhof, J & Grimaldo, E. 2018. Bycatch reduction in the Norwegian Deep-water Shrimp (*Pandalus borealis*) fishery with a double grid selection system. Fisheries Research, 208:267-273. doi.org/10.1016/j.fishres.2018.08.007.

Mantelatto, F.L.M & Fransozo, A. 1999. Characterization of the physical and chemical parameters of Ubatuba Bay, northern coast of São Paulo State, Brazil. Revista Brasileira de Biologia, 59: 23-31.

Marques, A.O.; Sousa, A.N.; Bernardes, V.P.; Bernardo, C.H.; Reis, D.M.; Godoy, A.T & Fransozo, A. 2021. Evaluation of caridean ecological distribution in the Ubatuba region, southeastern Brazilian coast using unsupervised machine learning technique. Marine Ecology: e12673. doi:10.1111/maec.12673

Miazaki, L.F.; Heckler, G.S.; Santos, A.P.F.; Castilho, A.L.; Pescinelli, R.A & Costa, R.C. 2021. Growth parameters, longevity, and mortality of the seabob shrimp *Xiphopenaeus* spp. (Decapoda: Penaeidae) in four important fishing regions of the southeastern Brazil. Fisheries Oceanography, 00: 1-16. doi: 10.1111 /fog.12533.

Moraes, L.E.; Paes, E.; Garcia, A.; Moller, O & Vieira, P. 2012. Delayed response of fish abundance to environmental changes: a novel multivariate time-lag approach. Marine Ecology Progress Series, 456, 159-168. doi.org/10.3354/meps09731

Pereira, N & D'Incao, F. 2012. Relationship between rainfall, pink shrimp harvest (*Farfantepenaeus paulensis*) and adult stock, associated with El Niño and La Niña phenomena in Patos Lagoon, southern Brazil. Journal of the Marine Biological Association UK 92, 1451-1456. doi.org/10.1017/S0025315412000021

Pérez-Farfante, I & Kensley, B. 1997. Penaeoid and Sergestoid shrimps and Pawns of the World. Keys and diagnoses for the families and genera. Éditions du Muséum national d histoire naturalle. Paris.

Perroca, J.F.; Rodrigues-Filho, J.L.; Fransozo, A & Costa, R.C. 2022. Variations in pink-shrimps *Farfantepenaeus brasiliensis* and *F. paulensis* juvenile abundance: clarifying ecological patterns and providing subsidies to management in shallow marine ecosystems. Fisheries Research 256: 106482. doi.org/10.1016/j.fishres.2022.106482

Pezzoli, A.; Cartacho, D.L.; Arasaki, E.; Alfredini, P & Sakai, R.O. 2013. Extreme events assessment methodology coupling rainfall and tidal levels in the coastal flood plain of the São Paulo North Coast (Brazil) for engineering projects purposes. Journal of Climatology and Weather Forecast, 1, 1. https://doi.org/10.4172/jcwf.1000103.

Piantkoski, E.L.; Costa, R.C.; Davanso, T.M.; Herrera, D.R & Simões, S.M. 2021. Which environmental factors are most relevant to the distribution of *Sicyonia dorsalis* (Penaeoidea: Sicyoniidae) in an upwelling region? Biologia. doi:0.2478/s11756-020-00676-8

Rosas, C.; Sánchez, A.; Díaz-Iglesia, E.; Brito, R.; Martinez, E & Soto, A.L. 1997.

Critical dissolved oxygen level to *Penaeus setiferus* and *Penaeus schmitti* postlarvae (PL10–18) exposed to salinity changes. Aquaculture, 152(1-4): 259-272. doi.org/10.1016/S0044-8486(96)01516-5

Santos, M.C.F & Freitas A.E.T.S. 2004. Estrutura populacional e pescado camarão branco *Penaeus schmitti* Burkenroad (Crustacea, Decapoda, Penaeidea) na Lagoa Papari, Município de Nísia Floresta (Rio Grande do Norte—Brasil). Boletim Técnico Científico do CEPENE 12: 23-42.

Santos, J.L.; Severino-Rodrigues, E & Vaz-Dos-Santos, A.M. 2008. Estrutura populacional do camarão-branco *Litopenaeus schmitti* nas regiões estuarina e marinha da Baixada Santista, São Paulo, Brasil. Boletim Instituto da Pesca, São Paulo 34: 375-389.

Santos, R.C.; Perroca, J.F.; Costa, R.C & Hirose, G. L. 2020. Population dynamics of *Farfantepenaeus subtilis* (Pérez-Farfante, 1967) and *Litopenaeus schmitti* (Burkenroad, 1936) (Decapoda: Penaeidae) and evidence of habitat partitioning in the northeast of Brazil. Regional Studies in Marine Science, 35: 101218. doi:10.1016/j.rsma.2020.101218

Seluchi, M.E.; Chou, S.C & Gramani, M. 2011. A case study of a winter heavy rainfall event over the Serra do Mar in Brazil. Geofisica Internacional, 50(1): 41-56.

Somers, E. 1987. Sediment type as a factor in the distribution of commercial prawn species in the western Gulf of Carpentaria, Australia. Australian Journal of Freshwater Research, 38, 133-149. doi.org/10.1071/MF9870133

Sugiura, N. 1978. Further analysis of the data by Akaike's information criterion and the finite corrections. Communications in Statistics, A7, 13-26. doi.org/10.1080/03610927808827599

Suguio, K & Martin, L. 1978. Formações quaternárias marinhas do litoral paulista e fluminense. Paper present at the International Symposium Coastal evolution in the Quaternary, São Paulo, SP. Retrieved from https://core.ac.uk/download/pdf/39879155.pdf.

Temming, A.; Bönisch, A.; Hagen, W.; Brenneken, C & Dänhardt, A. 2022. Unexpected high discard mortalities of juvenile brown shrimp (*Crangon crangon*) in the North Sea shrimp fishery. Fisheries Research, 252: 106354. doi.org/10.1016/j.fishres.2022.106354

Trenberth, K.E & Stepaniak, D.P. 2001. Indices of El Niño evolution. Journal of Climate 14, 1697-1701. doi.org/10.1175/1520-0442(2001)014<1697:LIOENO>2.0.CO;2

Tucker, M. 1988. Techniques in sedimentology. Oxford: Blackwell, Blackwell Scientific Publications, Boston 394p.

Turschwell, M.; Stewart-Koster, B.; Kenyon, R.; Deng, R.A.; Stratford, D.; Hughes, J.D & Pollino, C.A. 2022. Spatially structured relationships between white banana prawn (*Penaeus merguiensis*) catch and riverine flow in the Northern Prawn Fishery, Australia. Journal of Environmental Management, 319(1): 115761. doi.org/10.1016/j.jenvman.2022.115761

Vilarreal, H & Hernandez-Llamas, A., 2005. Influence of temperature on larval development of Pacific brown shrimp *Farfantepenaeus californiensis*. Aquaculture 249, 257-263. doi.org/10.1016/j.aquaculture.2005.03.039

Wentworth, C.K., 1999. A scale of grade and terms of cladistic sediments. J Geol. 30:377-392.

Wickham, H. 2016. ggplot2: Elegant Graphics for Data Analysis. Springer-Verlag New York. ISBN 978-3-319-24277-4.

Williams, A.B. 1984. Shrimps, Lobsters and Crabs of the Atlantic Coast of the Eastern United States, Maine to Florida. Smithsonian Institution Press, Washington, D.C. Wood, S.N. 2017. Generalized Additive Models: An Introduction with R. Chapman and Hall/CRC, Boca Raton, FL.

Zuur, A.F.; Ieno, E.N.; Walker, N.J.; Savaliev, A.A & Smith, G.M. 2009. Mixed effects models and extensions in R; Gail M, Krickeberg K, Samet JM, Tsiatis A, Wong W, editors. New York: Springer.

Supplementary material – Data exploration

1) Artemesia longinaris

1.1. Relationship between dependent and explanatory variables

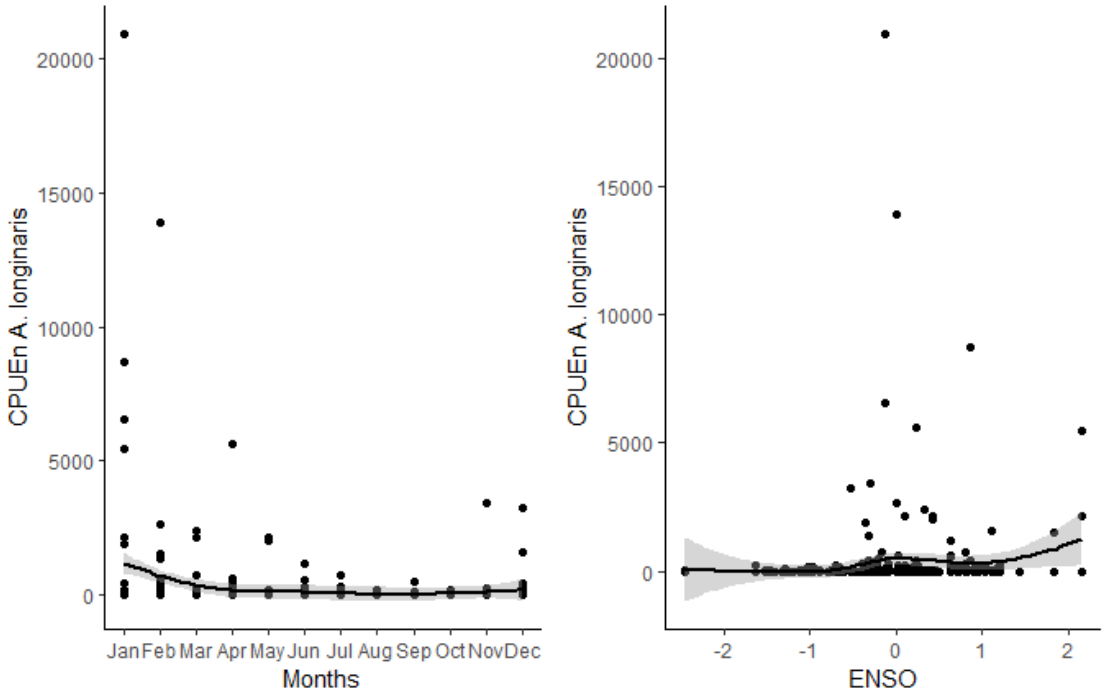

Fig. S1.1 – Scatterplots with a LOESS smoother between *A. longinaris* $CPUE_n$ and its covariates months and ENSO.

1.2. Outliers and dispersion pattern

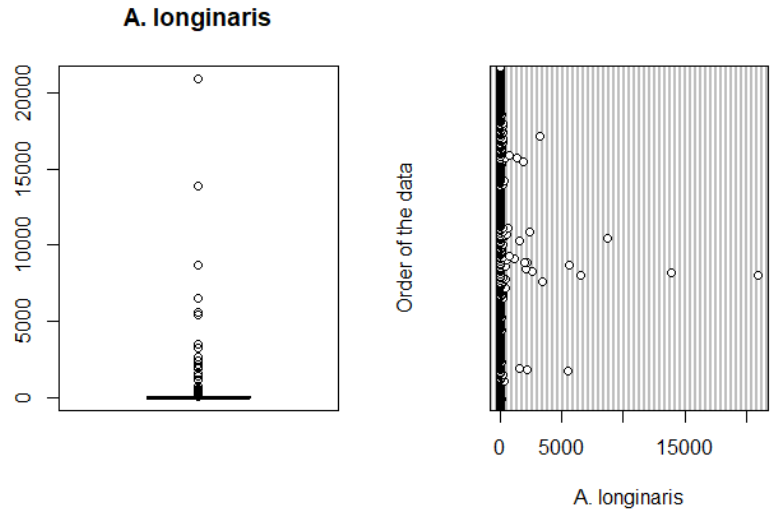

Fig. S1.2 – Box plot (Left) and Cleveland plot (Right) from *A. longinaris* $CPUE_n$.

1.3. Normality

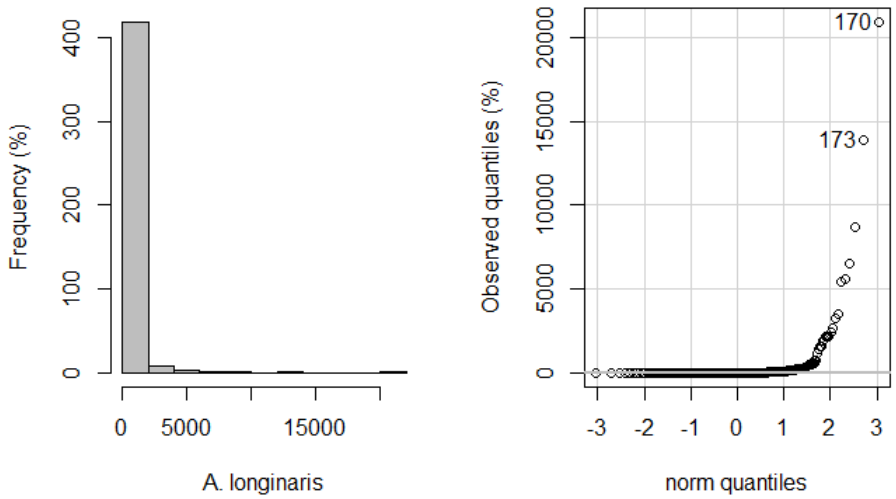

Fig. S1.3 – Histogram of *A. longinaris* $CPUE_n$. (Left) and Q-Q plots (Right) of observed diversity against hypothetical normal distribution.

1.4. Homogeneity

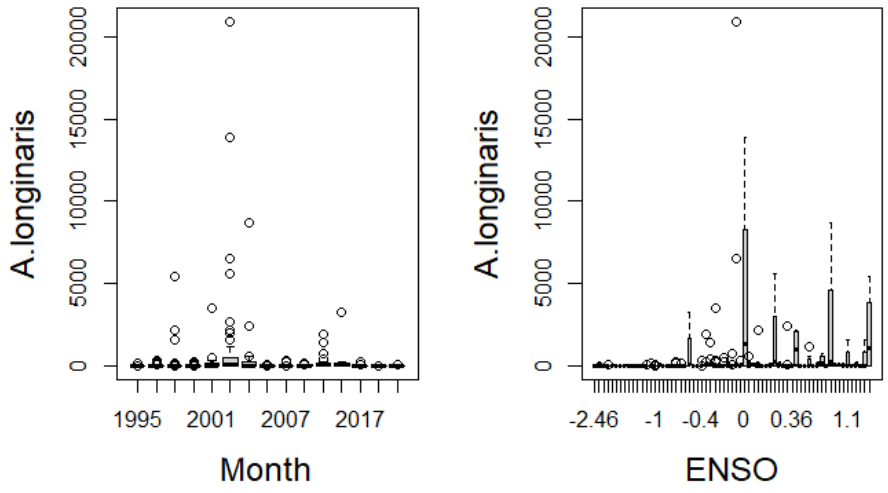

Fig. S1.4 – Month conditional box plot (Left) and ENSO conditional box plot (Right) of $CPUE_n$.

1.5. Independency

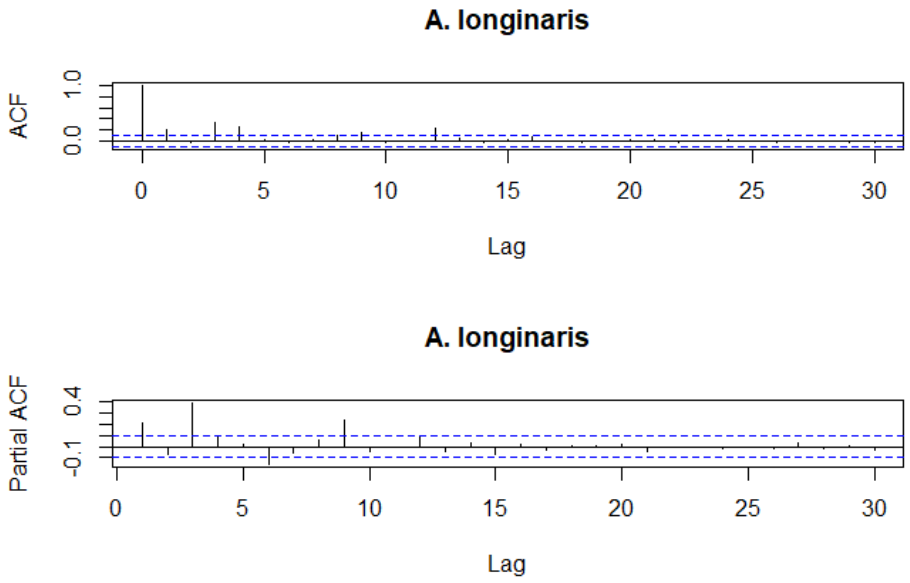

Fig. S1.5 – Auto-correlation function (ACF) and partial auto-correlation function (PACF) plot against time lag for *A. longinaris* $CPUE_n$.

1.6. Zeros

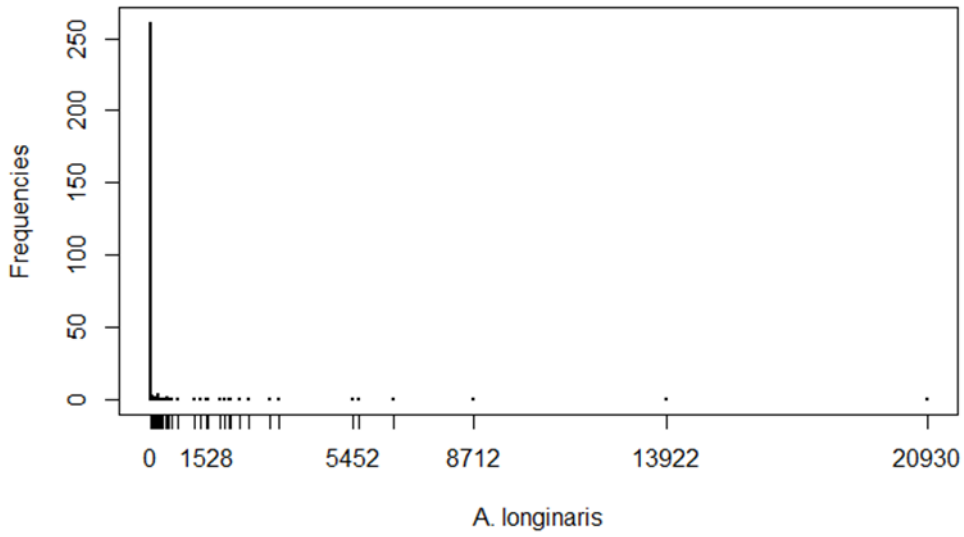

Fig. S1.6 – Frequency of *A. longinaris* $CPUE_n$.

1.7. Interaction

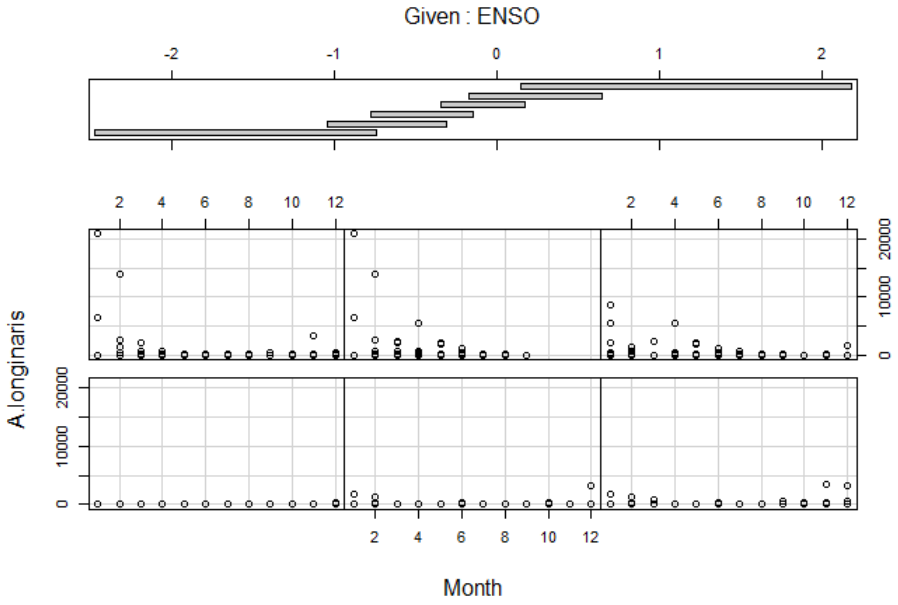

Fig. S1.7 – A coplot of *A. longinaris* $CPUE_n$ data against Month given the ENSO event.

1.8. Collinearity

Table. S1 – Values of VIF calculated for the numerical explicative variables. Temp – Bottom temperature (ºC), Sal – Bottom salinity, OM – Organic matter content (%), Phi – Granulometry and Rain2 – Rainfall -2.

Temp	Sal	OM	Phi	Rain2
1.0	1.09	1.07	1.06	1.06

2) ***Litopenaeus schmitti***

2.1. Relationship between dependent and explanatory variables

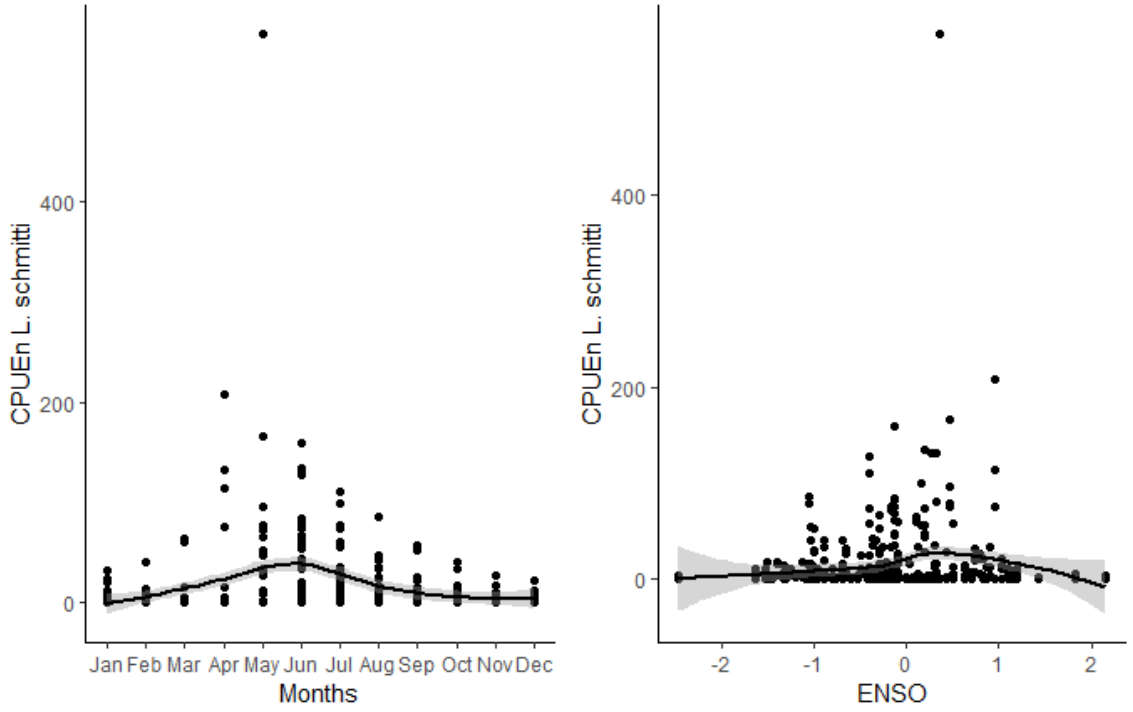

Fig. S2.1 – Scatterplots with a LOESS smoother between *L. schmitti* $CPUE_n$ and its covariates months and ENSO.

2.2. Outliers and dispersion pattern

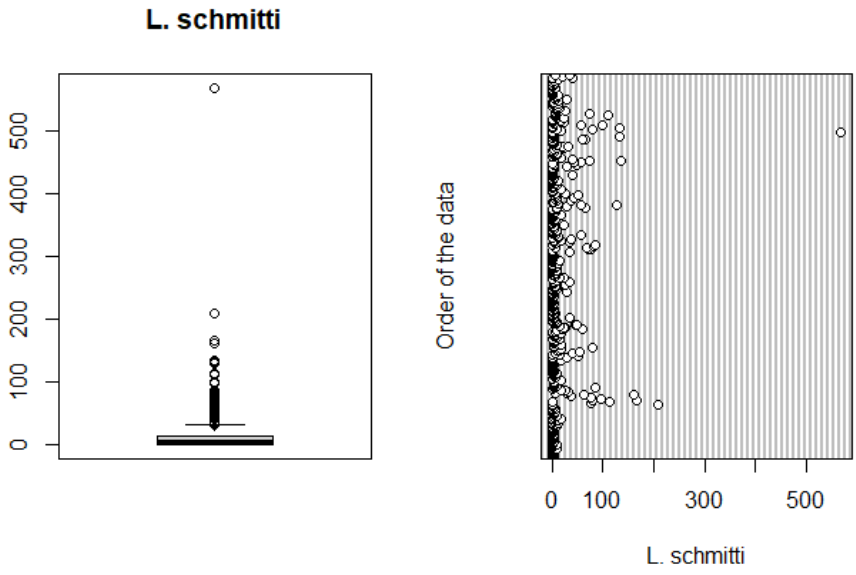

Fig. S2.2 – Box plot (Left) and Cleveland plot (Right) from *L. schmitti* $CPUE_n$.

2.3. Normality

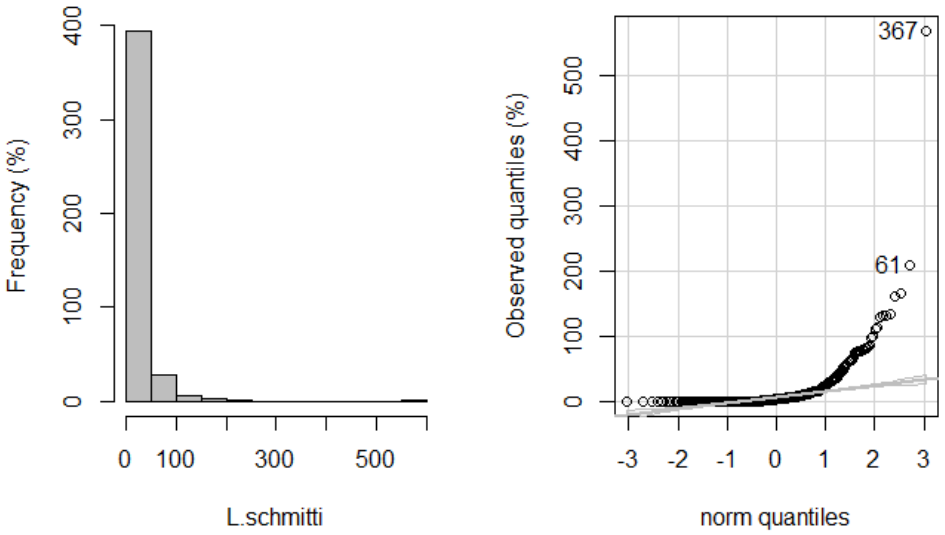

Fig. S2.3 – Histogram of *L. schmitti* $CPUE_n$. (Left) and Q-Q plots (Right) of observed diversity against hypothetical normal distribution.

2.4. Homogeneity

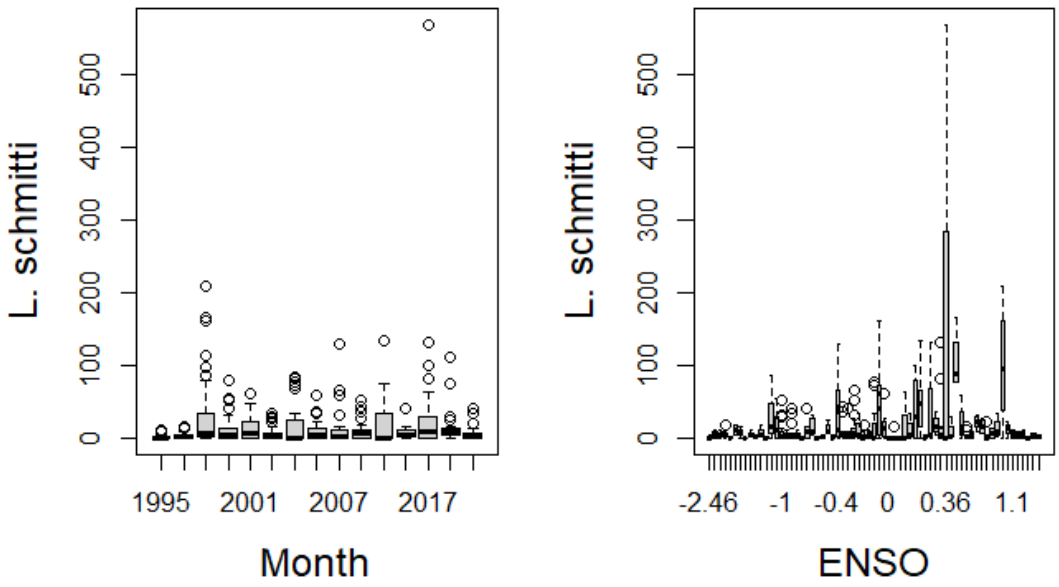

Fig. S2.4 – Month conditional box plot (Left) and ENSO conditional box plot (Right) of $CPUE_n$.

2.5. Independency

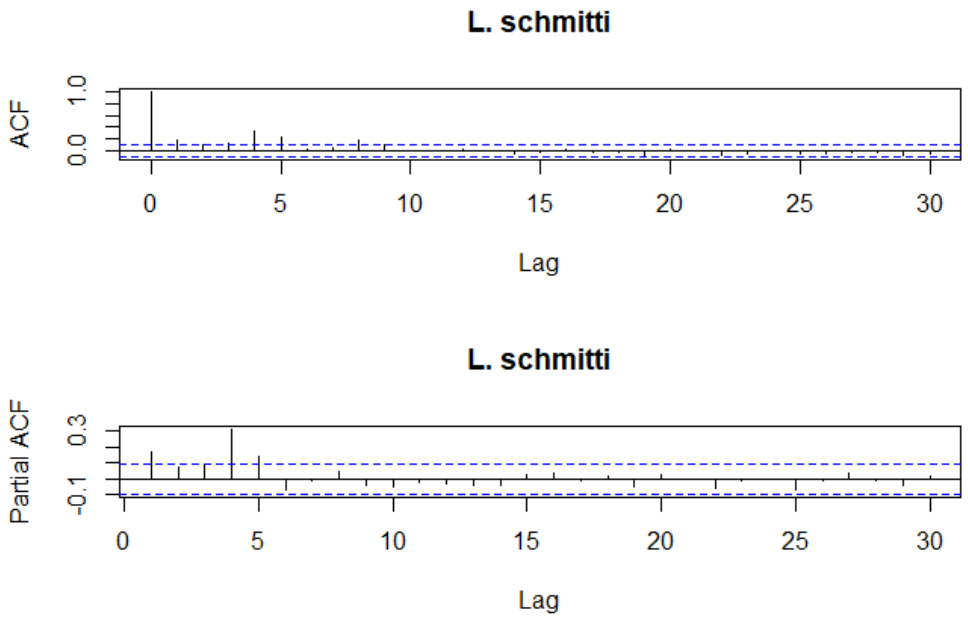

Fig. S2.5 – Auto-correlation function (ACF) and partial auto-correlation function (PACF) plot against time lag for *L. schmitti* $CPUE_n$.

2.6. Zeros

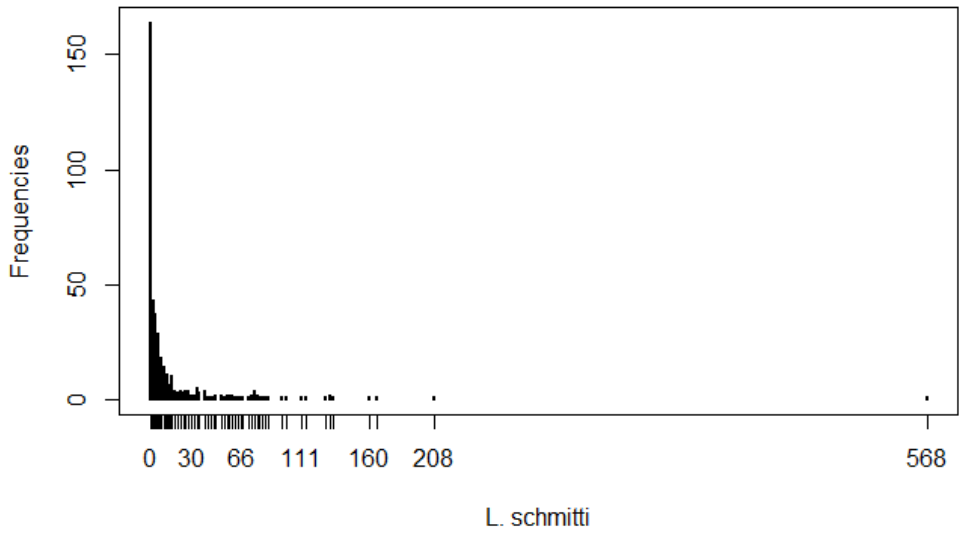

Fig. S2.6 – Frequency of *L. schmitti* $CPUE_n$.

2.7. Interaction

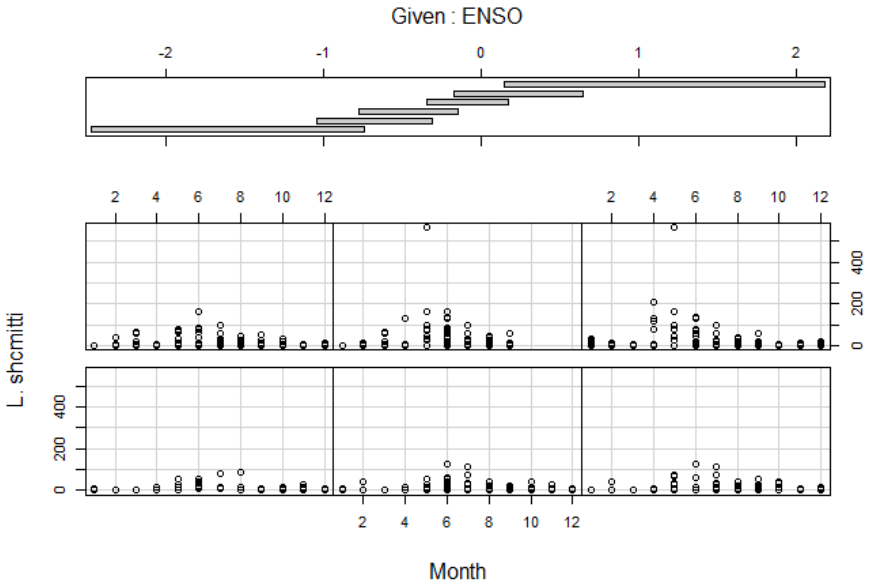

Fig. S2.7 – A coplot of *L. schmitti* $CPUE_n$ data against Month given the ENSO event.

2.8. Collinearity

Table. S2 – Values of VIF calculated for the numerical explicative variables. Temp – Bottom temperature (ºC), Sal – Bottom salinity, OM – Organic matter content (%), Phi – Granulometry and Rain – Rainfall.

Temp	Sal	OM	Phi	Rain
1.14	1.09	1.08	1.06	1.18

3) Pleoticus muelleri

3.1. Relationship between dependent and explanatory variables

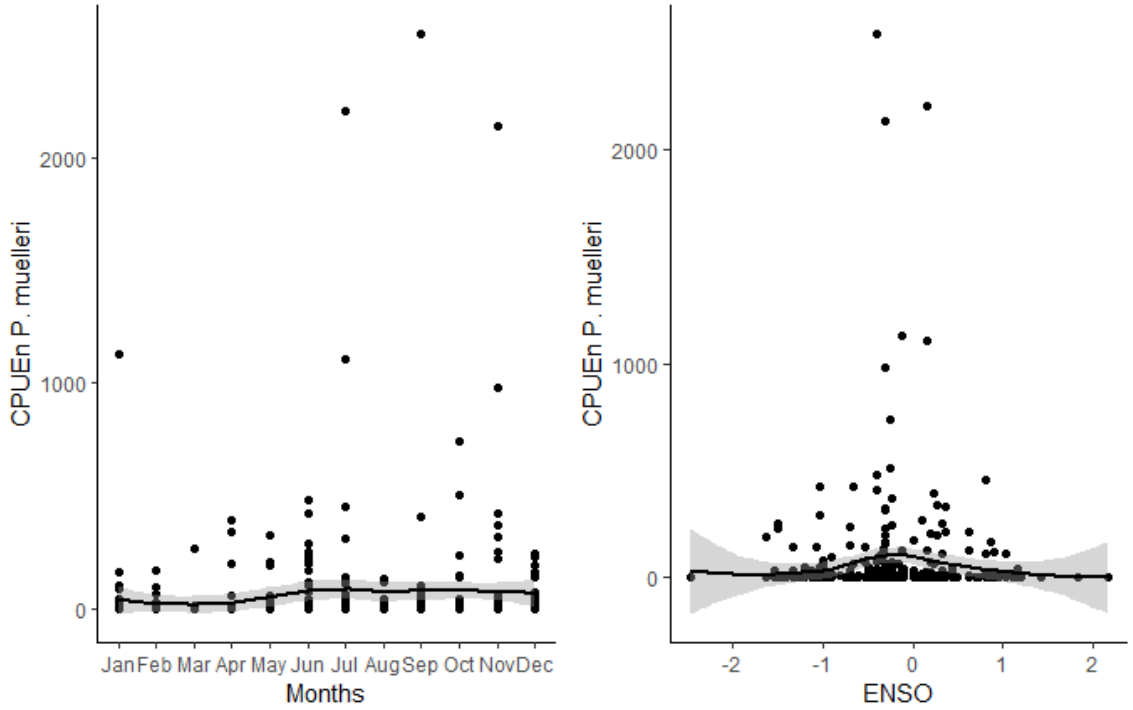

Fig. S3.1 – Scatterplots with a LOESS smoother between *P. muelleri* $CPUE_n$ and its covariates months and ENSO.

3.2. Outliers and dispersion pattern

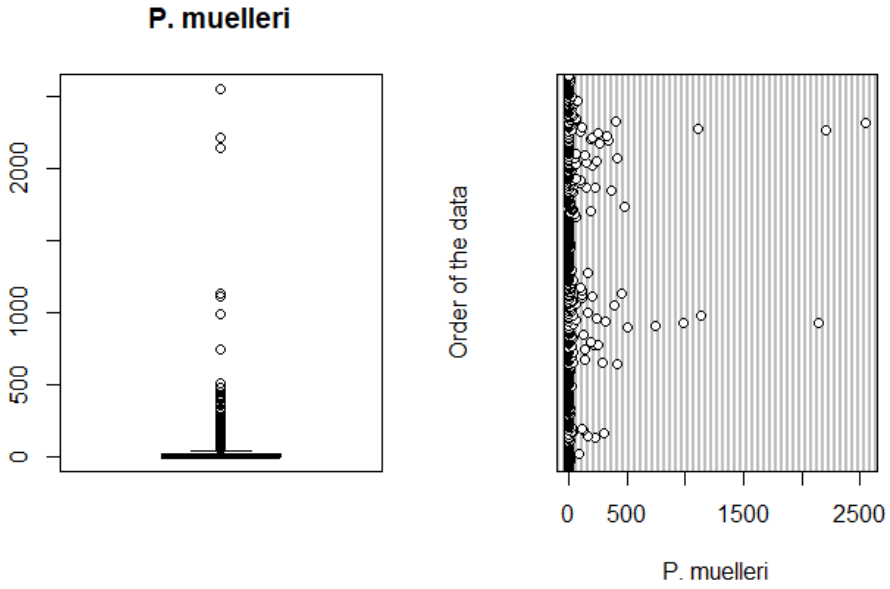

Fig. S2.2 – Box plot (Left) and Cleveland plot (Right) from *P. muelleri* $CPUE_n$.

3.3. Normality

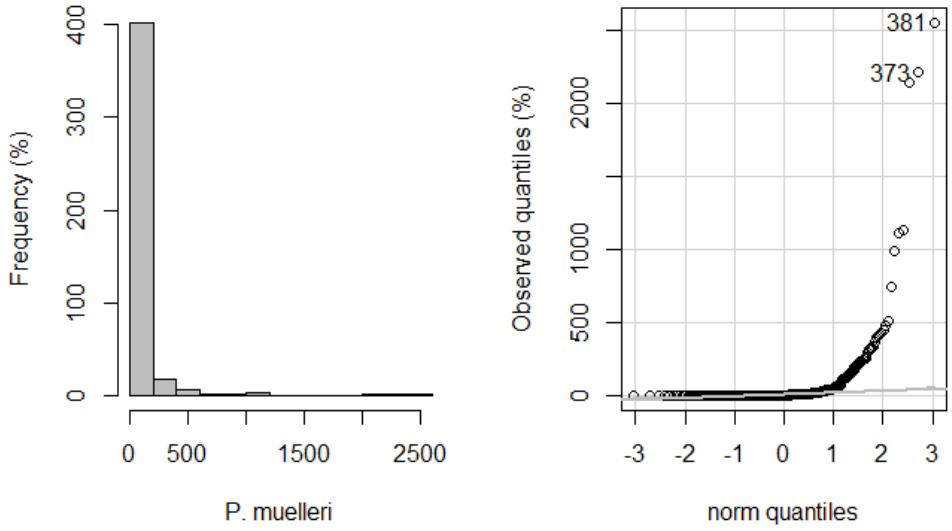

Fig. S3.3 – Histogram of *P. muelleri* $CPUE_n$. (Left) and Q-Q plots (Right) of observed diversity against hypothetical normal distribution.

3.4. Homogeneity

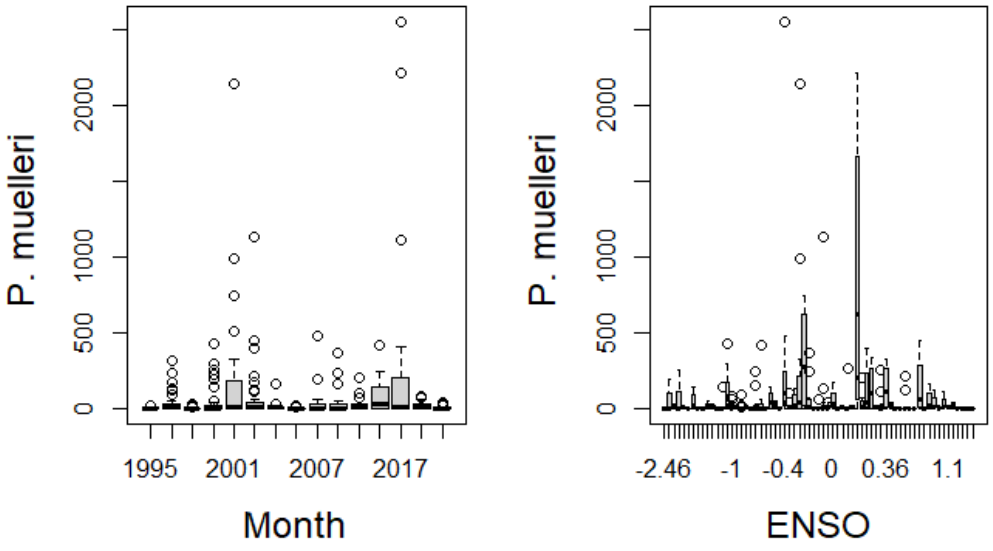

Fig. S3.4 – Month conditional box plot (Left) and ENSO conditional box plot (Right) of $CPUE_n$.

3.5. Independency

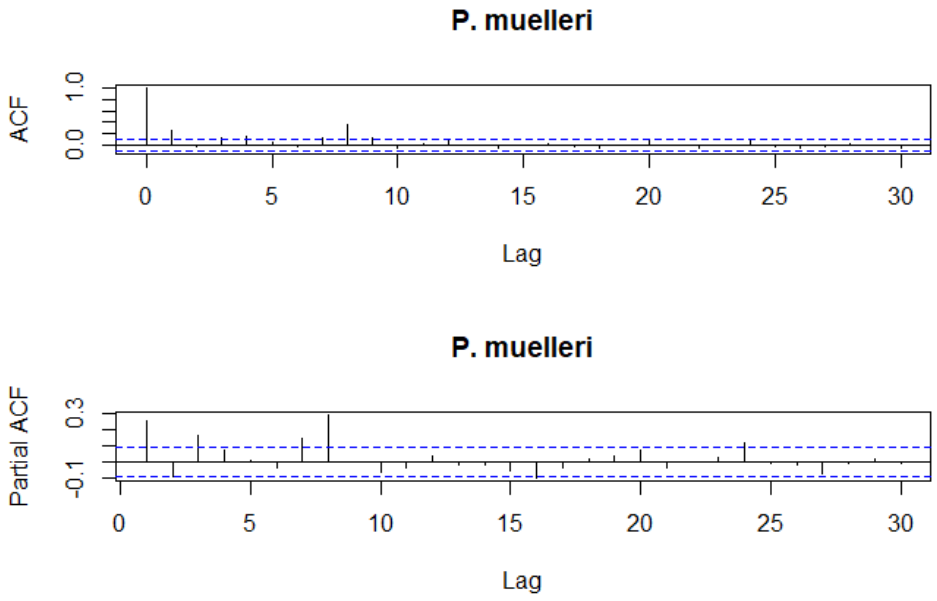

Fig. S3.5 – Auto-correlation function (ACF) and partial auto-correlation function (PACF) plot against time lag for *P. muelleri* $CPUE_n$.

3.6. Zeros

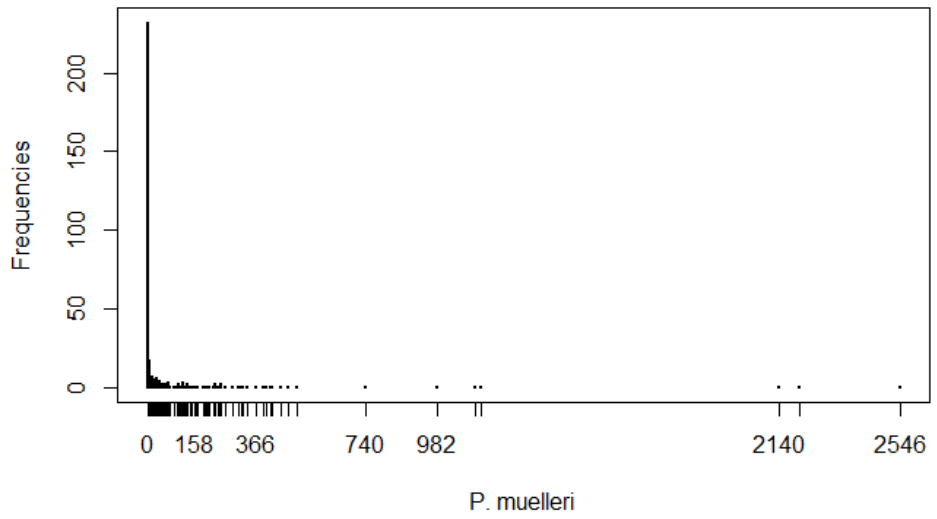

Fig. S3.6 – Frequency of *P. muelleri* $CPUE_n$.

3.7. Interaction

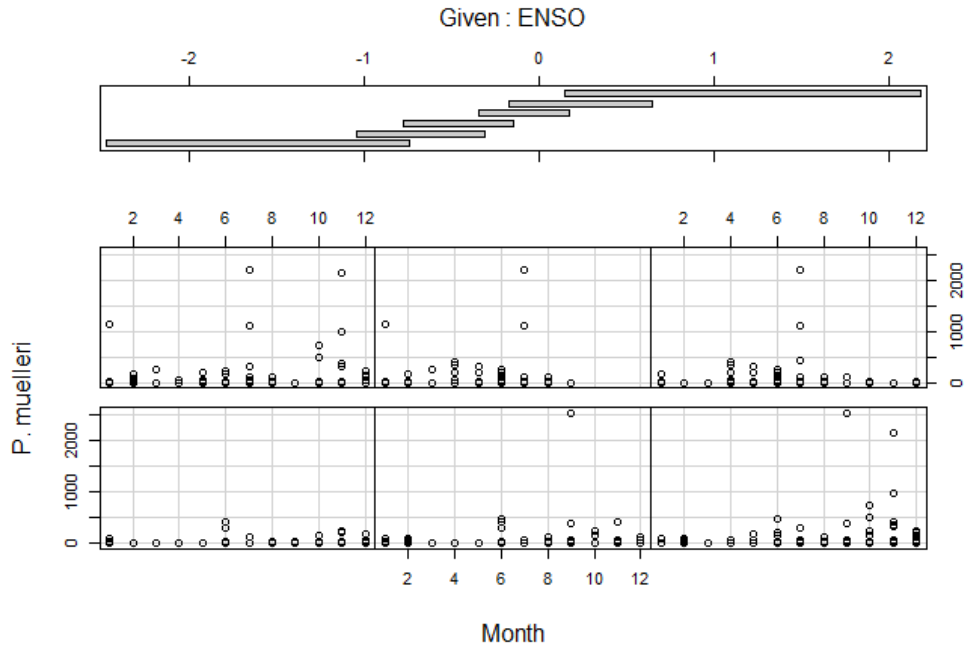

Fig. S3.7 – A coplot of *P. muelleri* $CPUE_n$ data against Month given the ENSO event.

3.8 Collinearity

Table. S3 – Values of VIF calculated for the numerical explicative variables. Temp – Bottom temperature (ºC), Sal – Bottom salinity, OM – Organic matter content (%), Phi – Granulometry and Rain – Rainfall.

Temp	Sal	OM	Phi	Rain
1.14	1.09	1.08	1.07	1.18

4) Rimapenaeus constrictus

4.1. Relationship between dependent and explanatory variables

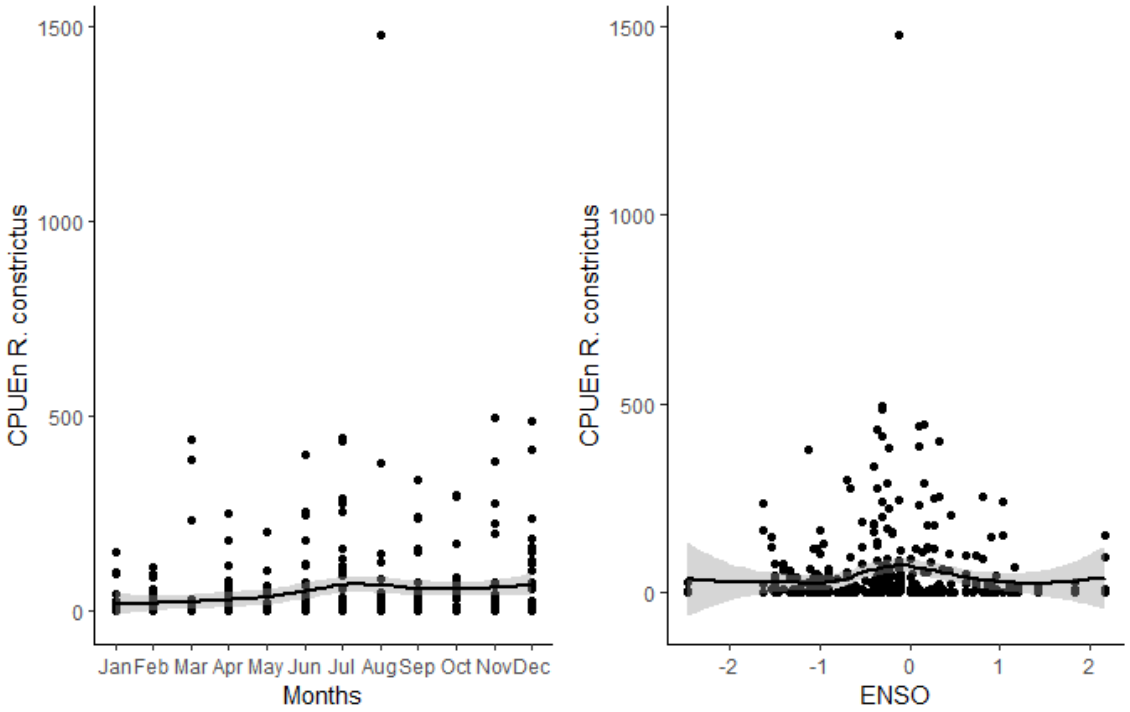

Fig. S4.1 – Scatterplots with a LOESS smoother between *R. constrictus* $CPUE_n$ and its covariates months and ENSO.

4.2. Outliers and dispersion pattern

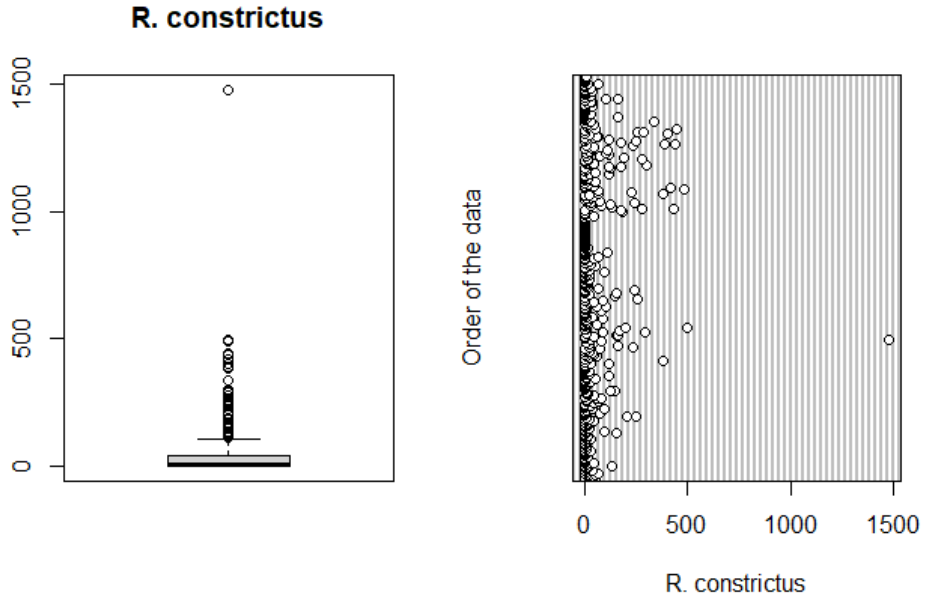

Fig. S4.2 – Box plot (Left) and Cleveland plot (Right) from *R. constrictus* $CPUE_n$.

4.3. Normality

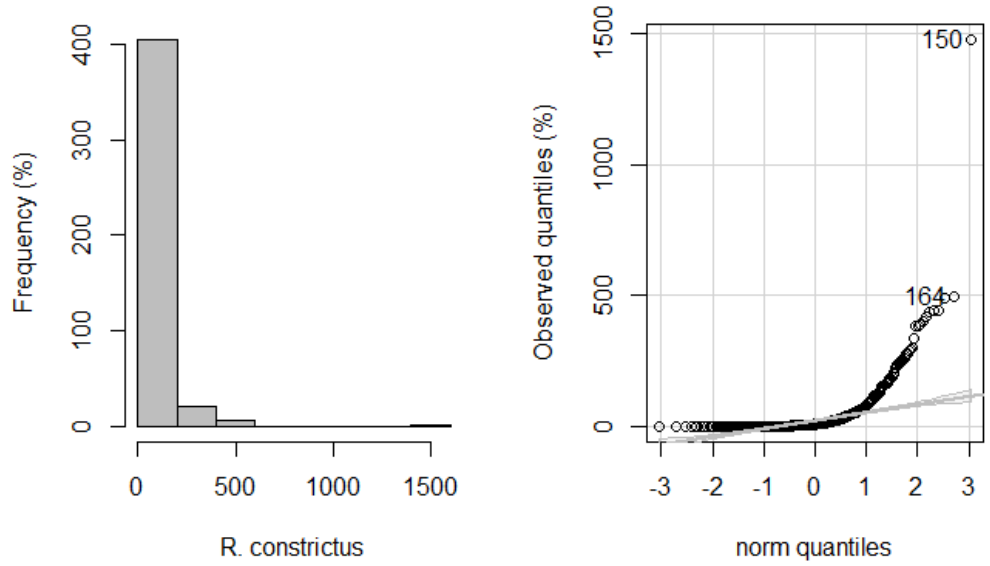

Fig. S4.3 – Histogram of *R. constrictus* $CPUE_n$. (Left) and Q-Q plots (Right) of observed diversity against hypothetical normal distribution.

4.4. Homogeneity

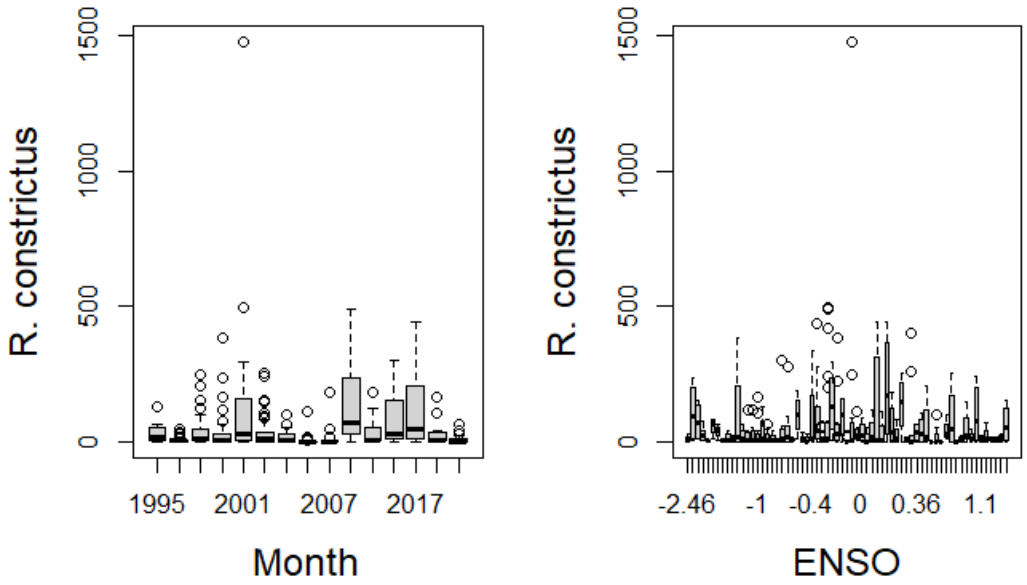

Fig. S4.4 – Month conditional box plot (Left) and ENSO conditional box plot (Right) of $CPUE_n$.

4.5. Independency

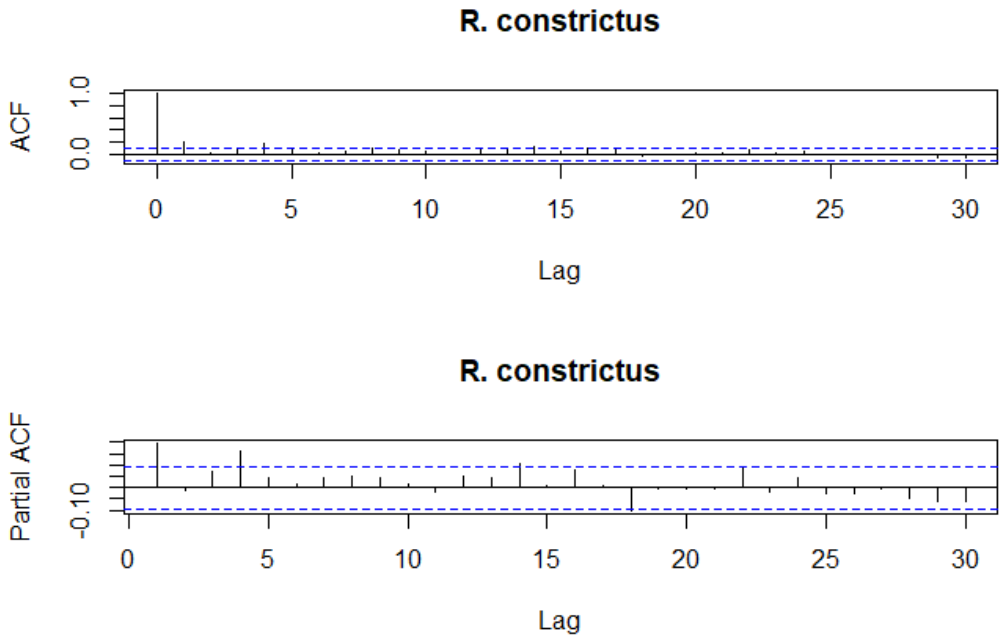

Fig. S4.5 – Auto-correlation function (ACF) and partial auto-correlation function (PACF) plot against time lag for *R. constrictus* $CPUE_n$.

4.6. Zeros

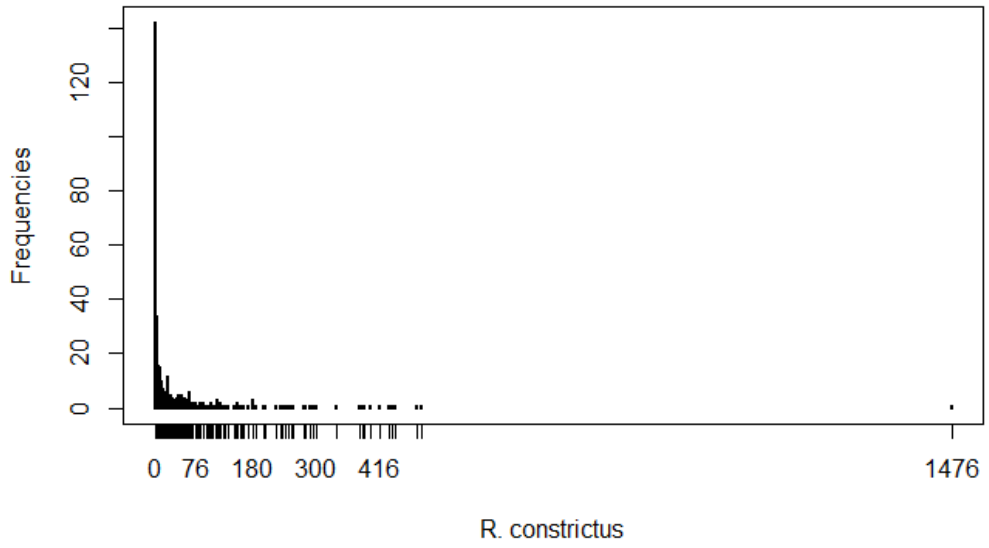

Fig. S4.6 – Frequency of *R. constrictus* $CPUE_n$.

4.7. Interaction

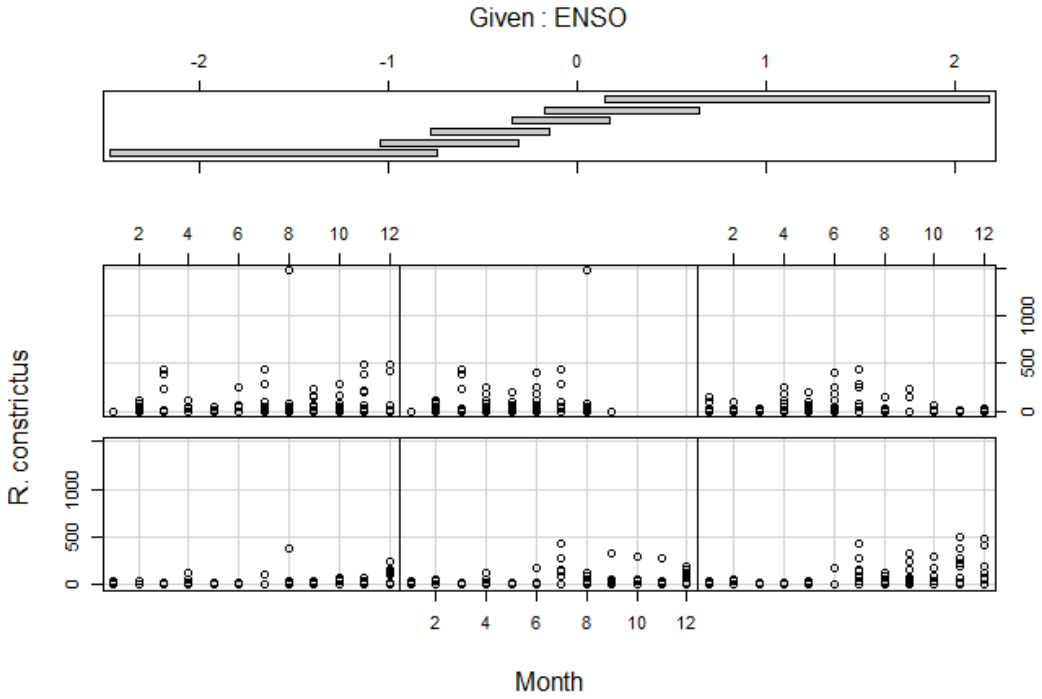

Fig. S4.7 – A coplot of *R. constrictus* $CPUE_n$ data against Month given the ENSO event.

4.8 Collinearity

Table. S4 – Values of VIF calculated for the numerical explicative variables. Temp – Bottom temperature (ºC), Sal – Bottom salinity, OM – Organic matter content (%), Phi – Granulometry and Rain – Rainfall.

Temp	Sal	OM	Phi	Rain
1.14	1.09	1.08	1.06	1.18

5) Sicyonia dorsalis

5.1. Relationship between dependent and explanatory variables

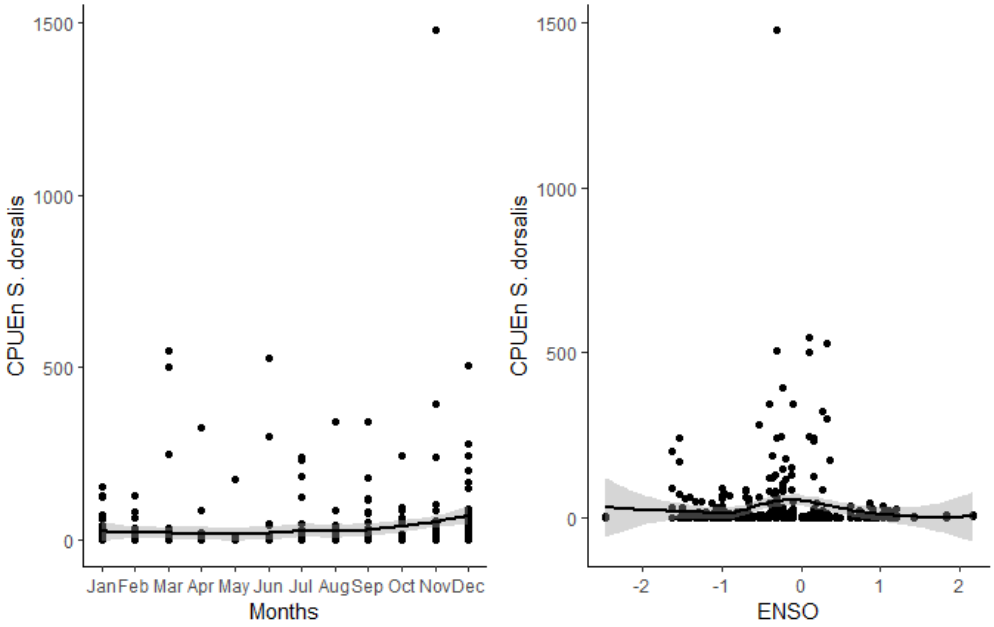

Fig. S5.1 – Scatterplots with a LOESS smoother between *S. dorsalis* $CPUE_n$ and its covariates months and ENSO.

5.2. Outliers and dispersion pattern

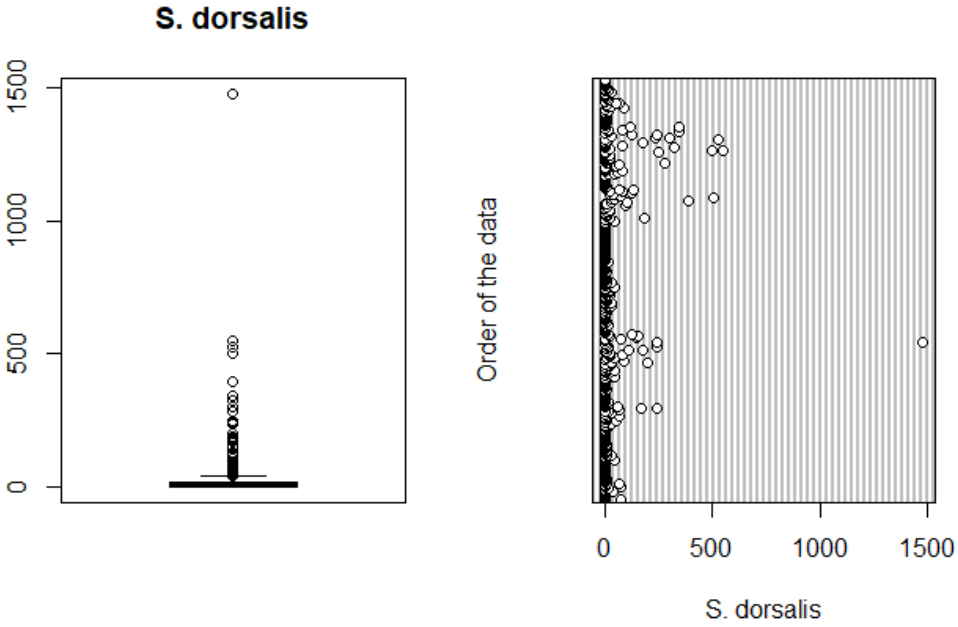

Fig. S5.2 – Box plot (Left) and Cleveland plot (Right) from *S. dorsalis* $CPUE_n$.

5.3. Normality

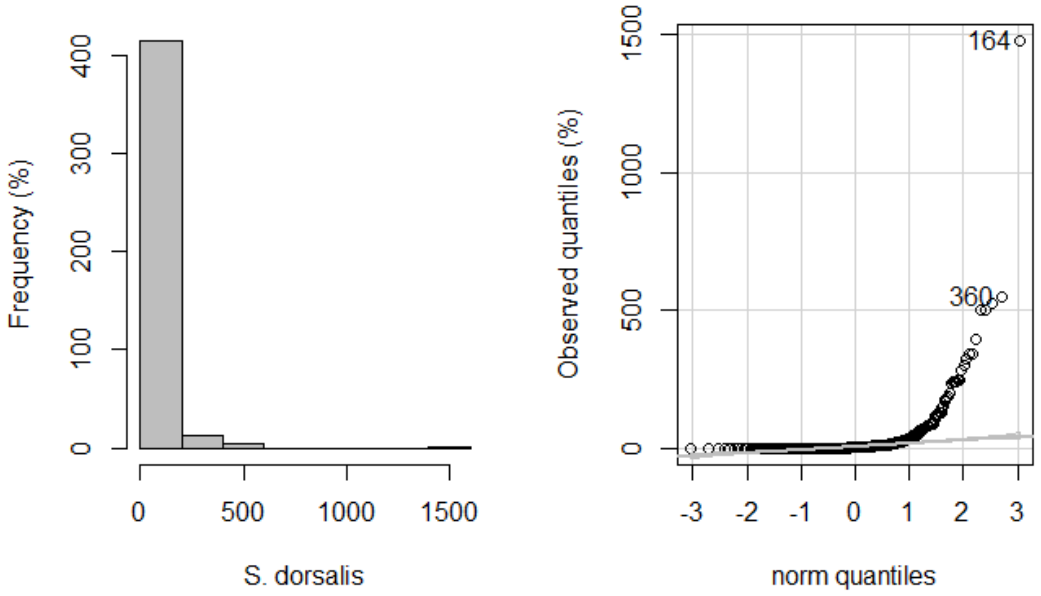

Fig. S5.3 – Histogram of *S. dorsalis* $CPUE_n$. (Left) and Q-Q plots (Right) of observed diversity against hypothetical normal distribution.

5.4. Homogeneity

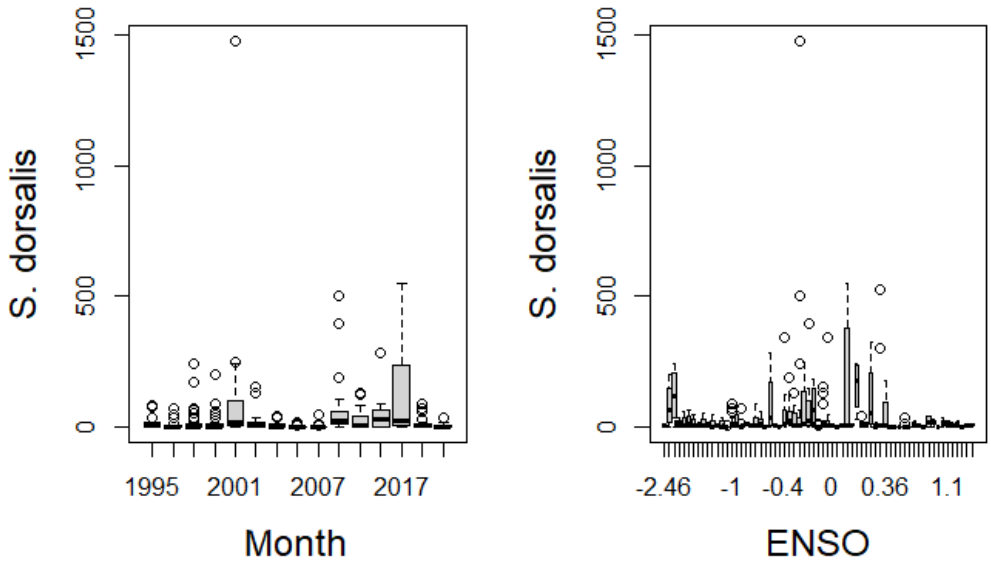

Fig. S4.4 – Month conditional box plot (Left) and ENSO conditional box plot (Right) of $CPUE_n$.

5.5. Independency

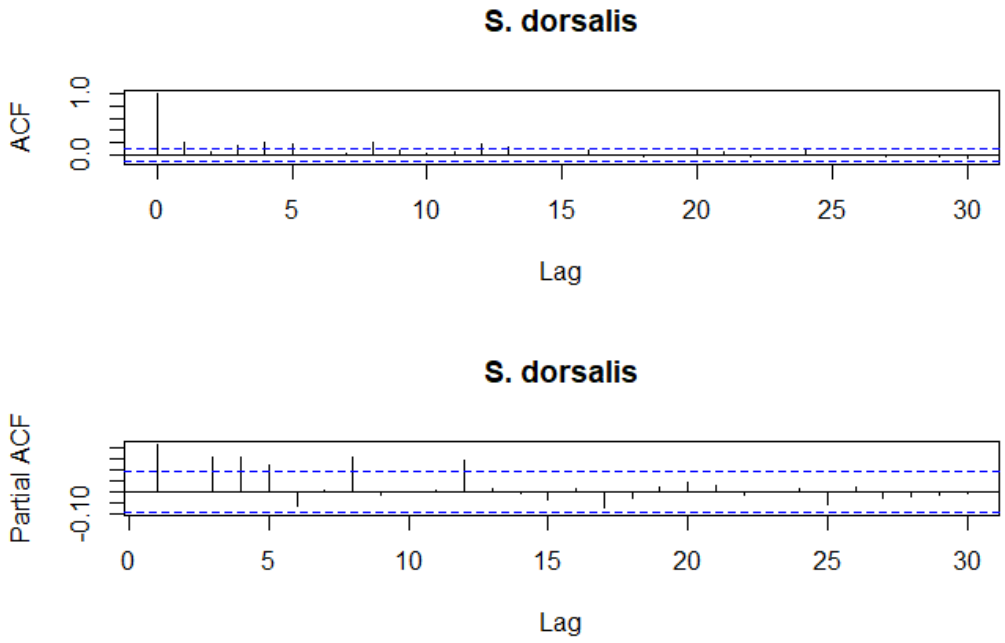

Fig. S5.5 – Auto-correlation function (ACF) and partial auto-correlation function (PACF) plot against time lag for *S. dorsalis* $CPUE_n$.

5.6. Zeros

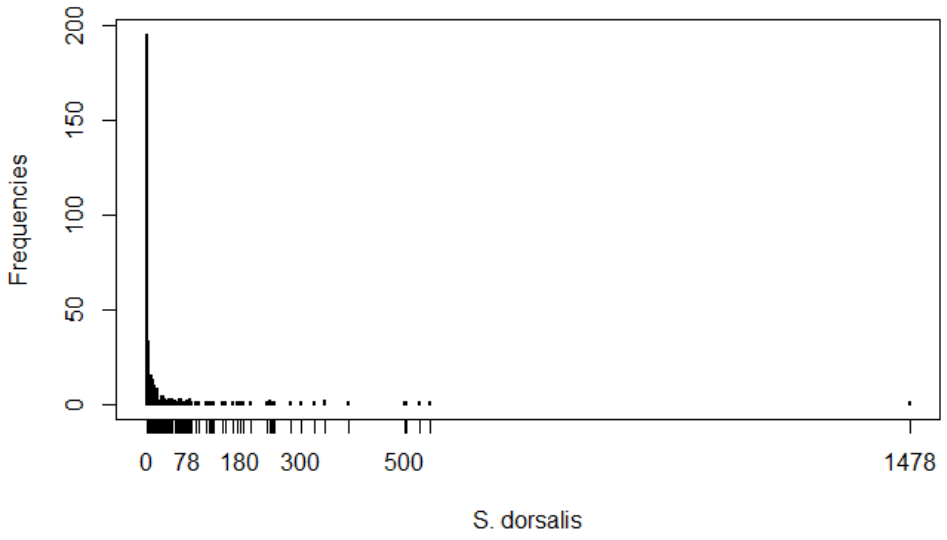

Fig. S5.6 – Frequency of *S. dorsalis* $CPUE_n$.

5.7. Interaction

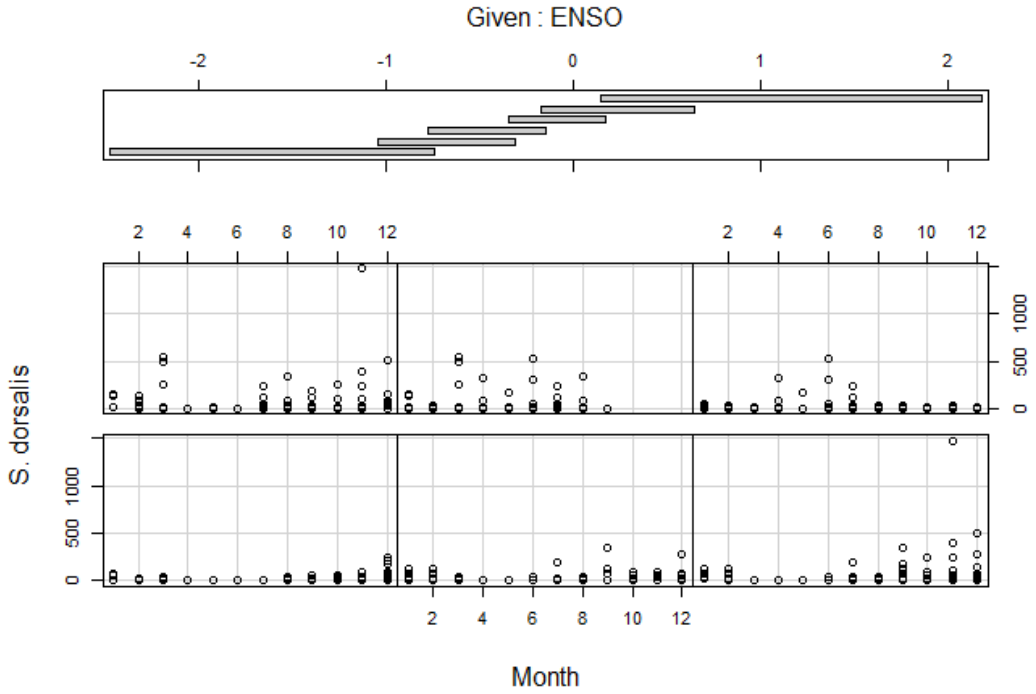

Fig. S5.7 – A coplot of *S. dorsalis* $CPUE_n$ data against Month given the ENSO event.

5.8 Collinearity

Table. S5 – Values of VIF calculated for the numerical explicative variables. Temp – Bottom temperature (ºC), Sal – Bottom salinity, OM – Organic matter content (%), Phi – Granulometry and Rain2 – Rainfall -2.

Temp	Sal	OM	Phi	Rain2
1.05	1.09	1.07	1.06	1.06

6) *Xiphopenaeus* spp.

6.1. Relationship between dependent and explanatory variables

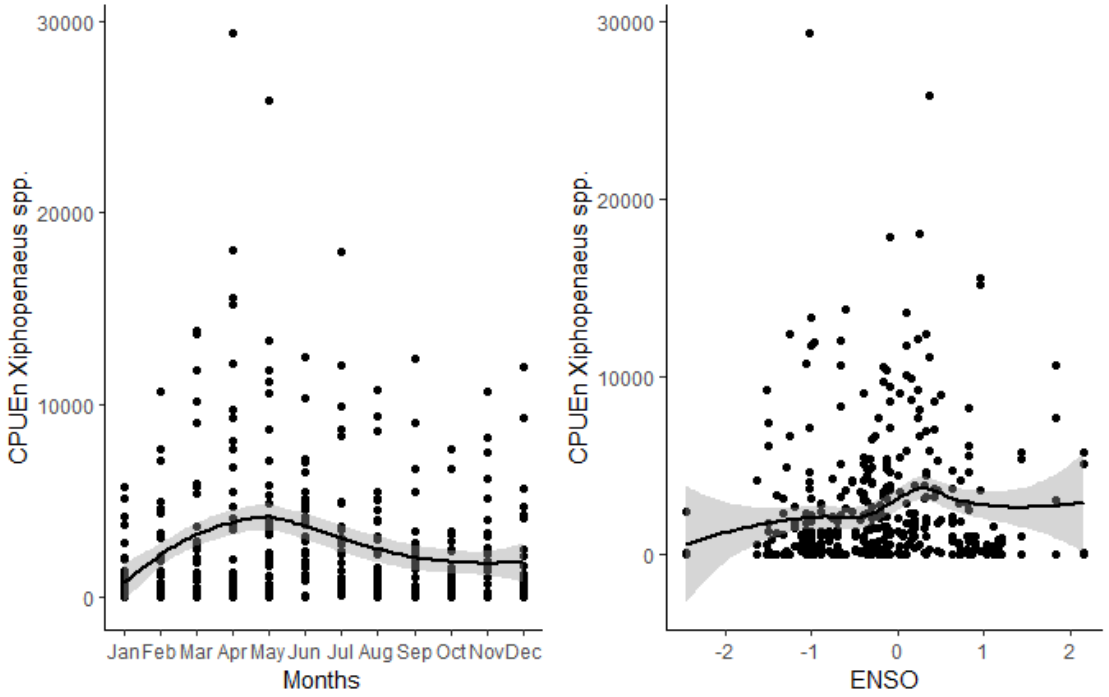

Fig. S6.1 – Scatterplots with a LOESS smoother between *Xiphopenaeus* spp. $CPUE_n$ and its covariates months and ENSO.

6.2. Outliers and dispersion pattern

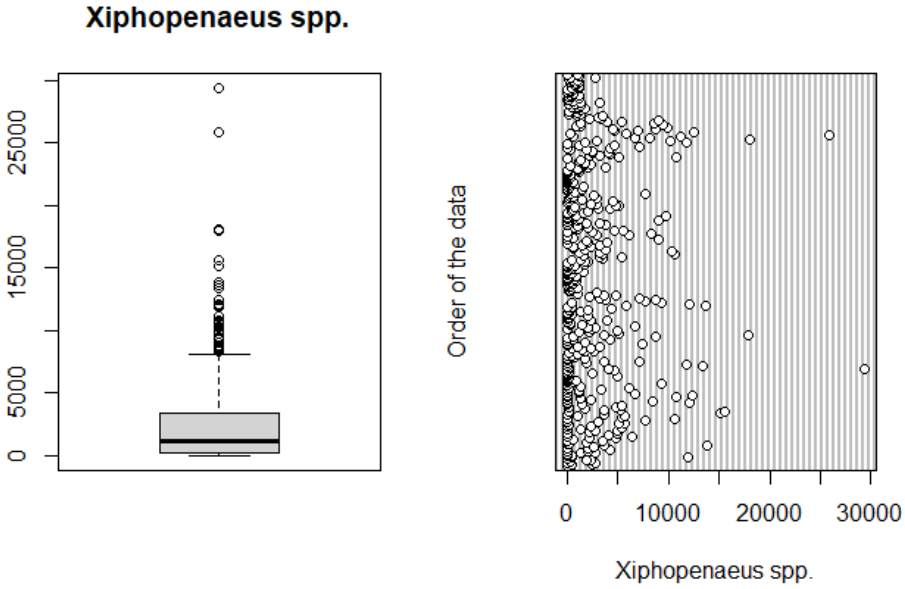

Fig. S6.2 – Box plot (Left) and Cleveland plot (Right) from *Xiphopenaeus* spp. $CPUE_n$.

6.3. Normality

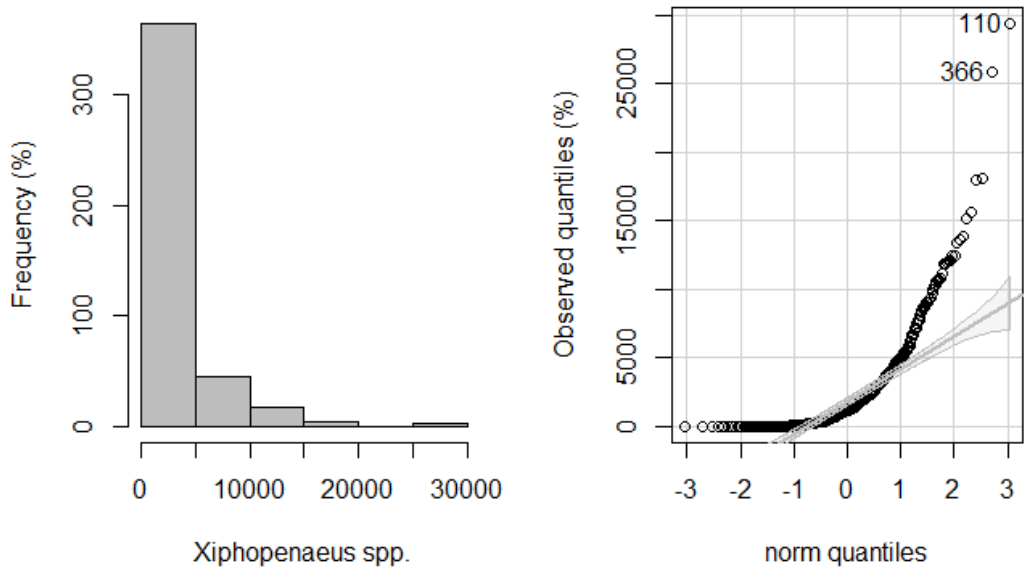

Fig. S6.3 – Histogram of *Xiphopenaeus* spp. $CPUE_n$. (Left) and Q-Q plots (Right) of observed diversity against hypothetical normal distribution.

6.4. Homogeneity

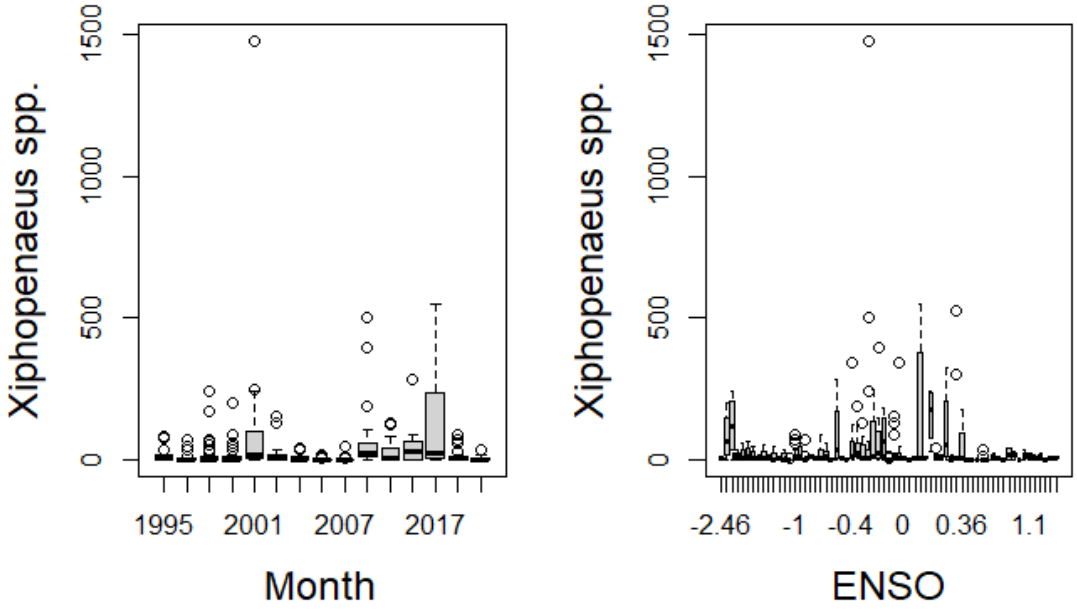

Fig. S6.4 – Month conditional box plot (Left) and ENSO conditional box plot (Right) of $CPUE_n$.

6.5. Independency

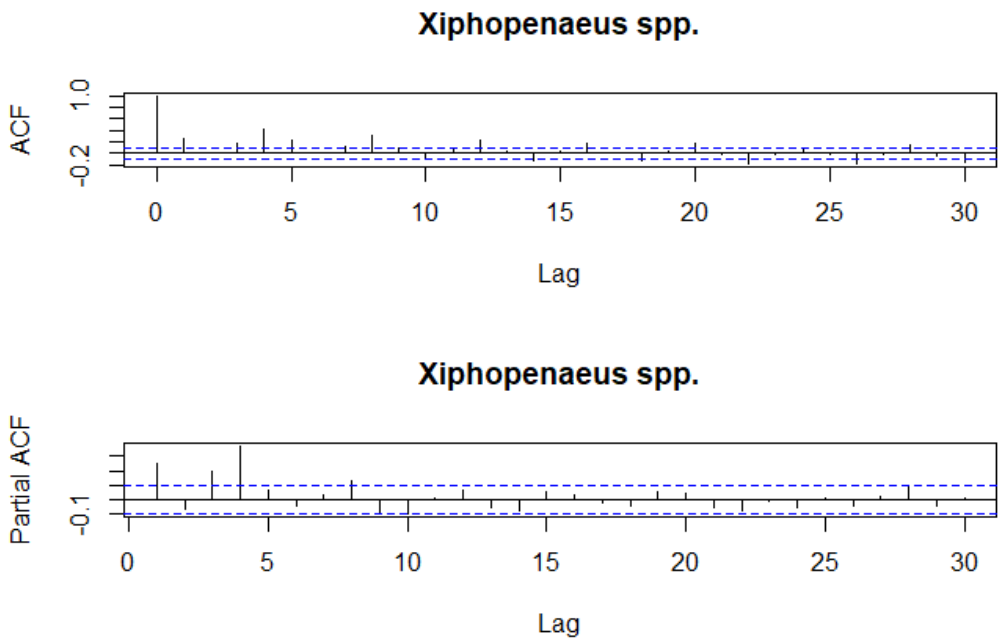

Fig. S6.5 – Auto-correlation function (ACF) and partial auto-correlation function (PACF) plot against time lag for *Xiphopenaeus* spp. $CPUE_n$.

6.6. Zeros

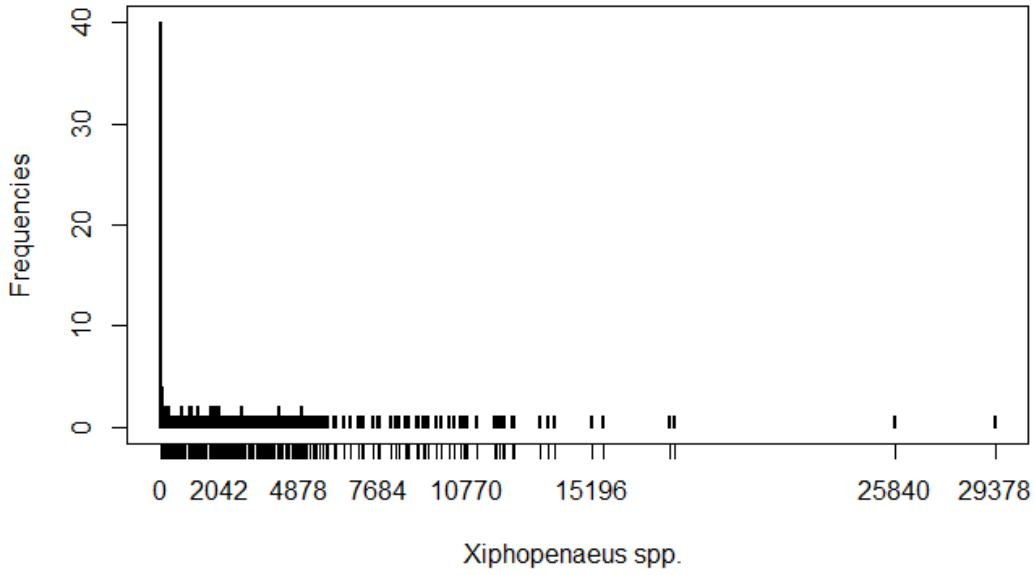

Fig. S6.6 – Frequency of *Xiphopenaeus* spp. $CPUE_n$.

6.7. Interaction

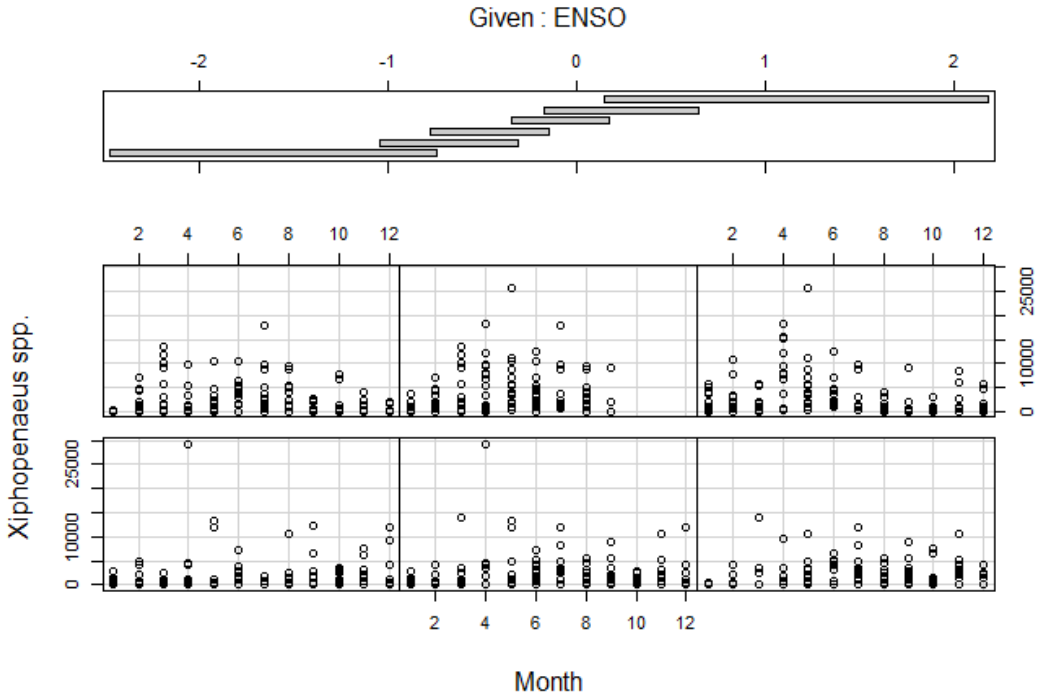

Fig. S6.7 – A coplot of *Xiphopenaeus* spp. $CPUE_n$ data against Month given the ENSO event.

6.8. Collinearity

Table. S6 – Values of VIF calculated for the numerical explicative variables. Temp – Bottom temperature (ºC), Sal – Bottom salinity, OM – Organic matter content (%), Phi – Granulometry and Rain2 – Rainfall -2.

Temp	Sal	OM	Phi	Rain2
1.05	1.09	1.07	1.06	1.06

7) Exhyppolysmata oplophoroides

7.1. Relationship between dependent and explanatory variables

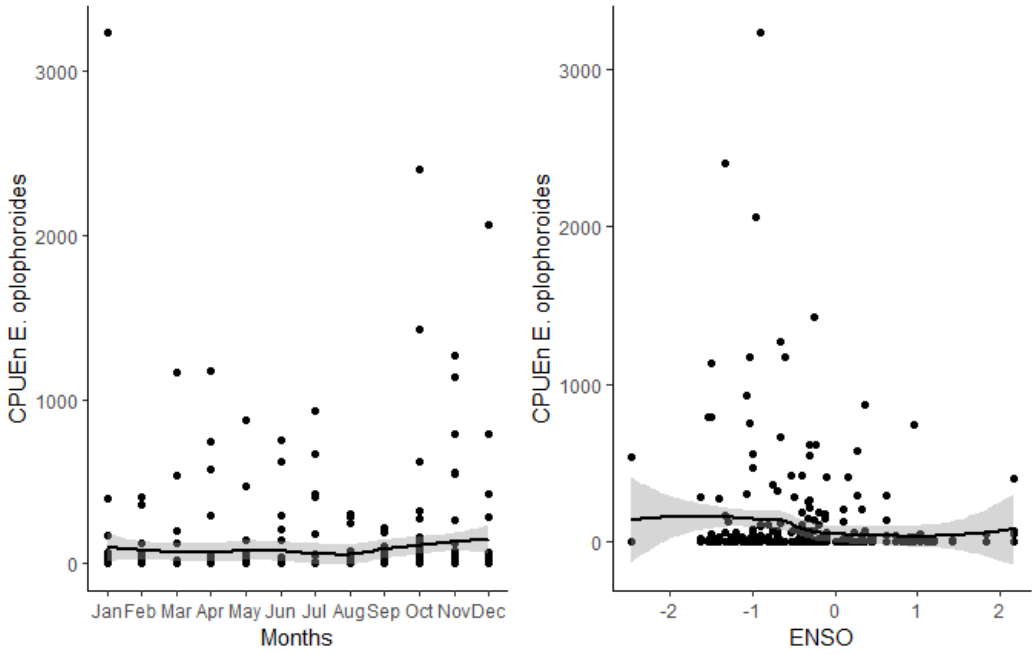

Fig. S7.1 – Scatterplots with a LOESS smoother between *E. oplophoroides* $CPUE_n$ and its covariates months and ENSO.

7.2. Outliers and dispersion pattern

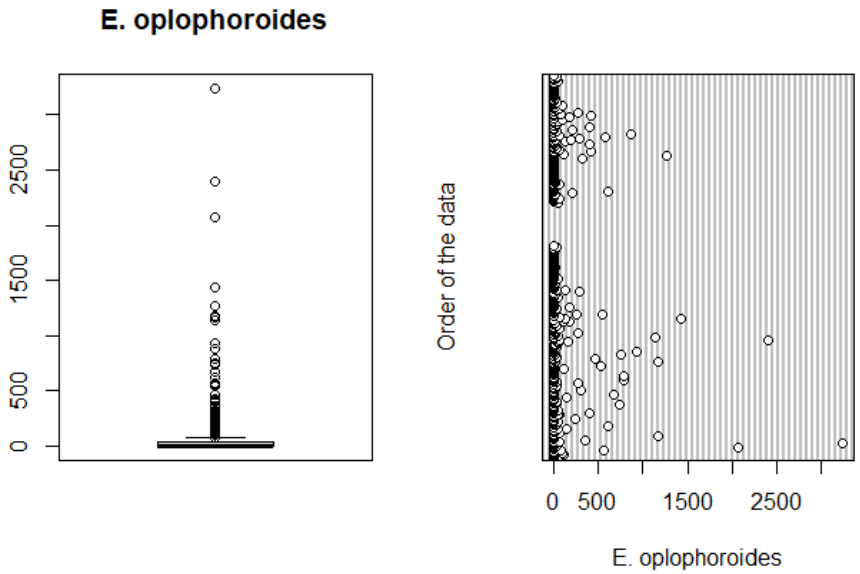

Fig. S7.2 – Box plot (Left) and Cleveland plot (Right) from *E. oplophoroides* $CPUE_n$.

7.3. Normality

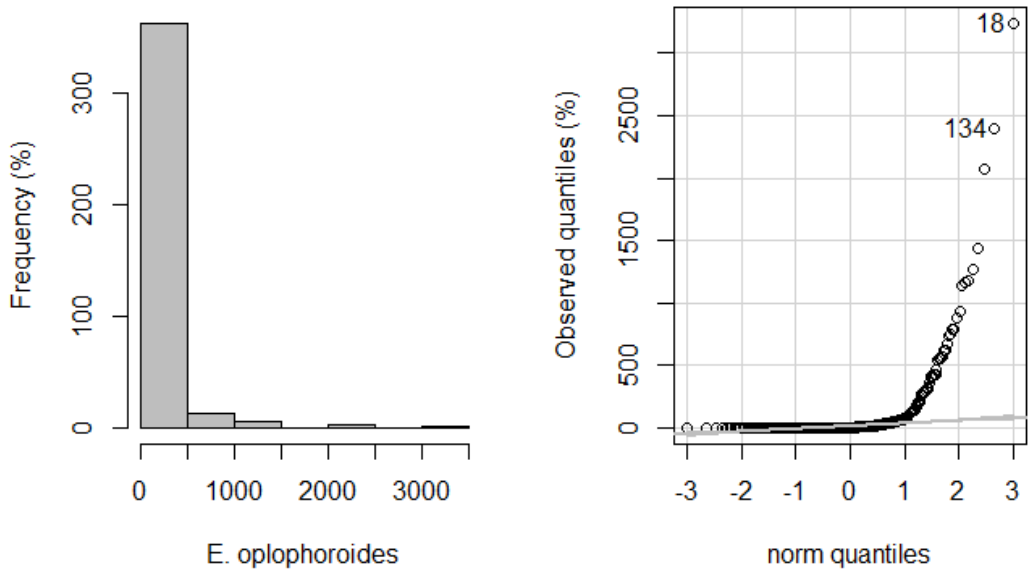

Fig. S7.3 – Histogram of *E. oplophoroides* $CPUE_n$. (Left) and Q-Q plots (Right) of observed diversity against hypothetical normal distribution.

7.4. Homogeneity

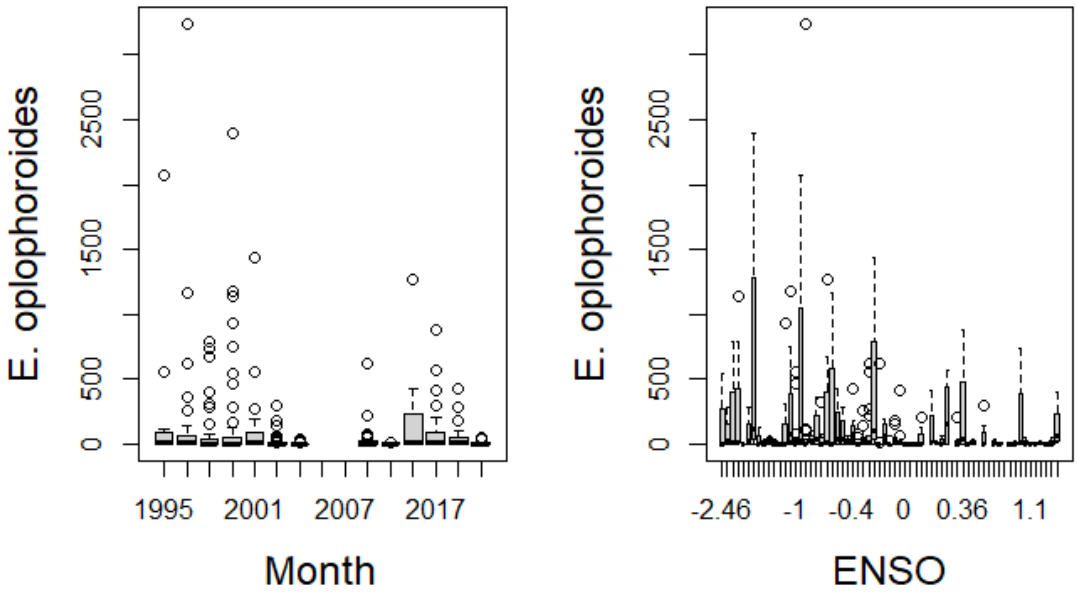

Fig. S7.4 – Month conditional box plot (Left) and ENSO conditional box plot (Right) of $CPUE_n$.

7.5. Independency

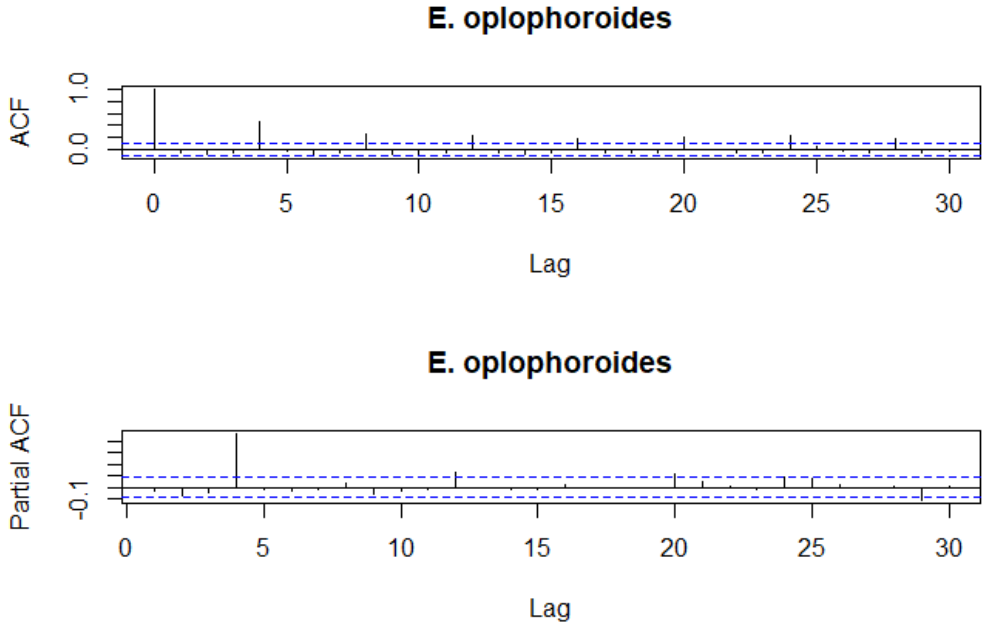

Fig. S7.5 – Auto-correlation function (ACF) and partial auto-correlation function (PACF) plot against time lag for *E. oplophoroides* $CPUE_n$.

7.6. Zeros

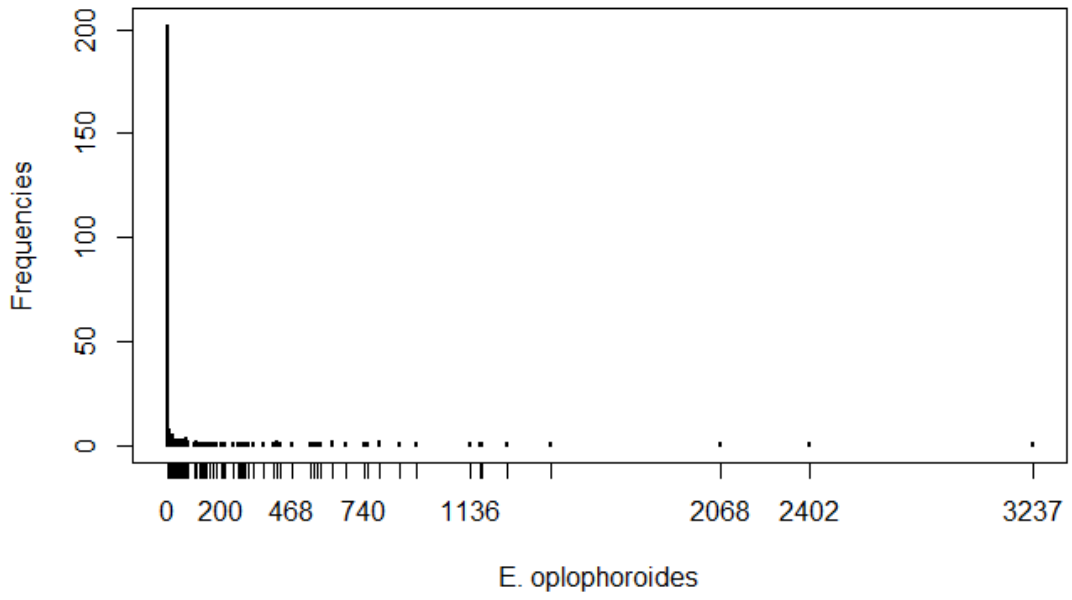

Fig. S7.6 – Frequency of *E. oplophoroides* $CPUE_n$.

7.7. Interaction

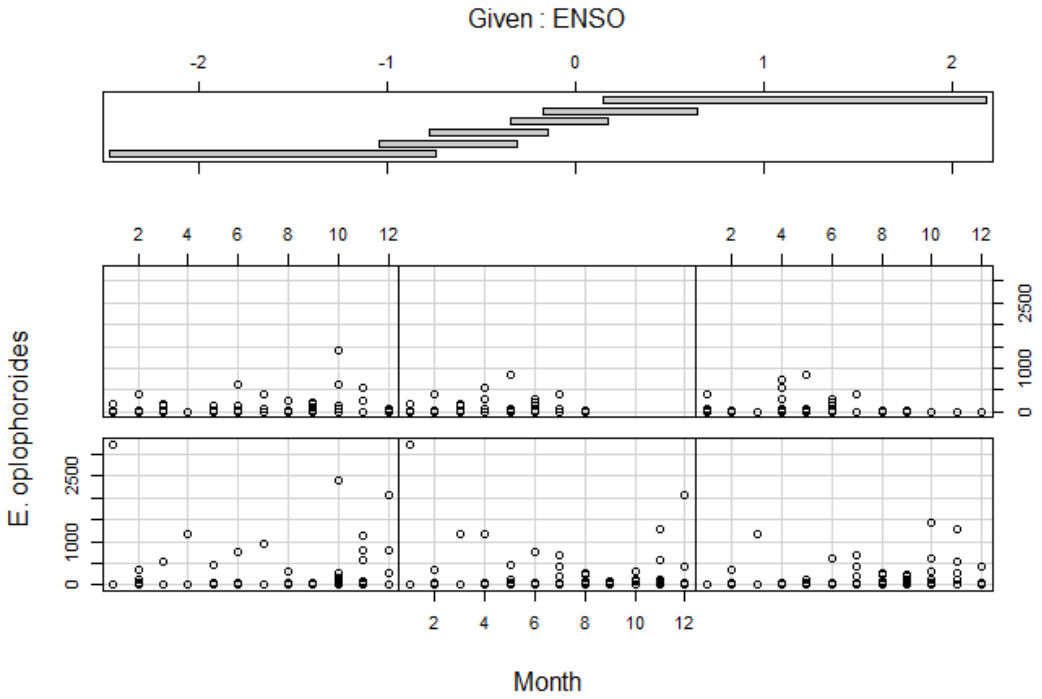

Fig. S7.7 – A coplot of *E. oplophoroides* $CPUE_n$ data against Month given the ENSO event.

7.8 Collinearity

Table. S7 – Values of VIF calculated for the numerical explicative variables. Temp – Bottom temperature (ºC), Sal – Bottom salinity, OM – Organic matter content (%), Phi – Granulometry and Rain2 – Rainfall -2.

Temp	Sal	OM	Phi	Rain2
1.06	1.06	1.06	1.04	1.07

8) Nematopalaemon schmitti

8.1. Relationship between dependent and explanatory variables

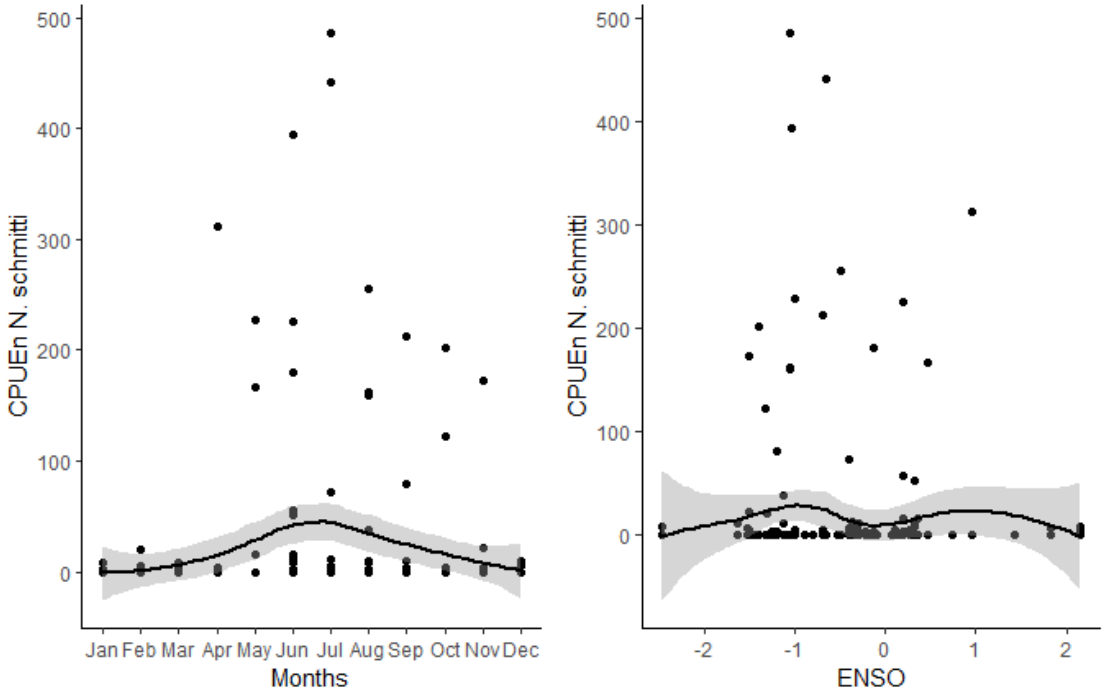

Fig. S8.1 – Scatterplots with a LOESS smoother between *N. schmitti* $CPUE_n$ and its covariates months and ENSO.

8.2. Outliers and dispersion pattern

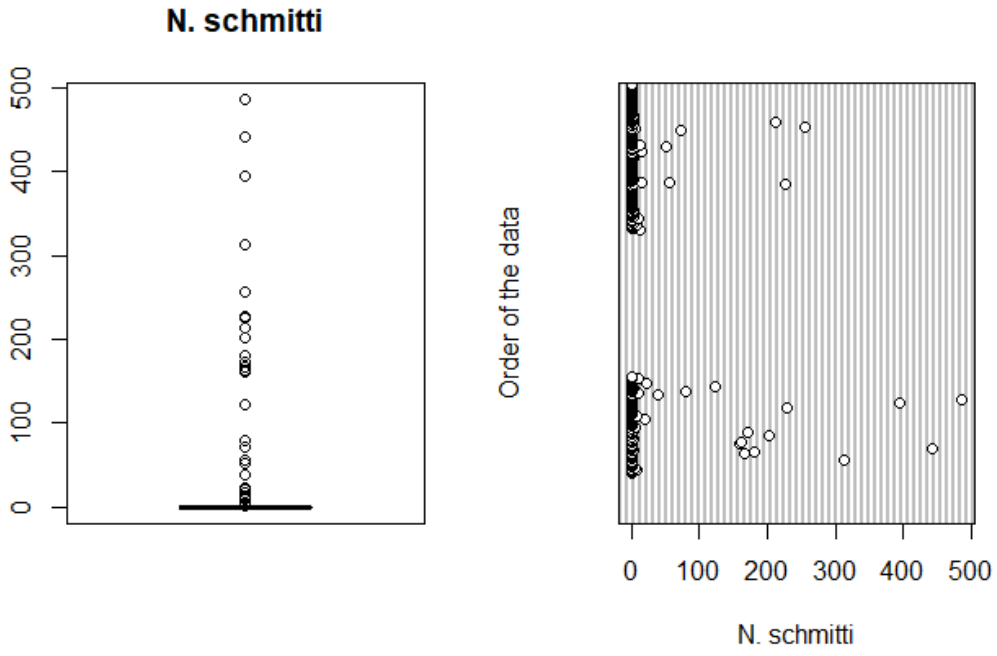

Fig. S8.2 – Box plot (Left) and Cleveland plot (Right) from *N. schmitti* $CPUE_n$.

8.3. Normality

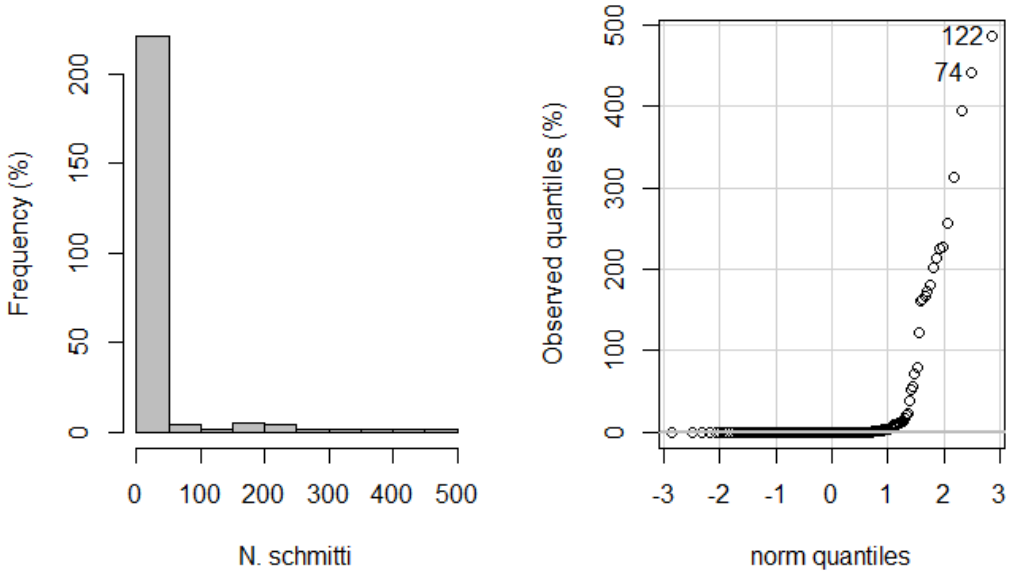

Fig. S8.3 – Histogram of *N. schmitti* $CPUE_n$. (Left) and Q-Q plots (Right) of observed diversity against hypothetical normal distribution.

8.4. Homogeneity

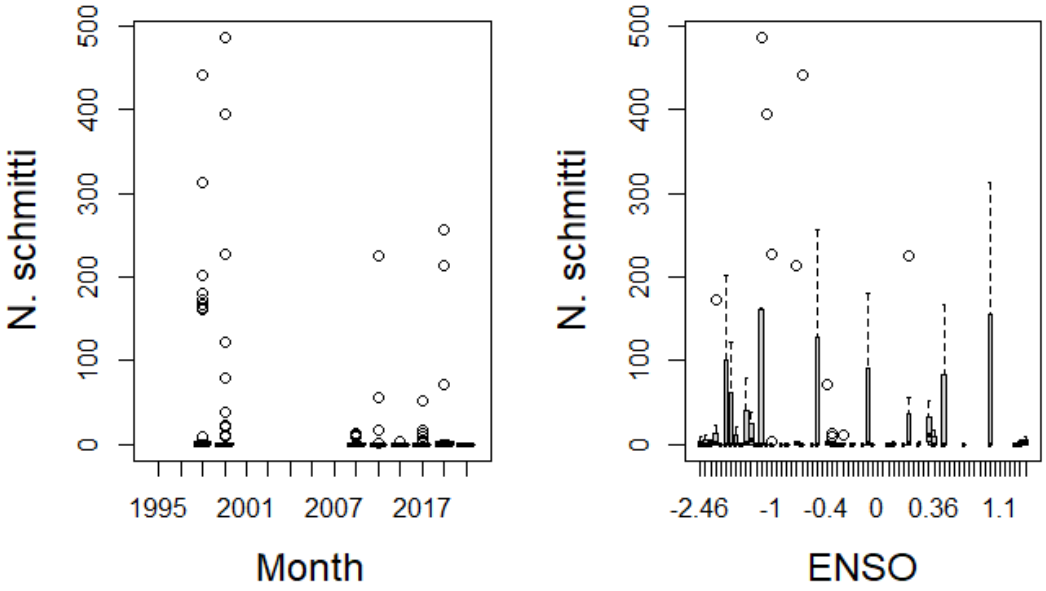

Fig. S8.4 – Month conditional box plot (Left) and ENSO conditional box plot (Right) of $CPUE_n$.

8.5. Independency

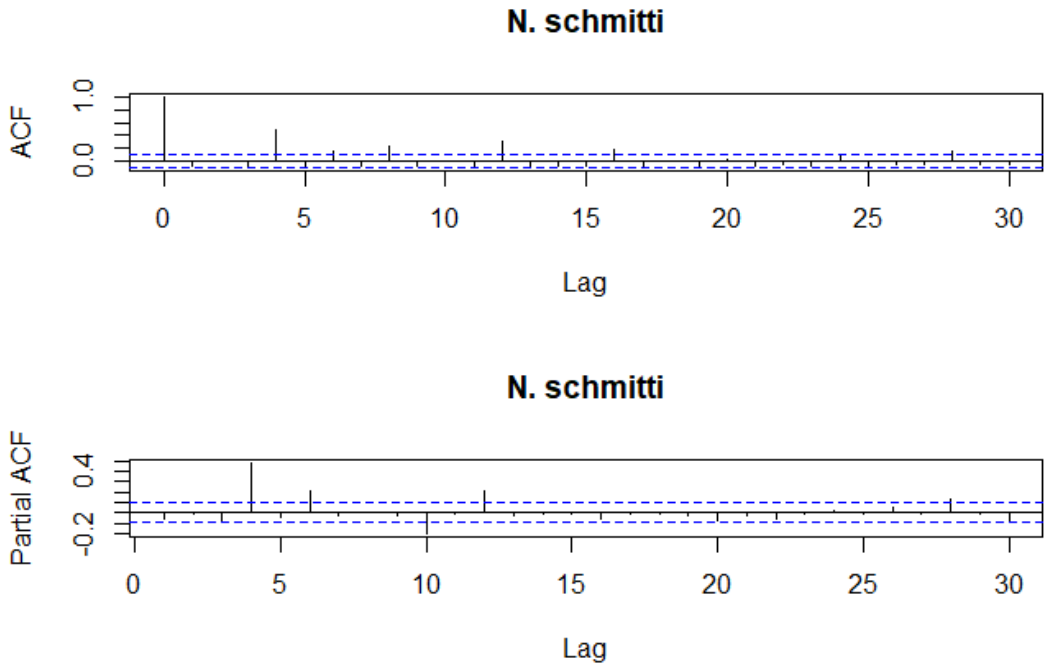

Fig. S8.5 – Auto-correlation function (ACF) and partial auto-correlation function (PACF) plot against time lag for *N. schmitti* $CPUE_n$.

8.6. Zeros

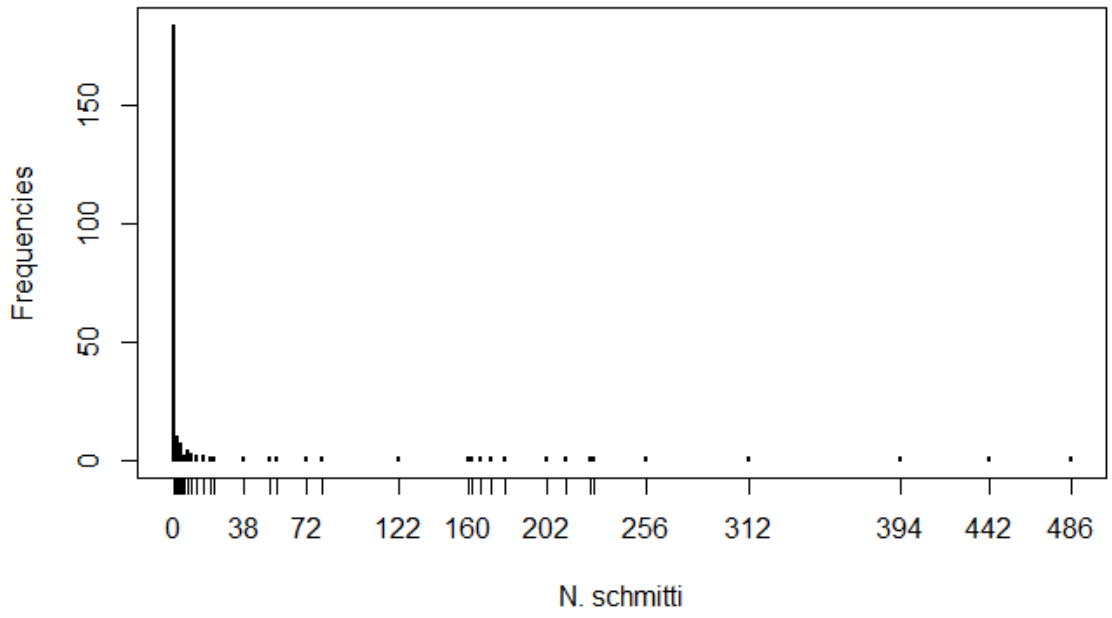

Fig. S8.6 – Frequency of *N. schmitti* $CPUE_n$.

8.7. Interaction

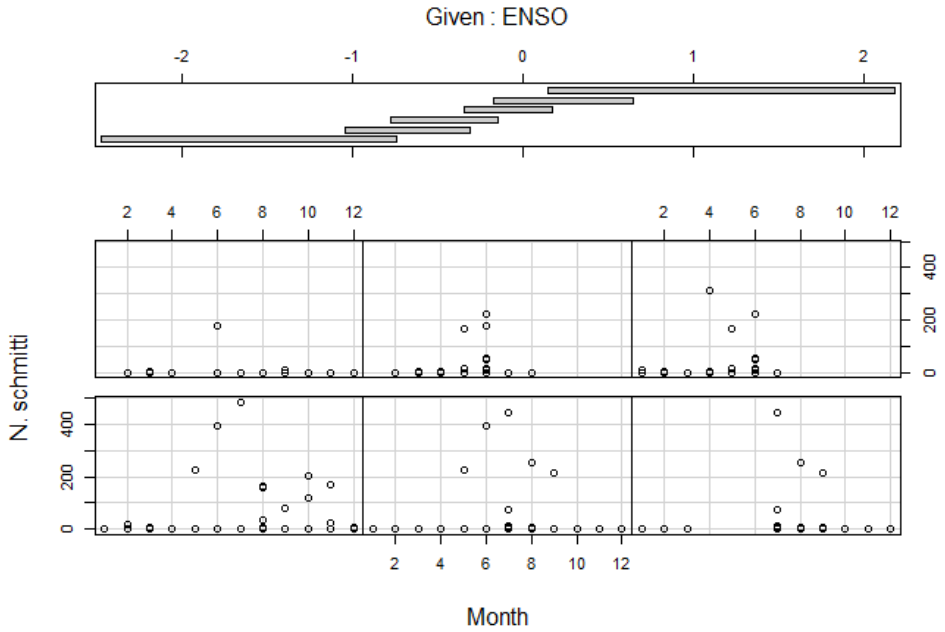

Fig. S8.7 – A coplot of *N. schmitti* $CPUE_n$ data against Month given the ENSO event.

8.8 Collinearity

Table. S8 – Values of VIF calculated for the numerical explicative variables. Temp – Bottom temperature (ºC), Sal – Bottom salinity, OM – Organic matter content (%), Phi – Granulometry and Rain – Rainfall.

Temp	Sal	OM	Phi	Rain
1.18	1.05	1.12	1.13	1.23

Capítulo 2

Long-term trends in shrimp abundance and diversity in a tropical bay

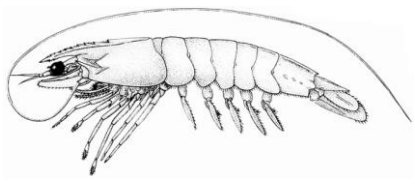

Long-term trends in shrimp abundance and diversity in a tropical bay

Abstract

Long-term monitoring is necessary to access the conservation status of commercial and non-commercial shrimp species. In this study we analyzed a fishery-independent dataset, that contained the abundance of nine shrimp species sampled in Ubatuba Bay, northern coast of São Paulo State, Brazil, over a 27-year period. We used the Principal Component Analysis (PCA) to investigate which species were associated at the bay, and the scores extracted from principal components (PCs) in which they were associated were used to represent the abundance of associated species. The variable PC1 represented *Farfantepenaeus brasiliensis*, *F. paulensis*, *Rimapenaeus constrictus*, *Xiphopenaeus* spp. and *Exhyppolysmata oplophoroides*. PC2 represented *Artemesia longinaris* and *Pleoticus muelleri*. PC3 represented *Litopenaeus schmitti* and *Sicyonia dorsalis*. Abundance of the species represented by PC1 did not vary through sampled years. Abundance of *A. longinaris* and *P. muelleri* were significatively higher in periods 4, 5 and 7. For *L. schmitti* and *S. dorsalis*, their abundance was significatively higher in period 7. Period 7 was also when diversity varied significatively, being higher than in other periods. Temperature was the environmental factor that influenced the variance in abundance of the species represented by PC2 and PC3, and also diversity. The decrease in temperature resulted in higher abundances. The lower temperatures are and indicator of the South Atlantic Central Water intrusion in the southeast coast. Also, higher values of ONI index (i.e., El Niño) results in decrease in the abundance of *L. schmitti* and *S. dorsalis*. Period 7, was a period of neutrality, in which the SACW effects were enhanced.

Keywords: Artisanal fisheries, Biodiversity, Penaeoidea, Trawling.

Introduction

Anthropogenic pressure is one of the main causes of biodiversity loss in the 21th century, to the point it was nominated the 'sixth mass extinction" (Leakey and Lewin 1992). While the prior extinction events in history were caused mostly by massive basaltic volcanic eruptions, impacts of asteroids, global climate changes, among others (Ward 2000; Keller 2008), current events of species loss result from human actions (e.g., deforestation, pollution, species introduction) (Chapin III et al., 2000).

In marine ecosystems, the main causes of biodiversity loss are linked to habitat degradation, climate change, and fishing. Ecosystem effects of fisheries include shifts in food-web structure, earlier age-at-maturity, fauna dominated by small sized individuals, mortality of non-targeted species (e.g., bycatch and ghost fishing), and reduction of habitat complexity (Kaiser, 2002). Out of all the fishing methods, bottom trawling is the most adopted in shrimp and prawn fisheries worldwide (Rezende et al., 2019; Hornborg et al., 2020; Lira et al., 2021).

Shrimps are fished offshore by industrial fleets and in coastal areas by artisanal ones. The industrial fleet is characterized by multiple large sized vessels owned by companies, that can fish for several days prior landing. The artisanal fishery however, consists of small owner-operated boats of less than 12 meters, that fishes in coastal areas targeting local sale (Pauly 2018). It has great economic and social importance specially in developing countries, being the main source of income and animal protein for families of fishers (Begossi et al., 2011).

In shallow tropical marine ecosystems, the artisanal fleet targets shrimps belonging to the superfamily Penaeoidea, as these areas are important nursing and recruiting grounds to commercial shrimps (Bauer, 2020). Therefore, trawling in coastal areas usually leads to great mortality of young individuals, which negatively impacts on

population dynamics, and consequently in stocks recovery overtime. Monitoring temporal trends in abundance is imperative to stocks assessment and management. While spatial patterns of organism's abundance and occurrence have been extensively investigated, studies accounting for species abundance over time are less common (Magurran, 2007), especially those whose data was collected using consistent methods over decades (Magurran & Henderson 2010).

In the present study, we evaluated shrimp abundance data using a 27-year period dataset from fishery-independent trawls conducted in the Ubatuba Bay, in southeastern Brazil. This bay is a traditional fishing ground for the seabob shrimp *Xiphopenaeus kroyeri* (Heller, 1862), one of the most economically and socially important species captured in the coast of São Paulo State (Graça-Lopes et al., 2007). In 2021, 77 double rigged boats were responsible for landing 132 ton of seabob shrimp in the municipality of Ubatuba (IP/APTA/SAA/SP, 2022).

The bycatch resulted from the seabob shrimp artisanal fisheries exceeds the biomass of targeted species, and after fishes, crustaceans are the most captured (Branco et al, 2015). Species of penaeoids such as the pink shrimps *Farfantepenaeus brasiliensis* (Latreille, 1817) and *F. paulensis* (Pérez-Farfante, 1967), the white shrimp *Litopenaeus schmitti* (Burkenroad, 1936), the Argentine stiletto shrimp *Artemesia longinaris* Bate, 1888, the Argentine red shrimp *Pleoticus muelleri* (Bate, 1888), the roughneck shrimp *Rimapenaeus constrictus* (Stimpson, 1874), and the lesser rock shrimp *Sicyonia dorsalis* Kingsley, 1878, are frequent and abundant in the *X. kroyeri* bycatch (Mantelatto et al., 2016; Bochini et al., 2019). With the exception of *S. dorsalis*, and the caridean shrimp *Exhippolysmata oplophoroides* (Holthuis, 1948), the remaining shrimp species are economically important.

Considering the importance of monitoring and an expected negative influence of

fisheries in the assemblage, the study investigated the long-term trends in shrimp species abundance and biodiversity in a tropical bay by answering the following questions: (i) which species are associated temporally? (ii) how did abundance and diversity vary through years?

Material and Methods

Study area

Located in the northern coast of São Paulo State, Ubatuba Bay, is part of the coastal portion of the Biogeographic Province of the State of São Paulo, a zone of faunal transition, in which the fauna is of tropical and Patagonian origin (Palacio, 1982; Sumida & Pires-Vanin, 1997). The bay has a total area of 8 Km2 (Mantelatto & Fransozo, 1999), and is protected from south and southeast waves from the open sea (Muniz et al., 2006).

Ubatuba Bay is included in the Cunhambebe sector of the marine protected area (MPA) in the northern coast of São Paulo State (Decree No. 53 525, October 08, 2008). This MPA was created to ensure the conservation and sustainable use of marine resources, therefore fishing is only permitted for the subsistence of local communities (i.e., artisanal fishing) outside the bay or within the bay in areas above 5 m of depth (Bernardes et al., 2020).

Data collection

Sampling was conducted monthly during nine years between September 1995 to June 2022 (Table 1) in four sites at the bay (Figure 1). Shrimps were captured through the years with the same shrimp fishing vessel, equipped with double rig nets, with 20 mm mesh in the wings and 18 mm mesh at the cord end, and towed at an average speed of 1.7 knots. Four hauls (half an hour per site – 18,000 m^2 per trawl) were carried out during daylight in the study area (Figure 1). The sites were chosen considering their position at the bay, depth and wave exposition. Site 1 is deeper and more exposed while Site 3 is the shallowest. As for Site 2, it is most influenced by wave action, whereas Site 4 is the most sheltered, with less wave action (Perroca et al., 2022). An echo sounder coupled to a GPS (Global Positioning System) was used to measure the depth of each sampling site and guarantee the location of the trawling (Table 2).

Table 1 – Sampling periods between 1995 and 2022 in Ubatuba Bay, southeastern coast of Brazil

1	September 1995 to August 1996
2	January to December 1998
3	January to December 1999
4	July 2001 to June 2002
5	July 2002 to June 2003
6	July 2006 to June 2007
7	July 2013 to June 2014
8	October 2016 to September 2017
9	July 2021 to June 2022

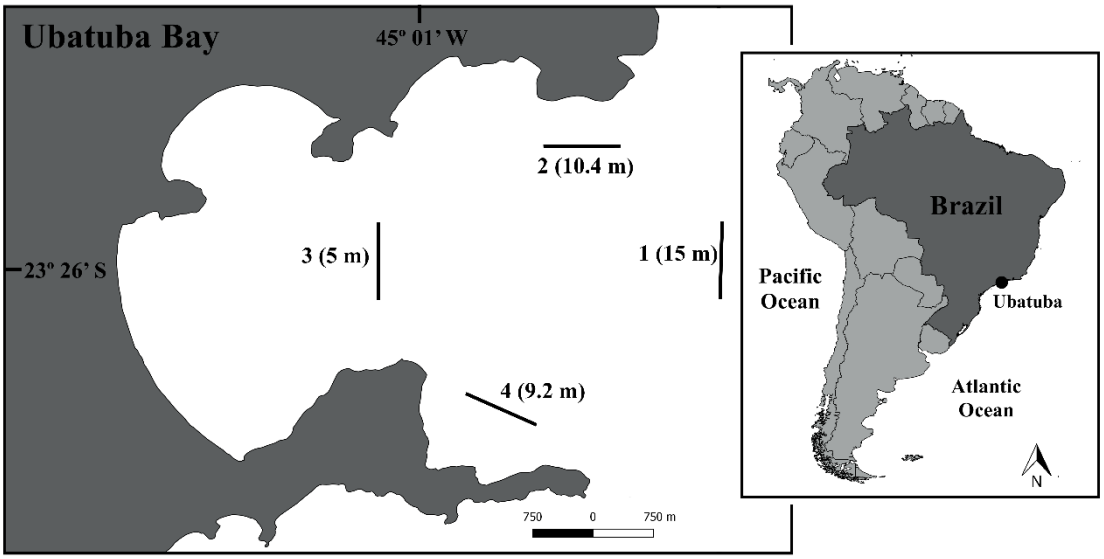

Figure 1 – The sampling sites (1, 2, 3 and 4) in Ubatuba Bay, São Paulo State, Brazil

Table 2 – Depth (m) and location (GPS) of each collection site.

Site	Depth (m)	Location (GPS)
1	15 m	23° 26' 42'' S / 44° 59' 57'' W
2	10.4 m	23° 25' 16'' S / 45° 00' 57'' W
3	5 m	23° 26' 48'' S / 45° 02' 12'' W
4	9.2 m	23° 26' 33'' S / 45° 03' 15'' W

After hauls, shrimps were packed in labeled plastic bags with ice, and kept in coolers until they arrived in the laboratory. Shrimps were identified according to Pérez-Farfante and Kensley (1997) and Costa et al. (2008), and counted (n). Additionally, with the description of a new seabob shrimp (i.e.; *Xiphopenaeus dincao* Carvalho-Batista, Terossi, Zara, Mantelatto, Costa, 2020) for the area, and the impossibility of identification of past sampled years all data regarding *X. kroyeri* will be considered in this work as *Xiphopenaeus* spp.

The samples were carried out by the NEBECC (Study Group on Crustacean Biology, Ecology and Culture) and LABCAM (Laboratory of Biology of Marine and Freshwater Shrimps) study groups of the São Paulo State University, as part of several master's and doctoral research projects.

Data analysis

Abundance was used to estimates indices of catch-per-unit-effort ($CPUE_n$: $shrimps.h^{-1}$) for each species to standardize response variables. Our dataset comprised nine response variables ($CPUE_n$ *A. longinaris*, $CPUE_n$ *F. brasiliensis*, $CPUE_n$ *F. paulensis*, $CPUE_n$ *L. schmitti*, $CPUE_n$ *P. muelleri*, $CPUE_n$ *R. constrictus*, $CPUE_n$ *S. dorsalis*, $CPUE_n$ *Xiphopenaeus* spp., $CPUE_n$ *E. oplophoroides*) and two explanatory variables (Periods, Sites).

The abundance matrix was used to estimate the Bray-Curtis dissimilarity matrix, in order to determine the statistical differences between shrimp assemblages among the sampling periods through a permutational multivariate analysis of variance (PERMANOVA; $p = 0.05$; Anderson, 2001). When differences in assemblages between different periods were confirmed, a multivariate Student's t test was applied with a significance level of 5% ($p < 0.05$). Then, and Indicator Species Analysis (ISA) (Dufrêne

& Legendre, 1997) was performed to the differences between the sampling periods highlighted by the PERMANOVA and its post-test, in order to determine which species are important in temporal patterns. The advantage of using the ISA, it is that it accounts for the abundance and frequency of species, and also is calculated independently for each species in the assemblage (Bakker, 2008). The PERMANOVA was performed using the vegan package (Oksanen et al., 2022), and its post-test using the function *pairwise* adonis from package pairwiseAdonis (Arbizu, 2020). The period 6 was removed from the PERMANOVA and ISA analysis due to the presence of NAs in the *E. oplophoroides* data. The Bray-Curtis dissimilarity matrix does not accept NAs; therefore, we choose to remove a sampling period instead of removing a specie.

To access temporal trends in species' abundance, first we identified which shrimp species were associated to each other at the bay, through an Analysis of Principal Components (PCA). A Hellinger transformation was used prior to the PCA, in order to reduce the effect of large abundances (Legendre & Gallagher, 2001). The resulting significative principal components (PCs) were fitted in a correlation matrix (Spearman's correlation) with the species $CPUE_n$ to correlate these variables. The variables *F. brasiliensis*, *F. paulensis*, *R. constrictus*, *Xiphopenaeus* spp., and *E. oplophoroides* were correlated with PC1. *Artemesia longinaris* and *P. muelleri* were correlated with PC2, and *L. schmitti* and *S. dorsalis* were correlated with PC3.

Generalized Linear Mixed Models (GLMMs) were fitted to each PC to investigate the variance in species abundance overtime. GLMMs were chosen because they provide a more flexible approach when analyzing nonnormal data when random effects are present (Bolker et al., 2008), such as the sampling sites. The variable Period was considered as the fixed effect, and the sites were considered as the random effect. Also due to the temporal dependency registered in the data exploration, the models contained

an autocorrelation structure of order 1. Models were fitted with the Tweedie family distribution, once data was non-continuous, non-normal, non-integer (Supplementary material). All models were adjusted with the function glmmTMB from the package glmmTMB (Brooks et al., 2017). The graphical outputs were plotted with packages ggplot2 (Wickham, 2016) and visreg (Breheny & Burchett, 2017).

GLMMs were also fitted to ecological models, in order to assess the influence of environmental factors and El Niño Southern Oscillation (ENSO) in the assemblage. For each PC we fitted models with all the environmental factors and explored the effect of dropping terms. All the models with $\Delta AICc < 2$ had substantial support to be considered as the best model (Burnham & Anderson, 2002). When more than one model presented $\Delta AICc < 2$ the most parsimonious model was chosen. The ecological models were also fitted with the Tweedie family distribution.

To analyze the temporal trends in shrimps' diversity, the original dataset was used to calculate the monthly taxonomical diversity by sites, for each sampling year, which was considered the alfa diversity. Then, alfa diversity was corrected based on the concept of "equivalent communities" (Jost 2006), and it was estimated that $q = 1$ (N1 = Shannon diversity) in order to present the same sensitivity to common and rare species (Hill, 1973; Jost 2006). This was considered the exponential of Shannon. The correction was performed using the package Vegan (Oksanen et al., 2022).

The values of the exponential of Shannon were considered as the response variable in order to access if there was variation in diversity of shrimps at the bay through time. A Generalized Linear Mixed model was fitted using the Period as the fixed effect and sites as random effects. This model also contained a correlation structure of order 1 due to temporal dependency on the biodiversity data. The model was fitted following the same methodology applied to the PCs data. All analyses were performed on RStudio, Version

1.4.1103 (R Studio Team, 2021).

Results

Environmental factors

Higher Rainfall mean values were registered in periods 1 and 2, and the lower mean values in periods 5 and 8 (Fig. 2A). The higher mean values of salinity were registered in period 7, and the lower in period 1 (Fig. 2B). As for temperature, the higher mean values were registered in period 8, and the lowest in period 3 (Fig. 2C). The higher mean values of organic matter content were registered in period 1, and the lower in period 5 (Fig. 2D). The highest mean values of Phi were registered in periods 5 and 8, and the lowest in period 9 (Fig. 2E). The higher ENSO mean values were recorded in periods 5 and 6, and the lower in period 3 (Fig. 2F).

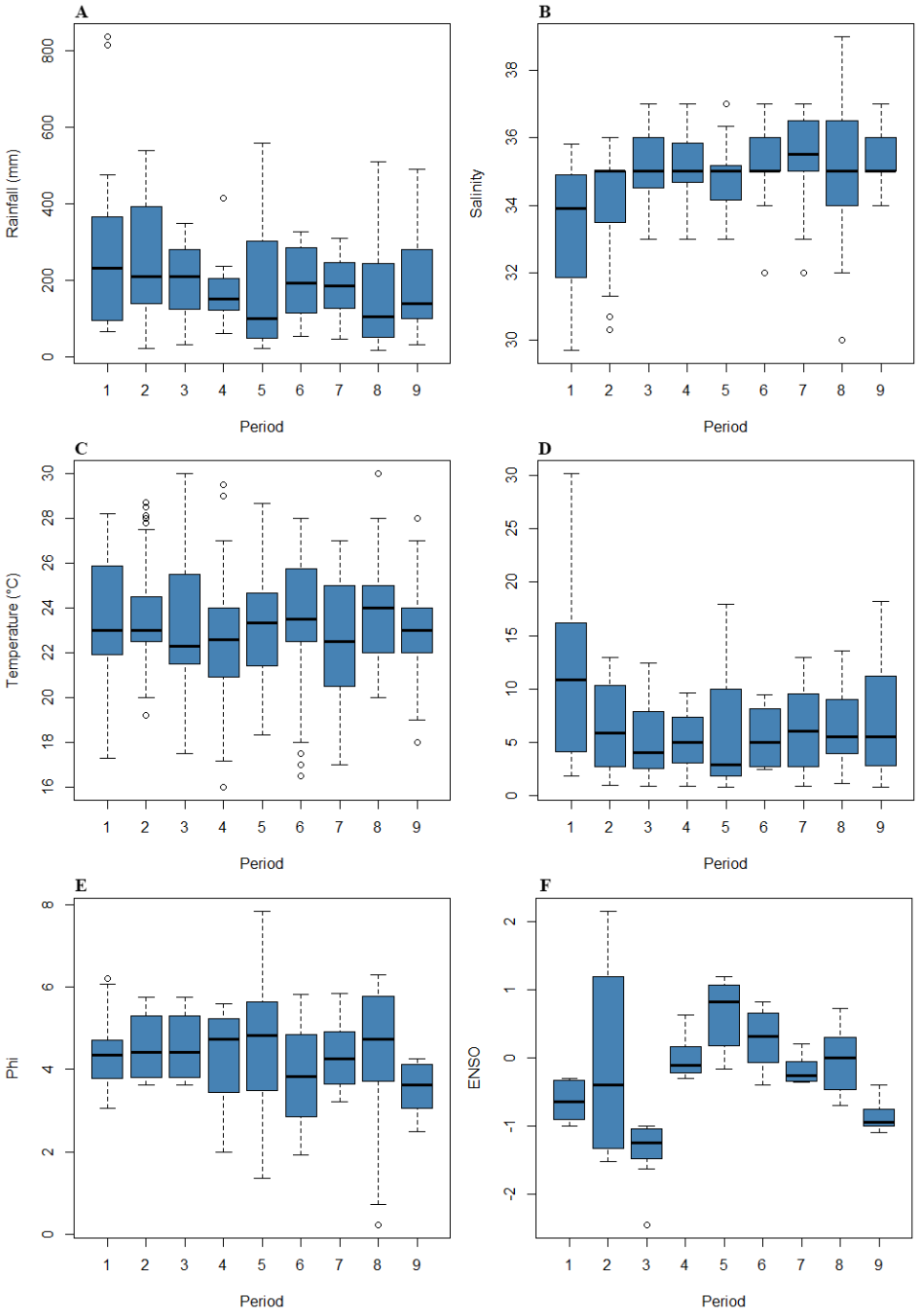

Figure 2 – Mean values, and minimum and maximum amplitudes of [A] Rainfall (mm), [B] Bottom water salinity, [C] Bottom water temperature (◦C), [D] Organic matter content, [E] Phi during, [F] El Niño Southern Oscillation the sampling period. (Mean; SD = standard deviation; Min = minimum; Max = maximum; Circles = outliers). Periods 1(1995-1996), 2 (1998), 3 (1999), 4 (2001-2002), 5 (2002-2003), 6 (2006-2007), 7 (2013-2014), 8 (2016-2017), 9 (2021-2022).

Abundance of sampled species

A total of 564016 shrimps were sampled in the Ubatuba Bay, in the 27-year period. The abundance of species per sampling period may be observed in figure 3. Among penaeoideans, *Xiphopenaeus* spp. was the most abundant (81.60%) with 460,268 individuals captured, followed by *A. longinaris* with 51,163 individuals (9.7%) and *P. muelleri* with 12,048 individuals (2.14%). The least abundant species were *L. schmitti* (0.56%) and *F. paulensis* (0.21%).

Regarding abundance by periods, *A. longinaris* was considerably more abundant in period 4, followed by period 5 (Fig. 3A). *Farfantepenaeus brasiliensis* was more abundant in period 7 (Fig. 3B), and *F. paulensis* in period 7, followed by period 2 (Fig. 3C). *Litopenaeus schmitti* was more abundant in period 8, followed by period 2 (Fig. 3D). *Pleoticus muelleri* was more abundant in period 8, followed by period 4 (Fig. 3E). *Rimapenaeus constrictus* was more abundant in period 8, followed by period 7 (Fig. 3F). *Sicyonia dorsalis* was more abundant in periods 8 and 4 (Fig. 3G). *Xiphopenaeus* spp. abundance was higher in period 8 (Fig. 3H), and *E. oplophoroides* in periods 1 and 3 (Fig. 3I).

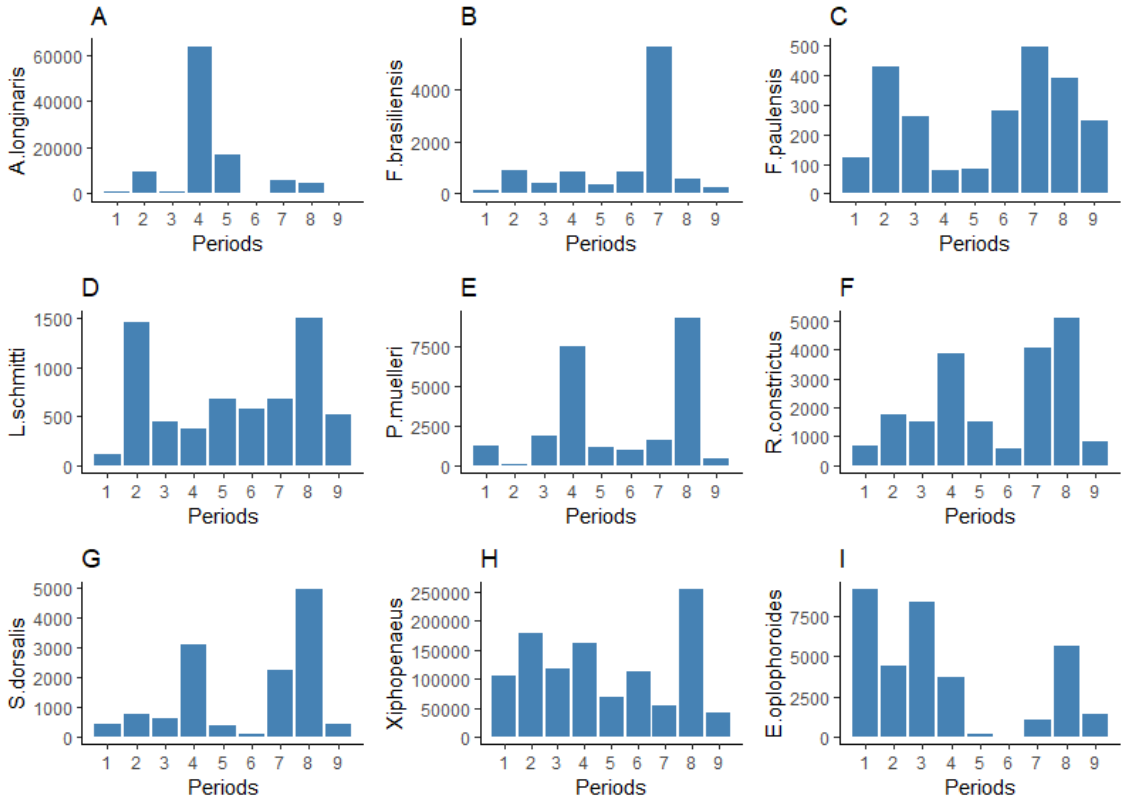

Figure 3 – Shrimp abundance by sampling periods in Ubatuba Bay, [A] *Artemesia longinaris* Spence Bate, 1888, [B] *Farfantepenaeus brasiliensis* (Latreille, 1817), [C] *Farfantepenaeus paulensis* (Pérez Farfante, 1967), [D] *Litopenaeus schmitti* (Burkenroad, 1936), [E] *Pleoticus muelleri* (Spence Bate, 1888), [F] *Rimapenaeus constrictus* (Stimpson, 1871), [G] Sicyonia dorsalis Kingsley, 1878, [H] *Xiphopenaeus* spp., [I] *Exhippolysmata oplophoroides* (Holthuis, 1948). Periods 1(1995-1996), 2 (1998), 3 (1999), 4 (2001-2002), 5 (2002-2003), 6 (2006-2007), 7 (2013-2014), 8 (2016-2017), 9 (2021-2022). There was no data available regarding *E. oplophoroides* catches for period 6.

Trends in species' abundance: assemblage variation

The PERMANOVA results indicated differences between the periods (p = 0.001; F = 6.3352) (Table 3). From the post-test results, differences were evidenced between the paired seasons: 1 and 7 (p = 0.028); 1 and 9 (p = 0.028); 2 and 5 (p = 0.028); 2 and 7 (p = 0.028); 2 and 9 (p = 0.028); 3 and 8 (p = 0.028); 3 and 9 (p = 0.028); 4 and 5 (p = 0.028); 4 and 7 (p = 0.028); 4 and 9 (p = 0.028); 5 and 8 (p = 0.028); 5 and 9 (p = 0.028); 7 and 8 (p = 0.028); 7 and 9 (p = 0.028); 8 and 9 (p = 0.028) (Table 4).

According to the results from the ISA, only five from the nine species are associated with at least one of the periods. *Artemesia longinaris* was associated with periods 4, 5 and 7. *Exhyppolysmata oplophoroides* was associated with all periods with exception of period 6 (not included in the analysis) and period 7. *Pleoticus muelleri* was associated with all periods with exception of period 6 (not included in the analysis) and period 2. At last, *L. schmitti* and *S. dorsalis* were associated with periods 2, 3, 4, 5, 7, 8 and 9.

Table 3 – Results of the PERMANOVA analysis applied to the shrimp assemblage in Ubatuba Bay. (DF = Degrees of freedom; SS = Sum of squares; F = F-value in the test; p (perm) = p-value obtained through the permutation test.

Factor	DF	SS	R^2	F	p (perm)
Periods	7	8.183	0.10651	6.3352	0.001***
Residual	372	68.645	0.89349		
Total	379	76.828	1.00000		

Table 4 – Pairwise-PERMANOVA results based on Bray-Curtis of shrimp assemblage in relation to periods. (DF = Degrees of freedom; SS = Sum of squares; F Model = F value by permutation; P-value = based on 9999 permutations. Bold values indicate significant differences ($p < 0.05$).

	DF	SS	F Model	R^2	P value	P adjusted
1 vs. 2	1	0.6455	2.1264	0.0221	0.048	1
1 vs. 3	1	0.3031	0.9589	0.0103	0.458	1
1 vs. 4	1	1.1140	3.7778	0.0386	0.004	0.112
1 vs. 5	1	0.8636	2.9480	0.0307	0.015	0.420
1 vs. 7	1	1.1669	3.8546	0.0393	0.001	**0.028**
1 vs. 8	1	1.5300	6.3724	0.0641	0.002	0.056
1 vs. 9	1	1.9318	8.0832	0.0791	0.001	**0.028**
2 vs. 3	1	0.5373	1.6811	0.0179	0.108	1
2 vs. 4	1	0.8228	2.7583	0.0285	0.025	0.700
2 vs. 5	1	1.6938	5.7140	0.0578	0.001	**0.028**
2 vs. 7	1	1.5152	4.9489	0.0500	0.001	**0.028**
2 vs. 8	1	0.8331	3.4203	0.0354	0.012	0.336
2 vs. 9	1	3.5425	14.6125	0.1345	0.001	**0.028**
3 vs. 4	1	1.1792	3.7950	0.0396	0.003	0.084
3 vs. 5	1	0.7662	2.4801	0.0265	0.016	0.448
3 vs. 7	1	0.6306	1.9783	0.02105	0.049	1
3 vs. 8	1	1.7789	6.9788	0.0712	0.001	**0.028**
3 vs. 9	1	1.9571	7.7167	0.0773	0.001	**0.028**
4 vs. 5	1	1.3955	4.8516	0.0495	0.001	**0.028**
4 vs. 7	1	1.7207	5.7846	0.0579	0.001	**0.028**
4 vs. 8	1	0.8269	3.5224	0.0364	0.002	0.056
4 vs. 9	1	3.9650	16.9645	0.1528	0.001	**0.028**
5 vs. 7	1	0.6153	2.0817	0.0218	0.046	1.000
5 vs. 8	1	2.6487	11.4082	0.1103	0.001	**0.028**
5 vs. 9	1	1.0378	4.4901	0.0460	0.001	**0.028**
7 vs. 8	1	2.8870	11.8948	0.1133	0.001	**0.028**
7vs. 9	1	1.8488	7.6531	0.0752	0.001	**0.028**
8 vs. 9	1	4.6805	26.2542	0.2201	0.001	**0.028**

Trends in species' abundance: Temporal models

The shrimp species *F. brasiliensis*, *F. paulensis*, *R. constrictus*, *Xiphopenaeus* spp. and *E. oplophoroides* were positively correlated with the PC1 axis in the PCA, therefore the PC1 scores were extracted and used to represent these species, creating the response variable PC1. The Generalized Linear Mixed Model fitted for the variance in PC1 did not show significant change for these species' abundance overtime (Table 5).

Artemesia longinaris and *P. muelleri* were negatively correlated with the PC2 axis in the PCA. The Generalized Linear Mixed Model fitted for the variance in PC2 showed that abundance was significant different in period 4 (GlmmTMB z-value = 2.60, p-value < 0.01), period 5 (GlmmTMB z-value = -2.04, p-value < 0.5) and period 7 (GlmmTMB z-value = 2.96, p-value < 0.05) (Table 6). Graphically it is possible to notice an increase in the species abundances in periods 4, 5 and 7 (Figure 4A).

The shrimps *L. schmitti* and *S. dorsalis* were negatively correlated with the PC3 axis in the PCA. The Generalized Linear Mixed Model fitted for the variance in PC3 showed that abundance was significant different in period 7 (GlmmTMB z-value = 2.39, p-value < 0.05) (Table 7). Graphically it is possible to notice an increase in the species abundances in period 7 (Figure 4B).

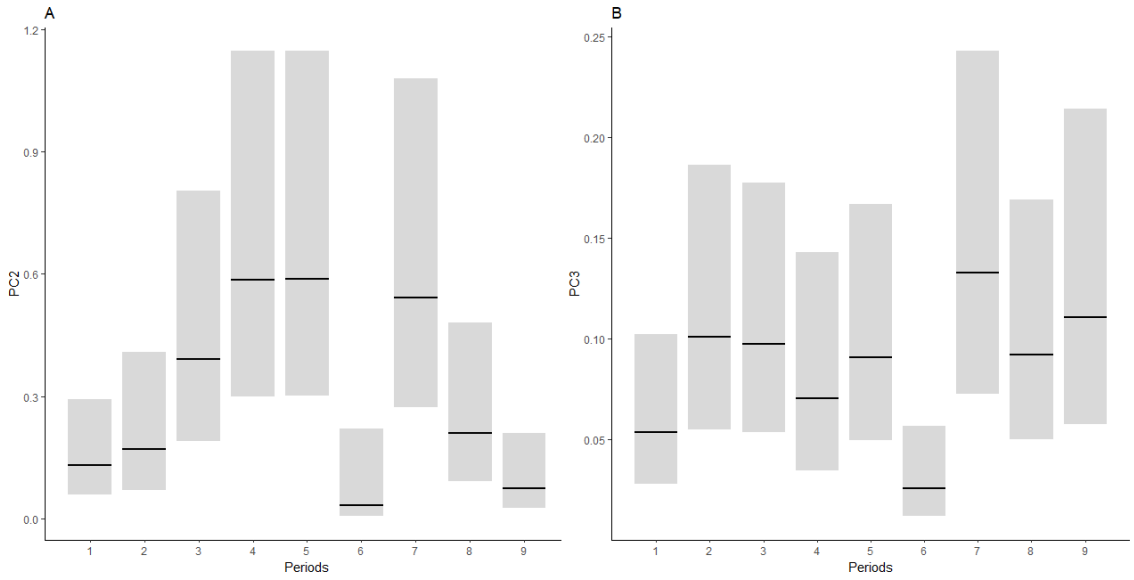

Figure 4 – Variation of [A] PC2 and [B] PC3 through the sampled periods in Ubatuba Bay.

Table 5 – Conditional model estimated from the fitted GLMM of PC1.

	Estimate	Std. Error	z value	P value
Intercept	-2.7867	0.7632	-3.651	< 0.001
Period 2	-0.7201	0.8407	-0.857	0.3916
Period 3	0.5430	0.8029	0.676	0.4988
Period 4	0.0630	0.8164	0.077	0.9384
Period 5	-0.0158	0.8224	-0.019	0.9846
Period 6	-0.3874	0.8447	-0.459	0.6465
Period 7	1.1478	0.7921	1.449	0.1473
Period 8	-1.2170	0.8720	-1.396	0.1628
Period 9	-1.1388	0.8746	-1.302	0.1929

Table 6 – Conditional model estimated from the fitted GLMM of PC2.

	Estimate	Std. Error	z value	P value
Intercept	-4.1910	0.9763	-4.293	< 0.001
Period 2	-0.4677	0.8132	-0.575	0.5651
Period 3	0.6598	0.7263	0.908	0.3636
Period 4	1.8009	0.6907	2.607	< 0.01
Period 5	1.7458	0.6988	2.498	< 0.5
Period 6	0.1481	0.7918	0.187	0.8515
Period 7	2.0419	0.6892	2.963	< 0.05
Period 8	0.4971	0.7359	0.676	0.4993
Period 9	-0.8192	0.8008	-1.023	0.3063

Table 7 – Conditional model estimated from the fitted GLMM of PC3.

	Estimate	**Std. Error**	**z value**	**P value**
Intercept	-2.7694	0.4454	-6.217	< 0.001
Period 2	0.6352	0.3941	1.612	0.1070
Period 3	0.6031	0.3876	1.556	0.1197
Period 4	0.3105	0.3994	0.777	0.4369
Period 5	0.5375	0.3888	1.383	0.1668
Period 6	-0.7250	0.4572	-1.586	0.1128
Period 7	0.8945	0.3735	2.395	< 0.05
Period 8	0.5433	0.3877	1.401	0.1611
Period 9	0.7521	0.3843	1.957	0.0503

Trends in species' abundance: Ecological models

Model selection for the ecological models of PC2 yielded in eight models with ΔAICc < 2 (Table 8). Following the principle of parsimony, the chosen best model was the model that contained the variables Sal (GlmmTMB z-value = 3.24, p-value < 0.005), Temp (GlmmTMB z-value = -3.23, p-value < 0.005), and Rain (GlmmTMB z-value = 3.40, p-value < 0.001). Abundance of *A. longinaris* and *P. muelleri* increases with higher salinity (Fig. 5A) and decreases with temperature increase (Fig. 5B). These species abundance also increase with increase in Rainfall (Fig. 5C).

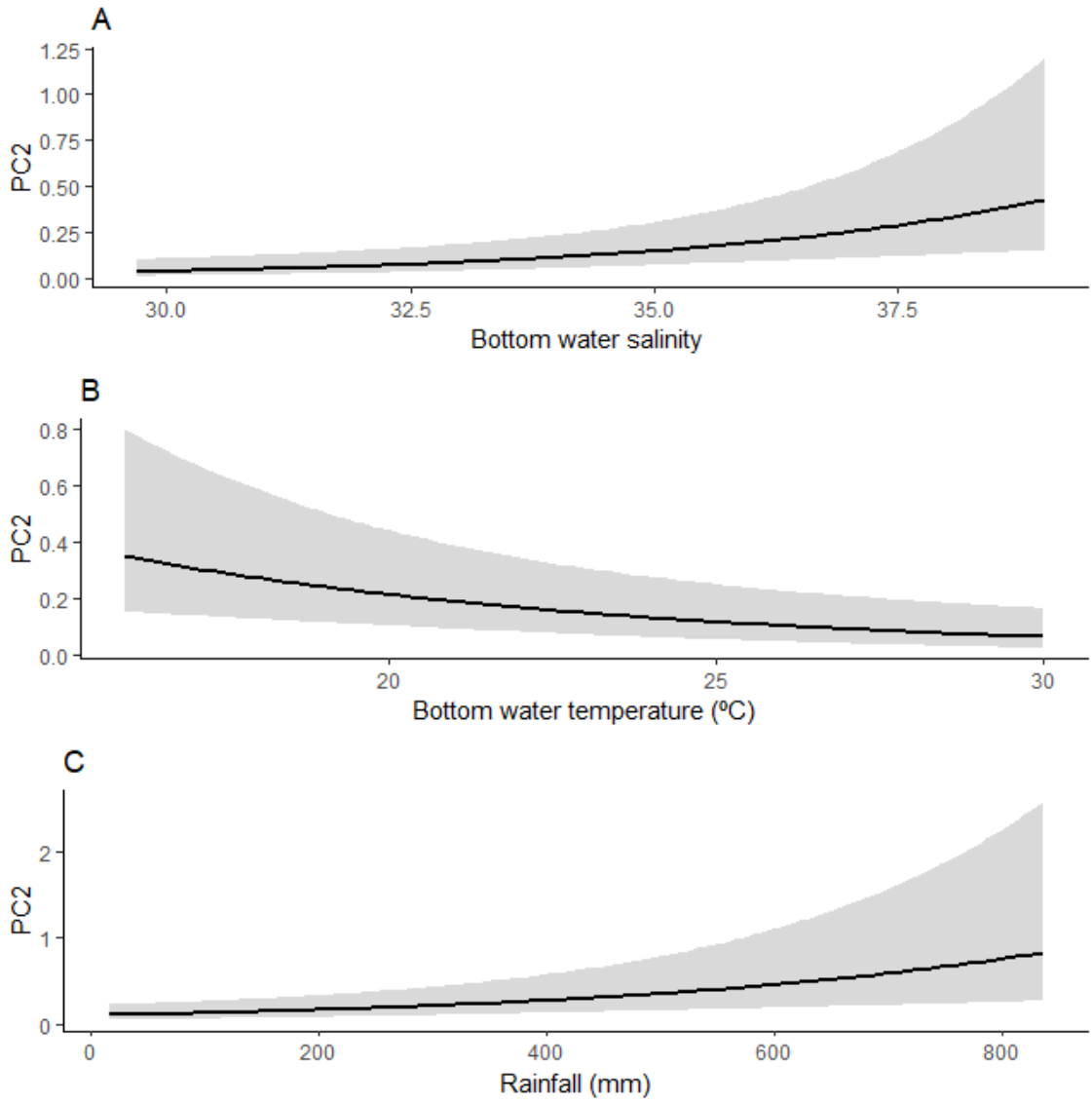

Figure 5 – Variation in PC2 and its relationship with the covariates selected in the best model: [A] Bottom water salinity, [B] Bottom water temperature (°C), and [C] Rainfall (mm).

Model selection for the ecological models of PC3 yielded in eight models with ΔAICc < 2 (Table 9). Following the principle of parsimony, the chosen best model was the model that contained the variables ENSO (GlmmTMB z-value = -2.30, p-value < 0.05), and Temp (GlmmTMB z-value = -6.37, p-value < 0.001). Abundance of *L. schmitti* and *S. dorsalis* decreases with ENSO intensity (Fig. 6A) and with increase in temperature (Fig. 6B).

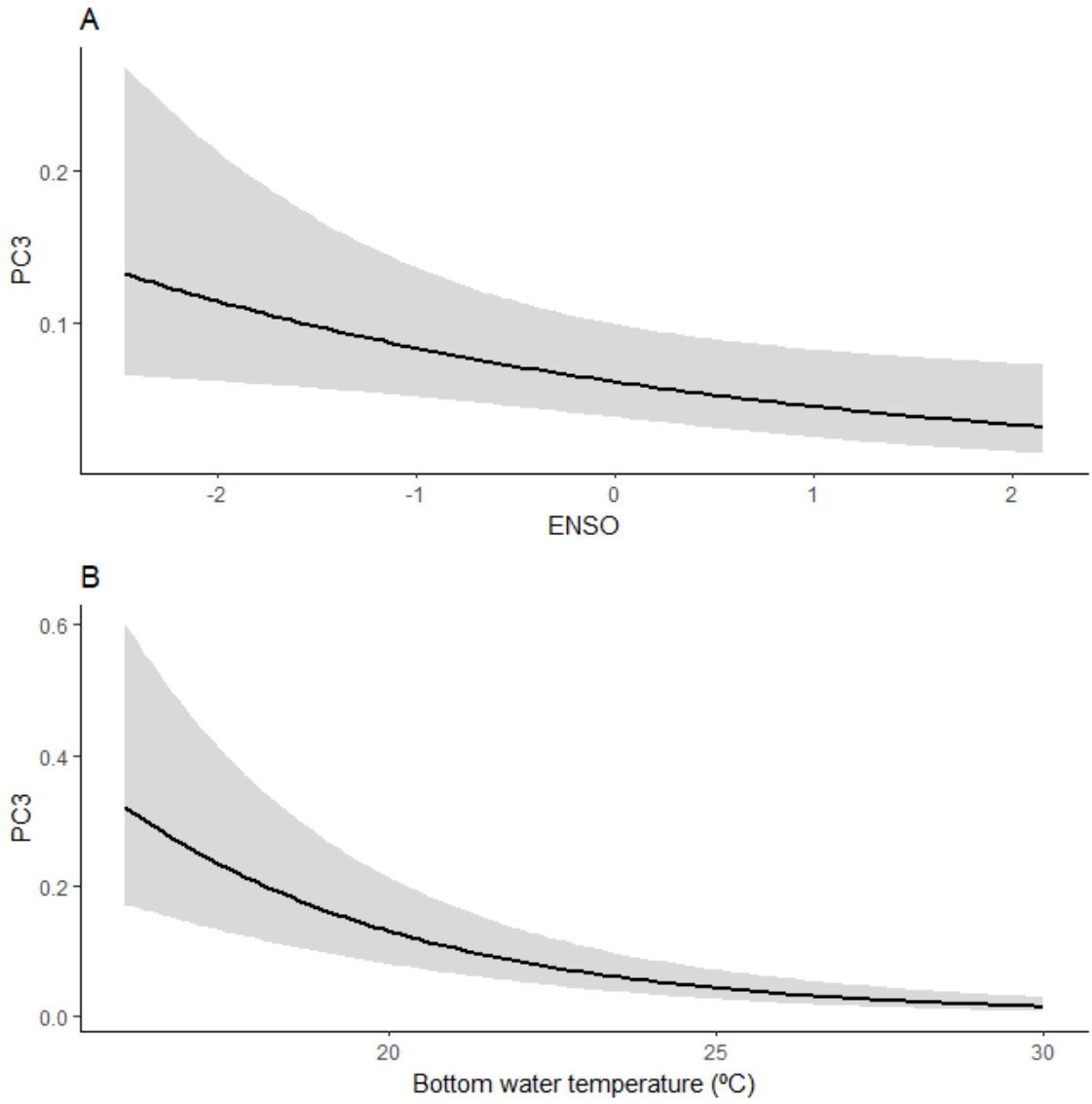

Figure 6 – Variation in PC3 and its relationship with the covariates selected in the best model: [A] ENSO, and [B] Bottom water temperature (°C).

Table 8 – Generalized Linear Mixed Models (GLMM) adjusted for PC2. LogLik = Log likelihood of a model; DF = Degrees of freedom; sigma^2 = variance.

Rank	Parameters	LogLik	Deviance	DF residuals	Sigma^2	AICc	ΔAICc
8	s(ENSO) + s(MO) + s(Phi)	-210.1	420.1	423	1.14	438.55	27.50
6	s(ENSO) + s(Phi)	-210.6	421.2	424	1.14	437.50	26.45
7	s(MO) + s(Phi)	-210.3	420.7	424	1.14	437.01	25.96
4	s(ENSO) + s(MO)	-210.1	420.2	424	1.14	436.53	25.48
16	s(ENSO) + s(MO) + s(Phi) + s(Rain)	-207.8	415.6	422	1.1	436.15	25.10
5	s(Phi)	-210.7	421.5	425	1.14	435.72	24.68
2	s(ENSO)	-210.7	421.4	425	1.14	435.70	24.65
3	s(MO)	-210.4	420.8	425	1.14	435.02	23.97
14	s(ENSO) + s(Phi) + s(Rain)	-208	416	423	1.1	434.40	23.35
15	s(MO) + s(Phi) + s(Rain)	-207.9	415.8	423	1.1	434.21	23.16
12	s(ENSO) + s(MO) + s(Rain)	-207.8	415.6	423	1.1	434.06	23.01
1	null	-210.9	421.7	426	1.14	433.92	22.88
13	s(Phi) + s(Rain)	-208	416	424	1.1	432.38	21.33
10	s(ENSO) + s(Rain)	-208	416	424	1.1	432.36	21.31
11	s(MO) + s(Rain)	-207.9	415.8	424	1.1	432.13	21.08
9	s(Rain)	-208	416.1	425	1.09	430.35	19.30
24	s(ENSO) + s(MO) + s(Phi) + s(Sal)	-204.5	409.1	422	1.08	429.62	18.57
38	s(ENSO) + s(Phi) + s(Temp)	-205.6	411.1	423	1.08	429.58	18.53
40	s(ENSO) + s(MO) + s(Phi) + s(Temp)	-204.5	409	422	1.07	429.52	18.47
39	s(MO) + s(Phi) + s(Temp)	-205.2	410.5	423	1.07	428.92	17.87
22	s(ENSO) + s(Phi) + s(Sal)	-205	410.1	423	1.09	428.48	17.43
37	s(Phi) + s(Temp)	-206	412	424	1.08	428.35	17.30
34	s(ENSO) + s(Temp)	-205.9	411.8	424	1.07	428.14	17.09
36	s(ENSO) + s(MO) + s(Temp)	-204.6	409.2	423	1.07	427.63	16.58
20	s(ENSO) + s(MO) + s(Sal)	-204.6	409.1	423	1.08	427.53	16.49
23	s(MO) + s(Phi) + s(Sal)	-204.6	409.1	423	1.08	427.53	16.48
35	s(MO) + s(Temp)	-205.4	410.7	424	1.07	427.07	16.02
33	s(Temp)	-206.3	412.6	425	1.07	426.90	15.85
18	s(ENSO) + s(Sal)	-205.1	410.2	424	1.08	426.52	15.47
21	s(Phi) + s(Sal)	-205.1	410.1	424	1.09	426.48	15.43
19	s(MO) + s(Sal)	-204.6	409.1	424	1.08	425.46	14.41
32	s(ENSO) + s(MO) + s(Phi) + s(Rain) + s(Sal)	-201.1	402.1	421	1.03	424.74	13.69

Table 8 – Continuation

Rank	Parameters	LogLik	Deviance	DF residuals	Sigma^2	AICc	ΔAICc
17	s(Sal)	-205.1	410.3	425	1.09	424.53	13.48
56	s(ENSO) + s(MO) + s(Phi) + s(Sal) + s(Temp)	-200.7	401.4	421	1.04	424.07	13.03
48	s(ENSO) + s(MO) + s(Phi) + s(Rain) + s(Temp)	-200.7	401.3	421	1.02	423.95	12.90
54	s(ENSO) + s(Phi) + s(Sal) + s(Temp)	-201.6	403.3	422	1.04	423.78	12.73
31	s(MO) + s(Phi) + s(Rain) + s(Sal)	-201.2	402.5	422	1.04	422.99	11.94
30	s(ENSO) + s(Phi) + s(Rain) + s(Sal)	-201.2	402.3	422	1.03	422.87	11.82
46	s(ENSO)+ s(Phi) + s(Rain) + s(Temp)	-201.1	402.3	422	1.02	422.82	11.77
28	s(ENSO) + s(MO) + s(Rain) + s(Sal)	-201.1	402.1	422	1.03	422.65	11.60
47	s(MO) + s(Phi) + s(Rain) + s(Temp)	-201	402.1	422	1.01	422.57	11.52
55	s(MO) + s(Phi) + s(Sal) + s(Temp)	-200.8	401.6	422	1.03	422.15	11.10
50	s(ENSO) + s(Sal) + s(Temp)	-201.8	403.7	423	1.04	422.08	11.03
52	s(ENSO) + s(MO) + s(Sal) + s(Temp)	-200.8	401.5	422	1.03	422.07	11.02
44	s(ENSO) + s(MO) + s(Rain) + s(Temp)	-200.7	401.4	422	1.02	421.90	10.86
53	s(Phi) + s(Sal) + s(Temp)	-201.6	403.3	423	1.04	421.71	10.66
29	s(Phi) + s(Rain) + s(Sal)	-201.4	402.9	423	1.04	421.30	10.25
45	s(Phi) + s(Rain) + s(Temp)	-201.3	402.7	423	1.01	421.11	10.07
42	s(ENSO) + s(Rain) + s(Temp)	-201.3	402.5	423	1.01	420.95	9.90
27	s(MO) + s(Rain) + s(Sal)	-201.2	402.5	423	1.04	420.92	9.87
26	s(ENSO) + s(Rain) + s(Sal)	-201.2	402.3	423	1.03	420.78	9.73
43	s(MO) + s(Rain) + s(Temp)	-201.1	402.1	423	1.01	420.55	9.50
51	s(MO) + s(Sal) + s(Temp)	-200.9	401.7	423	1.03	420.15	9.11
49	s(Sal) + s(Temp)	-201.8	403.7	424	1.04	420.01	8.96
41	s(Rain) + s(Temp)	-201.4	402.9	424	1.01	419.24	8.19
25	s(Rain) + s(Sal)	-201.4	402.9	424	1.04	419.21	8.16
64	s(ENSO) + s(MO) + s(Phi) + s(Rain) + s(Sal) + s(Temp)	-195.9	391.8	420	0.975	416.54	5.50
62	s(ENSO) + s(Phi) + s(Rain) + s(Sal) + s(Temp)	-196.2	392.5	421	0.974	415.11	4.06
63	s(MO) + s(Phi) + s(Rain) + s(Sal) + s(Temp)	-195.9	391.8	421	0.975	414.43	3.38
60	s(ENSO) + s(MO) + s(Rain) + s(Sal) + s(Temp)	-195.9	391.8	421	0.974	414.43	3.38
61	s(Phi) + s(Rain) + s(Sal) + s(Temp)	-196.3	392.6	422	0.976	413.08	2.03
58	s(ENSO) + s(Rain) + s(Sal) + s(Temp)	-196.3	392.5	422	0.973	413.06	2.01
59	s(MO) + s(Rain) + s(Sal) + s(Temp)	-195.9	391.8	422	0.975	412.33	1.28
57	**s(Rain) + s(Sal) + s(Temp)**	**-196.3**	**392.6**	**423**	**0.975**	**411.05**	**0.00**

Table 9 – Generalized Linear Mixed Model (GLMM) adjusted for PC3. LogLik = Log likelihood of a model; DF = Degrees of freedom; sigma^2 = variance.

Rank	Parameters	LogLik	Deviance	DF residuals	Sigma^2	AICc	ΔAICc
7	s(MO) + s(Phi)	-226.7	453.4	424	0.991	469.77	46.48
23	s(MO) + s(Phi) + s(Sal)	-225.5	451.1	423	0.987	469.49	46.20
3	s(MO)	-226.9	453.8	425	0.995	468.06	44.77
5	s(Phi)	-226.8	453.7	425	0.992	467.93	44.64
19	s(MO) + s(Sal)	-225.7	451.3	424	0.99	467.64	44.35
21	s(Phi) + s(Sal)	-225.6	451.1	424	0.988	467.47	44.17
1	null	-227	454	426	0.996	466.15	42.86
17	s(Sal)	-225.7	451.3	425	0.991	465.60	42.31
8	s(ENSO) + s(MO) + s(Phi)	-223.3	446.6	423	0.957	465.07	41.78
4	s(ENSO) + s(MO)	-223.7	447.3	424	0.963	463.68	40.39
6	s(ENSO) + s(Phi)	-223.4	446.9	424	0.958	463.20	39.91
31	s(MO) + s(Phi) + s(Rain) + s(Sal)	-221	441.9	422	0.949	462.44	39.15
24	s(ENSO) + s(MO) + s(Phi) + s(Sal)	-220.8	441.7	422	0.937	462.18	38.89
2	s(ENSO)	-223.7	447.5	425	0.964	461.74	38.45
29	s(Phi) + s(Rain) + s(Sal)	-221.1	442.3	423	0.952	460.70	37.41
20	s(ENSO) + s(MO) + s(Sal)	-221	442.1	423	0.94	460.49	37.20
27	s(MO) + s(Rain) + s(Sal)	-221	442.1	423	0.952	460.48	37.19
22	s(ENSO) + s(Phi) + s(Sal)	-220.8	441.7	423	0.938	460.10	36.81
13	s(Phi) + s(Rain)	-221.4	442.9	424	0.953	459.22	35.92
11	s(MO) + s(Rain)	-221.3	442.5	424	0.952	458.86	35.57
25	s(Rain) + s(Sal)	-221.2	442.4	424	0.954	458.70	35.40
18	s(ENSO) + s(Sal)	-221	442.1	424	0.94	458.41	35.12
9	s(Rain)	-221.5	443	425	0.955	457.23	33.94
32	s(ENSO) + s(MO) + s(Phi) + s(Rain) + s(Sal)	-215.5	431.1	421	0.905	453.69	30.40
16	s(ENSO) + s(MO) + s(Phi) + s(Rain)	-216.5	432.9	422	0.915	453.46	30.16
14	s(ENSO) + s(Phi) + s(Rain)	-216.7	433.4	423	0.919	451.86	28.56
28	s(ENSO) + s(MO) + s(Rain) + s(Sal)	-215.6	431.3	422	0.907	451.81	28.52
30	s(ENSO) + s(Phi) + s(Rain) + s(Sal)	-215.6	431.3	422	0.908	451.81	28.52
12	s(ENSO) + s(MO) + s(Rain)	-216.6	433.3	423	0.917	451.70	28.40
10	s(ENSO) + s(Rain)	-216.8	433.7	424	0.921	450.02	26.73
26	s(ENSO) + s(Rain) + s(Sal)	-215.7	431.5	423	0.909	449.88	26.59
15	s(MO) + s(Phi) + s(Rain)	-207.9	415.8	423	1.1	434.21	10.92

Table 9 – Continuation

Rank	Parameters	LogLik	Deviance	DF residuals	Sigma^2	AICc	ΔAICc
63	s(MO) + s(Phi) + s(Rain) + s(Sal) + s(Temp)	-205.3	410.5	421	0.823	433.14	9.84
55	s(MO) + s(Phi) + s(Sal) + s(Temp)	-206	412	422	0.828	432.53	9.24
59	s(MO) + s(Rain) + s(Sal) + s(Temp)	-205.5	410.9	422	0.825	431.43	8.14
47	s(MO) + s(Phi) + s(Rain) + s(Temp)	-205.4	410.9	422	0.823	431.40	8.11
61	s(Phi) + s(Rain) + s(Sal) + s(Temp)	-205.4	410.9	422	0.826	431.38	8.09
39	s(MO) + s(Phi) + s(Temp)	-206.5	412.9	423	0.829	431.35	8.06
51	s(MO) + s(Sal) + s(Temp)	-206.2	412.5	423	0.83	430.92	7.63
53	s(Phi) + s(Sal) + s(Temp)	-206.1	412.2	423	0.83	430.63	7.34
35	s(MO) + s(Temp)	-206.8	413.5	424	0.831	429.88	6.59
45	s(Phi) + s(Rain) + s(Temp)	-205.7	411.4	423	0.826	429.79	6.50
43	s(MO) + s(Rain) + s(Temp)	-205.7	411.3	423	0.825	429.76	6.47
37	s(Phi) + s(Temp)	-206.6	413.3	424	0.831	429.60	6.31
57	s(Rain) + s(Sal) + s(Temp)	-205.6	411.2	423	0.827	429.58	6.29
49	s(Sal) + s(Temp)	-206.3	412.6	424	0.831	428.94	5.65
41	s(Rain) + s(Temp)	-205.8	411.7	424	0.828	428.04	4.75
33	s(Temp)	-206.9	413.8	425	0.832	428.02	4.73
40	s(ENSO) + s(MO) + s(Phi) + s(Temp)	-203.6	407.2	422	0.811	427.71	4.42
56	s(ENSO) + s(MO) + s(Phi) + s(Sal) + s(Temp)	-202.3	404.6	421	0.804	427.26	3.97
64	s(ENSO) + s(MO) + s(Phi) + s(Rain) + s(Sal) + s(Temp)	-201.2	402.4	420	0.801	427.15	3.86
36	s(ENSO) + s(MO) + s(Temp)	-204	408.1	423	0.812	426.53	3.23
48	s(ENSO) + s(MO) + s(Phi) + s(Rain) + s(Temp)	-201.9	403.9	421	0.805	426.49	3.20
38	s(ENSO) + s(Phi) + s(Temp)	-203.7	407.5	423	0.813	425.89	2.60
52	s(ENSO) + s(MO) + s(Sal) + s(Temp)	-202.6	405.2	422	0.804	425.75	2.46
60	s(ENSO) + s(MO) + s(Rain) + s(Sal) + s(Temp)	-201.5	402.9	421	0.8	425.53	2.24
54	s(ENSO) + s(Phi) + s(Sal) + s(Temp)	-202.4	404.7	422	0.805	425.24	1.95
62	s(ENSO) + s(Phi) + s(Rain) + s(Sal) + s(Temp)	-201.3	402.6	421	0.802	425.24	1.95
44	s(ENSO) + s(MO) + s(Rain) + s(Temp)	-202.3	404.5	422	0.806	425.07	1.78
46	s(ENSO)+ s(Phi) + s(Rain) + s(Temp)	-202.2	404.3	422	0.808	424.83	1.53
34	**s(ENSO) + s(Temp)**	**-204.1**	**408.3**	**424**	**0.814**	**424.61**	**1.31**
50	s(ENSO) + s(Sal) + s(Temp)	-202.6	405.3	423	0.805	423.69	0.39
58	s(ENSO) + s(Rain) + s(Sal) + s(Temp)	-201.5	403	422	0.802	423.55	0.26
42	s(ENSO) + s(Rain) + s(Temp)	-202.4	404.9	423	0.809	423.29	0.00

Trends in species 'diversity: Temporal models

The Generalized Linear Mixed Model fitted for the variance in Exp_Shannon showed that diversity was significant different in period 7 (GlmmTMB z-value = 2.20, p-value < 0.05) (Table 14), being higher in comparison with other periods (Fig. 25).

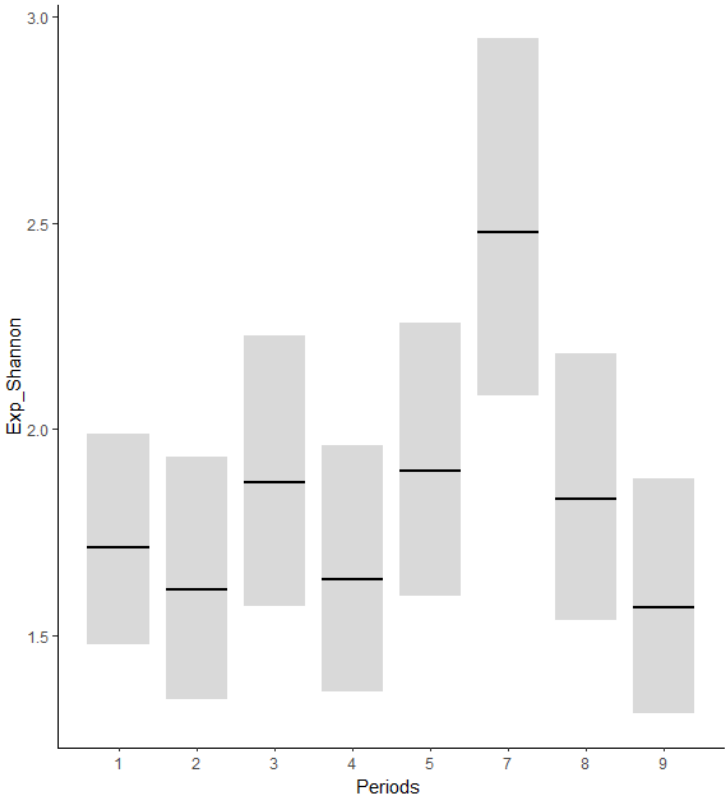

Figure 7 – Variation of Exp_Shannon trough the sampling periods in Ubatuba Bay.

Table 10 – Conditional model estimated from the fitted GLMM of Exp_Shannon.

	Estimate	Std. Error	z value	P value
Intercept	0.583778	0.098301	5.939	< 0.001
Period 2	-0.00843	0.111439	-0.076	0.9397
Period 3	0.091082	0.111455	0.817	0.4138
Period 4	-0.01262	0.111501	-0.113	0.9099
Period 5	-0.03399	0.111499	-0.305	0.7605
Period 7	0.245409	0.111447	2.202	< 0.05
Period 8	0.016795	0.111444	0.151	0.8802
Period 9	-0.09436	0.111451	-0.847	0.3972

Trends in species 'diversity: Ecological models

Model selection for the ecological models of Exp_Shannon yielded in nine models with ΔAICc < 2 (Table 27). Following the principle of parsimony, the chosen best model was the model that contained the variables Temp (GlmmTMB z-value = -3.27, p-value < 0.005). Shrimp diversity decreased with the increase in temperature (Fig. 26).

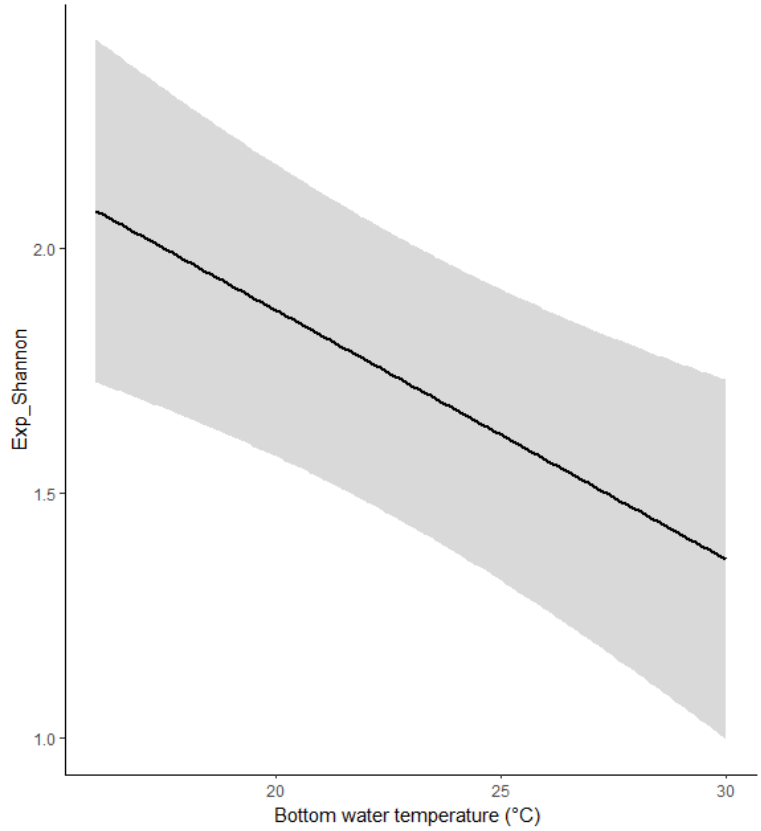

Figure 8 – Variation in Exp_Shannon and its relationship with the covariate selected in the best model: [A] Bottom water temperature (°C).

Table 11 – Generalized Linear Mixed Model (GLMM) adjusted for Exp_Shannon. LogLik = Log likelihood of a model; DF = Degrees of freedom; sigma^2 = variance.

Rank	Parameters	LogLik	Deviance	DF residuals	sigma^2	AICc	ΔAICc
31	s(MO) + s(Phi) + s(Rain) + s(Sal)	-468.2	936.4	375	0.60	954.84	12.20
27	s(MO) + s(Rain) + s(Sal)	-469.1	938.2	376	0.60	954.59	11.95
16	s(ENSO) + s(MO) + s(Phi) + s(Rain)	-468	936.1	375	0.60	954.58	11.94
15	s(MO) + s(Phi) + s(Rain)	-469	938	376	0.60	954.43	11.79
11	s(MO) + s(Rain)	-469.9	939.8	377	0.60	954.06	11.42
12	s(ENSO) + s(MO) + s(Rain)	-468.8	937.5	376	0.60	953.92	11.28
8	s(ENSO) + s(MO) + s(Phi)	-468.7	937.3	376	0.60	953.72	11.08
7	s(MO) + s(Phi)	-469.7	939.4	377	0.61	953.67	11.03
23	s(MO) + s(Phi) + s(Sal)	-468.5	937.1	376	0.60	953.47	10.84
32	s(ENSO) + s(MO) + s(Phi) + s(Rain) + s(Sal)	-466.4	932.8	374	0.59	953.41	10.77
3	s(MO)	-470.5	940.9	378	0.61	953.17	10.53
19	s(MO) + s(Sal)	-469.4	938.8	377	0.60	953.14	10.51
4	s(ENSO) + s(MO)	-469.3	938.6	377	0.60	952.93	10.29
29	s(Phi) + s(Rain) + s(Sal)	-468.2	936.4	376	0.60	952.79	10.15
28	s(ENSO) + s(MO) + s(Rain) + s(Sal)	-467.1	934.3	375	0.59	952.78	10.14
25	s(Rain) + s(Sal)	-469.1	938.2	377	0.60	952.51	9.87
14	s(ENSO) + s(Phi) + s(Rain)	-468.1	936.1	376	0.60	952.49	9.85
13	s(Phi) + s(Rain)	-469	938	377	0.60	952.35	9.71
9	s(Rain)	-469.9	939.8	378	0.60	952.00	9.36
10	s(ENSO) + s(Rain)	-468.8	937.5	377	0.60	951.83	9.19
24	s(ENSO) + s(MO) + s(Phi) + s(Sal)	-466.6	933.3	375	0.60	951.75	9.11
6	s(ENSO) + s(Phi)	-468.7	937.4	377	0.60	951.66	9.03
5	s(Phi)	-469.7	939.4	378	0.61	951.62	8.98
21	s(Phi) + s(Sal)	-468.6	937.2	377	0.60	951.49	8.85
30	s(ENSO) + s(Phi) + s(Rain) + s(Sal)	-466.5	932.9	375	0.59	951.43	8.79
1	null	-470.5	940.9	379	0.61	951.10	8.46
17	s(Sal)	-469.4	938.9	378	0.60	951.10	8.46
20	s(ENSO) + s(MO) + s(Sal)	-467.3	934.7	376	0.60	951.06	8.42
2	s(ENSO)	-469.3	938.6	378	0.60	950.86	8.22
26	s(ENSO) + s(Rain) + s(Sal)	-467.2	934.4	376	0.59	950.74	8.10
22	s(ENSO) + s(Phi) + s(Sal)	-466.7	933.5	376	0.59	949.86	7.22
18	s(ENSO) + s(Sal)	-467.4	934.8	377	0.60	949.09	6.45

Table 11 – Continuation

Rank	Parameters	LogLik	Deviance	DF residuals	sigma^2	AICc	ΔAICc
48	s(ENSO) + s(MO) + s(Phi) + s(Rain) + s(Temp)	-463.8	927.5	374	0.58	948.09	5.46
44	s(ENSO) + s(MO) + s(Rain) + s(Temp)	-464.5	929.1	375	0.59	947.58	4.94
63	s(MO) + s(Phi) + s(Rain) + s(Sal) + s(Temp)	-463.4	926.8	374	0.58	947.43	4.79
64	s(ENSO) + s(MO) + s(Phi) + s(Rain) + s(Sal) + s(Temp)	-462.3	924.7	373	0.58	947.36	4.73
59	s(MO) + s(Rain) + s(Sal) + s(Temp)	-464.4	928.8	375	0.59	947.25	4.61
47	s(MO) + s(Phi) + s(Rain) + s(Temp)	-464.3	928.5	375	0.59	947.00	4.36
60	s(ENSO) + s(MO) + s(Rain) + s(Sal) + s(Temp)	-463.1	926.3	374	0.58	946.88	4.24
43	s(MO) + s(Rain) + s(Temp)	-465.2	930.3	376	0.59	946.70	4.06
46	s(ENSO)+ s(Phi) + s(Rain) + s(Temp)	-463.8	927.5	375	0.59	946.00	3.36
40	s(ENSO) + s(MO) + s(Phi) + s(Temp)	-463.8	927.5	375	0.58	945.99	3.35
42	s(ENSO) + s(Rain) + s(Temp)	-464.6	929.1	376	0.59	945.53	2.89
36	s(ENSO) + s(MO) + s(Temp)	-464.6	929.1	376	0.59	945.49	2.85
55	s(MO) + s(Phi) + s(Sal) + s(Temp)	-463.5	926.9	375	0.58	945.41	2.77
56	s(ENSO) + s(MO) + s(Phi) + s(Sal) + s(Temp)	-462.4	924.8	374	0.58	945.38	2.74
61	s(Phi) + s(Rain) + s(Sal) + s(Temp)	-463.4	926.8	375	0.58	945.32	2.68
51	s(MO) + s(Sal) + s(Temp)	-464.4	928.9	376	0.59	945.28	2.64
62	s(ENSO) + s(Phi) + s(Rain) + s(Sal) + s(Temp)	-462.3	924.7	374	0.58	945.27	2.63
57	s(Rain) + s(Sal) + s(Temp)	-464.4	928.8	376	0.59	945.16	2.52
52	s(ENSO) + s(MO) + s(Sal) + s(Temp)	-463.2	926.5	375	0.58	944.95	2.31
45	s(Phi) + s(Rain) + s(Temp)	-464.3	928.5	376	0.59	944.93	2.29
39	s(MO) + s(Phi) + s(Temp)	-464.3	928.5	376	0.59	944.91	2.27
58	s(ENSO) + s(Rain) + s(Sal) + s(Temp)	-463.1	926.3	375	0.58	944.78	2.14
41	s(Rain) + s(Temp)	-465.2	930.4	377	0.59	944.69	2.06
35	s(MO) + s(Temp)	-465.2	930.3	377	0.59	944.63	1.99
38	s(ENSO) + s(Phi) + s(Temp)	-463.8	927.5	376	0.59	943.90	1.26
34	s(ENSO) + s(Temp)	-464.6	929.2	377	0.59	943.45	0.81
53	s(Phi) + s(Sal) + s(Temp)	-463.5	926.9	376	0.58	943.32	0.68
54	s(ENSO) + s(Phi) + s(Sal) + s(Temp)	-462.4	924.8	375	0.58	943.29	0.65
49	s(Sal) + s(Temp)	-464.5	928.9	377	0.59	943.21	0.57
50	s(ENSO) + s(Sal) + s(Temp)	-463.2	926.5	376	0.58	942.85	0.21
37	s(Phi) + s(Temp)	-464.3	928.5	377	0.59	942.84	0.21
33	**s(Temp)**	**-465.2**	**930.4**	**378**	**0.59**	**942.64**	**0.00**

Discussion

Many studies around the world have accessed long-term fluctuations in shrimp abundance (Haas et al., 2001; Siegel et al., 2005; Diop et al, 2007; Stallings et al., 2014). In Brazil, however, long term datasets are scarce. In the southern region Noleto-Filho et al. (2017) investigated temporal variation in juvenile size distribution of the pink shrimp *F. paulensis* from 1996 to 2012, and in the southeast region, Heckler et al. (2014) analyzed the long-term patterns of spatial and temporal distribution in the seabob shrimp *Xiphopenaeus kroyeri* population.

In this study, the temporal models indicated that there was no significant variation in the abundance of *F. brasiliensis*, *F. paulensis*, *R. constrictus*, *Xiphopenaeus* spp. and *E. oplophoroides* from 1995 to 2022. The lack of significance in the models fitted for pink-shrimp species probably indicates that the closed season is effective for the maintenance of these populations in Ubatuba Bay, even if protecting them only partially as observed by Perroca et al. (2022a). In Brazilian fisheries, the normative instruction IBAMA nº 189/2008 forbade fishing during the pink shrimp juvenile's recruitment from March 1 to May 31, in the marine area between the parallels 21º18'04,00 "S (frontier between Espirito Santo and Rio de Janeiro States) and 33º40'33,00 "S (Arroio Chuí, RS).

However, the effectiveness of this protection measure was heavily discussed once it did not include all shrimp species (Simões et al., 2017), especially those who are not targeted by fisheries. From 2023, the normative SAP/MAPA nº656 changed the closed season from January 28 to April 30, within the same geographic range from the previous normative, seeking to adequate the fishing closure with pink shrimp recruitment. Considering that pink shrimps in Ubatuba Bay start recruiting from January (Perroca et al., 2022a) and there was no significant variation in the populations in the past 27 years, it is expected that these overexploited populations (Perroca et al., 2022b) could start

recovering. As pink shrimps have relative high fecundity, fast growth and a short life cycle, their stocks may recover if the fishing intensity is reduced and the management is adequate to prevent recruitment overfishing (Haimovici & Cardoso, 2017). Still, the removal of May from the closed season can be potentially prejudicial to the population, once it's the time in which the juveniles are recruiting from the bay to the adult stock offshore. This calls for continuing monitoring at the area.

Considering the stabilization trends for the shrimp populations in the area, it seems that *Farfantepenaeus* spp. may be acting as an umbrella species to the other shrimp populations at a certain degree. An umbrella species is a species whose conservation is expected to confer protection to a large number of cooccurring species (Fleishman et al., 2000).

Rimapenaeus constrictus population probably did not variated significantly over the sampled years because the species is mostly found in site 3 (i.e., 5 m deep), where fishing is forbidden, so the species is not being impacted from such activity. Also, the seabed of algae that comes with the trawling makes it difficult to sort shrimps at the boat, making it a more time-consuming activity (field observation). As for *E. oplophoroides*, its population may not have varied significantly over the sampled years, because its peak in abundance (i.e., September to December) don't coincide with the higher catches in the target species at the bay, *Xiphopenaeus* spp. As soon as the closed season ceased in May 31, the fishing vessels would focus on capturing seabob shrimp, with higher catches registered in June and July (IP/APTA/SAA/SP, 2023). Therefore, we could assume that even though *E. oplophoroides* constitutes part of the seabob shrimp bycatch, this fishery it is not impacting this population enough to lead in significant changes overtime.

The *Xiphopenaeus* spp. abundance did not variated significantly at the bay. As we saw previously, these shrimps peaked in abundance during the closed season, which could

explain the population stability. Also, its juveniles are more abundant in site 3 (field observation). Heckler et al. (2014) also did not find differences in *Xiphopenaeus kroyeri* abundance between the studied periods in Ubatuba Bay. Seabob shrimp present a short life cycle, living up to 2 years in Ubatuba Bay (Miazaki et al., 2021), and have high fecundity (Miazaki, 2021), therefore it has the ability to recover its population, much like pink shrimp.

Artemesia longinaris and *P. muelleri* abundances were significatively higher in periods 4, 5 and 7 in comparison with other periods. In periods 4, 5 and especially 7 the lowest values of bottom water temperature were registered, which could indicate the SACW intrusion. As observed in the ecological models for these grouped species (PC2), their abundances increase with temperature decrease. These species are mostly subtropical, both occurring in the Western Atlantic. *A. longinaris* is distributed from Brazil (i.e., between the states of Rio de Janeiro and Rio Grande do Sul) to Argentina, and *P. muelleri* from Brazil (i.e., between the states of Espirito Santo and Rio Grande do Sul) (Mantelatto et al., 2022).

These species were also influenced by salinity, with abundances increasing in higher salinities. The SACW has as its characteristics, temperature bellow 18°C and salinity bellow 36, however salinity is higher to the area between the coast and 50 km (Castro Filho et al., 1987). Another environmental factor that was significant in the increase of these subtropical species was rainfall. Higher values of rainfall reflected in higher abundances. *A. longinaris* abundance peaks in summer, and *P. muelleri* peaks in spring, both being the rainiest seasons. These seasons are also when the SACW comes near the coast in Southeast Brazil. In Southern Brazil, temperature and abundance also modulated these species abundance. Dumont & D'Incao (2008) observed that *A. longinaris* concentrates greater densities in areas of low temperature and high salinity

associated to summer upwelling, while *P. muelleri* also occurs in greater densities in areas of low temperature, but on the contrary, it is able to tolerate lower salinities.

As for *L. schmitti* and *S. dorsalis* they were significatively more abundant in period 7. The ecological models for these grouped species (PC3) indicated that their abundance decreases with the increase in the ONI index, which indicates periods of El Niño. Also, lower temperatures also lead to increase in abundance for this species.

Period 7 was a neutral period, and periods of neutrality enhances the SACW intrusion (Castro Filho et al., 1987). Thus explains the higher abundance of these species in this period, especially because *S. dorsalis* abundance peaks in spring. *Sicyonia dorsalis* also shows preference for lower values of temperature (Castilho et al., 2008). *L. schmitti* however, being mostly a tropical species (Mantelatto et al., 2022) does not show a preference for lower temperature values, which indicates that this result is probably being influenced by grouping both species.

PERMANOVA analysis indicated that species composition within the shrimp assembly variated in several of the sampled years, with periods 7, 8 and 9 differing from other periods the most. The ISA indicated that from the nine species analyzed, only five contribute to changes in the assembly diversity. *Artemesia longinaris* was linked with period 7; *E. oplophoroides* with periods 8 and 9; *P. muelleri*, *L. schmitti* and *S. dorsalis* with periods 7, 8 and 9. These species were the ones that abundance varied trough years, with exception of *E. oplophoroides*. However, as observed in the GLMM models, diversity was only significantly different in period 7, in which it was higher than in other periods. Diversity also decreases with the increase in temperature, which reflects the preference of *A. longinaris*, *P. muelleri*, *L. schmitti* and *S. dorsalis* to lower temperatures.

Since most species abundance did not vary significatively in the past 27 years, and those species in which abundance varied was due to environmental changes, we may

assume that the shrimp assemblage in Ubatuba Bay have been stable, and the fishing impacts of the seabob fishery did not contribute to decrease diversity. Nonetheless, the area is a hotspot for several species of shrimp and other organisms. Therefore, long-term studies of the communities living there, caught as species of commercial interest or accidentally, are essential for monitoring, which leads to efficient measures to protect this ecosystem.

References

Anderson, M.J. 2001. A new method for non-parametric multivariate analysis of variance. Austral Ecology 26: 32-46. https://doi.org/10.1111/j.1442-9993.2001.01070.pp.x.

Arbizu, M.P. 2020. pairwiseAdonis: Pairwise multilevel comparison using adonis. R package version 0.4.

Bakker, J.D. 2008. Increasing the utility of Indicator Species Analysis. Journal of Applied Ecology 45:1829 -1835. doi.org/10.1111/j.1365-2664.2008.01571.x

Bauer, R. 2020. Shrimp Fisheries In: Fisheries and Aquaculture. Edited by: Gustavo Lovrich and Martin Thiel, Oxford University Press.

Begossi, A; May, P.H.; Lopes, P.F.; Oliveira, L.E.C.; Vinha, V & Silvano, R.A.M. 2011. Compensation for environmental services from artisanal fisheries in SE Brazil: Policy and technical strategies. Ecological Economics 71: 25-32. doi.org/10.1016/j.ecolecon.2011.09.008

Bernardes, V.P.; Souza, A.N.; Bernardo, C.H.; Teixeira, G.M.; Costa, R.C.; Mantelatto, F.L & Fransozo, A. 2020. Comparison of the spatio-temporal distribution of the roughneck shrimp *Rimapenaeus constrictus* (Stimpson, 1874) (Crustacea, Penaeoidea) from monthly samples collected 20 years apart: Effects of a marine protected area in southeastern Brazil. Marine Ecology, 41: e12605. doi: 10.1111/maec.12605

Bochini, G.L.; Stanski, G.; Castilho, A.L & Costa, R.C. 2019. The crustacean bycatch of seabob shrimp *Xiphopenaeus kroyeri* (Heller, 1862) fisheries in the Cananéia region, southern coast of São Paulo, Brazil. Regional Studies in Marine Science, 31: 100799. doi.org/10.1016/j.rsma.2019.100799

Bolker, M., Brooks, M.E., Clark, C.J., Geange, S.W., Poulsen, J.R., Stevens, M.H.H & White, J.S.S. 2008. Generalized linear mixed models: a practical guide for ecology and evolution Benjamin. Trends in Ecology & Evolution 24(3): 127-135. doi.org/10.1016/j.tree.2008.10.008

Branco, J.O.; Junior, F.F & Christoffersen, M.L. 2015. Bycatch fauna of seabob shrimp trawl fisheries from Santa Catarina State, southern Brazil. Biota Neotropica, 15(2): e20140143. doi.org/10.1590/1676-06032015014314

Brooks, M.E.; Kristensen, K.; van Benthem, K.J.; Magnusson, A.; Berg, C.W.; Nielsen, A.; Skaug, H.J.; Maechler, M & Bolker, B.M. 2017. "glmmTMB Balances Speed and Flexibility Among Packages for Zero-inflated Generalized Linear Mixed Modeling."

The R Journal 9(2): 378-400. doi:10.32614/RJ-2017-066.

Carvalho-Batista, A.; Terossi, M.; Zara, F.J & Costa, R.C. 2020. Validation of *Xiphopenaeus dincao* Carvalho-Batista, Terossi, Zara, Mantelatto & Costa and *Xiphopenaeus baueri* Carvalho-Batista, Terossi, Zara, Mantelatto & Costa (Decapoda: Penaeidae) from western Atlantic. Zootaxa. 4772(3): 597-599. doi.org/10.11646/zootaxa.4772.3.10

Castilho, A.L.; Furlan, M.; Costa, R.C & Fransozo, V. 2008. Abundance and temporal-spatial distribution of the rock shrimp *Sicyonia dorsalis* Kinsgley, 1878 (Decapoda, Penaeoidea) from the northern coast of São Paulo state, Brazil. Seckenbergiana maritima, 38(1): 75-83.

Castro-Filho, B.M.; Miranda, L.B & Myao, S.Y. 1987. Condições hidrográficas na plataforma continental ao largo de Ubatuba: Variações sazonais e em média escala. Boletim do Instituto Oceanográfico, 35:13-51.

Chapin III, F.; Zavaleta, E.; Eviner, V. et al. 2000. Consequences of changing biodiversity. Nature 405, 234-242. https://doi.org/10.1038/35012241

Diop, H.; Keithly Jr, W.R.; Kazmierczak Jr, R.F & Shaw, R.F. 2007. Predicting the abundance of white shrimp (*Litopenaeus setiferus*) from environmental parameters and previous life stages. Fisheries Research, 86: 31-41. doi.org/10.1016/j.fishres.2007.04.004

Dornelas, M.; Magurran, A.E.; Buckland, S.T.; Chao, A.; Chazdon, R.L.; Colwell, R.K.; Curtis, T.; Gaston, K.J.; Gotelli, N.J.; Kosnik, M.A.; McGill, B.; McCune, J.L.; Morlon, H.; Mumby, P.J.; Øvrea°s, L.; Studeny, A & Vellend, M. 2013. Quantifying temporal change in biodiversity: challenges and opportunities. Proceedings of the Royal Society B 280: 20121931. doi.org/10.1098/rspb.2012.1931

Dufrêne, M & Legendre, P. 1997 Species assemblages and indicator species: the need for a flexible asymmetrical approach. Ecological Monographs 67: 345-366.

Dumont, L.F & D'Incao, F. 2008. Distribution and abundance of the argentinean (*Artemesia longinaris*) and red (*Pleoticus muelleri*) prawns (Decapoda:Penaeoidea) in Southern Brazil during the commercial double-rig trawl fishery season. Nauplius 16(2): 83-94.

Fleishman, E.; Murphy, D.D & Brussard, P.F. 2000. A new method for selection of umbrella species for conservation planning. Ecological Applications, 10:569–579. doi.org/10.1111/j.1523-1739.2004.00450.x

Franco, A.C.N.P.; Schwarz Junior, R.; Pierri, N & Santos, G.C. Levantamento,

sistematização e análise da legislação aplicada ao defeso da pesca de camarões para as regiões Sudeste e Sul do Brasil. Boletim do Instituto de Pesca, 5(4): 687-699.

Haas, H.L.; Lamon III, E.C.; Rose, K.A & Shaw, R.F. 2001. Environmental and biological factors associated with the stage-specific abundance of brown shrimp (*Penaeus aztecus*) in Louisiana: applying a new combination of statistical techniques to long-term monitoring data. Canadian Journal of Fisheries and Aquatic Sciences, 58: 2258-2270. doi.org/10.1139/cjfas-58-11-2258.

Haimovici, M & Cardoso, L.G. 2017. Long-term changes in the fisheries in the Patos Lagoon estuary and adjacent coastal waters in Southern Brazil. Marine Biology Research, 13: 135-150. doi.org/10.1080/17451000.2016.1228978

Heckler, G.S.; Costa, R.C.; Fransozo, A.; Rosso, S & Shimizu, R.M. 2014. Long-term Patterns of Spatial and Temporal Distribution in the Seabob Shrimp *Xiphopenaeus kroyeri* (Decapoda: Penaeidae) Population in Southeastern Brazil. Journal of Crustacean Biology, 34(1-3): 326-333. doi.org/10.1163/1937240X-00002231

Holbrook, S.J.; Schmitt, R.J & Stephens, J.A. Jr. 1997. Changes in an assemblage of temperate reef fishes associated with a climate shift. Ecological Applications, 7: 1299-1310.

Hornborg, S.; Hobday, A.J.; Ogier, E.; Fleming, A.; Thomas, L & Hartog, J.R. 2020. Challenges and insights from holistic sustainability reporting for shrimp fisheries in different jurisdictions. ICES Journal of Marine Science, 77(6): 2022-2032. doi.org/10.1093/icesjms/fsaa048

IBAMA (Brazilian Institute of Environment and Renewable Natural Resources). 2008 – http://www.ibama.gov.br/biodiversidade-aquatica/periodos-dedefeso/defesos

IP/APTA/SAA/SP. 2022. Estatística Pesqueira Marinha e Estuarina do Estado de São Paulo. Consulta On-line. Programa de Monitoramento da Atividade Pesqueira Marinha e Estuarina do Estado de São Paulo. Instituto de Pesca (IP), Agência Paulista de Tecnologia dos Agronegócios (APTA), Secretaria de Agricultura e Abastecimento do Estado de São Paulo (SAA/SP). [accessed: 2022 November 1].http://www.propesq.pesca.sp.gov.br/.

IP/APTA/SAA/SP. 2023. Estatística Pesqueira Marinha e Estuarina do Estado de São Paulo. Consulta On-line. Programa de Monitoramento da Atividade Pesqueira Marinha e Estuarina do Estado de São Paulo. Instituto de Pesca (IP), Agência Paulista de Tecnologia dos Agronegócios (APTA), Secretaria de Agricultura e Abastecimento do Estado de São Paulo (SAA/SP). [accessed: 2023 May 12].

Jackson, J.B.C.; Kirby, M.X.; Berger, W.H.; Bjorndal, K.A.; Botsford, L.W.; Bourque, B.J.; Bradbury, R.H.; Cooke, R.; Erlandson, J.; Estes, J.A.; Hughes, T.P.; Kidwell, S.; Lange, C.B.; Lenihan, H.S.; Pandolfi, J.M.; Peterson, C.H.; Steneck, R.S.; Tegner, M.J & Warner, R.R. 2001. Historical overfishing and the recent collapse of coastal ecosystems. Science, 293: 629-638.

Keller, G. 2008. Cretaceous climate, volcanism, impacts, and biotic effects. Cretaceous Research, 29:754–771. doi.org/10.1016/j.cretres.2008.05.030.

Leakey, R & Lewin R. 1992. The sixth extinction: patterns of life and the future of humankind. Doubleday, London

Lira, A.S; Lucena-Frédou, F & Le Loc'h, F. 2021. How the fishing effort control and environmental changes affect the sustainability of a tropical shrimp small scale fishery. Fisheries Research, 235: 105824. /doi.org/10.1016/j.fishres.2020.105824

Magurran, A.E. 2007. Species abundance distributions over time. Ecology Letters, 10: 347–354. doi.org/10.1111/j.1461-0248.2007.01024.x

Mantelatto, F.L.M.; Bernardo, C.H.; Silva, T.E.; Bernardes, V.P.; Cobo, V.J & Fransozo, A. 2016. Composição e distribuição de crustáceos decápodes associados à pesca do camarão-sete-barbas *Xiphopenaeus kroyeri* (Heller, 1862) no litoral norte do estado de São Paulo. Boletim do Instituto de Pesca, 42: 307-326. doi.org/10.20950/1678-2305.2016v42n2p307

Mantelatto, F.L.; Tamburus, A.F.; Carvalho-Batista.; Rossi, N.; Buranelli, R.C.; Pantaleão, J.A.F.; Teles, J.N.; Zara, J.F.; Carvalho, F.L.; Bochini, G.L.; Terossi, M.; Robles, R.; Castilho, A.L & Costa, R.C. 2022. Checklist of decapod crustaceans from the coast of the São Paulo state (Brazil) supported by integrative molecular and morphological data: V. Dendrobranchiata and Pleocyemata [Achelata, Astacidea, Axiidea, Caridea (Alpheoidea and Processoidea excluded), Gebiidea, Stenopodidea]. Zootaxa, 5121 (1): 001-074. https://doi.org/10.11646/zootaxa.5121.1.1

Miazaki, L.F. 2021. Parâmetros reprodutivos e populacionais dos camarões sete-barbas *Xiphopenaeus* spp. (Decapoda: Penaeidae) na região sudeste do Brasil: uma abordagem interdisciplinar. PhD. Dissertation.

Muniz, P.; Pires-Vanin, A.M.S.; Martins, C.C.; Montone, R & Bicego, M.C. 2006. Trace metals and organic compounds in the benthic environment of a subtropical embayment (Ubatuba Bay, Brazil). Baseline / Marine Pollution Bulletin, 52: 1090-1117.

Noleto-Filho, E.M.; Pucciarelli, P & Dumont, L.F.C. 2017. Spatial and temporal variation in juvenile size distribution of the pink shrimp (*Penaeus paulensis*) in the Patos

Lagoon Estuary, Brazil. Marine Biology Research, 13: 62-73. doi.org/10.1080/17451000.2016.1248851

Oksanen J, Simpson G.L, Blanchet F.G, Kindt R, et al. 2022. Vegan: Community Ecology Package. R package version 2.6-4. Available at https://CRAN.R-project.org/package=vegan.

Palacio, F.J. 1982. Revision zoogeografica marina del sur del Brasil. Boletim do Instituto Oceanográfico, 31(l):69-92.

Pauly, D. 2018. The future of artisanal fishing. Science, 360 (6385): 161. doi.org/10.1126/science.aas9431

Perroca, J.F.; Rodrigues-Filho, J.L.; Fransozo, A & Costa, R.C. 2022a. Variations in pink-shrimps *Farfantepenaeus brasiliensis* and *F. paulensis* juvenile abundance: clarifying ecological patterns and providing subsidies to management in shallow marine ecosystems. Fisheries Research 256: 106482. doi.org/10.1016/j.fishres.2022.106482

Perroca, J.F.; Miazaki, L.F.; Fransozo, A.; Freire, F.A.M & Costa, R.C. 2022b. Growth, longevity and mortality of pink-shrimps Farfantepenaeus brasiliensis and F. paulensis in southeastern Brazil. Marine and Fishery Sciences (MAFIS), 35(2): 209-222. https://doi.org/10.47193/mafis.3522022010503

Pinheiro, J.C & Bates, D.M. 2000. Linear Mixed-Effects Models: Basic Concepts and Examples. In: Mixed-Effects Models in Sand S-PLUS. Statistics and Computing. Springer, New York, NY. https://doi.org/10.1007/978-1-4419-0318-1_1

Pinheiro, J.; Bates, D & R Core Team. 2022. nlme: Linear and Nonlinear Mixed Effects Models. R package version 3.1-160, https://CRAN.R-project.org/package=nlme. RStudio Team (2021). RStudio: Integrated Development Environment for R. RStudio, PBC, Boston, MA URL http://www.rstudio.com/.

Rezende, G.A.; Rufener, M.C.; Ortega, I.; Ruas, V.M & Dumont, L.F.C. 2019. Modelling the spatio-temporal bycatch dynamics in an estuarine small-scale shrimp trawl fishery. Fisheries Research, 219: 105336. doi.org/10.1016/j.fishres.2019.105336

Siegel, V.; Groger, J.; Neudecker, T.; Damm, U & Jansen, S. 2005. Long-term variation in the abundance of the brown shrimp *Crangon crangon* (L.) population of the German Bight and possible causes for its interannual variability. Fisheries Oceanography, 14:1, 1-16. doi.org/10.1111/j.1365-2419.2004.00301.x

Stallings, C.D.; Brower, J.P.; Heinlein Loch, J.M & Mickle, A. 2014. Commercial trawling in seagrass beds: bycatch and long-term trends in effort of a major shrimp fishery. Marine Ecology Progress Series, 513: 143-153. doi.org/10.3354/meps10960

Sumida, P.Y.G & Pires-Vanin, A.M.S. 1997. Benthic associations of die shelfbreak and upper slope off Ubatuba-SP, south-eastern Brazil. Estuaries, Coastal and Shelf Science, 44:779-784

Ward, P.D. 2000. Rivers in time. The search for clues to earth's mass extinctions. Columbia University Press, New York

Supplementary material – Data exploration

PCs

1. Relationship between dependent and explanatory variables

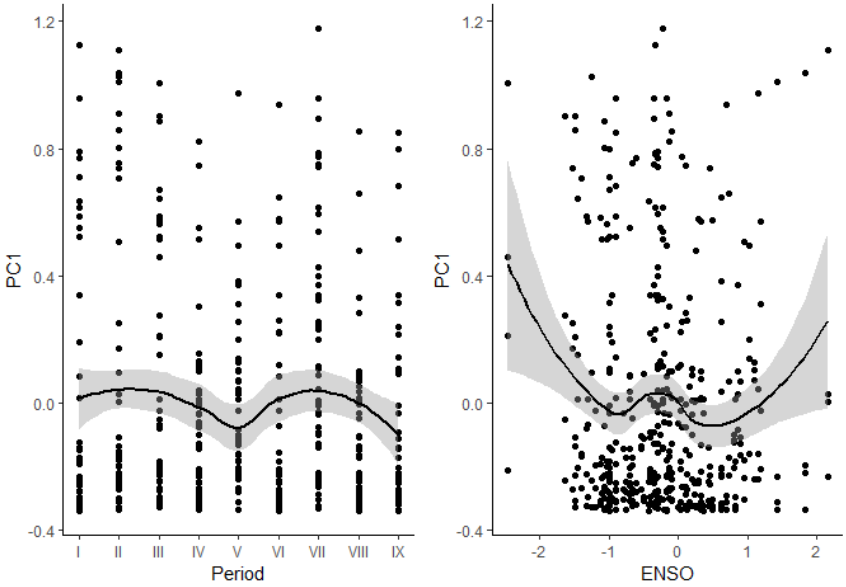

Fig. S1 – Scatterplots with a LOESS smoother between PC1 and its covariates Period and ENSO.

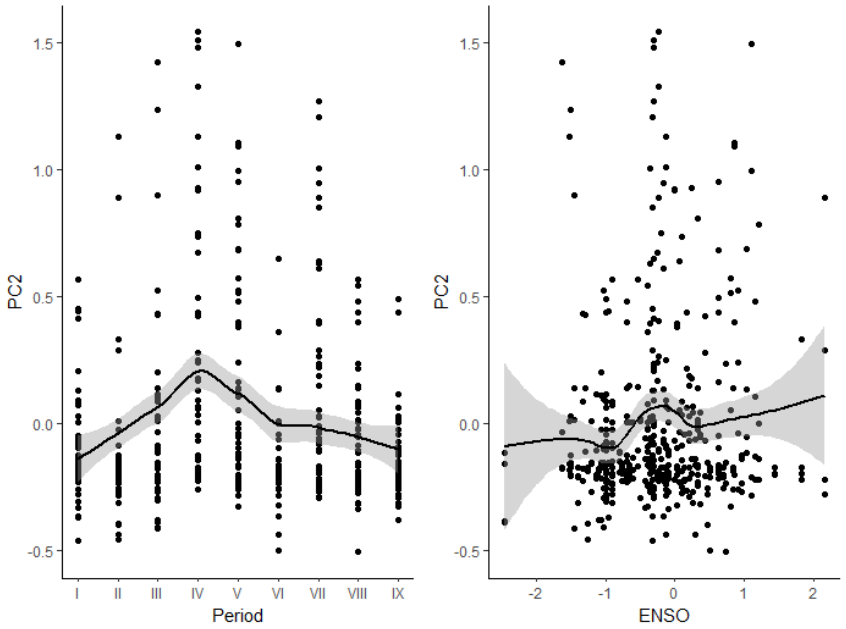

Fig. S2 – Scatterplots with a LOESS smoother between PC2 and its covariates Period and ENSO.

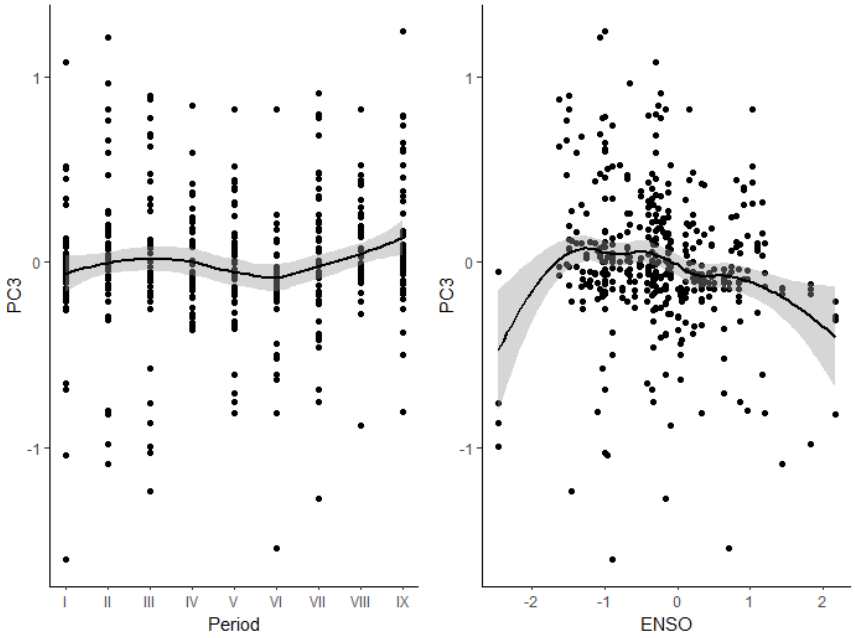

Fig. S3 – Scatterplots with a LOESS smoother between PC3 and its covariates Period and ENSO.

2. Outliers and dispersion pattern

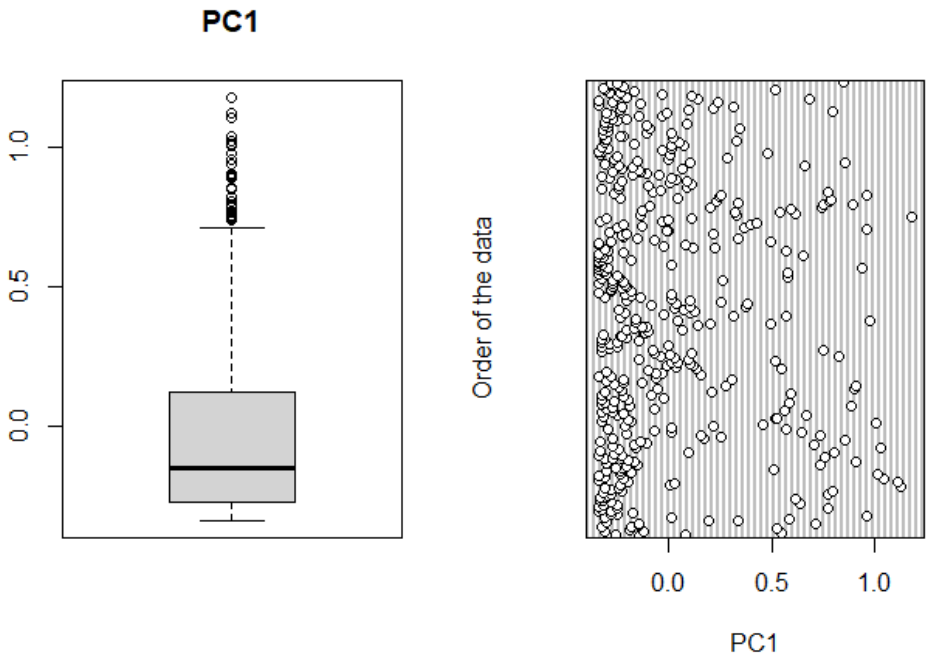

Fig. S4 – Box plot (Left) and Cleveland plot (Right) from PC1.

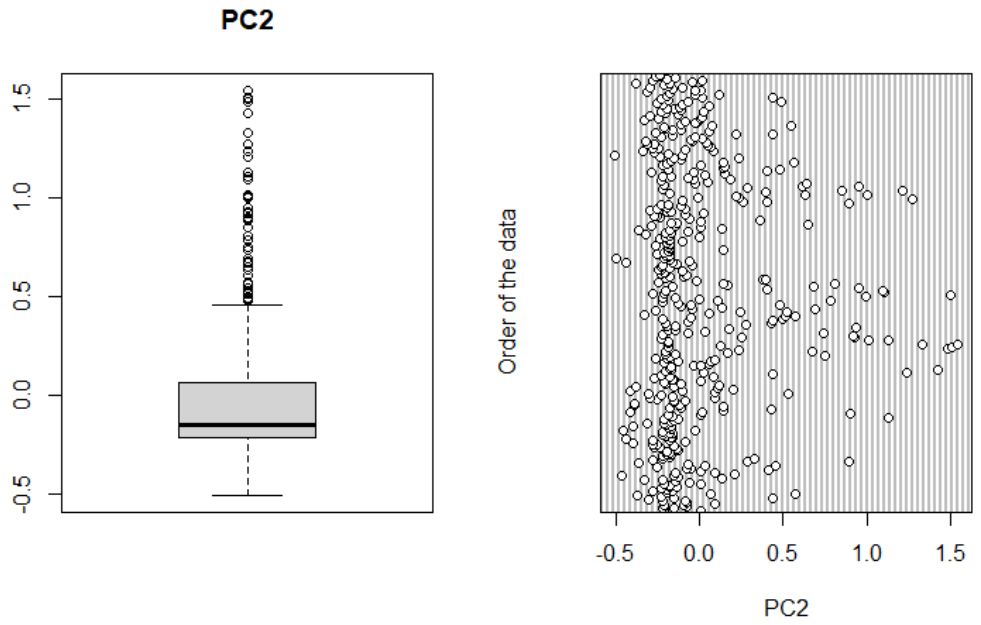

Fig. S5 – Box plot (Left) and Cleveland plot (Right) from PC2.

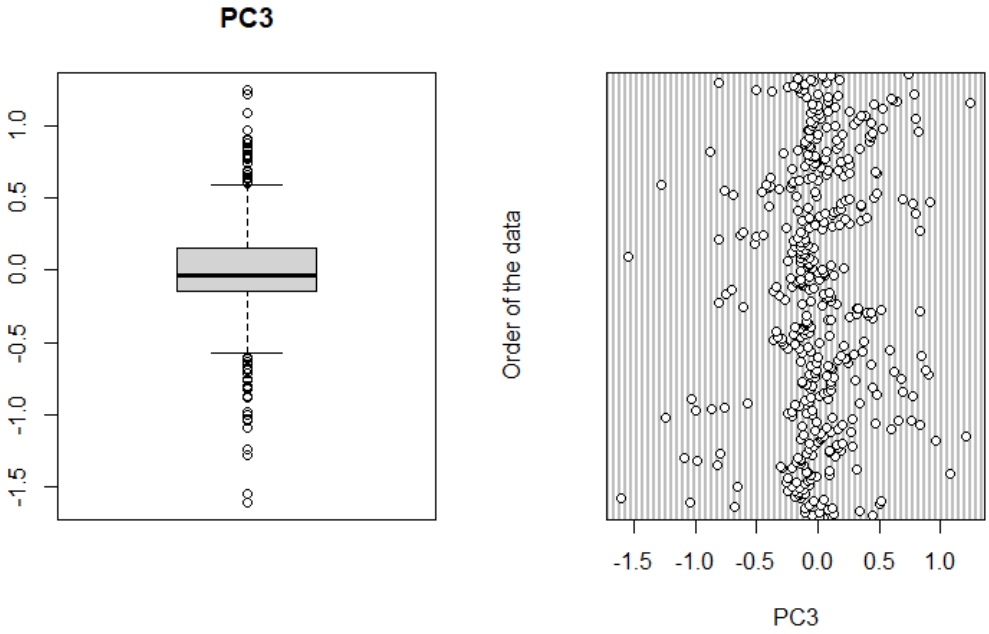

Fig. S6 – Box plot (Left) and Cleveland plot (Right) from PC3.

3. Normality

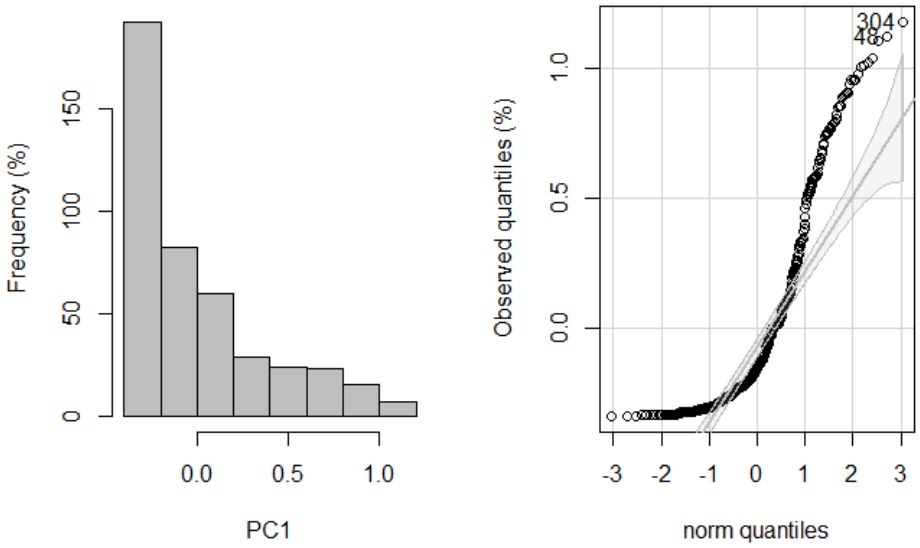

Fig. S7 – Histogram of CP1 (Left) and Q-Q plots (Right) of observed diversity against hypothetical normal distribution.

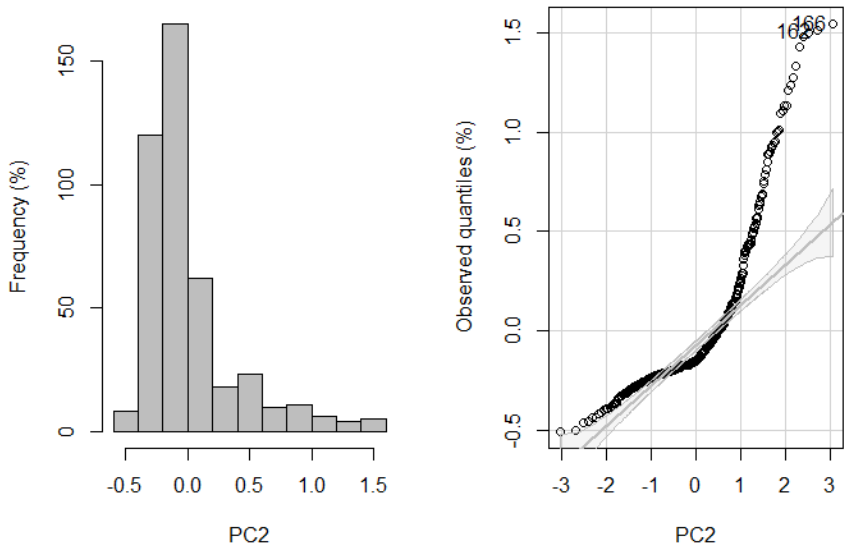

Fig. S8 – Histogram of CP2 (Left) and Q-Q plots (Right) of observed diversity against hypothetical normal distribution.

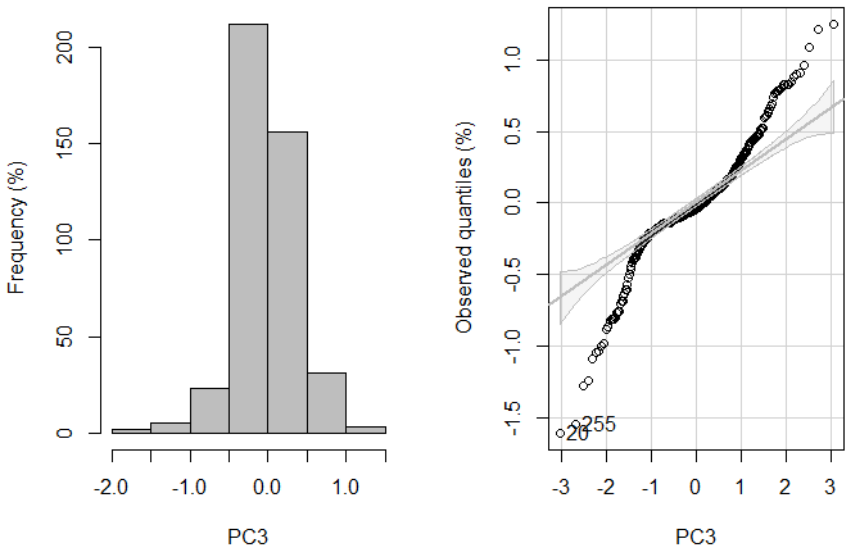

Fig. S9 – Histogram of CP3 (Left) and Q-Q plots (Right) of observed diversity against hypothetical normal distribution.

4. Homogeneity

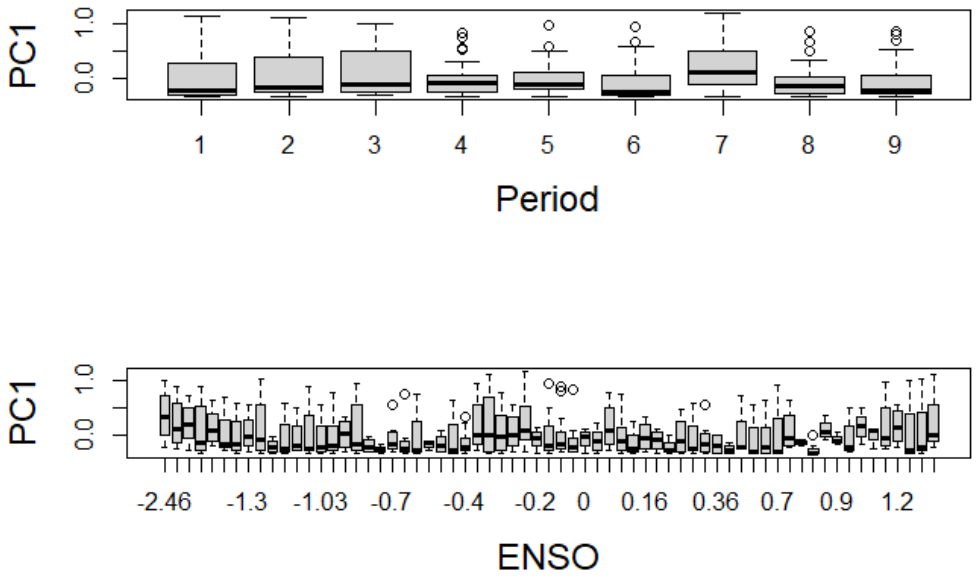

Fig. S10 – Period conditional box plot (Upper) and ENSO conditional box plot (Lower) of CP1.

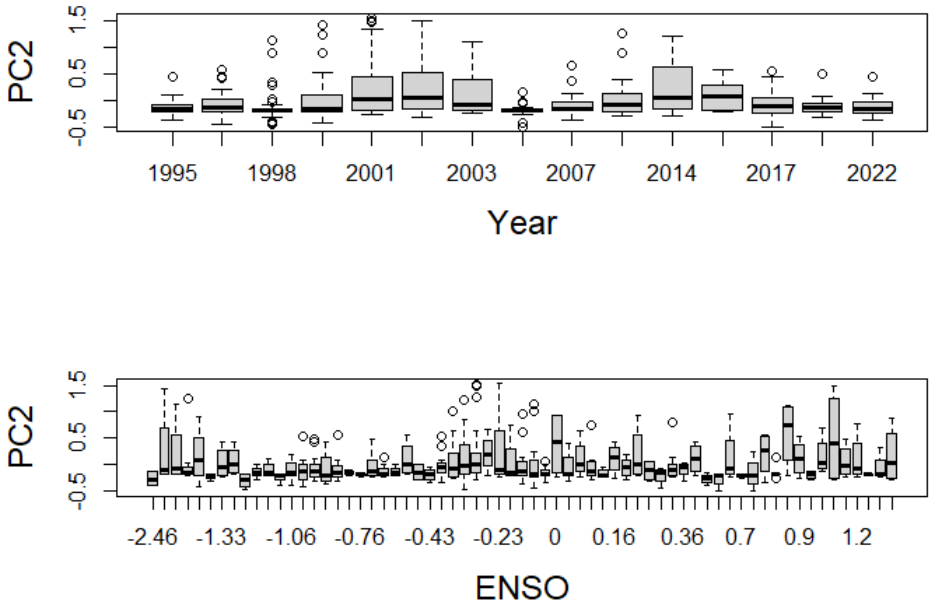

Fig. S11 – Period conditional box plot (Upper) and ENSO conditional box plot (Lower) of CP2.

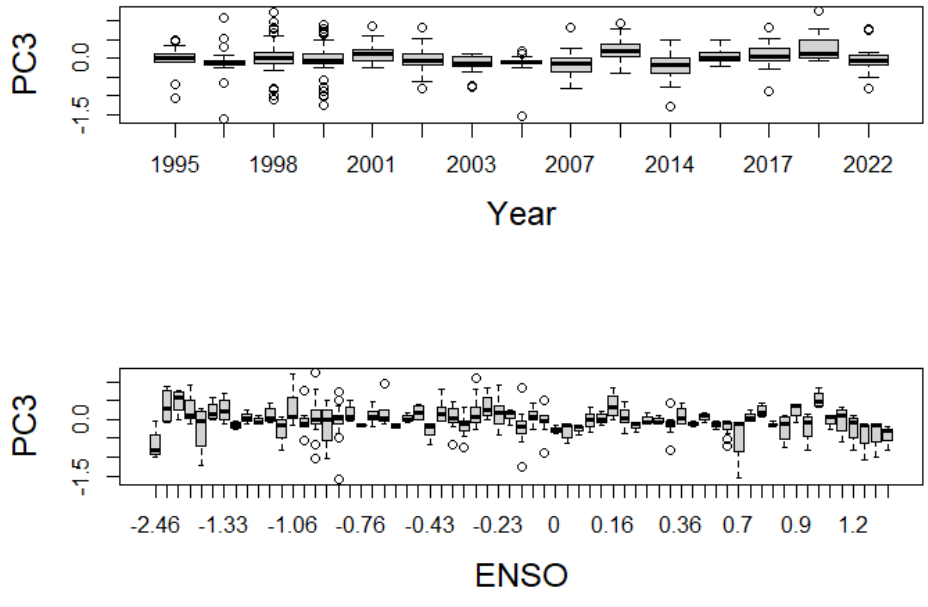

Fig. S12 – Period conditional box plot (Upper) and ENSO conditional box plot (Lower) of CP3_t.

5. Independency

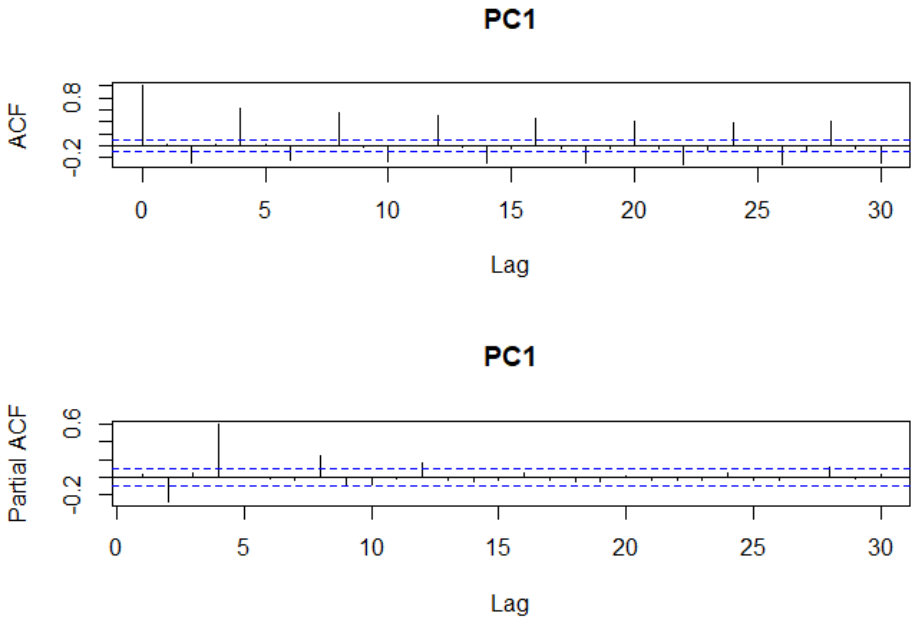

Fig. S13 – Auto-correlation function (ACF) and partial auto-correlation function (PACF) plot against time lag for CP1.

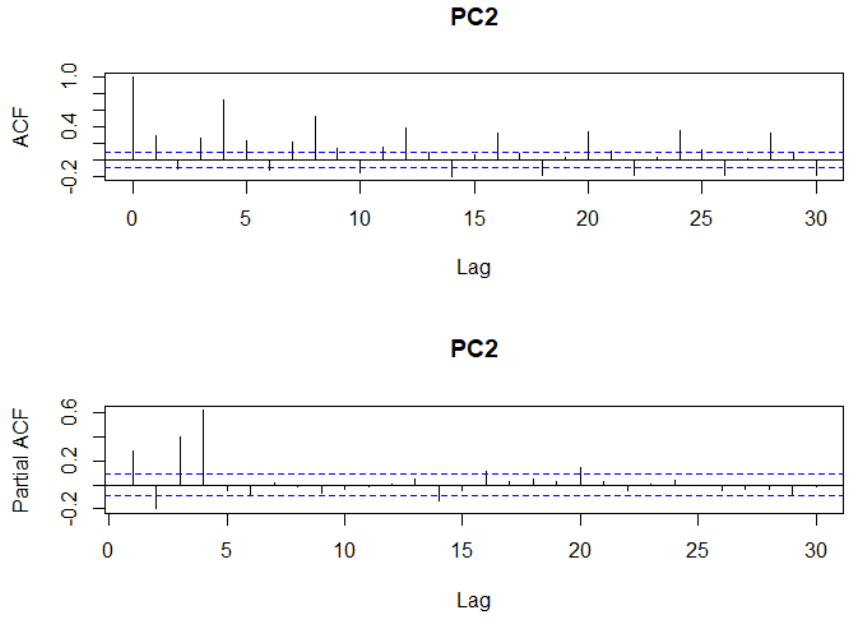

Fig. S14 – Auto-correlation function (ACF) and partial auto-correlation function (PACF) plot against time lag for CP2.

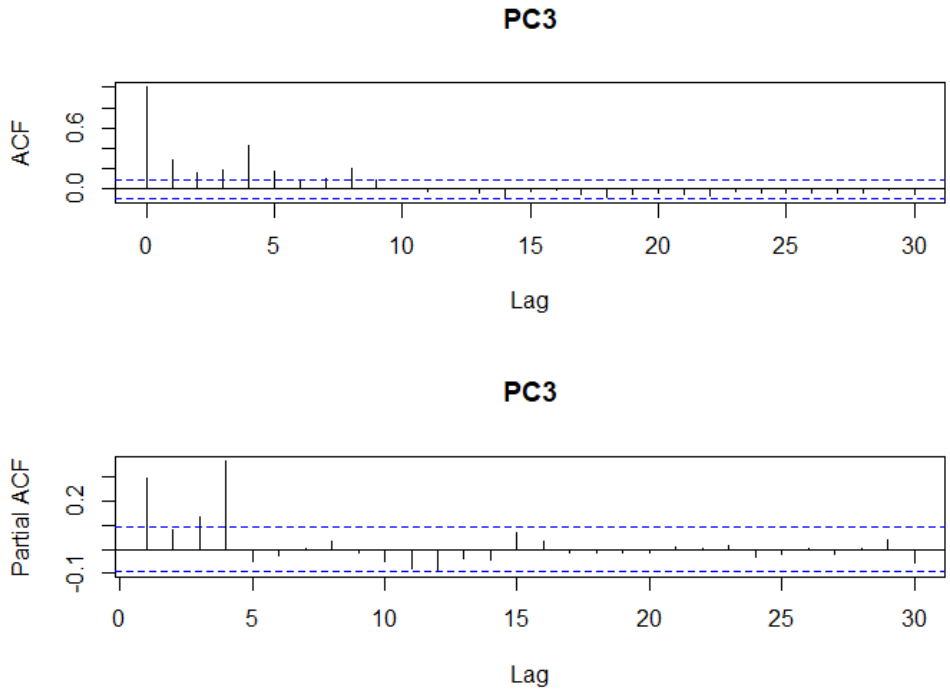

Fig. S15 – Auto-correlation function (ACF) and partial auto-correlation function (PACF) plot against time lag for CP3.

6. Zeros

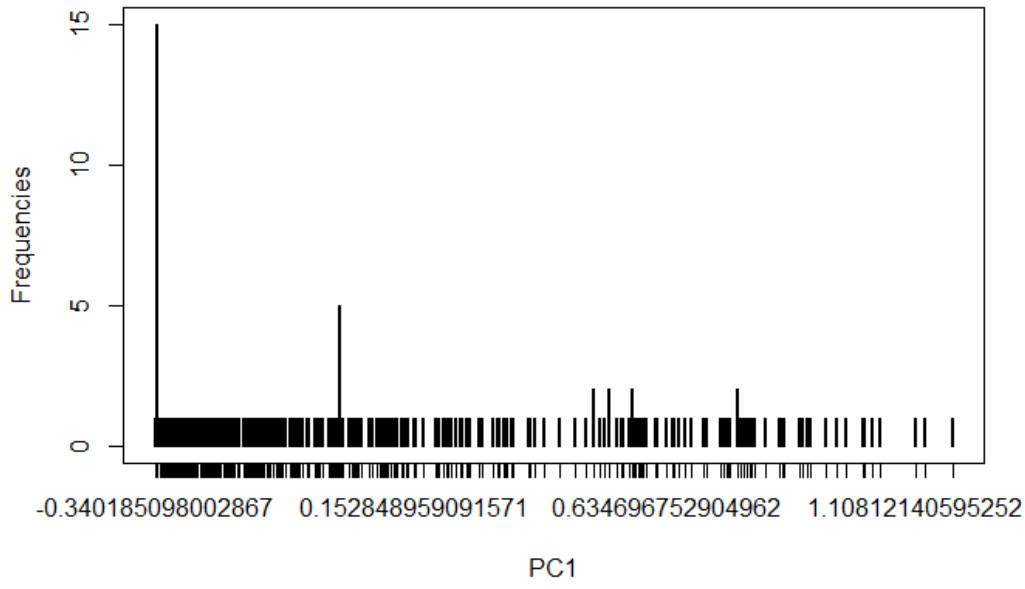

Fig. S16 – Frequency of CP1.

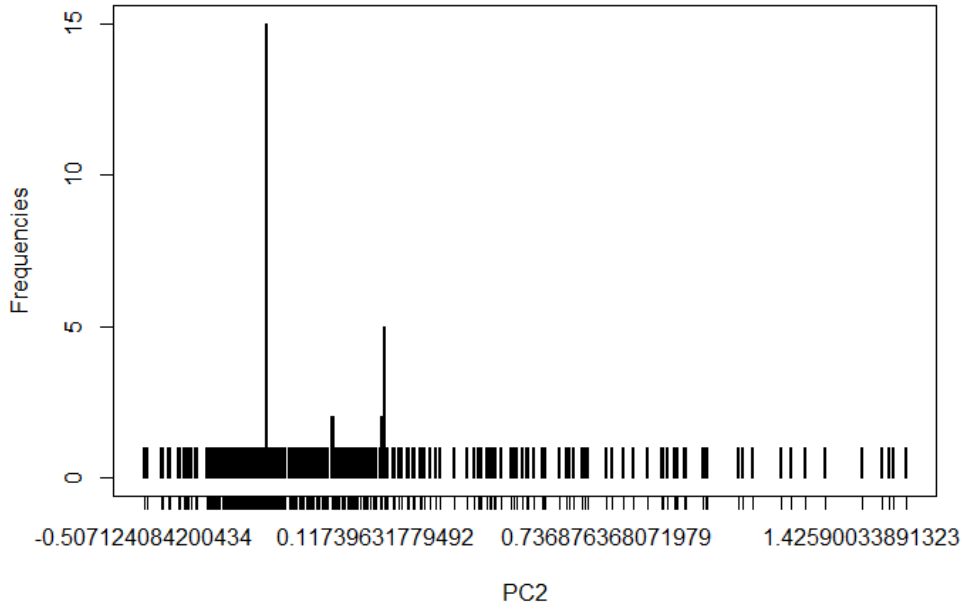

Fig. S17 – Frequency of CP2.

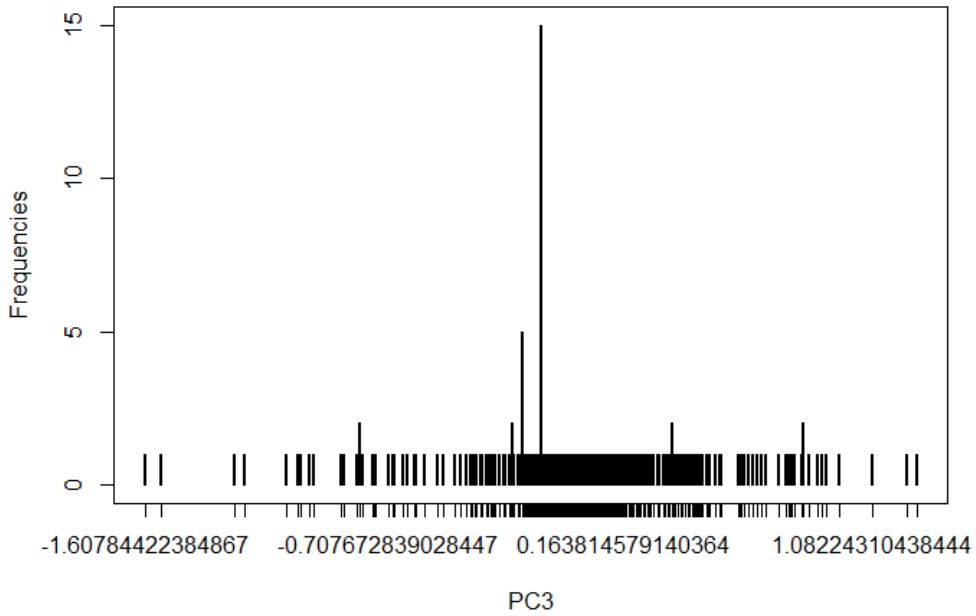

Fig. S18 – Frequency of CP3.

7. Interaction

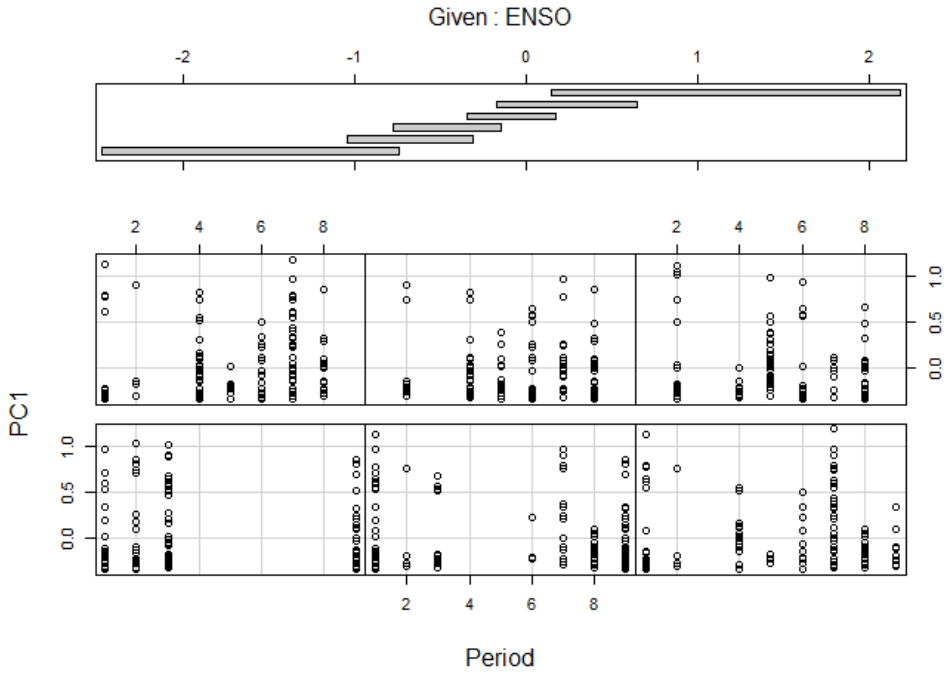

Fig. S19 – A coplot of CP1 data against Period given the ENSO event.

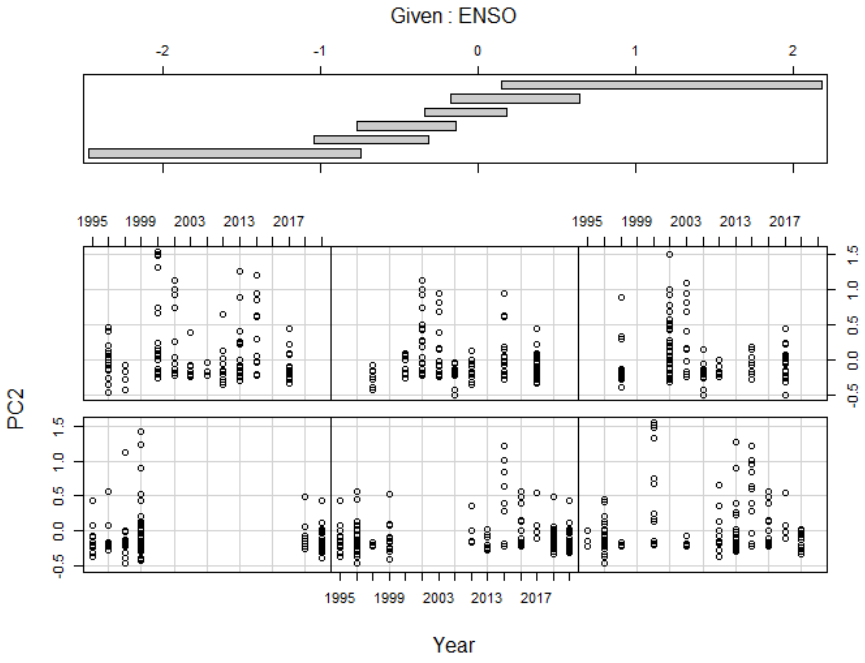

Fig. S20 – A coplot of CP2 data against Period given the ENSO event.

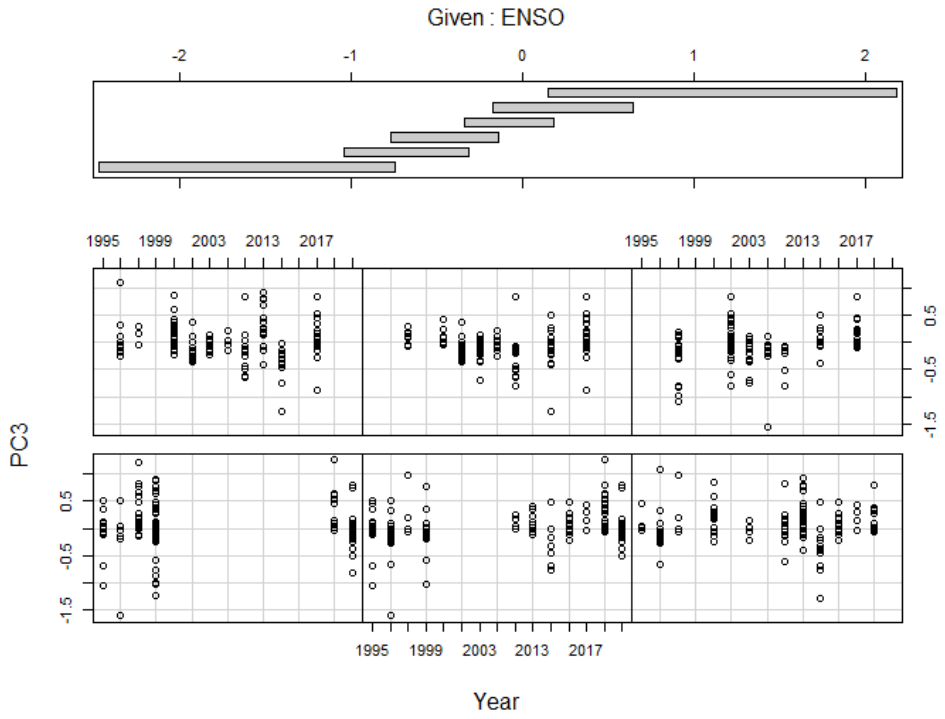

Fig. S21 – A coplot of CP3 data against Period given the ENSO event.

8. Collinearity

Table. S1 – Values of VIF calculated for the numerical explicative variables. Temp – Bottom temperature (ºC), Sal – Bottom salinity, OM – Organic matter content (%), Phi – Granulometry and Rain – Rainfall.

Temp	Sal	OM	Phi	Rain	ENSO
1.15	1.15	1.08	1.07	1.19	1.06

Diversity

9. Relationship between dependent and explanatory variables

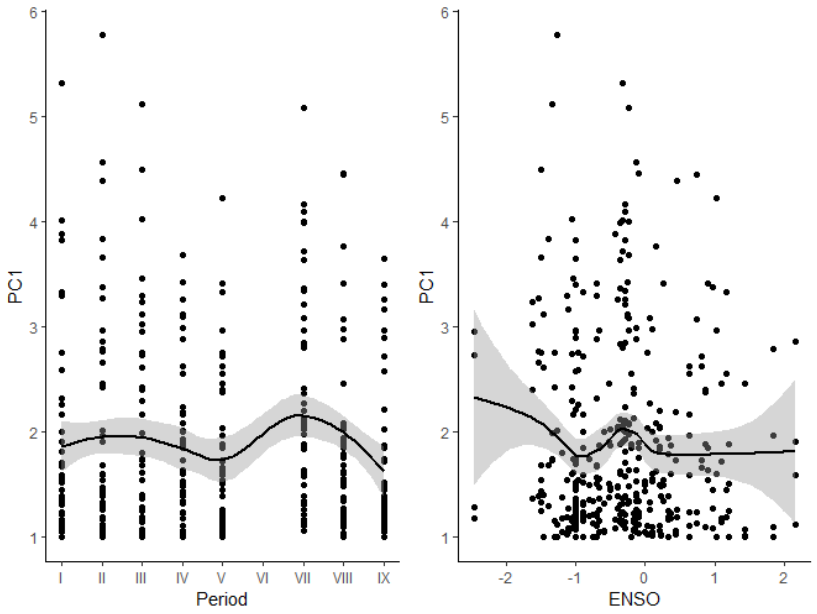

Fig. S22 – Scatterplots with a LOESS smoother between Diversity and its covariates Period and ENSO.

10. Outliers and dispersion pattern

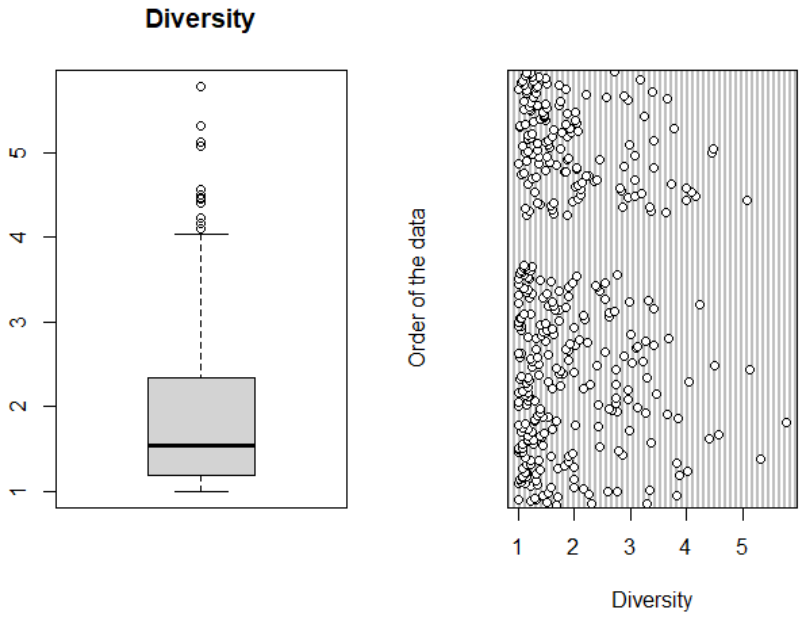

Fig. S23 – Box plot (Left) and Cleveland plot (Right) from Diversity.

11. Normality

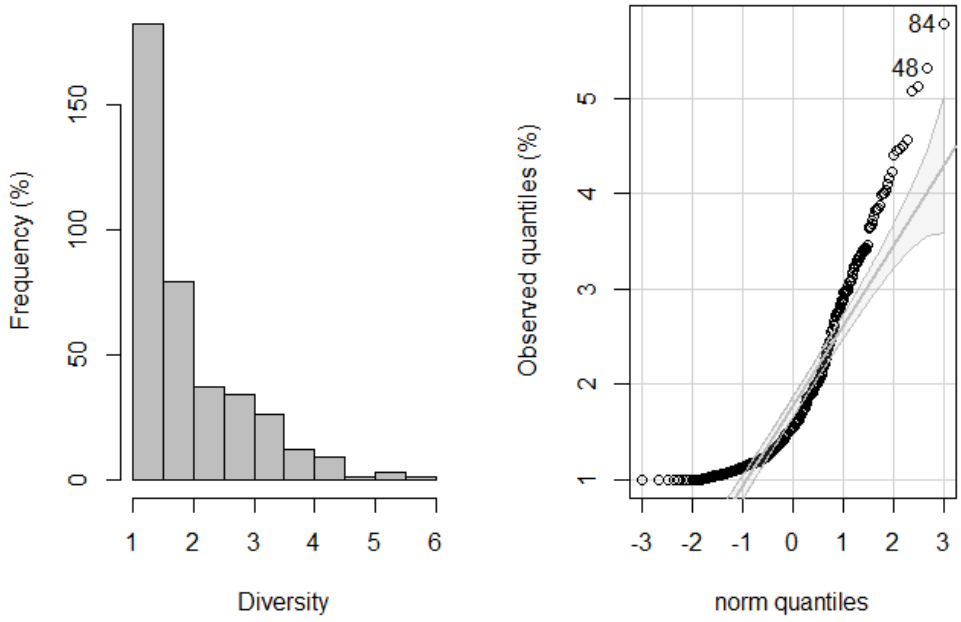

Fig. S24 – Histogram of Diversity (Left) and Q-Q plots (Right) of observed diversity against hypothetical normal distribution.

12. Homogeneity

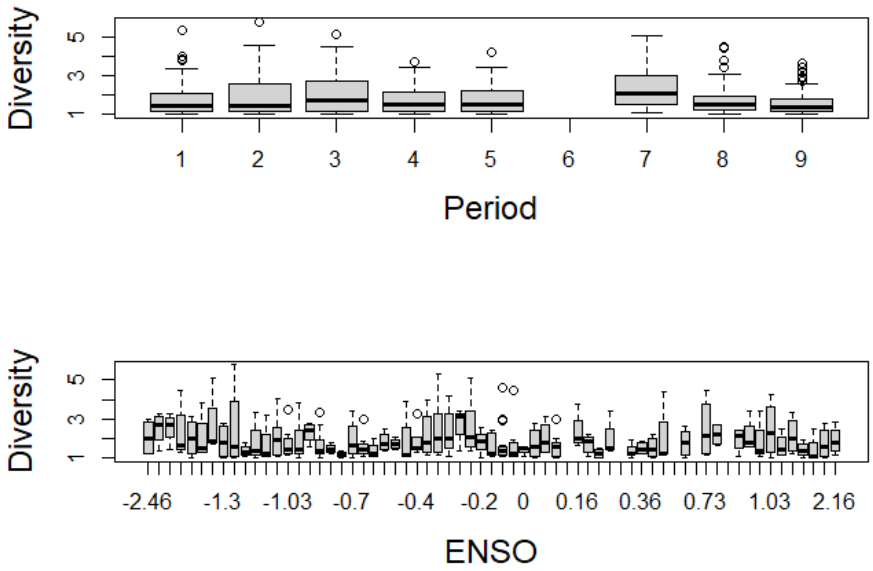

Fig. S25 – Period conditional box plot (Upper) and ENSO conditional box plot (Lower) of Diversity.

13. Independency

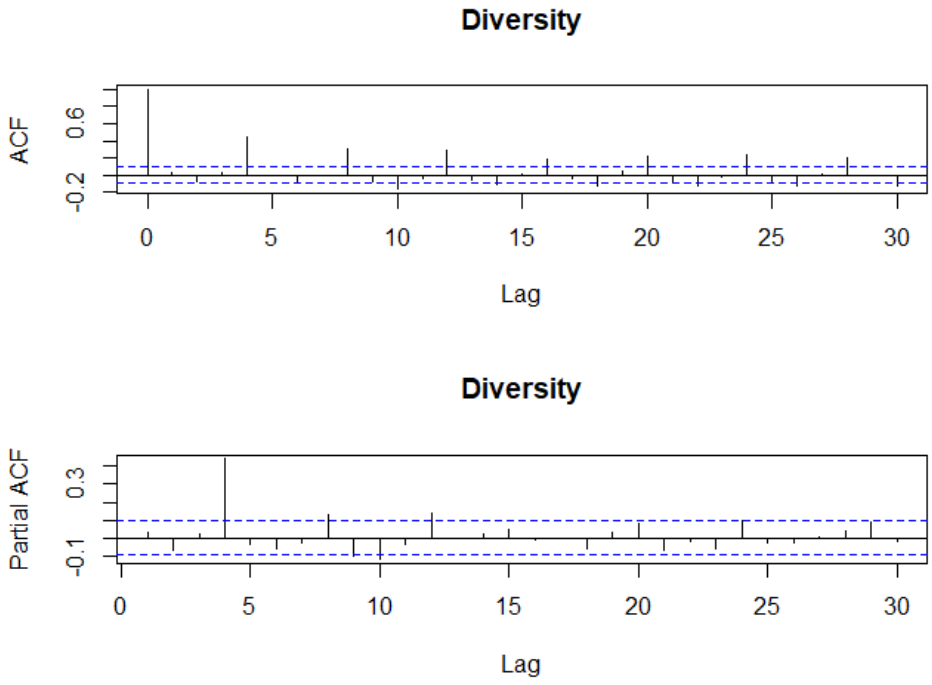

Fig. S26 – Auto-correlation function (ACF) and partial auto-correlation function (PACF) plot against time lag for Diversity index.

14. Zeros

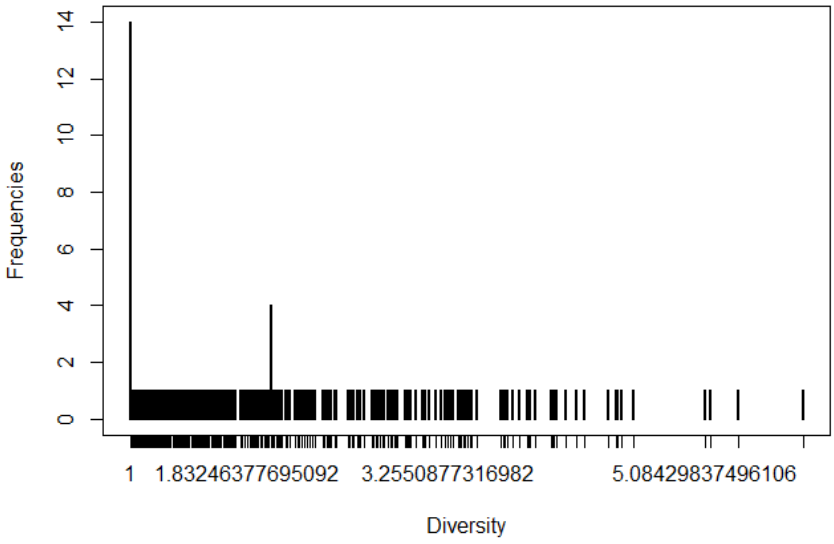

Fig. S34 – Frequency of Diversity data.

15. Interaction

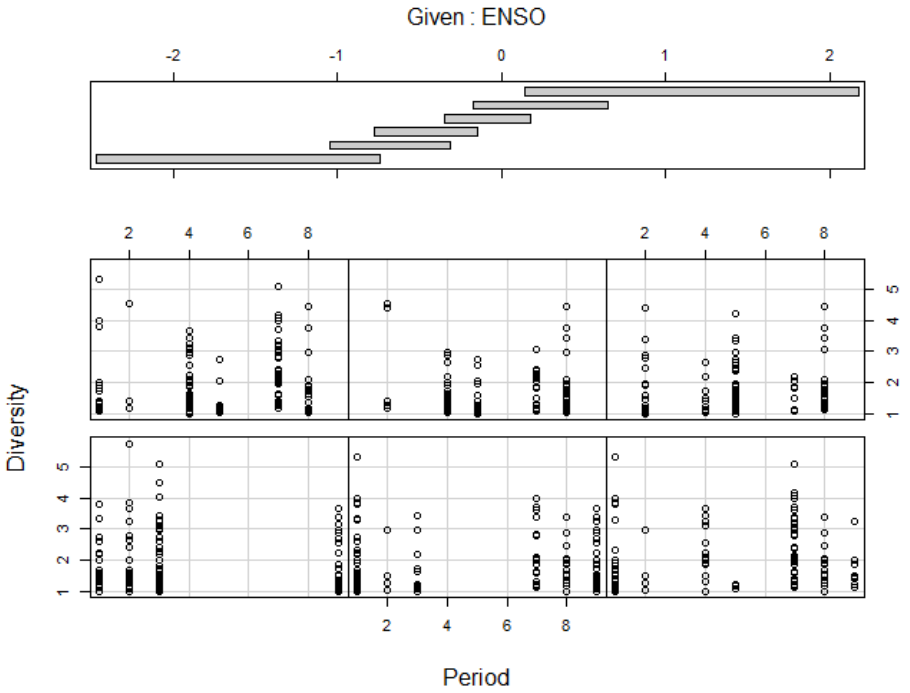

Fig. S35 – A coplot of Diversity data against Period given the ENSO event.

16. Collinearity

Table. S2 – Values of VIF calculated for the numerical explicative variables. Temp – Bottom temperature (ºC), Sal – Bottom salinity, OM – Organic matter content (%), Phi – Granulometry and Rain – Rainfall.

Temp	Sal	OM	Phi	Rain	ENSO
1.23	1.20	1.16	1.06	1.06	1.07

Considerações finais

Os resultados nos permitiram observar a variação temporal e espacial da abundância das espécies que compõem a assembleia de camarões da Enseada de Ubatuba durante os meses do ano e sua relação com os fatores ambientais (capítulo 1), e a variação da abundância e diversidade entre os anos amostrais, ao longo de nove anos entre um intervalo de 27 anos de coleta (capítulo 2).

Pudemos observar que a distribuição espacial das espécies na Enseada está intrinsecamente ligada ao seu ciclo de vida. Espécies com dependência do estuário em seu ciclo de vida foram encontradas em maior abundância nas áreas mais rasas, ao passo que as espécies que não dependem de tal habitat para seu desenvolvimento foram encontradas nas porções mais profundas da Enseada. Temporalmente, foi possível observar uma variação da presença de algumas espécies ao longo dos meses. Esta variação temporal está ligada tanto aos ciclos reprodutivos bem como a variação nos fatores ambientais. Eventos de ENSO influenciaram a abundância dos camarões. Períodos de neutralidade favoreceram o aumento na abundância de *A. longinaris*, *P. muelleri*, *R. constrictus*, *S. dorsalis* e *N. schmitti*. Em La Niña, houve aumento na abundância de *P. muelleri* e *S. dorsalis*. Já o El Niño, favoreceu a abundância de *L. schmitti* e *R. constrictus*. A variável ambiental Phi esteve presente nos modelos de todas as espécies avaliadas, sendo um fator preponderante na presença dos camarões.

Também foi possível observar que não houve variação significativa da abundância *F. brasiliensis*, *F. paulensis*, *R. constrictus*, *Xiphopenaeus* spp., e *E. oplophoroides* entre os anos amostrais. No que se refere aos camarões-rosa, o período de defeso estipulado para as espécies que esteve vigente até 2022 (i.e., 1º março a 31 de maio), aparentou estabilizar as populações ainda que cobrindo parcialmente o recrutamento juvenil na Enseada. O novo período de defeso a partir de 2023 ocorre de 28 de janeiro a 30 de abril.

Espera-se que a inclusão de janeiro seja benéfica para as populações, uma vez que é a partir deste mês que os juvenis entram na Enseada para completar seu desenvolvimento. No entanto a retirada de maio pode potencialmente ser prejudicial para as populações, sendo o período no qual os juvenis recrutam para a população adulta. Dessa forma, o monitoramento contínuo na área se faz necessário para a avaliação da eficácia deste novo período. A abundância de *Xiphopenaeus* spp. provavelmente não se alterou devido a abundância dos juvenis ocorrer no ponto 3, local onde a pesca é proibida.

As espécies que variaram em sua abundância ao longo do período amostral foram *A. longinaris*, *P. muelleri*, *L. schmitti* e *S. dorsalis*. As primeiras duas espécies ocorreram em maior abundância nos períodos 4 (jul/2001-jun/2002), 5 (jul/2002-jun2003) e 7 (jul/2013-jun/2014), e as duas últimas apenas para o período 7. O período 7 também foi o período no qual a maior diversidade foi registrada. A variação da abundância destas espécies e da diversidade na Enseada de Ubatuba entre os anos esteve intrinsecamente relacionada com a variação da temperatura. Os períodos de maior abundância e diversidade foram aqueles que apresentaram menores valores de temperatura de fundo.

Considerando que não ocorreu variação significativa de *F. brasiliensis*, *F. paulensis*, *R. constrictus*, *Xiphopenaeus* spp., e *E. oplophoroides* ao longo dos anos, e que as abundâncias de *A. longinaris*, *P. muelleri*, *L. schmitti* e *S. dorsalis* são influenciadas pela variação ambiental, com cautela, podemos deduzir indiretamente que a assembleia de camarões está estável na Enseada de Ubatuba.

Devemos considerar também que este é um estudo realizado com dados independentes da pesca. Uma vez que nosso esforço amostral se manteve constante ao longo dos anos, os fatores ambientais e períodos amostrais são as principais variáveis explicativas consideradas. Sugerimos paralelamente o estudo com dados dependentes da pesca para avaliar se estes resultados se repetem. Também podemos concluir que estudos

de longo prazo são essenciais para o monitoramento de espécies impactadas pela atividade pesqueira, e para a avaliação da eficácia de medidas de mitigação de tal atividade econômica.